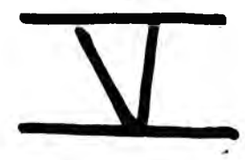

NUCLEAR MAGNETIC RESONANCE STUDIES OF MOLECULAR GEOMETRY AND CONFIGURATION

A Thesis submitted to the Council for Academic Awards in Partial Fulfillment of the requirement for the Degree of Doctor of Philosophy

by

Mohamed F Patel B.Sc.

Department of Chemistry,

Sir John Cass School of Physical Sciences and Technology

City of London Polytechnic,

London EC3.

March 1984

Abstract

Nuclear Magnetic Resonance Studies of Molecular Geometry and Configuration

Nuclear Magnetic Resonance (nmr) spectroscopy has been employed to determine molecular geometries, anisotropies in the indirect spin-spin couplings and chemical shifts, quadrupolar coupling constant, signs of indirect spin-spin coupling constants and conformational preferences of selected molecules by using isotropic and oriented solvents. The equilibrium geometries of the linear molecules CH_3HgCCH (I), $CH_3HgCCCH_3$ (II) and $(CF_3)_2Hg$ (III) were determined, and the geometrical parameters obtained were consistent with those which might be expected. ^{199}Hg shielding anisotropies of +6550, +6101 and +4071 ppm respectively for the above molecules were obtained by using nematic liquid crystals. These anisotropies when compared with that obtained in $(CH_3)_2Hg$ show that the carbon triple bond in I and in II, and the fluorines in III, are responsible for the the withdrawal of electrons from the mercury $6p_z$ orbitals, and an increase in occupancy of the $6p_x$ and $6p_y$ orbitals. The ^{19}F shielding anisotropy along the C-F bond in III was +105 ppm and this is in agreement with results obtained by solid state nmr. The signs of the indirect couplings $^nJ(HHg)$ (n=2-4) in I and II, and the signs of $^2J(FHg)$ and $^4J(FF)$ in III were determined by analysing the appropriate nematic spectrum. Evidence of anisotropies in J(FHg), J(FF) and J(FF) were found from the study of III partially oriented in a liquid crystal. ^1H and ^2D nmr spectra of partially oriented CH_3HgCCD were used to obtain the deuterium quadrupolar coupling constant in this molecule.

The geometry of the $(C_6F_5)P$ system (IV) in $(C_6F_5)(C_6H_5)_2P$ determined by liquid crystal nmr, was consistent with that in similar molecules, and in addition, an anisotropic contribution of 3% was found in $^3J(PF)$ when the sign of this coupling was assumed to be positive. $^{19}F\{^1H\}$ and $^{31}P\{^1H\}$ spectra of $(\underline{p}\text{-}C_6FH_4)_3P$ (V) partially oriented in a nematic liquid crystal showed evidence of anisotropy in $^5J(PF)$, and anisotropy in J(FF) was found if the CPC interbond angle in this molecule and in $(C_6H_5)_3P$ were assumed to be the same. $^{19}F\{^1H\}$ and $^{31}P\{^1H\}$ spectra of $(\underline{o}\text{-}C_6FH_4)_3P$ (VI) partially oriented in a liquid crystal showed conclusively the absence of free rotation about the P-C bonds, but they were consistent with their being either a single conformation or rapid interconversion between preferred conformers. ^{31}P shielding anisotropies in V and VI were determined to be +6 ppm and +40 ppm respectively.

^{13}C nmr data established that trimesitylphosphine (VII) in solution adopts the chiral propeller conformation at $-68^{\circ}C$, and tetramesityldiphosphine (VIII) adopts the gauche configuration at the slow exchange limit. The energy barriers to rotation about the P-mesityl bond in VII and P-P bond in VIII were obtained from ^{13}C nmr and band shape analysis.

M.F. Patel

Acknowledgment

It is a pleasure to acknowledge the continuous encouragement and much advice given to me by my supervisor, Professor W. McFarlane throughout this study. I would also like to thank Dr. I.J. Colquhoun and Dr. J. D. Dalton for helpful discussions and Dr. B. Wood for assistance in recording some of the nmr spectra. Thanks are also due to the computer centre at the City of London Polytechnic for providing computing facilities and the Inner London Education Authority for the award of a research assistantship.

Statement of Advanced Studies

The author has attended the lecture course in Fortran programming at the City of London Polytechnic, and has attended the NMR Summer School in Nottingham in 1982. In addition, the author has attended research meetings and seminars in nmr.

"Men love to wonder, and that

is the seed of our science."

Emerson, Society and Solitude.

CONTENT

Chapter 1 INTRODUCTION

Nuclear Magnetic Resonance (nmr) spectroscopy has now been available to chemists for over 25 years. In this time it has been extensively used for obtaining detailed information on chemical systems at the molecular level. Initial work was carried out on continuous wave spectrometers and only the most receptive nuclei ^{1}H and ^{19}F could be observed easily. In 1970 the use of Fourier transform (FT) techniques, high-field magnets and computer controlled operation greatly enhanced the scope of nmr spectroscopy. Thus at present, very high-field operation, multinuclear capability, high resolution work in solids, two dimensional operation and spin imaging have been included in the armoury of nmr spectroscopy. This thesis deals with obtaining information about geometries, conformational preferences, energies of bond rotation, and chemical environment by nmr of liquids and solution systems and molecules dissolved in liquid crystals.

1.1 Aspects of Nmr of Molecules Dissolved in Isotropic Solvents

This type of system is by far the most studied by nmr[1]. The analysis of nmr spectra of molecules dissolved in isotropic solvents is dominated by two parameters; the isotropic chemical shift differences and the indirect spin-spin coupling constants(J). The chemical shift arises because of shielding of the nuclei from the external magnetic field by the electrons, and thus nuclei with different electronic environments will have different chemical shifts (or shielding constants). As a knowledge of absolute values of shielding would involve consideration of the external magnetic field and the sample shape,

it is more convenient to report shieldings relative to those for certain nuclei in a standard. However, the nmr spectra for a given compound are governed by intramolecular chemical shift differences, i.e the chemical shift positions of each nucleus corresponding to its electronic environment. The indirect spin-spin couplings constant is observed as a splitting and is caused by interaction between pairs of nuclei in the molecule. It is not dependant upon the external magnetic field and is reported in Hertz(Hz). The magnitude of the coupling constant depends upon the chemical environment, and is a measure of the degree of interaction between the coupled nuclei. As both chemical shifts and coupling constants are governed by chemical environments, they are of great use in structural determination[2]. In fact more is known about the structural dependence of coupling constants than about chemical shifts.

A very important feature of the relationship between the indirect coupling and the geometry is that when all other factors are constant then the magnitudes of two and three bond couplings depend upon the dihedral angle ϕ (Fig 1.1)[2]. This type of relationship is known as Karplus[3], and the Karplus relationship can be used to predict the angle in molecules of unknown conformation from the following equation;

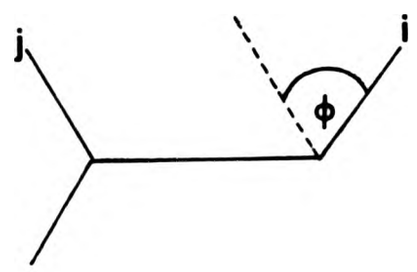

Fig 1.1

$$J = A + B\cos\phi + C\cos\phi \qquad 1.1$$

where A, B, and C are constants determined from model compounds. In Chapter 7 the determination of conformational preferences of

selected aromatic phosphines directly from the magnitudes of two and three bond P-C coupling constants will be described. For example in tris(2,4,6-trimethylphenyl)phosphine at low temperature the ^{13}C nmr spectrum gave two different magnitudes of the $^{3}J(PC)$ and this implies that at this temperature one of the ortho carbons has a large dihedral angle with respect to the phosphorus lone pair, while the other has not. Thus nmr of molecules in isotropic phases can be used to determine conformational preferences.

Nmr spectra which can predict conformational preferences can in principle also be used to determine energy barriers to internal rotation[4]. For example at low temperature, the ^{13}C nmr spectrum of tris(2,4,6-trimethylphenyl)phosphine shows two different sites for the ortho ^{13}C nuclei implying in molecular terms a pronounced dominance of one conformer as described above. As the temperature is raised, the spectrum shows "site exchange" between the two ortho ^{13}C signals which corresponds to rotation about the PC bond. At the fast exchange limit a single ortho ^{13}C resonance is observed, implying that rotation about the PC bond is now fast compared to the nmr time scale(1s to 10^{-3}s). So, in principle spectra obtained between the slow and fast exchange limits can be used to determine rates of exchange. This can be done by band-shape analysis[5], and the rates can then be interpreted in terms of energy barriers to internal rotation. Thus variable temperature nmr spectra and band-shape analysis can be use to determine information to energy barriers as long as the rate of exchange is within the nmr time scale.

1.2 Nmr of Molecules Oriented in Liquid Crystals

For molecules dissolved in isotropic solvents the molecular tumbling causes all anisotropic contributions to average out to zero, and the corresponding spectrum gives isotropic chemical shifts and indirect coupling constants. However if the molecules are fixed in a particular orientation then it should in principle be possible to obtain anisotropic information. Nematic liquid crystals serve as valuable solvents since they provide a convenient medium for orienting the molecules[6]. In the anisotropic phase of liquid crystals the intermolecular forces between the solute and solvent molecules cause the solute molecules to become partially oriented. The liquid crystal restricts rotational motion but permits translational motion and so all the intermolecular anisotropic contributions are still averaged out. The spectra of molecules oriented in liquid crystals will now include only the intramolecular contributions to the indirect coupling constant and chemical shifts, and their anisotropies[7].

The concentrations of solute in liquid crystals used throughout the work reported in this thesis were low, and therefore only the most receptive nuclei were observed, namely ^{1}H, ^{19}F, and ^{31}P. ^{13}C nmr spectra were ruled out in this work, but ^{199}Hg nmr spectra were obtained after relatively long accumulation times (2000 transients).

Analysis of the nmr spectra of oriented molecules gives anisotropic and indirect coupling constants. The indirect coupling constant, J(i,j), is dependant upon the electronic environment and is transmitted through the electrons between the

coupled nuclei i and j. The anisotropic coupling, D(i,j), is a combination of two terms; the direct dipolar coupling, D_{ij}^{dir}, and the anisotropic contribution to the indirect coupling constant, D_{ij}^{ind}. The direct dipolar coupling is dependant on the internuclear distance r_{ij} and the orientation of the internuclear axis ij, and is independent of the electronic environment (cf indirect coupling constant). The anisotropic contribution to the indirect coupling is dependant upon the electronic environment of the nuclei involved, and is transmitted through the electrons (indirect). This latter contribution is zero for a pair of protons but between fluorines it can be significant[7,8]. Contributions between other pairs of nuclei are reported in Chapter 2. Thus if the contribution of anisotropy to the indirect coupling and the orientation of the molecule are known, then the anisotropic coupling can be used for determining precise geometrical parameters[7]. This technique for determining geometrical parameters has been modified to include the influence of molecular vibration[9] and the results obtained compare well with those from other methods. Also, if the geometry is known, then D^{ind} can be determined, and this should in principle help in the understanding of the mechanism involved in spin-spin coupling. However, there are few results on D^{ind} at the present which are in agreement with theoretical models.

In Chapters 3 and 4 the determination of the geometries of linear mercuric molecules, and in Chapters 5 and 6 the geometries of fluorine-substituted aromatic phosphines are discussed. These molecules are suitable for this type of study as geometries determined by nmr in oriented media can then be compared with those obtained by other methods. In Chapters 4-6 the

contributions to the indirect F-F, Hg-F, and P-F couplings are examined.

The shielding constant (σ) of a nucleus in an isotropic solvent depends only on the average environment of the nucleus being observed.

$$\sigma_{iso} = \frac{1}{3}(\sigma_{xx} + \sigma_{yy} + \sigma_{zz}) \qquad 1.2$$

For oriented samples the spectra give anisotropic contributions to the shielding and thus a combination of the isotropic and anisotropic shieldings can in principle give the separate values of σ_{ij}, and hence provide more detailed information about the molecule[7,10,11]. Some nuclei, like for example ^{199}Hg, have a large chemical shift anisotropy which can be measured with fair precision[10-12]. This can then be discussed with existing theories on nuclear shielding[13-14]. Also, as in the case of linear mercuric molecules the sign of the mercury chemical anisotropy is known and this can be used to determine the sign of the orientation parameter which in turn can be used to determine the sign of the indirect coupling[11]. In Chapters 3-6 the determination of the signs of selected indirect couplings and ^{19}F and ^{199}Hg shielding anisotropies in the above molecules are discussed.

The technique for studying molecules oriented in liquid crystals has been also applied for determining quadrupolar coupling constants in suitable molecules[8] and conformational preferences when the intramolecular motion is within the nmr time scale[8] Hence in Chapter 2 this technique is discussed in detail and in Chapters 3 to 6 the technique is applied to suitable molecules.

1.3 References

1 Specialist Periodical Report. Nuclear Magnetic Resonance. The Chemical Society; Annual Reports in Nmr Spectroscopy, Ed. G.A. Webb, Academic Press, London; Nmr and the Periodical Table, Eds. R.K. Harris and B.E. Mann, Academic Press, London.

2 References 10-25 in Chapter 7.

3 M. Karplus, J. Chem. Phys., 30, 11(1959).

4 B.E. Mann, Prog in Nmr specty., 11, 95(1977); Practical Nmr Spectroscopy, M.L. Martin, G.J. Martin, and J.J. Delpuech, Heydon Press 1980.

5 S.O. Chan and L.W. Reeves, J. Amer. Chem. Soc., 95, 670(1973).

6 Molecular Structure and Properties of Liquid Crystals, G.W. Gray, Academic Press N.Y. 1962.

7 P. Diehl and C.L. Khetrapal, NMR-Basic Principles and Progress Vol 1, Springer-Verlag, N.Y. 1969; Nmr Spectroscopy using Liquid Crystal Solvents, J.W. Emsley and J.C. Lindon, Pergamon, N.Y. 1975; C.L. Khetrapal and A.C. Kunwar, Advances in Magnetic Resonance Vol 9, 301(1977).

8 Chapter 2.

9 References 16-18 and 25 in Chapter 2.

10 J.D. Kennedy and W. McFarlane, J. Chem. Soc. Farad. Trans. 2, 72, 1653(1976).

11 Chapters 3 and 4.

12 J. Jokisaari and P. Diehl, Org. Mag. Res., 13(5), 359,(1980).

13 N.F. Ramsey, Phys. Rev., 91, 303(1953); C.J. Jameson and H.S. Gutowsky, J. Chem. Phys., 40, 1714(1964).

Chapter 2

Introduction to the Nmr of Molecules Oriented in Liquid Crystals

2.1 Introduction

In nuclear magnetic resonance experiments electromagnetic radiation is applied to a sample which is placed in a static magnetic field. If a nucleus in the sample has a magnetic moment, the magnetic component of the electromagnetic radiation causes transitions between spin states of the magnetic moment. It is the local magnetic fields at the sites of the nuclei that are responsible for there being different transition frequencies. The local magnetic field is given by the sum of the field produced by surrounding electrons and the field due to interaction with other nuclei in the sample. The former field describes shielding at the nucleus whereas the latter field is characteristic of coupling caused by surrounding nuclei. The shielding at the nucleus can be split into two contributions; the isotropic and anisotropic shieldings. Likewise the coupling term can also be differentiated into two categories; isotropic and anisotropic couplings. The anisotropic contribution differs from the isotropic term in that anisotropic measurements are dependant upon the direction the measurements are made from. In nmr experiments the measurements are carried out relative to the external magnetic field.

In nmr studies of liquids and gases, and of molecules dissolved in liquids, the anisotropic contributions mentioned above average out to zero, due to rapid tumbling of the molecules, and the nmr spectrum consists of fewer and generally sharper lines. Hence in the nmr spectra of molecules which are tumbling

Chapter 2

Introduction to the Nmr of Molecules Oriented in Liquid Crystals

2.1 Introduction

In nuclear magnetic resonance experiments electromagnetic radiation is applied to a sample which is placed in a static magnetic field. If a nucleus in the sample has a magnetic moment, the magnetic component of the electromagnetic radiation causes transitions between spin states of the magnetic moment. It is the local magnetic fields at the sites of the nuclei that are responsible for there being different transition frequencies. The local magnetic field is given by the sum of the field produced by surrounding electrons and the field due to interaction with other nuclei in the sample. The former field describes shielding at the nucleus whereas the latter field is characteristic of coupling caused by surrounding nuclei. The shielding at the nucleus can be split into two contributions; the isotropic and anisotropic shieldings. Likewise the coupling term can also be differentiated into two categories; isotropic and anisotropic couplings. The anisotropic contribution differs from the isotropic term in that anisotropic measurements are dependant upon the direction the measurements are made from. In nmr experiments the measurements are carried out relative to the external magnetic field.

In nmr studies of liquids and gases, and of molecules dissolved in liquids, the anisotropic contributions mentioned above average out to zero, due to rapid tumbling of the molecules, and the nmr spectrum consists of fewer and generally sharper lines. Hence in the nmr spectra of molecules which are tumbling

rapidly only isotropic shieldings (or chemical shifts) and isotropic coupling constants are observed. These parameters, obtained from the interpretation of isotropic nmr spectra, have proved to be invaluable to chemists for the determination of the molecular structures of unknown compounds. However, the process of eliminating all anisotropic contributions by using isotropic solvents can be said to impose a considerable loss of information. This information can be recovered if the molecular motion in the sample can be restricted so that the solute molecule adopts a preferred orientation for a sufficient length of time. Under such circumstances the anisotropic contributions will no longer average out to zero and this in turn will provide information about molecular geometry and the environment of the nuclei.

The inability of isotropic nmr to provide precise geometrical data led nmr spectroscopists to study solid materials. The work involved using powdered samples and single crystals. In solid state nmr we expect to observe anisotropic coupling via dipolar interaction between nuclei in the molecule and between neighbouring molecules. The spectrum will then consist of a broad resonance and in principle certain geometrical data may be determined by analyzing the shape of the band. In practice this is not always possible. The magnetic dipolar-dipolar coupling (which averages out to zero in the case of isotropic nmr) is strong, and to eliminate it high power decoupling is required and consequently causes technical problems [1]. Another problem is that some nuclei, for example carbon-13, have very long spin-lattice relaxation times thus leading to low sensitivity. However this problem can be overcome by special pulse sequences which transfer magnetization from one nucleus to another. This

technique is called Cross-Polarization [2]. Another problem encountered in solid state nmr is that shielding constants are anisotropic and the nmr spectrum of a powdered sample would show a distribution of chemical shifts corresponding to all orientations of the molecule. For say ^{13}C, such a range may be up to 200ppm and thus all that will be observed would be a broad band. This problem can be eliminated by spinning the sample at a special angle which has the effect of removing the orientation dependence of the shielding [3]. This procedure is known as Magic Angle Spinning and the special angle is set at $54^{o}44'$ to the applied field. For a Magic Angle Spinning experiment using a spectrometer operating at 25MHz the spinning rate required is about 2.5KHz which suggests that as we go to high field technical problems will be encountered. The techniques described (magic angle spinning, high power decoupling and cross polarization) or a combination of them to study solid state nmr have in some cases been successful in obtaining information on the geometry of both small and large molecules. However the experiments described do have their limitations because of technical problems.

In 1963 Saupe and Englert[4] used liquid crystals as solvents to restrict the motion of the solute, and since then nmr studies of molecules oriented in liquid crystal solvents have been extensively used [5]. The liquid crystal restricts the rotational motion in the sample but permits translational motion so that coupling to neighbouring molecules is no problem. The method does not require modification of the nmr spectrometer, and nmr spectra of molecules oriented in liquid crystal solvents are acquired in the conventional way. As expected the analysis of the spectra will be more complicated than of the corresponding isotropic

spectra, but this can be accomplished by using computer programs for systems of up to 8-10 spins.

2.2 Liquid Crystal Solvents

Certain organic compounds consist of rod-like molecules with benzene rings, and they have the property that they show two distinct melting points. The lower melting point is a transition between the solid and the liquid crystalline phases, and the higher melting point is the transition between the liquid crystalline phase and the isotropic liquid phase. Such compounds are called liquid crystals, and there are 3 types. These are smectic, nematic, and cholesteric; their difference lies in the degree of ordering that takes place. The smectic liquid crystal phase is the most ordered and cholesteric the least well ordered of the three. In the course of this study the nematic liquid crystalline phase was found to be satisfactory as a solvent and all further discussion will be devoted to this type. In appendix 2.1 physical data of some liquid crystal solvents are compiled and Fig 2.1 gives a representation of the molecular arrangement in a nematic solvent.

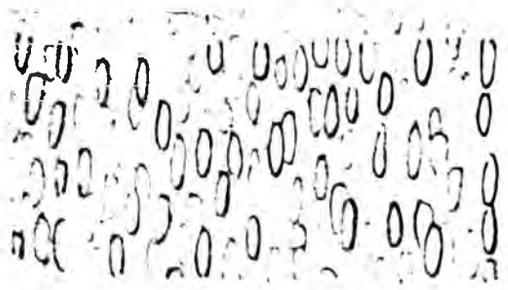

Fig 2.1 Molecular Arrangement in the Nematic Phase

When molecules are dissolved in liquid crystal solvents they behave differently in the two phases. In the isotropic phase the behaviour of the molecule is comparable to that found in "normal" solution and the nmr spectrum gives the isotropic chemical shifts and coupling constants in the usual way. The liquid crystalline phase (or nematic phase) of the solvent has anisotropic properties, and the intermolecular forces between the molecules of the solute and solvent cause the solute molecules to become partially oriented. The molecular motion in the nematic phase is however still sufficiently rapid to average out the inter-molecular dipolar couplings, and nmr spectra of molecules oriented in liquid crystal solvents will give anisotropic and isotropic contributions to the chemical shifts and intramolecular coupling constants.

Proton nmr spectra of molecules partially oriented in nematic liquid crystal solvents show an absence of sharp signals due to the solvent. This is not the case in "normal" nmr of solute dissolved in organic (isotropic) solvents. The reason for this is that nematic liquid crystal solvents have molecules which have a larger number of protons (usually more that 30). The large number of protons and the complex direct dipolar interactions between these protons would give a spectrum of the liquid crystal as a broad band of some 20KHz width. The spectrum corresponding to the molecules in solute would then lie upon the broad band. However if a suitable weighting function is applied to the FID signal prior to transformation most of the signal from the solvent is lost in the noise and we obtain a reasonable quality spectrum corresponding to the solute molecules. An example of this artificial treatment of the FID whereby the signals from the

solvent are lost in the baseline, and signals from the solute give relatively sharp lines is shown for acetone partially oriented in Phase IV (fig 2.2). Spectra of nuclei not present in the liquid crystal itself (e.g. ^{19}F, ^{31}P etc.) cause no problems and require no baseline modification.

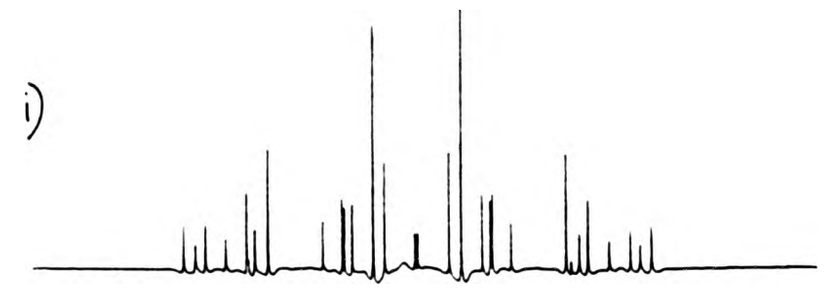

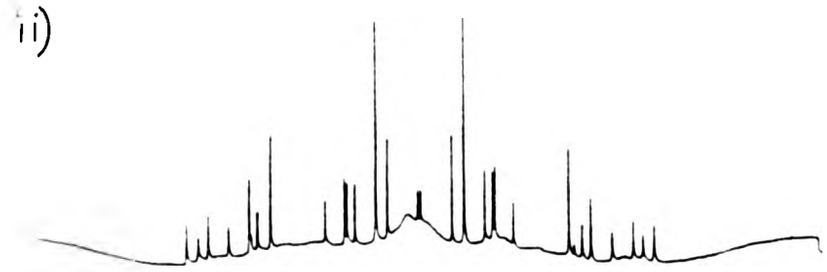

Fig 2.2

Nmr spectra of Acetone Oriented in Phase V; i) with baseline modification, ii) without baseline modification.

2.3 Basic Theory

High resolution nmr both of molecules dissolved in isotropic and in anisotropic solvents is now well understood. The nuclear spin Hamiltonian for the isotropic phase is given by the following equations.

$$h^{-1}H_{ns} = -\sum_J \nu_j \hat{I}_{jz} + \sum_{J<k} J(j,k)\hat{I}_j.\hat{I}_k \qquad 2.1$$

$$\nu_j = \frac{\gamma_I}{2\pi} B_o(1-\sigma_j) \qquad 2.2$$

The definition of the symbols is as follows: ν_j is the isotropic

chemical shift, $\hat{I}$ is the spin operator, J_{jk} is the indirect isotropic coupling constant between nuclei j and k, σ_j is the shielding constant, γ is the magnetogyric ratio, and B_o is the applied magnetic field. The nuclear spin Hamiltonian for the anisotropic phase is given by Equation 2.3.

$$h^{-1}H_{ns,a} = -\sum_j \nu_{ja}\hat{I}_{jz} + \sum_{j<k}(J(j,k)+2D_{jk}^{tot})\hat{I}_j.\hat{I}_k \qquad 2.3$$

$$\nu_{ja} = \frac{\gamma_j}{2\pi}B_o(1-\sigma_j-\sigma_{ja}) \qquad 2.4$$

where D_{jk}^{tot} is the total dipolar (or anisotropic) coupling constant, ν_{ja} is the anisotropic chemical shift, and σ_{ja} is the anisotropic shielding constant. Comparison of Equations 2.1 and 2.3 shows that Equation 2.3 contains additional terms. It is not difficult to see that in the case of rapid molecular tumbling, when all anisotropic contributions average out to zero, Equation 2.3 becomes identical with 2.1. Consequently, computer programs already existing for the analysis of spectra of molecules in isotropic media [6] (e.g. LAOCOON 1968) were readily modified for oriented systems[7] (e.g. LAOCOON LC). A description of the input and output of LAOCOON LC is shown in Appendix 2.2

2.4 Direct Dipolar Coupling Constants

From the analysis of nmr spectra of molecules oriented in the nematic phase, values for the anisotropic chemical shifts and the anisotropic and isotropic coupling constants will be obtained. The isotropic coupling constant J_{ij} (or the indirect spin-spin coupling) arises from the interaction between nuclei in the same molecule and this is transmitted through the electrons. In some cases this interaction can also have a component that is

anisotropic and this is called the indirect dipolar coupling D_{ij}^{ind} or the anisotropic J coupling, J_{ij}^{aniso}. This is again transmitted through the electrons. The magnitude of this is incorporated in the total anisotropic coupling constant D_{ij}^{total}. The remaining anisotropic coupling contribution is independent of the electrons, and is called the direct dipolar coupling D_{ij}^{dir}. D_{ij}^{dir} depends on the internuclear distance as r_{ij}^{-3} and the orientation. Hence the total anisotropic contribution to the coupling is given by the sum of the individual anisotropic couplings. Thus

$$D_{ij}^{total} = D_{ij}^{dir} + D_{ij}^{ind} \qquad 2.5$$

As we shall see later, for a pair of protons the D^{ind} tends to zero [8], whereas for a pair of fluorine nuclei this contribution may be significant [9]. At present, we shall concentrate on the direct dipolar coupling, and the indirect dipolar coupling will be dealt with in Section 2.8 .

The direct dipolar coupling between two nuclei i and j is obtained by taking the average value over all inter and intra molecular motions, and is given by the following equations.

$$D_{ij}^{dir} = -\frac{K(i,j)}{2}\left\langle \frac{3\cos^2\theta_{ij} - 1}{r_{ij}^3} \right\rangle \qquad 2.6$$

$$K(i,j) = \frac{\gamma_i \gamma_j}{4\pi^2} \qquad 2.7$$

where θ_{ij} is the angle between the magnetic field direction and the axis connecting nuclei i and j that are a distance r_{ij} apart, and <> implies the average value of. Values of K(i,j) for pairs of nuclei i, j are complied in Table 2.1.

Table 2.1

The Magnitude of K(i,j) for different pairs of Nuclei

Nuclear Pairs i,j	$K(i,j)/HzA^3$
^1H - ^1H	120066.66
^1H - ^{19}F	112957.24
^1H - ^{31}P	48606.5
^1H - ^{199}Hg	21432.13
^{13}C - ^{19}F	28401.0
^{13}C - ^{31}P	12221.2
^{19}F - ^{19}F	106268.79
^{19}F - ^{31}P	45728.38
^{19}F - ^{199}Hg	20163.08

In Equation 2.3 it was noted that in the course of molecular tumbling the anisotropic terms averages out to zero. It is this term $3Cos^2\theta_{ij}-1/r_{IJ}^3$ which when integrated over all possible orientations (or angles θ) that becomes zero, and thus reduces Equation 2.3 to 2.1. If nuclei i and j belong to the same "rigid" part of the molecule then equation 2.6 can be written as

$$D_{IJ}^{dir} = -K(i,j) \times S_{ij}/r_{IJ}^3 \qquad 2.8$$

where S_{ij} is the orientation parameter describing the orientation of the vector i,j in terms of the internuclear axis ij, and now r_{ij} is constant (if the effect of molecular vibration is ignored). Sometimes the symmetry of the molecule can be such that a series of equations similar to Equation 2.8 can be derived for different pairs of nuclei r,s. For example

$$D_{rs}^{dir} = -K(rs) \times S_{ij}/r_{rs}^3 \qquad 2.8(a)$$

What is required now is to solve the series of equations of the form 2.8(a) for each measured D_{rs}^{dir} so as to determine the internuclear distance r_{rs}. This could be done once the orientation tensor has been determined, and this is our next aim.

2.5 The Orientation Tensor

The orientation tensor S is a parameter that describes the orientation of a molecule and is dependant upon temperature and concentration, as well as the molecular properties. Hence for every different liquid crystal nmr experiment a new value for S is required to be calculated. When a solute is dissolved in a liquid crystal solvent and then placed in a magnetic field, the molecules of the solute will take up a preferred average orientation. As the external magnetic field in the nmr experiment is applied in one particular direction (z direction) then the preferred orientation of the solute molecules can be related to the direction of the magnetic field. As Equation 2.8 stands, S_{ij} is given in terms of the internuclear axis i,j, but it would be more useful to write S in terms of Cartesian coordinates. Saupe [10] and Snyder [11] have shown that the orientation of any molecule may be described by an S matrix whose elements S_{pq} (in our case p,q=x,y,z) are given by Equation 2.9

$$S_{pq} = \langle 3\mathrm{Cos}\theta_p \mathrm{Cos}\theta_q - \delta_{pq} \rangle \qquad 2.9$$

$$p,q = x,y,z \qquad \delta_{pq} = 0 \text{ if } p \neq q \text{ and } \delta_{pq} = 1 \text{ if } p = q$$

where the angle θ_p is the angle the Cartesian coordinate axis p makes with the magnetic field direction. From equation 2.9 it can be seen that S_{ij} must lie between -0.5 and +1. Thus when the internuclear vector i,j is parallel to the magnetic field

direction S_{ij}= +1, and when it is perpendicular to this direction S_{ij}= -0.5.

We will now consider some of the properties of the S matrix. The elements of a 3x3 S matrix are listed below.

$$S = \begin{bmatrix} S_{xx} & S_{xy} & S_{xz} \\ S_{yx} & S_{yy} & S_{yz} \\ S_{zx} & S_{zy} & S_{zz} \end{bmatrix}$$

Important properties of the S matrix are that it is symmetric ($S_{pq} = S_{qp}$), and its trace is zero:

$$S_{xx} + S_{yy} + S_{zz} = 0 \qquad 2.10$$

The S matrix also has a property whereby an S matrix given in one coordinate system can be related to that in a another system. Thus S_{ij} is then related to S_{pq} by

$$S_{ij} = \sum_{pq} \text{Cos}\alpha_{ijp}\text{Cos}\alpha_{ijq}S_{pq} \qquad 2.11$$

That is ;

$$\begin{aligned} S_{ij} = {} & S_{xx}\cos^2\alpha_{ijx} + S_{yy}\cos^2\alpha_{ijy} \\ & + S_{zz}\cos^2\alpha_{ijz} + 2S_{xy}\cos\alpha_{ijx}\cos\alpha_{ijy} \\ & + 2S_{xz}\cos\alpha_{ijx}\cos\alpha_{ijz} + 2S_{yz}\cos\alpha_{ijy}\cos\alpha_{ijz} \end{aligned} \qquad 2.11$$

where α_{ijp} is the angle the vector i,j makes with the coordinate axis p (cf Fig 2.3).

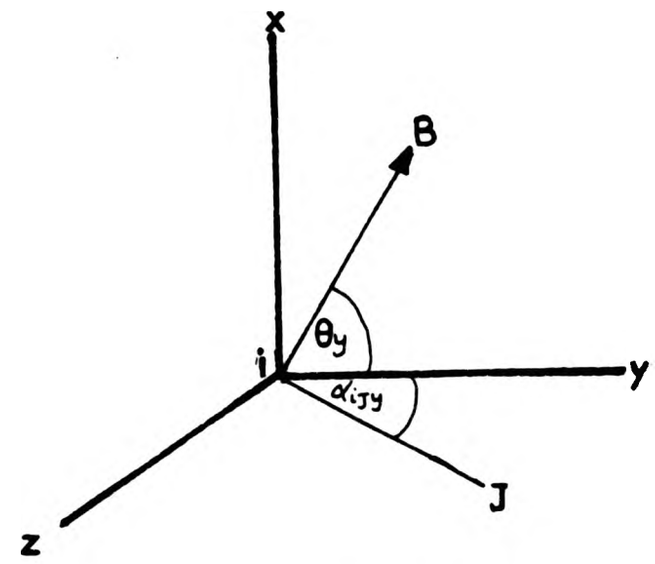

Fig 2.3

The maximum number of elements S_{pq} that need to be calculated for the S matrix is 6. Using the equation for the trace of S this number is reduced to 5. Hence for a molecule with no symmetry 5 elements of the S matrix are required. However, sometimes we can use the symmetry of the molecule to reduce this number further. For example, if we take a molecule with C_3 symmetry and let the C_3 axis run parallel to one of the coordinate axes, then only one independent orientation tensor need to be determined. However if a molecule contains 2 perpendicular planes of symmetry (e.g. a mono substituted benzene), then 2 independent S_{pq} values need to be calculated. In Table 2.2 the number of independent S values required to be calculated are listed, subject to symmetry and a suitable coordinate axis.

Table 2.2 Number of Parameters necessary for the description of Orientation

Symmetry of the molecule	Number of independent elements of the S-matrix	Independent elements of the S-matrix
3-fold or greater axis	1	S_{zz}
2 perpendicular planes	2	S_{zz}, $S_{xx} - S_{yy}$
1 plane	3	S_{xx}, S_{yy}, S_{zz}
none	5	S_{xx},S_{yy},S_{xy}, S_{xz},S_{yz}

Once the orientation tensor S_{ij} can be written in terms of S_{pq}, then S_{ij} can be solved by substitution into equation 2.8 .

$$D_{IJ}^{dir} = -K(i,j) \times S_{ij} / r_{IJ}^{3} \qquad 2.8$$

$$S_{ij} = \sum_{p,q} \cos\alpha_{ijp} \cos\alpha_{ijq} S_{pq} \qquad 2.11$$

For every independent S_{ij} required we need corresponding pairs D_{IJ}^{dir} and r_{ij}. The value of D^{dir} is obtained from the analysis of the oriented spectrum, and the internuclear distance is obtained from the molecular geometry of either the same molecule or a similar one. Once the value of S_{ij} has been determined, then for each remaining experimental direct dipolar coupling the corresponding internuclear distance can be calculated (using equation 2.8b). This method of obtaining geometrical parameters relies heavily on determining an accurate value of S_{ij} first, which is dependant on r_{ij} and D_{IJ}^{dir}. The precision with which the direct dipolar coupling constant can be

obtained depends upon the quality of the anisotropic spectrum. The value of r_{ij} on the other hand relies on the accuracy to which this parameter was determined by previous studies. Hence the method of determining geometries from the anisotropic nmr spectrum is not completely reliable, unless certain structural parameters are precisely known. However, as the method calculates geometry by using a known value of r_{ij} to determine S_{ij}, and then using this value of S_{ij} to calculate other internuclear distances r_{rs} from corresponding observed D_{rs}^{dir}, the geometrical parameters obtained are in fact ratios of internuclear distances. When comparing geometrical information from other techniques with that obtained from oriented nmr it is advisable to compare ratios of internuclear distances and not individual distances.

The direct dipolar coupling in Equation 2.8 depends upon two factors, S the orientation parameter and r the internuclear distance. The internuclear distance should be constant in one particular phase, and up to now it has been assumed that when the molecules in a solute are dissolved in the anisotropic phase they will orient in one particular way only. This was found to be untrue when studying certain molecules like acetylene [12], methanol [13], and methyl fluoride [14], where it was found that such molecules can take up more than one average orientation in the anisotropic phase. These situations should therefore serve as a warning when determining geometries by this method. It is therefore advisable, when using nmr of molecules oriented in anisotropic solvents to determine structures, to work with more than one orientation; e.g by changing temperature, solvent or concentration.

2.6 Effects Of Molecular Vibration

Since the first discussion on the calculation of molecular geometries of molecules oriented in anisotropic solvents[4], many experimental results have shown that it is necessary to take into account the effects of molecular vibrations[15-20]. It was not until 1971 that Meiboom and Snyder included vibrational effects in their calculation of the geometry of benzene dissolved in a nematic phase[15]. They found that corrections for the influence of vibration on the direct dipolar couplings needed to be applied for small distances and only between light atoms. Since then Diehl has also studied the geometry of benzene and calculated the vibrational correction averaged over the whole molecule using normal coordinates of the molecule obtained from its force field [16-18]. It is this model that will be discussed later on.

The ultimate aim in using the method for structural determination by nmr is to compare its results with results obtained by other methods (e.g X-ray, microwave, electron diffraction etc.). Before this can be done we have to make sure that comparisons are being made between identical parameters at the same temperature and phase. In practice these conditions are not always met. Nmr studies of oriented species must use molecules dissolved in liquid crystals, whereas for example electron diffraction, X-ray and microwave spectroscopy do not require solvents at all. Also the nmr method cannot determine geometry directly from dipolar coupling constants alone but must be used in conjunction with other techniques of structure determination. Thus changes in the geometry with temperature and phase have to be assumed to be small, and the value (or values) for the orientation parameter (or parameters) can be obtained in

most cases with reasonable precision.

The comparison between different techniques for structure determination must be made between identical parameters. In nmr we determine geometry from the relationship between the orientation, the direct dipolar coupling and $\langle r^{-3} \rangle$. In electron diffraction, experiments are performed on gases and what is measured is $\langle r^{-1} \rangle$. For rotational spectroscopy measurements are made from the moment of inertia and the moment of inertia depends on $\langle r^{2} \rangle$. These three averages are not equal when the bond length can change. Hence if comparisons were made of structural parameters without considering vibrational effects, this would in some cases lead to results that differ considerably, as was found for the CH bond length in benzene. The results from rotational spectroscopy [21], Raman spectroscopy[22], and nmr [23] showed that the differences in the CH internuclear distances (without vibrational correction) were greater than can be attributed to experimental error. However when these values were compared after vibrational corrections, there was agreement between them. Hence the inclusion of vibrational averaging in the calculations of geometry and orientation by nmr will increase the accuracy of measurements of the parameters that have been derived. We shall define the geometry calculated with vibrational corrections as the equilibrium geometry. This differs from the rigid geometry in that internuclear distances in the equilibrium geometry are based upon the average positions of the nuclei after harmonic approximations to the vibrations have been accounted for.

The model for the determination of the molecular geometry by nmr of oriented species with the inclusion of vibrational effects involves determining the difference between observed direct

dipolar couplings D^{obs} and those calculated from the molecular geometry when nuclei are in their equilibrium position D^{e}. If D^{obs} is close to D^{e} then the relationship between the observed and calculated dipolar couplings can be expressed as a Taylor series

$$D_{ij}^{obs} = D_{ij}^{e} + \sum_{p,q} \Delta p_{ij} \frac{\partial D_{ij}^{e}}{\partial p} + \frac{1}{2} \sum_{pq} \Delta p_{ij}^{2} \frac{\partial^2 D_{ij}^{e}}{\partial p^2} \qquad 2.13$$

The quantity Δp is the mean amplitude of vibration and is a function of the anharmonic term in the potential function of the vibrating molecule. Such terms are only known for small molecules and have to be ignored in our problem[24-26]. The quantity Δp^2 is the mean square amplitude of vibration and is calculated from the normal coordinates of the molecular vibration[24-26]. The normal coordinate of the vibration can be evaluated from the force field and the Cartesian coordinates of the molecule.

$$D_{ij}^{e} = D_{ij}^{obs} - \tfrac{1}{2}\sum_{p,q} \Delta p_{ij}^{2} \frac{\partial^2 D_{ij}^{e}}{\partial p^2} = D_{ij}^{obs} - D_{ij}^{vib} \qquad 2.14$$

A program for calculating D^{vib}, the direct dipolar coupling contribution to vibration has been written by Diehl, and the form of its input and output are illustrated in Appendix 2.3. The program calculates the the values for D^{e} from the orientation tensor and geometry. Entering the force field then gives D^{vib}. The equilibrium geometry is then determined by iterating first on the orientation parameter, followed by iteration on the geometry until there is consistency between the experimentally determined D^{obs} and D^{obs} calculated from the program.

2.7 Shielding Anisotropies

The Hamiltonian for an oriented system (Equation 2.3) contains terms that describe the isotropic and anisotropic shielding constants of the nuclei that are under consideration, i.e. σ_j and σ_{ja}. Hence from analysis of the nmr spectra of oriented molecules, the values of the shielding constants can be determined. In isotropic media, the molecules are changing their orientation rapidly with respect to the applied magnetic field and what is observed is an average chemical shift i.e. an average environment of the nucleus that we are observing. However, in the anisotropic phase the molecules behave as though they remain fixed in a particular orientation for a sufficient length of time to allow the shielding constant of the nucleus at that particular orientation to be determined. In nmr, shielding constants are measured as chemical shifts and reported in ppm relative to a standard, and not in absolute terms of shielding. This is because, to be able to quote absolute values of shielding requires knowledge of the chemical shift of a bare nucleus and this is not generally available. Hence in nmr we report on the changes in environment of nucleus in a particular molecule as compared with a standard. The convention used is that resonances to high frequency correspond to a positive chemical shift (or negative shielding).

The shielding constants observed from an anisotropic spectrum describe a relationship between the components of the shielding tensors. Hence for each experiment or each orientation a corresponding relationship between the shielding in all the directions would be obtained.

In general the shielding anisotropy is given by the following equation

$$\sigma(\text{nem}) - \sigma(\text{iso}) = \frac{2}{3} \sum_{p,q} \sigma_{pq} S_{pq} \qquad 2.15$$

where σ (nem) and σ (iso) are the shielding constants in the isotropic and nematic phases respectively, and σ_{pq} is the shielding tensor in the pq direction. To determine the shielding anisotropy we need to solve Equation 2.15. σ (nem) can be obtained directly from chemical shift measurements in the anisotropic spectra. The isotropic shielding must also be determined at the same temperature and concentration, and in the same phase. The magnitude of this parameter can not be determined directly from the anisotropic spectrum. However Buckingham[27] has pointed out that the observed chemical shift in most cases is linearly dependant upon temperature. Hence by plotting the isotropic chemical shift against temperature and then extrapolating back to the nematic temperature the isotropic chemical shift in the nematic phase can be deduced. We shall now consider the form of Equation 2.15 for molecules with a particular symmetry.

From equation 2.15 for molecules with 3-fold symmetry we obtain

$$\sigma(\text{nem}) - \sigma(\text{iso}) = \frac{2}{3} S_{zz} \Delta\sigma \qquad 2.16$$

$$\text{where } \Delta\sigma = \sigma_{\parallel} - \sigma_{\perp} \qquad 2.17$$

and taking the C_3 symmetry axis to be parallel with the z axis. $\sigma_{\parallel}$ and $\sigma_{\perp}$ in equation 2.17 are the shieldings parallel and perpendicular to the z direction. The equation for the isotropic

shielding is

$$\sigma_{iso} = \frac{1}{3}(\sigma_{xx} + \sigma_{yy} + \sigma_{zz}) \qquad 2.18$$

Equations 2.16 and 2.18 can then be solved simultaneously to determine $\sigma_{\parallel}$ and $\sigma_{\perp}$.

A shielding anisotropy experiment for molecules having symmetry that is lower than 3-fold can only yield relationships between the shielding components. For example, for a molecule with 2-fold symmetry

$$\sum_{p,q} \sigma_{pq} S_{pq} = S_{xx}\sigma_{xx} + S_{yy}\sigma_{yy} + S_{zz}\sigma_{zz} \qquad 2.19$$

To obtain the individual components for the shielding tensor three truly independent experiments are required. Sometimes using three different orientations will give three different ratios for the calculated orientation parameters, and three different values for differences between the isotropic and nematic chemical shifts. From these three different orientations, three equations of the form 2.15 can then be derived and solved simultaneously to give the three components of the shielding tensor. The different orientations may be obtained by using the same solvent or different solvents. In practice by varying the concentration in the same solvent or a different solvent very rarely can independent orientations be obtained.

Shielding anisotropy experiments can also give the sign of the orientation tensor if the sign of the shielding anisotropy is already known. It is sometimes possible to predict the sign of the anisotropy from the geometry of the molecule. For example, the mercury nucleus in the linear molecule dimethylmercury should have a positive shielding anisotropy because the electronic

circulation about the symmetry axis will be relatively unhindered (positive shielding contribution), and will be restricted when the electronic circulation is perpendicular to this direction (therefore the shielding is negative). As the anisotropy is given by $\sigma_{\parallel} - \sigma_{\perp}$, then in dimethylmercury the mercury shielding anisotropy must be positive. Once the sign of the shielding anisotropy is known, the sign of the orientation tensor can be derived using Equation 2.15. This in turn gives the sign of the direct dipolar coupling constant using equation 2.8. In the analysis of all nmr spectra the signs of all the couplings are interchangeable. That is to say a reversal of the signs of all the couplings leaves the spectrum unchanged. Hence what is required is the sign of any one of the couplings and then the signs of the remaining couplings will follow. Thus by using the sign of the dipolar coupling derived from the orientation tensor we can deduce the signs of all the anisotropic couplings, and more interestingly, the signs of the J couplings. This process of deriving the signs of couplings from the the sign of the shielding anisotropy can obviously be reversed, that is a knowledge of the sign of any one of the couplings can lead to the the sign of the chemical shift anisotropy.

Another method by which the sign of the orientation parameter can be predicted is by using the possible range of values of S. As the orientation parameter must lie between -0.5 and +1 then certain measured values of S can only have one sign. For example if the S tensor was determined to be 0.7 then its sign would have to be positive.

2.8 Anisotropy To The Indirect Spin-Spin Coupling

It was mentioned in Section 2.4 of this chapter that the total (observed) anisotropic coupling, D^{tot}, is not always purely dipolar (D^{dir}), but may have a significant anisotropic contribution from the indirect spin-spin coupling, J^{aniso} or D^{ind}. In isotropic media, due to rapid molecular tumbling, this contribution averages out to zero. However in the anisotropic phase, J^{aniso} may no longer be zero, and the nmr of oriented molecules can in principle be used to determine its magnitude.

The experimental determination of J^{aniso} cannot be made as a separate quantity; that is it cannot be detected on its own. It is determined by taking the difference between the experimental dipolar coupling and the dipolar coupling calculated from the known geometry with the assumption that J^{aniso} is zero (Equation 2.5). Thus the accuracy to which J^{aniso} can be calculated depends upon the precision of D^{tot} and D^{dir}. The error in D^{tot} is dependant upon the quality of the spectrum, and the error in D^{dir} on the geometrical parameters used to calculate the orientation tensor. To improve the accuracy of J^{aniso} vibrational corrections should be included when determining D^{dir}. Hence one way of determining J^{aniso} is by observing the difference between D^{tot} and D^{dir} [28]. Another way of measuring J^{aniso} is to determine the orientation tensor at different concentrations and by using different anisotropic solvents. Unlike the direct dipolar coupling, J^{aniso} does not necessarily change linearly with orientation, and if J^{aniso} does exist, then different ratios between the orientation parameters will be detected for each experiment [29,30]. Once J^{aniso} has been determined the next step is to calculate the individual

components of J^{aniso}.

The components of the anisotropic indirect coupling can be calculated from J^{aniso} using equation 2.20.

$$J^{aniso} = \frac{2}{3} \sum_{p,q} S_{pq} J^{pq} \qquad 2.20$$

where p and q belong to the coordinate axis x,y,z. The isotropic coupling is given by;

$$J^{iso} = \frac{1}{3}(J^{xx} + J^{yy} + J^{zz}) \qquad 2.21$$

By solving Equations 2.20 and 2.21 we can determine the components of the indirect coupling (J^{xx}, J^{yy}, etc.).

Taking for example a molecule with C_3 symmetry we have the relationship between the orientation parameters

$$S_{zz} = -S_{xx}/2 = -S_{yy}/2 \qquad 2.22$$

Then J^{aniso} is given by

$$J^{aniso} = S_{zz}(J^{zz} - \frac{1}{2}(J^{xx} + J^{yy})) \qquad 2.23$$

where the internuclear vector ij lies parallel to the C_3 and the z axes. This gives

$$J^{xx}_{ij} = J^{iso}_{ij} - J^{aniso}_{ij}/2S_{zz} \qquad 2.24$$

$$J^{zz}_{ij} = J^{iso}_{ij} + J^{aniso}_{ij}/2S_{zz} \qquad 2.24$$

Using Equations 2.21 and 2.24 we can solve for J^{xx}_{ij} , J^{yy}_{ij} and J^{zz}_{ij}.

components of J^{aniso}.

The components of the anisotropic indirect coupling can be calculated from J^{aniso} using equation 2.20.

$$J^{aniso} = \frac{2}{3} \sum_{p,q} S_{pq} J^{pq} \qquad 2.20$$

where p and q belong to the coordinate axis x,y,z. The isotropic coupling is given by;

$$J^{iso} = \frac{1}{3}(J^{xx} + J^{yy} + J^{zz}) \qquad 2.21$$

By solving Equations 2.20 and 2.21 we can determine the components of the indirect coupling (J^{xx}, J^{yy}, etc.).

Taking for example a molecule with C_3 symmetry we have the relationship between the orientation parameters

$$S_{zz} = -S_{xx}/2 = -S_{yy}/2 \qquad 2.22$$

Then J^{aniso} is given by

$$J^{aniso} = S_{zz}(J^{zz} - \frac{1}{2}(J^{xx} + J^{yy})) \qquad 2.23$$

where the internuclear vector ij lies parallel to the C_3 and the z axes. This gives

$$J_{ij}^{xx} = J_{ij}^{iso} - J_{ij}^{aniso}/2S_{zz} \qquad 2.24$$

$$J_{ij}^{zz} = J_{ij}^{iso} + J_{ij}^{aniso}/2S_{zz} \qquad 2.24$$

Using Equations 2.21 and 2.24 we can solve for J_{ij}^{xx} , J_{ij}^{yy} and J_{ij}^{zz}.

Another method for the determination of the individual components of J^{aniso} is possible when there are in the molecule two internuclear vectors that are parallel. When two internuclear vectors ij and kl are parallel to each other, the direct dipolar couplings of the two will be dependant upon their nuclear constant K(i,j) (or K(k,l) and their internuclear distances. This is not the same for J^{aniso} for the same internuclear vectors. Hence we can obtain two equations for J^{aniso}

$$J_{ij}^{aniso} = S_{pp}[J_{ij}^{pp} - (J_{ij}^{qq}+J_{ij}^{rr})] + (S_{qq}-S_{rr})(J_{ij}^{qq}-J_{ij}^{rr}) \ldots\ldots \quad 2.25$$

$$J_{kl}^{aniso} = S_{pp}[J_{kl}^{pp} - (J_{kl}^{qq}+J_{kl}^{rr})] + (S_{qq}-S_{rr})(J_{kl}^{qq}-J_{kl}^{rr}) \ldots\ldots \quad 2.25$$

and solve simultaneously, once the orientation parameters have been determined.

When there are no convenient symmetry relationships between the internuclear vectors, then the detection of J^{aniso} relies on determining the difference between the observed anisotropic couplings and the anisotropic couplings calculated with the assumption that J^{aniso} is zero. If the number of observed dipolar couplings is greater than the number of independent orientation parameters to be calculated, and the molecular geometry is known from other sources, then J^{aniso} can be estimated in the following way. It is possible to obtain a different value for J^{aniso} for each concentration from the difference between the calculated and observed dipolar couplings. The corresponding orientation tensors for each concentration can also be determined. The different concentration may be made up using one solvent or different solvents. Thus an equation of the form of 2.20 can be derived for each concentration. If n

components of J^{aniso} are required then at least n+1 equations of the form of 2.20 must be derived. By solving these equations simultaneously the individual components of J^{aniso} can be obtained. However it should be stated that the number of occasions in which any of these procedures has been used successfully is small.

Comparisons between experimentally determined values of J^{aniso} and those calculated theoretically have been interpreted in various ways. Where agreement has been poor the following reasons have been suggested to account for the discrepancies.

i) The indirect coupling may be temperature and solvent dependant (if different solvents were used to determine isotropic and anisotropic couplings).

ii) Molecules at different sites in the anisotropic phase may have different molecular orientations.

When J^{aniso} is small, discrepancies have been accounted for by suggesting,

iii) Neglect of molecular vibration,

iv) The geometrical parameters used to calculate S were not correct.

v) Errors in the measurement of the experimental dipolar couplings.

In general it has been found that H-F indirect couplings are less anisotropic [29] than F-F indirect couplings [31-34], and proton-proton couplings are not anisotropic[35]. In Table 2.3 we list the contribution of J^{aniso} for the pairs of nuclei that have so far been studied. The table acts as rough guide for deciding when the magnitude of J^{aniso} may be significant, and when it should not be ignored in using nmr of oriented molecules

to determine molecular geometries.

Table 2.3

Percentage Anisotropic Contributions to the Indirect Spin-Spin Coupling Between Pairs of Nuclei

Coupling	Percent[a]	Reference
^{1}H - X	0	X= ^{1}H[35-38], ^{13}C[39], ^{15}N[40], ^{29}Si[41], ^{31}P[42], $^{111,113}Cd$[43], ^{199}Hg[36-38,44]
^{1}H- ^{19}F	0.2-0.5	Fluorinated benzenes [31-34]
^{1}H- ^{19}F	0.2-1.0	Fluoroethylenes [45]
^{13}C- ^{13}C	12	Ethylenes[46], Dimethylmercury[47]
^{13}C- ^{19}F	0.8	[39]
^{13}C-^{199}Hg	50	[47]
^{19}F- ^{19}F	16	[31-34,45,48]
^{19}F- ^{31}P	0	[42,49,50]
^{19}F- ^{31}P	50	Phosphoryl Fluoride [51]
^{19}F-^{199}Hg	50	[52]

a) Percent = $J^{aniso} \times 100/D_J^{dir}$

2.9 The Quadrupolar Interactions

A nucleus with spin I greater than 1/2 has a quadrupole moment. The quadrupole moment Q is the measure of the departure of the nuclear charge distribution from the spherical shape. Owing to the molecular tumbling any molecular electrical field gradient acting on the nuclear charge changes rapidly with respect to a particular axis thus leading to various energies of transitions. It is this variation in the electrostatic energy around the nucleus that gives rise to the quadrupole coupling constant. In liquids where there is molecular tumbling, the motion is fast and this enables the coupling to become zero. However due to short spin relaxation times line broadening is a common feature in spectra of molecules containing nuclei with I greater than 1/2. For anisotropic phases, the motion is no longer isotropic and line broadening is again observed but the quadrupole splitting can now be measured also. Nuclei such as iodine and chlorine have large quadrupole moments leading to rapid relaxation, and this makes it difficult to measure their quadrupolar splittings [53]. The deuteron (I=1) on the other hand, has a small quadrupole coupling constant and even with the effects of line broadening, the value of the coupling can be measured without a great deal of difficulty [53]. Thus we shall discuss the use of quadrupolar coupling using the deuteron as an example.

The deuterium spectrum of an oriented molecule containing a single deuteron is a doublet with splitting Δ from which the quadrupole coupling constant (eQV_{zz}/h) can be determined using the following equation.

$$eQV_{zz}/h = 2\Delta/3S_{zz} \qquad 2.27$$

where S_{zz} is the orientation tensor and the z axis lies along the direction of the deuteron bond. Typical values of Δ are of the order of 100KHz and therefore the effect of temperature gradients in the sample is to give broad peaks with line widths of about 150Hz. This is a common feature of anisotropic deuterium spectra, and broad lines are not primarily a consequence of short spin relaxation time of the deuteron nucleus. The orientation tensor must be measured from the same sample at the same temperature. Again, the precision to which the quadrupolar coupling can be measured is dependant upon the internuclear distance used to calculate the orientation parameter. Hence to improve the accuracy of measurement of the coupling constant the effects due to molecular vibration should be included in the calculation. If the quadrupolar coupling constant is known from a different experiment the magnitude and sign of the orientation parameter can then be determined. This is quite a useful method to obtain a value of the orientation parameter which is independent of internuclear distance.

Besides using eQV_{zz}/h to determine S_{zz}, this parameter can be used to derive the electronic structure along the deuteron bond. In eQV_{zz}/h, eQ is the electrical quadrupole moment and V_{zz} is the distribution of charge along this bond. To determine V_{zz} a detailed knowledge of the wave function for all the electrons around the bond is required. Only V_{zz} for hydrogen is known [53]. However the magnitude of V_{zz} depends almost entirely on the way the lowest available (non spherical) orbitals are occupied. Hence from the magnitudes of the quadrupole coupling constants the electronic environment of the bond to the

deuteron can be deduced. Table 2.4 lists some of the quadrupole coupling constants that have been measured and the types of hybrid orbital involved in the bond to the deuteron are reported.

Table 2.4

Some Deuterium Quadrupolar Coupling Constants

Molecule	Quadrupolar Coupling Constant (KHz)	Nature of hybrid orbital[a]	Ref
DCN	199 ±3	sp	54
DC≡CD	200 ±10	sp	55
$CH_3C{\equiv}D$	199 ±2	sp	54
C_6D_6	183 ±10	sp^2	56
CH_3CD_3	167 ±12	sp^3	56

a) The hybrid orbital of the carbon directly bonded to the deuteron.

2.10 Conclusion

The nmr of oriented molecules has been developed with considerable success for the determination of anisotropic parameters which cannot be measured by isotropic nmr. These results augment those obtained from solid state nmr. In this chapter the techniques whereby molecules oriented in liquid crystal solvents can be used to determine structure and to derive the anisotropy of couplings and shieldings have been discussed. The anisotropic contributions to the coupling may be indirect

spin-spin or quadrupolar and can give insight into the electronic environment of chemical bonds. The shielding anisotropy gives information about the environment of the nucleus that is under consideration. The internuclear distances and bond angles obtained from dipolar couplings can help to derive the possible geometry of the oriented species, and in this respect it is the only available technique for the determination of molecular geometries in the liquid phase. However the technique has its limitations. One of these limitations is that it is best suited to small organic molecules. In the case of large molecules, low concentrations would be required, otherwise a unique orientation would not exist over the whole phase. Also it may be difficult to obtain good quality spectra of oriented large molecules, because of the requirement of low concentration, and in any case the analysis of the spectrum would be complicated. Another limitation of this technique is that only molecules that dissolve with ease in liquid crystal solvents can be studied. Hence few inorganic molecules can be studied by this method. In the chapters to follow this technique will be applied on a series of interesting molecules and the usefulness and problems experienced in these studies will be discussed.

APPENDIX 2.1 Liquid Crystal Solvents Used

i) Phase IV: p-n-Butyl-p'-methoxyazoxybenzene

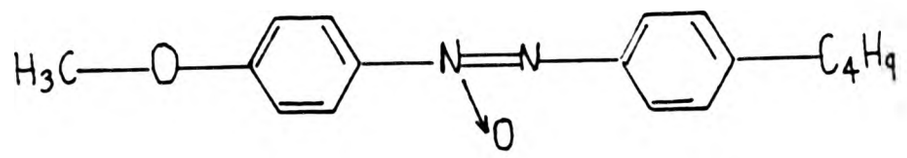

nematic range +16 to +76°C

ii) Phase V: 65 mole percent of Phase IV and

35 mol percent of p-ethyl-p'-methoxyazoxybenzene

65 mole percent of Phase IV +

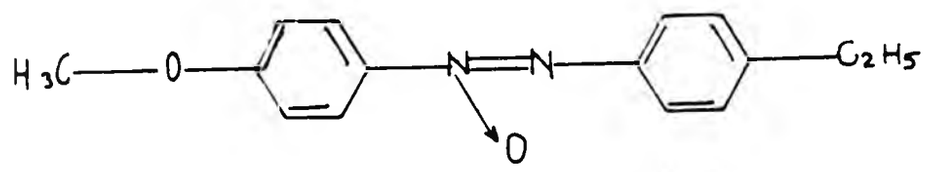

nematic range -5 to +75°C

iii) EBBA: N-(p-Ethoxybenzylidene)p-n-butylaniline

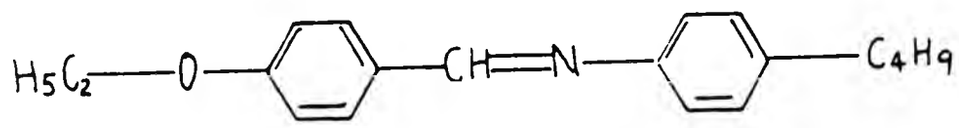

nematic range +32.5 to +81°C

APPENDIX 2.2

Input for LAOCOON LC[7]

```
1,5,H
-10000,20000,.01
1,1,1,1,2
8900.87,8941.69,8941.69,8941.69,-5000
0,0,0,68.6
-203.92,-203.92,-203.92,-139.927
0,0,-146
5522.72,5522.72,-490.8
0,-146
5522.72,-490.8
-146
-490.8
```

Output of LAOCOON LC

```
1                    LAOCOON LC
                     CASE   1H

NN= 5
FREQUENCY RANGE -10000.0 to  20000.0  MINIMUM INTENSITY .010

        ISO VALUE      CHEMICAL SHIFT

             1        W(1)=   8900.870
             1        W(2)=   8941.690
             1        W(3)=   8941.690
             1        W(4)=   8941.690
             2        W(5)=  -5000.000
COUPLING CONSTANTS              ANISOTROPIC COUPLING CONSTANTS[a]
J(1,2)=      0.000                   DD(1,2)=   -203.920
J(1,3)=      0.000                   DD(1,3)=   -203.920
J(1,4)=      0.000                   DD(1,4)=   -203.920
J(1,5)=     68.600                   DD(1,5)=   -139.927
J(2,3)=      0.000                   DD(2,3)=   5522.720
J(2,4)=      0.000                   DD(2,4)=   5522.720
J(2,5)=   -146.000                   DD(2,5)=   -490.800
J(3,4)=      0.000                   DD(3,4)=   5522.720
J(3,5)=   -146.000                   DD(3,5)=   -490.800
J(4,5)=   -146.000                   DD(4,5)=   -490.800
       FREQUENCY  INTENSITY   CORRESPONDING LINE NUMBERS
      -5990.863     1.000          5
      -5919.475     1.000         12
      -5033.029     0.348         80
            .         .            .
            .         .            .
            .         .            .
      17617.565     2.819        120
      18000.021     0.215        124
           END OF CASE   1
```

a) Anisotropic Couplings are twice the value of the anisotropic couplings defined in equation 2.6.

APPENDIX 2.3

Input for VIBRA

```
GEOM          11   1
CH3HGCH3
     1                          2    1    1
     2                          3    4    1
     3                          3    5    1
     4                          1    1    6
     5                          1    1    7
     6                          1    1    8
     7                          9    1   11
     8                         10    4   11
     9                         10    5   11

   11
0.          1.02658     -.51329     .88904      -.88904     .36639
2.46039     4.55439
-1.02658    0.51329     4.92078
FMAT           11
S*          1     1     4
S*          1     2     4
S*          1     3     4
B*          3     1     4     3
B*          3     1     4     2
B*          3     2     4     3
SS          5     1     4     2     4
SS          5     2     4     3     4
SS          5     1     4     3     4
SS          7     3     4     4     5
SB          8     6     7     7     6     8
SB          8     6     7     7     6     9
SB          8     6     8     7     6     8
 .          .     .     .     .     .     .
 .          .     .     .     .     .     .
 .          .     .     .     .     .     .
 .          .     .     .     .     .     .
BB         15     3     4     5     7     6     5
BB         15     3     4     5     8     6     5
BB         15     3     4     5     9     6     5
L*         16     6     5     4     2
O*         16     6     5     4     2

   16
4.74        2.38        .433        .146        .016        .031
-.075       .007
.1408       .0975       .0873       .0252       -.0297      -.0213
.0265       .1035
NCOR             1
1.008        1.008       1.008       12.         12.00       12.
1.008       1.008
1.008
COVM           11
     1     2
     1     4
     1     5
     1     6
```

```
    1    7
    1    8

303.
AMPL
DVIB           11   11
     1 H        2 H
     1 H        4 C13
     1 H        5 HG
     1 H        6 H
     1 H        7 H
     1 H        8 H

-.10748     .21496
STOP
```

OUTPUT FOR VIBRI

ATOMIC COORDINATES ... CH3HGCH3

N	X	Y	Z
1	1.02658	0.00000	0.00000
2	-0.51329	0.88904	0.00000
3	-0.51329	-0.88904	0.00000
4	0.00000	0.00000	0.36639
5	0.00000	0.00000	2.46039
6	0.00000	0.00000	4.55439
7	-1.02658	0.00000	4.92078
8	0.51329	0.88904	4.92078
9	0.51329	-0.88904	4.92078

THE S_TENSOR ...CH3HGCH3

(SXX)	S(ZZ)	S(XZ)	S(XY)	S(YZ)
-0.10748	0.21496	0.00000	0.00000	0.00000

THE D_VALUES ...CH3HGCH3

N1	N2	D(EQUIL)	HARM.COR.	= TOTAL	PERCENT
1 H	2 H	2296.47	-90.83	2205.64	-4.12
1 H	4 C13	1656.85	-137.70	1519.15	-9.06
1 H	5 HG	-189.10	2.77	-186.33	-1.49
1 H	6 H	-235.33	-0.61	-235.94	0.26
1 H	7 H	-132.45	0.00	-132.44	-0.00
1 H	8 H	-190.56	-1.10	-191.67	0.58

2.11 References

1 M. Mehring, "High Resolution Nmr Spectroscopy in Solids", Nmr Basic Principles and Progress Vol 11, ed. P. Diehl, E. Fluck and R.K.R. Kosfeld.

2 A. Pines, M.G. Gibby and J.S. Waugh, J. Chem. Phys., 59, 569(1973).

3 E.R. Andrew, Prog. Nmr Specty. Vol 8, 1(1971).

4 A. Saupe and G. Englert, Phys. Rev. Lett., 11, 462(1963).

5 C.L. Khetrapal and A.C. Kunwar, Advances in Magnetic Resonance Vol 9, 301(1977) references 2-22.

6 S. Castellano and A.A. Bother-By, J. Chem. Phys., 41, 3863(1964).

7 C.M. Woodman, Mol. Phys., 13, 365(1967).

8 M. Barfield. Chem. Phys. Letts, 4, 518, (1970); ibid 5, 365, (1970)

9 G.J. den Otter and C. MacLean, Chem. Phys. Letts, 19, 571(1973).

10 A. Saupe, Z Naturforsch, A19, 161(1964).

11 L.C. Snyder, J. Chem. Phys., 43, 4041(1965).

12 L.C. Snyder and S. Meiboom, J. Chem. Phys., 44, 4057(1966).

13 P. Diehl, M. Reinhold, A.S. Tracey and E. Wullschleger, Mol. Phys., 30, 1781(1975)

14 E.E. Burnell, J.R. Council and S.E. Ulrich, Chem. Phys. Letts., 31, 395(1975).

15 S. Meiboom and L.C. Snyder. Acct Chem. Res., 4, 81(1971).

16 P. Diehl, S. Sýkora and E. Wullschleger, Mol. Phys., 29, 305(1975).

17 G. Englert, P. Diehl and W. Niederberger, Z. Naturforsch, A26, 1829(1971).

18 P. Diehl and W. Niederberger. J. Mag. Res., 9, 495(1973).

19 J. Bulthuis, Nmr in Liquid Crystalline Solvents, Portland Oreg. 1974.

20 L.C. Snyder and S. Meiboom J. Chem. Phys., 47, 148(1967).

21 A. Langseth and B.P. Stoicheff, Can. J. Phys., 34, 350(1956).

22 K. Tamagawa and T. Iijima, quoted as private communication in ref 21.

23 P. Diehl and W. Niederberger, J. Mag. Res., 9, 495(1973).

24 N. J. Lucas, Mol. Phys., 22, 147(1971).

25 N. J. Lucas, Mol. Phys., 22, 233(1971).

26 N. J. Lucas, Mol. Phys., 23, 825(1972).

27 A.D. Buckingham, E.E. Burnell and C.A. deLange, J. Amer. Chem. Soc., 90, 2972(1968).

28 G.J. Otter and C. MacLean, Chem. Phys., 3, 119(1974).

29 J. Bulthuis and C. MacLean, Chem. Phys. Letts., 21, 611(1973).

30 H. Nakatsurji, I. Morishmima, H. Kota and T. Yonezawa, Bull. Chem. Soc. Japan, 44, 2010(1971).

31 J. Gerritsen and C. MacLean, Spectrchimica Acta, 27A, 1495(1971).

32 G.J. den Otter, J. Gerritsen and C. MacLean, J. Mol. Struct, 16, 379,(1973).

33 G.J. den Otter, W. Heijser, and C. MacLean, J. Mag. Res., 13 11(1974).

34 J. Gerritsen, G. Koopmans, H.S. Rollema and C. MacLean, J. Mag. Res., 8, 20(1972).

35 M. Barfield, Chem. Phys. Letts., 4, 518(1970); ibid 5, 316(1970).

36 J. Jokisaari and J. Kuonanoja, J. Mol. Struct., 68, 173(1980).

37 J. Jokisaari and J. Kuonanoja, Org. Mag. Res., 3, 5(1980).

38 J.D. Kennedy and W. McFarlane, J. Chem. Soc. Farad. Trans. 2, 72, 1653(1976).

39 R. Ditchfield and L.C. Snyder, J. Chem. Phys., 56, 5823(1972).

40 J.M. Briggs, E.J. Rahkmaa and E.W. Randall, J. Mag. Res., 17, 55(1975).

41 R. Alder and A. Lowenstein, J. Amer. Chem. Soc., 96, 5336(1974).

42 N. Zumbulyadis and B.P. Dailey, Mol. Phys., 27, 633(1974).

43 J. Dalton, J.D. Kennedy, W. McFarlane and J.R. Wedge, Mol. Phys., 34, 215(1977).

44 Chapter 3.

45 G.J. den Otter and C. MacLean, J. Mag. Res., 20, 11,(1975).

46 P. Diehl, S. Sýkora and E. Wullschleger, Mol. Phys., 29, 305(1975).

47 C. Schumann, H. Dreeskamp and K. Hildenbrand, J. Mag. Res., 18, 97(1975).

48 J. Degelaen, P. Diehl and W. Niederberger, Org. Mag. Res., 4, 721(1972).

49 N. Zumbulyadis and B.P. Dailey, Mol. Phys., 26, 777(1973).

50 A.J. Montana, N. Zumbulyadis and B.P. Dailey, J. Chem. Phys., 66, 1850(1977).

51 P.K. Bhattacharya and B.P. Dailey, Mol. Phys., 28, 209(1974); J. Bulthuis and C.A. deLange, J. Mag. Res., 14, 13(1974).

52 Chapter 4.

53 E.A.C. Lucken. Nuclear Quadrupole Coupling Constant Academic Press N.Y. 1969.

54 W.J. Caspary, F. Millet, M. Reichbach and B.P. Dailey, J. Chem. Phys., 51, 623(1967).

55 C.H. Anderson, Ph.D thesis Harvard University, Camb., Mass., 1961.

56 F.S. Millet and B.P. Dailey, J. Chem. Phys., 56, 3249(1972).

Chapter 3

THE STUDY OF METHYLETHYNYLMERCURY AND METHYL-1-PROPYNYLMERCURY ORIENTED IN A LIQUID CRYSTAL SOLVENT

3.1 Introduction

Nmr studies of molecules oriented in liquid crystal solvents have been extensively used to determine molecular geometries and anisotropic parameters which average out to zero in mobile liquids. The anisotropic parameters which have been measured by this technique include shieldings, and indirect and quadrupolar coupling constants. In this work, some of these parameters in methylethynylmercury ($CH_3HgC{\equiv}CH$) and methyl-1-propynylmercury ($CH_3HgC{\equiv}CCH_3$) oriented in the solvent Merck Phase IV were determined. By replacing the acetylenic proton in methylethynylmercury with a deuteron, it was possible to calculate the deuterium quadrupole coupling constant.

Numerous organo-mercuric compounds have been studied by isotropic nmr, whereas for the nmr of oriented molecules the list includes dimethylmercury [1-6], methyl-trifluoromethylmercury [7], methylmercuric nitrate [8] and the methylmercuric halides [9-10]. These molecules have a linear C-Hg-X (X = carbon, nitrogen, halogen) skeleton and C_3 symmetry. It is the symmetry of these molecules that makes them attractive to study by nmr, as molecules with 3-fold symmetry require only one independent orientation parameter to be calculated. The geometries determined for these mercuric molecules by oriented nmr showed that anisotropic contributions to the indirect J(HH) and J(HgH) couplings can be assumed to be zero[1-10]. The precision to which geometrical

parameters can be determined using the nmr of oriented molecules depends also upon including vibrational corrections in the calculation. Methylethynylmercury and methyl-1-propynylmercury are a good choice in this respect, as their normal coordinate analyses have been published [11,12]. Hence, the following factors help to determine quite accurately the equilibrium geometry of both molecules. These factors are:-

i) Only one independent orientation parameter is required to be calculated.

ii) The experimental anisotropic HH and HgH couplings are purely dipolar.

iii) The experimental dipolar couplings can be corrected for vibrations.

Another factor that makes linear organo-mercury compounds interesting is that the mercury atom in such compounds has a large shielding anisotropy. In dimethylmercury the shielding anisotropy was measured to be +7500 ppm [1], and in methyl mercuric halides it was about +5500 ppm [10]. Such a large anisotropy therefore can be measured with relatively fair precision. As the molecules studied here have 3-fold symmetry then the components of the shielding parallel and perpendicular to the linear skeleton can be determined using a single orientation. Also by knowing the sign of the shielding anisotropy, the sign of the orientation parameter can be derived, and this can assist in assigning the signs of all the coupling constants present.

The analysis of the nmr spectrum of suitable molecules oriented in liquid crystals has been shown to be a useful method for the measurement of small quadrupolar coupling constants [13-18]. The quadrupolar coupling constants measured by this

technique include those in molecules containing the deuteron and nitrogen-14. The magnitude of the constant can then be used to determine the type of hybrid orbital involved in the bond to the quadrupolar nucleus. Thus the measurement of the deuterium quadrupolar coupling constant in methylethynylmercury-d_1 will give a qualitative picture of the electronic environment of the bond to deuterium.

3.2 Experimental

Methylethynylmercury and methyl-1-propynylmercury were provided by Dr. B. Wrackmeyer, and Phase IV (Merck) was obtained commercially. All three compounds were used without further purification.

Oriented samples were prepared in 5mm nmr tubes by dissolving about 20-50mg of compound in 0.5g of Merck Phase IV. The temperature of the solution was raised above the nematic/isotropic transition temperature of the liquid crystal solvent, and after thoroughly mixing the sample, the solution was allowed to cool. The actual concentration of the samples was not determined. Both compounds were also studied in deuterated benzene.

All ^{1}H, ^{2}D and ^{199}Hg nmr experiments were carried out on a Jeol FX90Q multi-nuclear spectrometer operating at 89.56 MHz, 13.7 MHz and 15.96 MHz respectively. The spectrometer was equipped for variable temperature operation. The ^{1}H and ^{199}Hg spectra of molecules dissolved in Phase IV were recorded with external D_2O lock and the ^{2}D spectrum was obtained using an external locking signal from Lithium-7. Anisotropic spectra were obtained with the sample tube not spinning and at room temperature

(+22°C), whereas isotropic spectra of molecules dissolved in Phase IV were obtained with the sample tube spinning and at +65°C. In the mercury shielding anisotropy experiments, spectra were recorded at a series of temperatures above the nematic/isotropic transition temperature of the solution. The isotropic spectrum for molecules dissolved in deuterated benzene was recorded at room temperature. All spectra were obtained without proton decoupling.

The three spectral intervals of the proton spectrum of oriented methylethynylmercury covering the two outer and the central regions were recorded separately. Each region was recorded from 2000 scans with a frequency range of 2 KHz and a pulse width of 25μs. This number of scans was adequate to observe ^{199}Hg satellites. The FIDs were transformed with an artificial line broadening function so as to give an average line width of 5 Hz. The proton spectrum of oriented methyl-1-propynylmercury in Phase IV was recorded with a spectral width of 30 KHz and using the same pulse width as before. In order to observe ^{199}Hg satellites about 2000 scans were required. The FIDs were transformed with a line broadening function to give an average line width of 5 Hz in the central region of the spectrum, and 25 Hz in the outer wings. The isotropic proton spectrum of both compounds was measured using the same pulse width as before and a spectral width of 1 KHz. Also fewer scans were required to observe the ^{199}Hg satellites.

The ^{199}Hg spectrum for both compounds was recorded by accumulating 1000 scans with a spectral width of 4 KHz. The pulse width used was 20.4μs. The FIDs were transformed with an artificial line broadening function to give an average line width

of 20 Hz.

Dimethylmercury was used as a reference for ^{199}Hg chemical shifts. For neat dimethylmercury Ξ (^{199}Hg) is equal to 17910780 Hz [10], where Ξ (X) is the resonating frequency of nucleus X at that field which will give a TMS proton resonance at exactly 100 MHz. The usefulness of Ξ is that we no longer need internal references, as the frequencies can be locked to the spectrometer master oscillator. If R is the reference compound and ν(X) is the observed frequency of X then Ξ (X) can be determined by the following equation;

$$\Xi (X) = \nu(X) . \Xi (R)/\nu(R) \qquad 3.1$$

where ν(R) is the resonance frequency of R observed at the same field as ν(X). Then δ values for a given resonance X may be calculated using

$$\delta(X) = \Xi (X) - \Xi (R)/ \Xi (R) \qquad 3.2$$

The ^{2}D spectrum of methylethynylmercury-d_1 oriented in a liquid crystal would consist of a doublet with a splitting of the order of 100 KHz. Thus the peaks at low and high frequencies in the deuterium spectrum had to be recorded separately using the appropriate carrier frequency. Each ^{2}D spectrum was recorded with spectral width of 50 KHz and pulse width of 24μs. The summation of 500 scans was transformed with a line broadening function to give a line width of 150 Hz.

Anisotropic spectra were analysed using LAOCOON LC[19]. The output of LAOCOON LC for a non-iterative computation from a given set of chemical shifts and coupling constants is an ordered table of frequencies and intensities of the lines expected in the nmr

spectrum. The ordered table was transferred to a plotting routine, written by ourselves, where a Lorentzian lineshape is applied to the lines. Where the satellite region of the spectrum was required to be plotted, the intensities of the lines were reduced to 16 percent of the total intensity of the proton spectrum so as to incorporate the natural abundance of the ^{199}Hg.

The harmonic vibrational corrections to the dipolar coupling constants were calculated with the aid of the computer program VIBRA[20] and the force field obtained from Imai[11,12].

3.3 Results

3.3.1 Indirect Spin-Spin and Anisotropic Couplings

Methylethynylmercury

The proton spectrum with natural abundance mercury satellites (^{199}Hg has natural abundance of 16 percent) of oriented methylethynylmercury in Phase IV is shown in Fig 3.1(a). This spectrum was analysed as an AB_3 (A= acetylenic proton and B= methyl proton) spin system with C_3 symmetry using formulae for the line positions given by Englert et al[6], and the computer program LAOCOON LC[19]. The program requires as its input, chemical shift positions for each nucleus, and the corresponding isotropic and anisotropic coupling constants. To use the formulae for the line positions to calculate all the input for the program was found not to be simple. However, as a first approximation the indirect spin-spin couplings (J) between protons were measured from the proton spectrum using deuterated benzene as the solvent.

Fig 3.1 Experimental (below) and Computed (overleaf) ^1H nmr spectra including ^{199}Hg satellites of Methylethynylmercury partially oriented in Phase IV

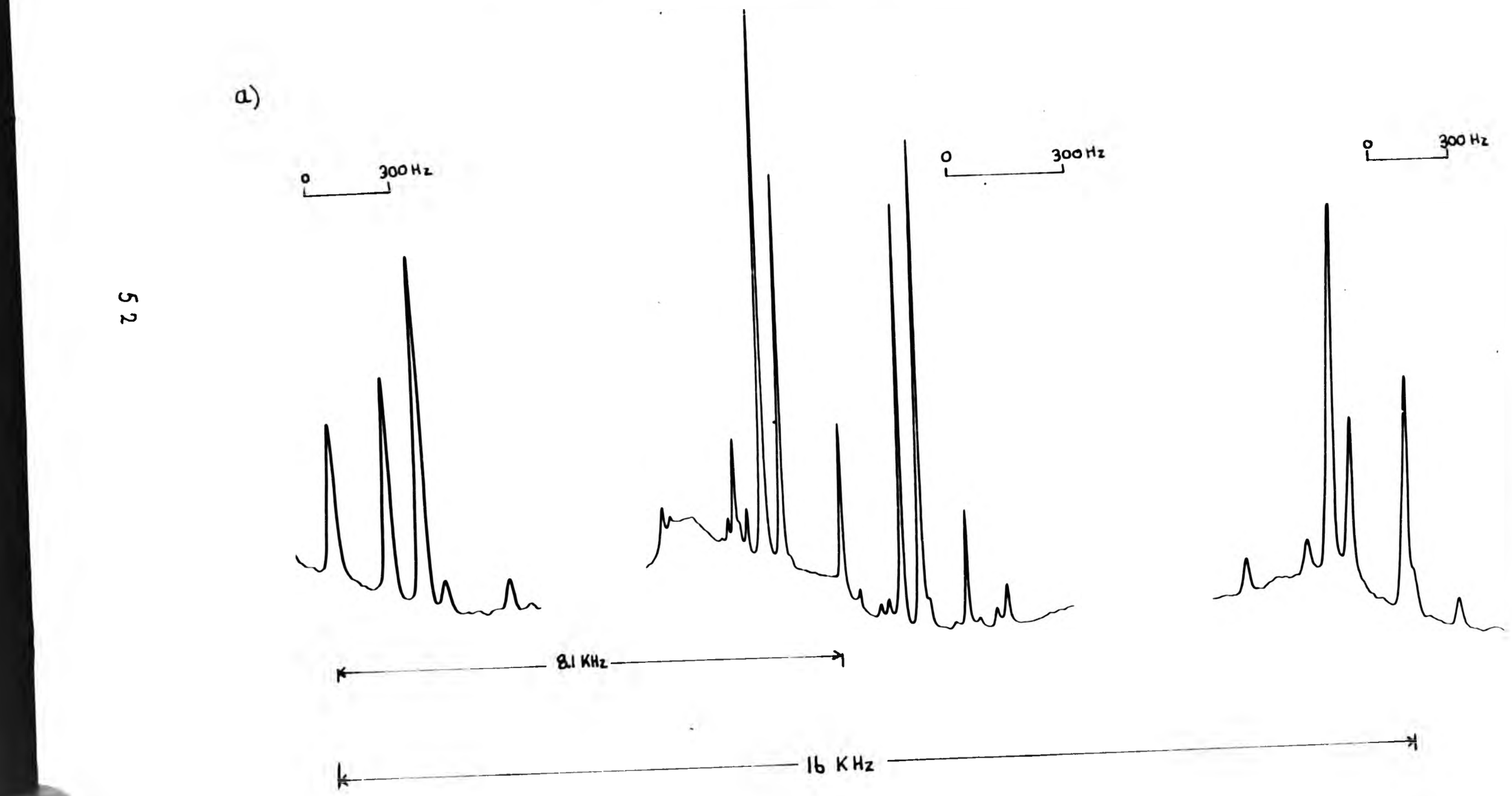

Fig 3.1(b)

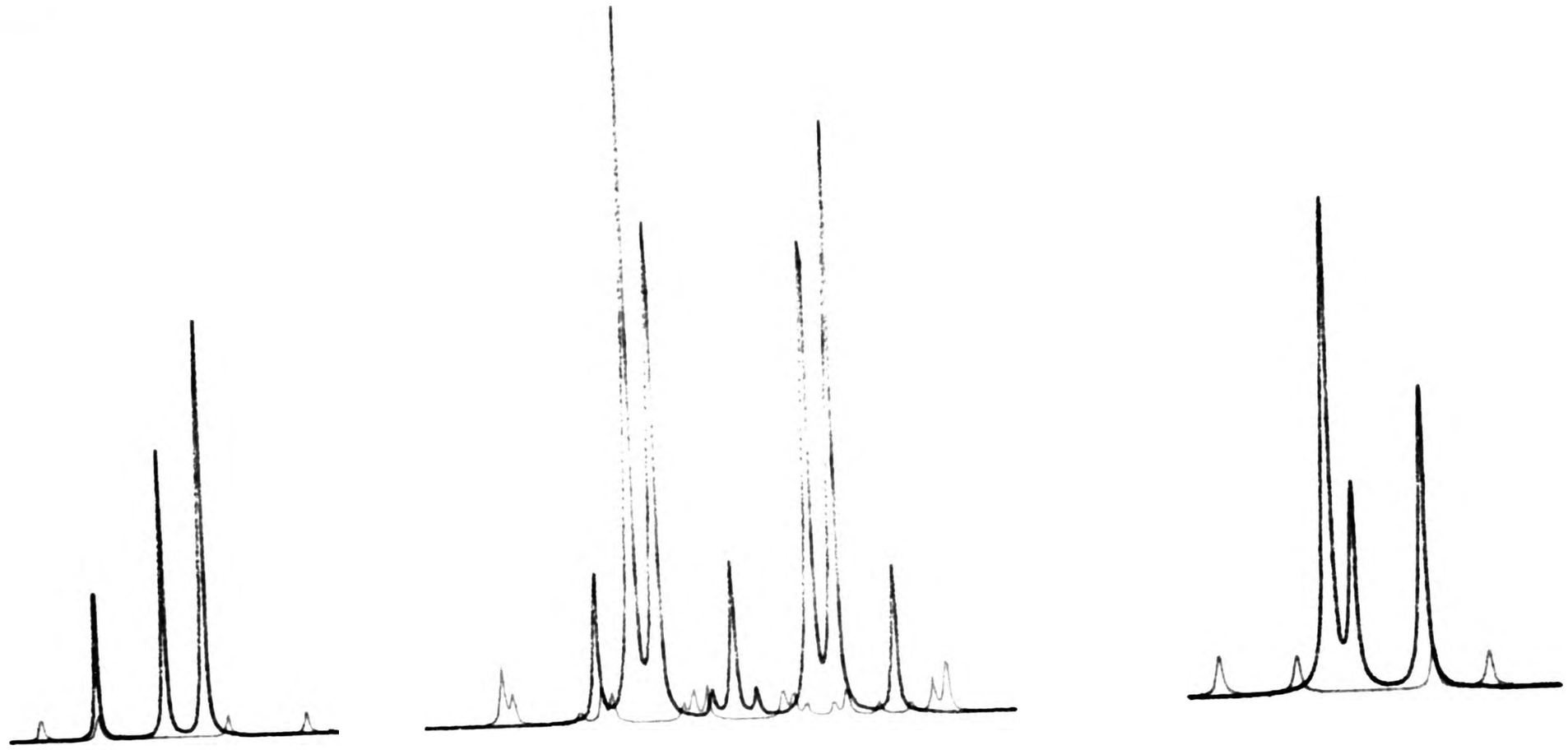

The long range proton-proton J coupling was found to be too small to measure and was taken as zero. The chemical shift positions for the two types of proton were approximated from the isotropic spectrum of methylethynylmercury in Phase IV.

An estimate for the dipolar $^2D(HH)$ coupling was derived from the formulae of the line positions. It was found that the two outermost lines in the proton spectrum of the oriented molecule were separated by approximately $6.^2D(HH)$. From this estimate of $^2D(HH)$ the value for the other dipolar coupling, $^5D(HH)$ was determined. For an AB_3 spin system with C_3 symmetry, and with the z axis taken to be parallel with the C_3 axis, then:

$$S_{AB} = (3\cos^2\gamma - 1)S_{zz}/2 \qquad 3.3$$

$$S_{BB} = S_{zz}/2 \qquad 3.4$$

$$S_{zz} = -S_{xx}/2 = -S_{yy}/2 \qquad 3.5$$

where γ is the angle between the z axis and the AB bond and S is the orientation parameter. Then:

$$D(BB) = -K(BB) \times S_{BB}/r_{BB}^3 \qquad 3.6$$

and

$$D(AB) = -K(AB) \times S_{AB}/r_{AB}^3 \qquad 3.7$$

where K(ij) is the nuclear constant defined in Section 2.4 and r is the internuclear distance.

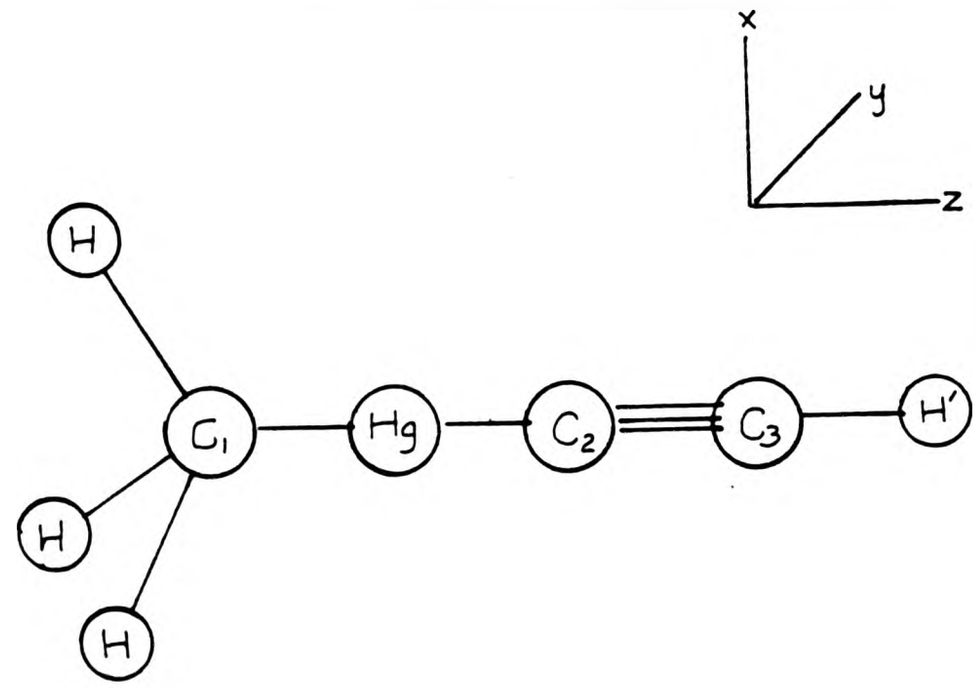

Fig 3.2

Numbering of atoms in Methylethynylmercury

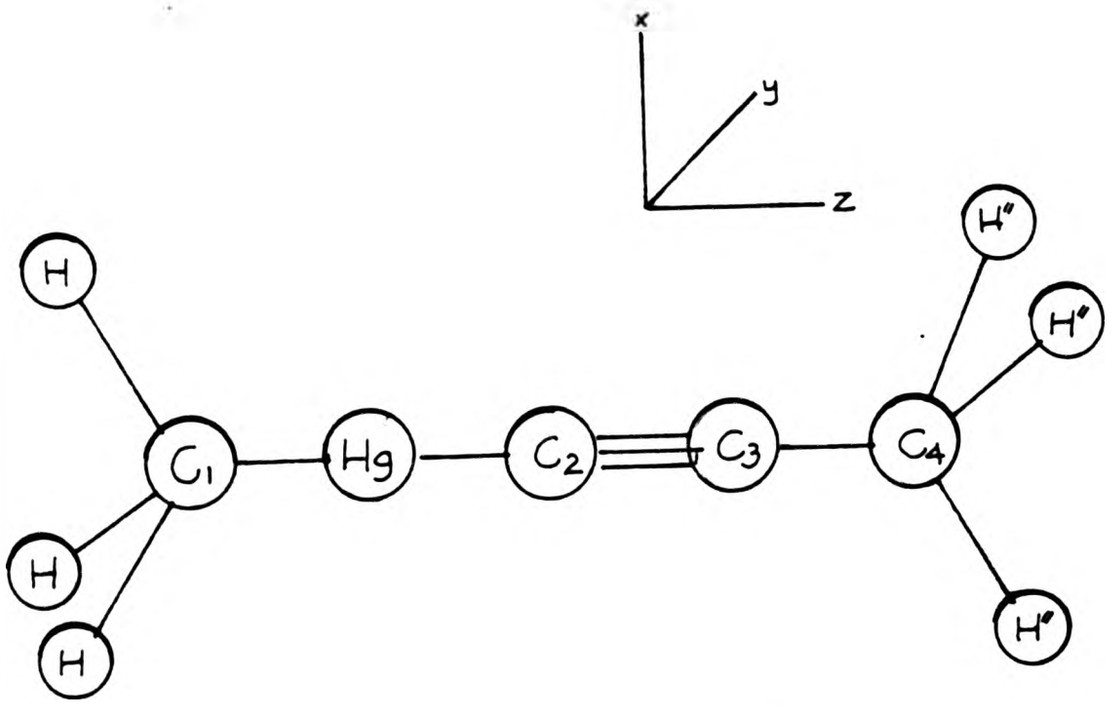

Fig 3.3

Numbering of atoms in Methyl-1-propynylmercury

Table 3.1 Preliminary Geometrical Parameters for Methyl-1-propynylmercury(II) and Methylethynylmercury(II)[a]

$r(C_2C_3)$	= 1.21A	$r(HgC_1)$	= 2.08A
$r(HgC_2)$	= 2.05A	$r(C_1H)$ and $r(C_4H")$	= 1.097A
$r(C_3C_4)$	= 1.46A	$r(C_3H')$	= 1.06A
$\angle HC_1H$	= 108.85°	$\angle H"C_4H"$	= 108.5°

a) Numbering refers to Figs 3.2 and 3.3.

Using the geometry as listed in Table 3.1 and A=H' and B=H (where H' and H denote the acetylenic proton and the methyl proton respectively) the magnitude of $^5D(HH')$ was estimated. Using the estimated values for the nmr parameters from the proton spectrum of oriented methylethynylmercury, the computed spectrum was calculated using LAOCOON LC. Once the computed spectrum had a recognizable resemblance to the experimental one, then iteration in LAOCOON LC was used to obtain accurate values for the nmr parameters of the anisotropic spectrum. The parameters that gave the best fit to the experimental spectrum are summarized in Table 3.2 and the computed proton spectrum of methylethynylmercury using these parameters is shown in Fig 3.1(b).

The next step was to analyse the mercury satellite region of the anisotropic spectrum. The indirect spin-spin couplings J(HgH) were measured from the proton spectrum with natural abundance Hg-199 satellites of methylethynylmercury in deuterated benzene. The $^2J(HgH)$ and $^3J(HgH)$ couplings were found to be -147.7 Hz and +68.6 Hz respectively. The sign of $^2J(HgH)$ was taken to be negative from double resonance experiments carried out on dimethylmercury by Mclauchlan et al[21].

Table 3.2

Selected Nmr Data of Methylethynylmercury in Phase IV

Nmr Parameter	Sample		
	A[a]	B[a]	C[b]
$\delta(H)-\delta(H')$/ppm [c]	0.53	0.68	0.51
$^{2}D(^{1}H-^{1}H)$/Hz	2664.1 ±2	2761.4 ±2	2604.1 ±1
$^{5}D(^{1}H-^{1}H)$/Hz	-98.9 ±4	-102.0 ±4	-96.7 ±2
$^{2}D(^{1}H-^{199}Hg)$/Hz		-245.4 ±2	-231.4 ±2
$^{3}D(^{1}H-^{199}Hg)$/Hz		-69.6 ±2	-66.0 ±2
$^{5}J(^{1}H-^{1}H)$/Hz	0.0	0.0	0.0
$^{2}J(^{1}H-^{199}Hg)$/Hz [d]	-146.0 ±1	-146.0 ±1	-146.0 ±1
$^{3}J(^{1}H-^{199}Hg)$/Hz [d]	68.6 ±1	68.6 ±1	68.6 ±1
$^{5}D(HH)/^{2}D(HH)$	-0.03712	-0.03692	-0.03713
$^{2}D(HHg)/^{2}D(HH)$		-0.08887	-0.08886
$^{3}D(HHg)/^{2}D(HH)$		-0.02521	-0.02535
$^{3}D(HHg)/^{2}D(HHg)$		0.28362	0.28522

a) Spectrum obtained at proton frequency of 60 MHz.

b) Spectrum obtained at proton frequency of 90 MHz.

c) H' denotes acetylenic proton

d) solvent used deuterated benzene and benzene mixture

The sign of $^3J(HgH)$ was determined from the analysis of the satellite region of the anisotropic proton spectrum. $^2D(HgH)$ was estimated from an assumed geometry and using Equations 3.3 and 3.7 where now B denotes Hg. The anisotropic coupling for $^3D(HHg)$ was approximated from the following equation;

$$^3D(H'Hg) = K(HHg) \times S_{zz}/r^3_{H'Hg} \qquad 3.8$$

As before, using the estimated values for the input parameters of LAOCOON LC the mercury satellite spectrum of the oriented molecule was calculated. Once this spectrum had a recognizable resemblance to the experimental spectrum, then the option of iteration available in LAOCOON LC was used. This made it possible to obtain accurate values for the nmr parameters of the satellite region in the anisotropic spectrum. The parameters that best fit the spectrum are reported in Table 3.2. The computed satellite region and the computed proton spectrum with mercury satellites using the nmr parameters in Table 3.2 are shown in Fig 3.1(b).

Methyl-1-propynylmercury

The proton spectrum with natural abundance mercury satellites of partially anisotropic methyl-1-propynylmercury in Phase IV is depicted in Fig 3.4(a). The analysis of the oriented spectrum was carried out as an A_3B_3 spin system (where A,B= methyl protons at either end of the molecule) using formulae for the line positions given by Englert *et al*[6] and LAOCOON LC. As in the case of the analysis of the oriented methylethynylmercury, estimates of the input parameters for LAOCOON LC were required to be calculated.

Fig 3.4 Experimental (below) and Computed (overleaf) 90 MHz ^1H nmr spectra including ^{199}Hg satellites of Methyl-1-propynylmercury partially oriented in Phase IV

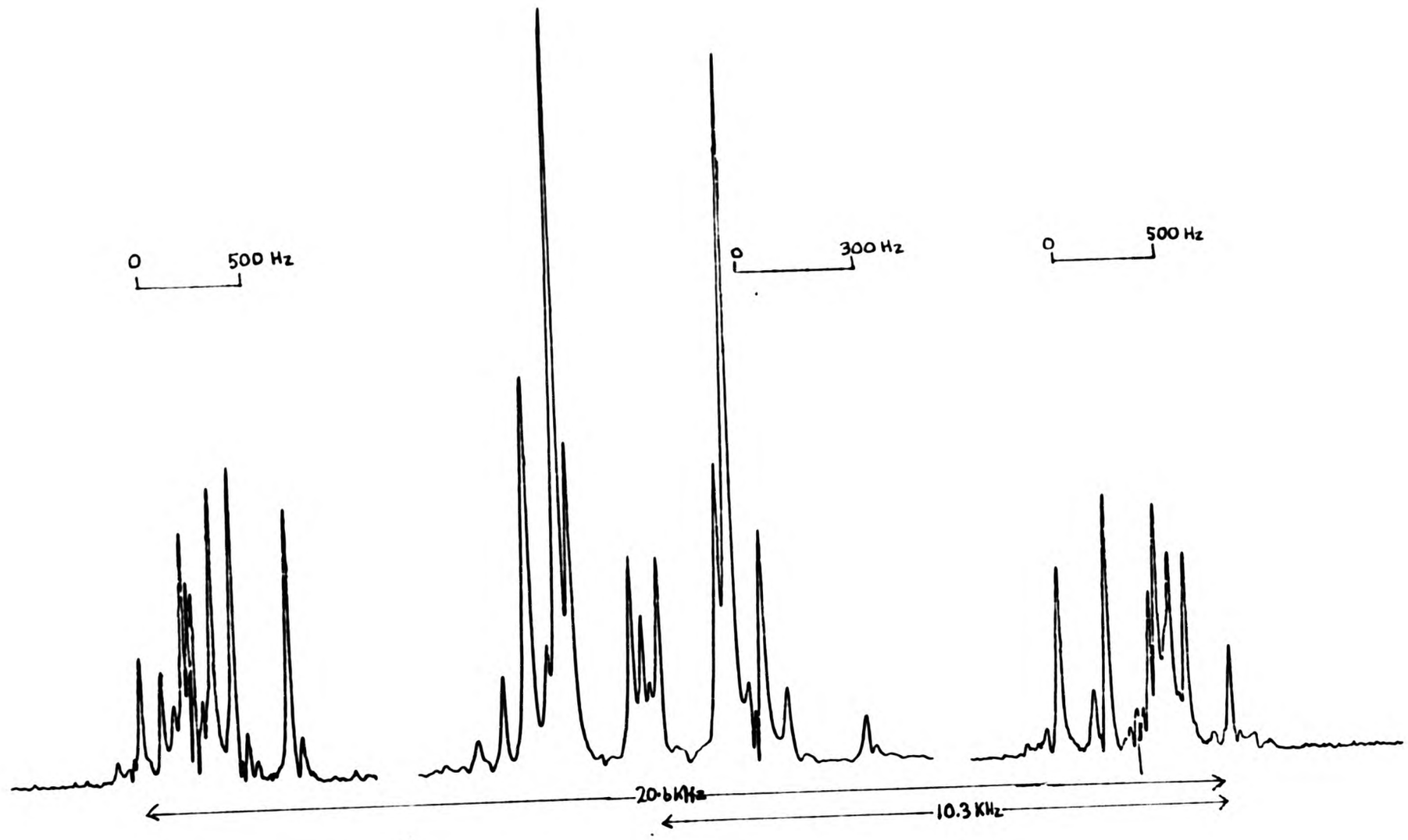

Fig 3.4 Experimental (below) and Computed (overleaf) 90 MHz ^1H nmr spectra including ^{199}Hg satellites of Methyl-1-propynylmercury partially oriented in Phase IV

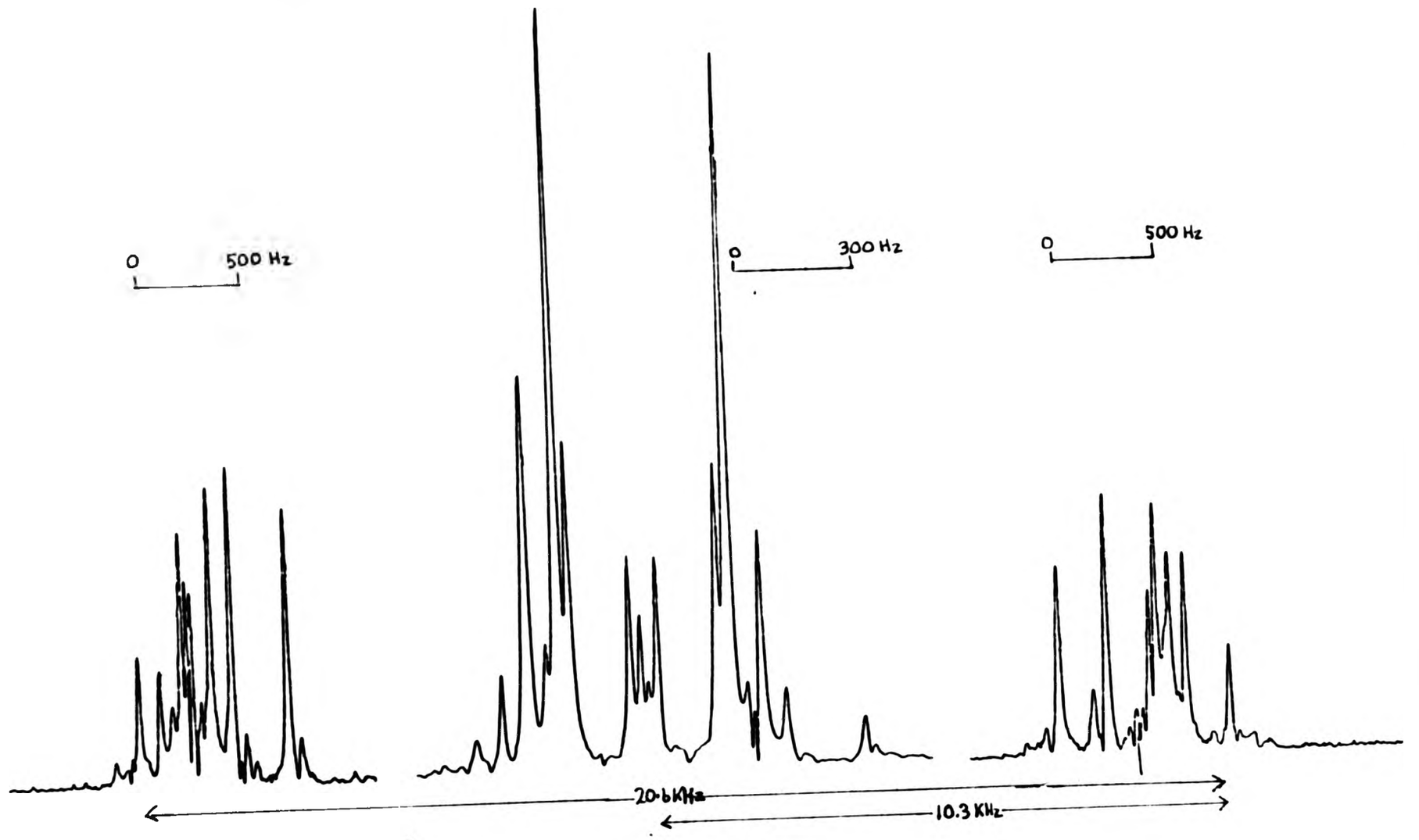

Fig 3.4(b)

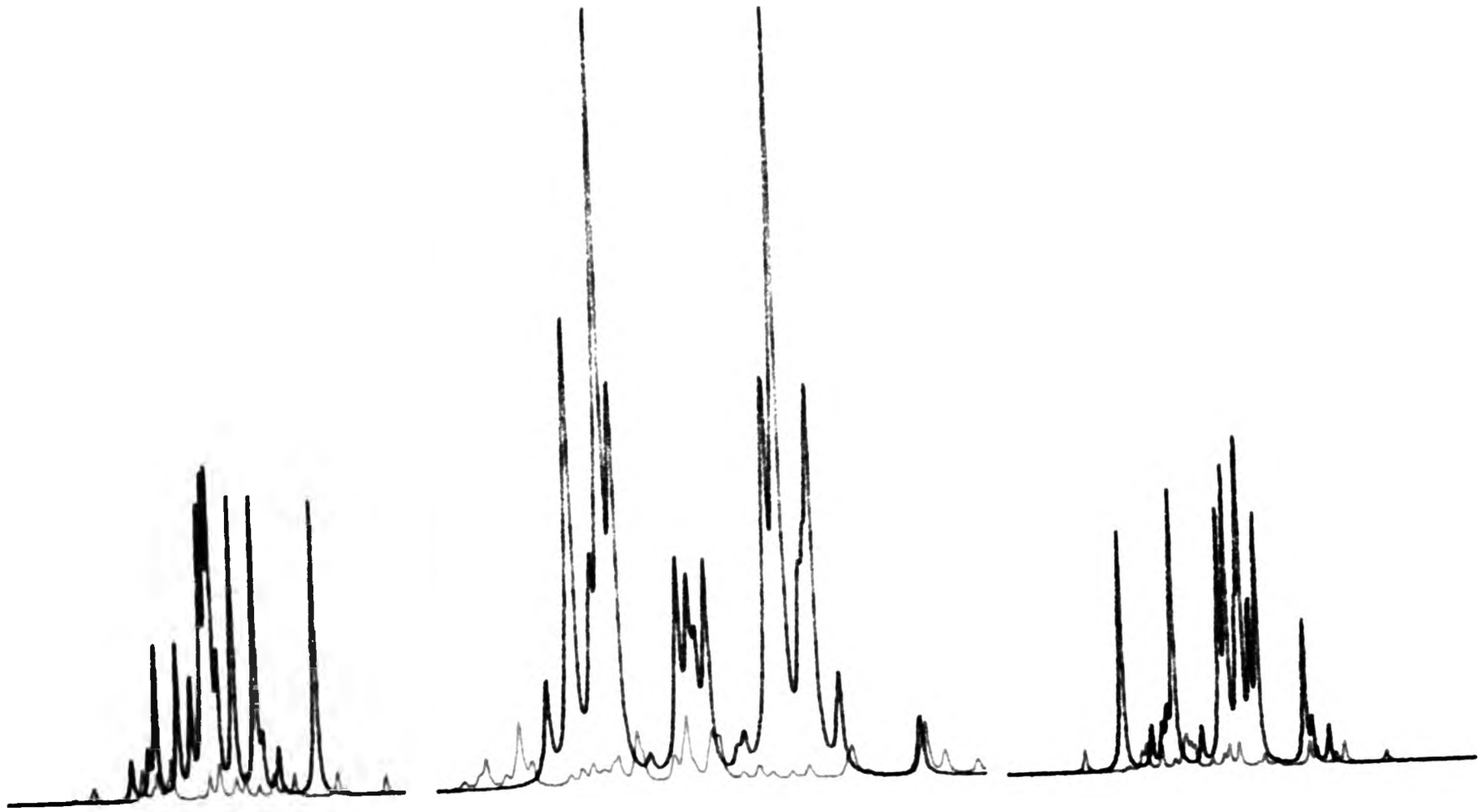

The proton-proton indirect spin-spin coupling was measured from the proton spectrum using deuterated benzene as the solvent, and was found to be zero. The chemical shift difference between the two types of protons was also estimated from the same spectrum. The proton spectrum (Fig 3.4a) is not symmetrical about the centre as might be expected, because the proton chemical shifts for the two methyls are different. At this stage it can also be assumed that the geometries for the two methyl are not identical, and this implies that the two geminal $^2D(HH)$ couplings will not be the same. To estimate these dipolar couplings it was found that one of the couplings could be roughly determined from the separation of the two wings in the proton spectrum. The separation of the wings is equal to approximately $3.^2D(HH)$. The next step was to determine D"(HH"), where D" is the dipolar coupling between protons of two methyl groups, H" denotes the proton belonging to the methyl attached to the acetylenic carbon, and H is the other methyl proton. The following equations were used:

$$^2D(HH) = -K(HH) \times S_{zz}/2r^3_{HH} \qquad 3.9$$

and

$$^6D"(HH") = -K(HH)\langle S/R^3\rangle \qquad 3.10$$

where R is the internuclear distance H-H", $S=(3\cos^2\Phi-1)$, Φ is the variable angle between the z axis (C_3 axis) and the internuclear vector R, and $\langle\rangle$ is the mean value. D" was determined from $^2D(HH)$ for the eclipsed and the staggered conformers and for free rotation of the methyls. It was found that the differences in values of D" from the three conformations were too small to permit any discrimination. The calculation was carried out using the computer program COM1PM whose listing is shown in appendix 3.1. The magnitude of D(H"H") was taken to be

within 40-50 Hz of the value of D(HH); hence trial spectra with different values of D(H"H") were calculated using LAOCOON LC. Once the trial spectrum gave a recognizable resemblance to the experimental one, then iteration was used to obtain accurate values for the nmr parameters. The parameters that best fit the experimental spectrum are summarized in Table 3.3.

Once the anisotropic proton spectrum of methyl-1-propynyl-mercury was analysed, the next step was to analyse the satellite region. The satellite region of the anisotropic spectrum of the oriented molecule was not simple, as most of the lines were hidden under main proton signals. Only six lines could be separated from the main spectrum and their positions were found to be sensitive to $^{2}D(HgH)$. The indirect spin-spin J(HgH) couplings were measured from the proton spectrum with natural abundance ^{199}Hg satellites using deuterated benzene as the solvent. $^{2}D(HgH)$ was estimated using equation 3.7, and then was accurately determined using the iteration option in LAOCOON LC. The $^{4}D(HgH")$ dipolar coupling was determined using Equation 3.7 and the geometry obtained from the long range proton proton dipolar coupling. The best fit parameters for the satellite region are summarized in Table 3.3. The computed proton spectrum with natural abundance ^{199}Hg satellites of methyl-1-propynylmercury partially oriented in Phase IV are shown in Fig 3.4(b) using parameters in Table 3.3.

Table 3.3

Selected Nmr Data of Methyl-1-propynylmercury in Phase IV

Nmr Parameter	Sample		
	A[a]	B[b]	C[b]
$\delta(H)-\delta(H")$/ppm [c]	1.8	1.88	1.88
$^{2}D(^{1}H-^{1}H)$/Hz	2942 ±2	3327 ±2	3276 ±2
$^{2}D(^{1}H"-^{1}H")$/Hz	2923 ±2	3303 ±2	3257 ±2
$^{6}D(^{1}H-^{1}H")$/Hz	-77 ±4	-87 ±4	-86 ±4
$^{2}D(^{1}H-^{199}Hg)$/Hz	-260 ±4	-294 ±4	-290 ±4
$^{4}D(^{1}H"-^{199}Hg)$/Hz [d]	42 ±4	48 ±4	47 ±4
$^{6}J(^{1}H"-^{1}H")$/Hz	0.0	0.0	0.0
$^{2}J(^{1}H-^{199}Hg)$/Hz [e]	-144 ±1	-144 ±1	-144 ±1
$^{4}J(^{1}H-^{199}Hg)$/Hz [e]	-19 ±1	-19 ±1	-19 ±1
$^{2}D(H"H")/^{2}D(HH)$	0.9939	0.9928	0.9943
$^{6}D(HH")/^{2}D(HH)$	-0.0265	-0.0262	-0.0263
$^{6}D(HH")/^{2}D(H"H")$	-0.0266	-0.0264	-0.0265
$^{2}D(HHg)/^{2}D(HH)$	-0.0886	-0.0886	-0.0886
$^{4}D(H"Hg)/^{2}D(HHg)$	-0.1630	-0.1632	-0.1633

a) Spectrum obtained at proton frequency of 90 MHz.

b) Spectrum obtained at proton frequency of 60 MHz.

c) H denotes proton belonging to methyl attached directly to mercury and H" denotes proton belonging to methyl attached to triple bonded carbon.

d)Calculated from geometry obtained from $^{6}D(HH")$ and $^{2}D(HHg)$.

e) Solvent used deuterated benzene/benzene mixture

3.3.2 Force Field for Methylethynylmercury and Methyl-1-propynylmercury

Once the experimental anisotropic couplings had been determined, the next stage was to evaluate the equilibrium structure for both compounds. To do this, the harmonic vibrational corrections to the experimental dipolar couplings were calculated using the computer program VIBRA, partly written by Diehl[20]. The program requires the coordinates to define the geometry and the unsymmetrized force constants. Symmetrical force constants and geometries for both compounds were obtained from Imai[11,12]. The symmetrical force constants had to be unsymmetrized; i.e the symmetry force constants given as elements of an F matrix had to be decomposed into internal force constants. The symmetry coordinates, the symmetry force constants and the corresponding expressions for the internal coordinates are summarized in Table 3.4 for both molecules. From the relationship between the symmetry coordinates and their internal coordinates, the unsymmetrized force constants were calculated. For example, in Table 3.4 the symmetry coordinate F(1,1) corresponds to the internal coordinate R4, which from Fig 3.5 describes the stretch for the bond between the acetylenic proton and the adjacent carbon atom. In this case the force constant for the symmetry coordinate can be transferred directly into the unsymmetrized force constant. However F(2,2) in Table 3.4 corresponds to a symmetry coordinate which is the sum of two internal coordinates, f(r) and f(rr), where r denotes CH stretch in the methyl and rr corresponds to the interaction between two f(r) stretches. To calculate the individual contribution for the two internal coordinates it is necessary to solve simultaneously the symmetry coordinate

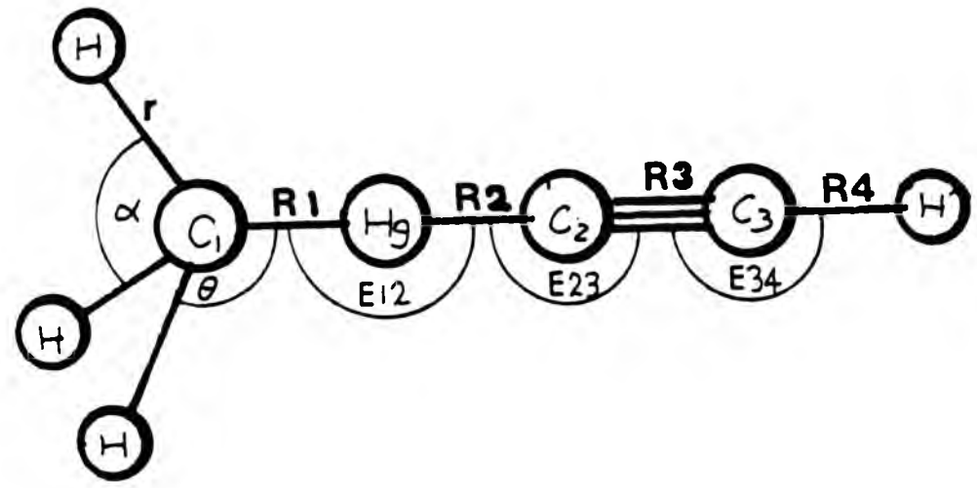

Fig 3.5

Internal Coordinates of Methylethynylmercury

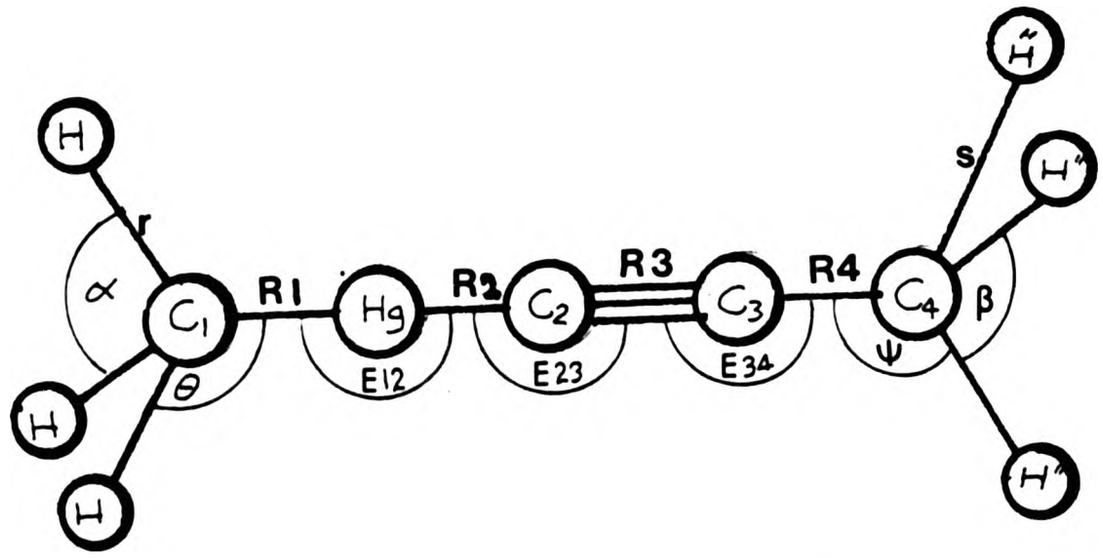

Fig 3.6

Internal Coordinates of Methyl-1-propynylmercury

Table 3.4

Force constants[a] of Methylethynylmercury and Methyl-1-propynylmercury in Symmetry coordinates, and the relationship between symmetry and internal coordinates.

Symmetry Coordinate	Internal Coordinate	Symmetry force Constant	
		M-1-pM[c]	MEM[d]
F(1,1)	f(s)+2f(ss)	4.890	
F(2,2)	f(r)+2f(rr)	4.630	4.551
F(3,3)	f(R3)	14.098	14.676
F(4,4)	f(β)+2f(ββ)	0.571	
F(5,5)	f(α)+2f(αα)	0.552	0.512
F(6,6)	f(R4)	5.752	5.752
F(7,7)	f(R1)	2.478	2.538
F(8,8)	f(R2)	2.992	2.832
F(9,9)	f(r)-f(rr)	4.721	4.739
F(10,10)	f(s)-f(ss)	4.648	
F(11,11)	f(β)-f(ββ)	0.546	
F(12,12)	f(α)-f(αα)	0.514	0.512
F(13,13)	f(ψ)-f(ψψ)	0.68	
F(14,14)	f(θ)-f(θθ)	0.428	0.435
F(15,15)	f(E3,4)	0.3017	0.232
F(16,16)	f(E2,3)	0.1274	0.239
F(17,17)	f(E1,2)	0.0535	0.301
F(2,5)	3f(rα)	-0.548	-0.61
F(3,6)	f(R3R4)		-0.197
F(4,6)	3f(R4β)	-0.189	
F(5,7)	3f(R1α)	-0.096	-0.067
F(7,8)	f(R1R2)	-0.471	-0.134
F(15,16)	f(E34 E 23)	0.124	0.084

a) The stretching force constants are given in mdyne/A, the deformation force constants in mdyne.A, and the stretching-deformation interaction constants in mdyne.

b) As represented in Figs 3.4 and 3.5

c) Methyl-1-propynylmercury

d) Methylethynylmercury

Table 3.5 The Force constants for Methyl-1-propynylmercury and Methylethynylmercury in Internal coordinate representation

Internal Coordinate	Force constant[a]	
	M-1-pM[c]	MEM[d]
f(r)	4.691	4.676
f(rr)	-0.03	-0.063
f(s)	4.729	
f(ss)	-0.08	
f(R1)	2.478	2.538
f(R2)	2.992	2.832
f(R3)	14.098	14.676
f(R4)	5.168	5.752
f(R1 R2)	-0.471	-0.134
f(R3 R4)		-0.197
f(α)	0.43	0.433
f(α α)	0.006	0.011
f(β)	0.4501	
f(β β)	0.007	
f(θ)	0.190	0.19
f(ψ)	0.420	
f(rα)	-0.1661	-0.185
f(R1α)	-0.0504	-0.035
f(R4β)	0.1893	
f(E34)	0.302	0.1809
f(E23)	0.1274	0.0964
f(E12)	0.0535	0.0706
f(E34 23)	0.124	0.047

a) Force constants in mdyne/A

b) As represented in Figs 3.5 and 3.6.

c) Methyl-1-propynylmercury

d) Methylethynylmercury

expressions given by F(2,2) and F(8,8). Likewise, all the symmetry coordinates were decomposed into internal coordinates, and they are summarized in Table 3.5 for both molecules. The requirement for using VIBRA is that all force constants are entered in mdyne/A. The symmetry force constants reported in references 11,12 were in mdyne/A for stretches, mdyne.A for bends, and mdyne for interactions between stretch and bend. To standardize the symmetry force constant for a bend involving

nuclei i,j,k, it is multiplied by $1/(r_{ij}.r_{jk})$ where r is the internuclear distance in A. For the symmetry force constant involving interaction between bend i,j,k and stretch ij, the multiplication factor is $1/(r_{ij}.r_{ik})^{1/2}$. Throughout the calculation the molecular geometry summarised in Table 3.1 has been used.

3.3.3 ^{199}Hg Shielding Anisotropy in Methylethynylmercury and Methyl-1-propynylmercury

The ^{199}Hg shielding anisotropies in methylethynylmercury and methyl-1-propynylmercury were determined and are reported in Table 3.6. The mercury shielding anisotropy ($\Delta\sigma(^{199}Hg)$) is given by the following expression;

$$\Delta\sigma(^{199}Hg) = 3\ (\sigma(nem) - \sigma(iso))/2S_{zz} \qquad 3.11$$

where $\sigma(nem)$ and $\sigma(iso)$ are the shieldings in the nematic and isotropic phases respectively. The shielding in the nematic phase was determined from the mercury chemical shift measured in the anisotropic mercury spectrum. $^2D(HH)$ was measured from the proton spectrum using the same concentration and at the same temperature. Once the experimental $^2D(HH)$ was determined, it was corrected for harmonic vibrations and then S_{zz} was calculated using Equation 3.6. The isotropic mercury shielding was also required to be measured at the same temperature. This was done by measuring mercury chemical shifts at various temperatures above the nematic/isotropic transition temperature of the solution and then plotting a graph of mercury chemical shift against temperature (see Figs 3.7 and 3.8). The isotropic shielding at the nematic temperature (the temperature at which the

spectrum of the oriented molecule was measured) was then obtained by extrapolation. In Table 3.6 the parameters used in the calculation of $\triangle\sigma(^{199}Hg)$ in methylethynylmercury and methyl-1-propynylmercury are reported.

Table 3.6 Isotropic Chemical Shift, Chemical Shift Differences, S_{zz} and ^{199}Hg Shielding Anisotropies of Methylethynylmercury and Methyl-1-propynylmercury

	Methylethynyl mercury	Methyl-1-propynyl-mercury
ν(iso)/Hz	16040593 ±50	16041160 ±50
$\delta^{199}Hg$/ppm[a]	-465.3 ±3	-429.9 ±3
ν(nem) - ν(iso)/Hz	-19007 ±50	-22408 ±50
σ(nem) - σ(iso)/ppm	+1189 ±3	+1402 ±3
S_{zz}	+0.2630 ±.002	+0.3134 ±.002
S_{zz} (v.c)	+0.2723 ±.002	+0.3447 ±.002
$\sigma_{\parallel} - \sigma_{\perp}$/ppm	+6780 ±20	+6711 ±20
$\sigma_{\parallel} - \sigma_{\perp}$/ppm (v.c)	+6550 ±20	+6101 ±20

v.c obtained from the coupling constant corrected for harmonic vibrations.

a) Chemical shift relative to mercury in dimethylmercury.

Fig 3.7 Plot of ^{199}Hg chemical shift against temperature for Methyl ethynylmercury in Phase IV

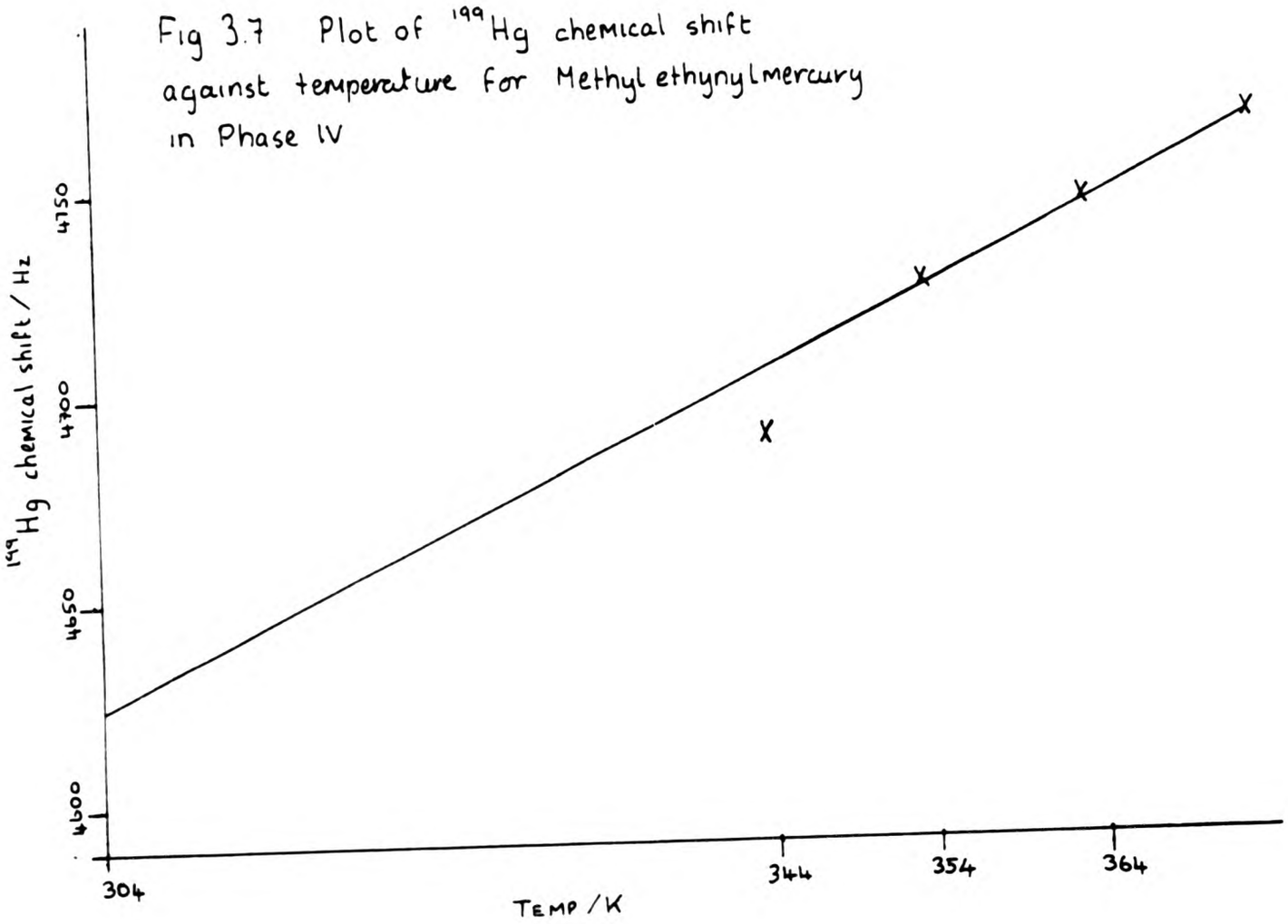

Fig 3.8 Plot of ^{199}Hg chemical shift against temperature for Methyl-1- propynylmercury in Phase IV

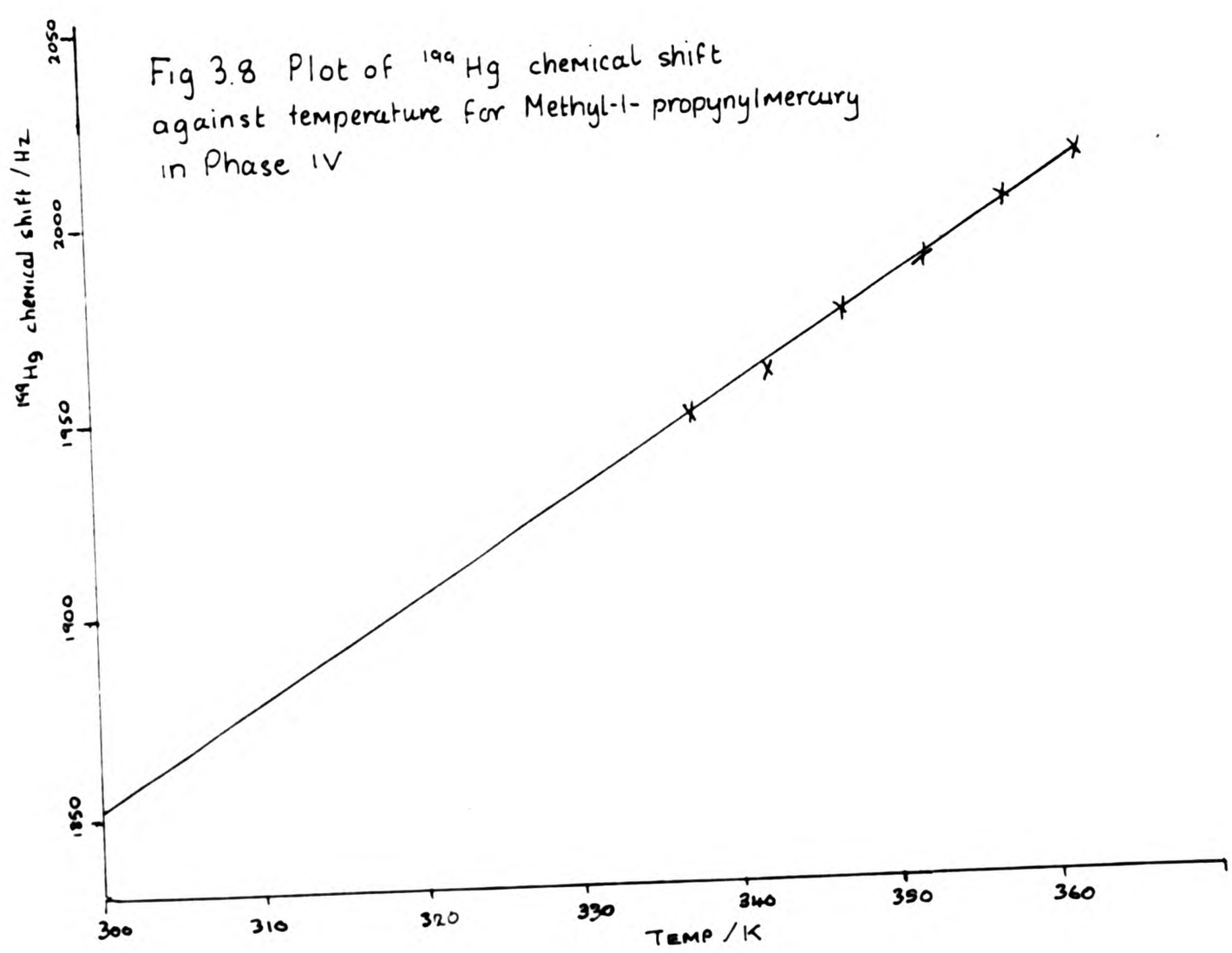

The calculation of $\Delta\sigma(^{199}Hg)$ in methylethynylmercury is shown here as an example.

The frequency of the nematic chemical shift of mercury in methylethynylmercury is

ν(nematic)= 5586(±50) +36000 +15980000 Hz

= 16021586 ±50 Hz

By extrapolation to 304K ν(isotropic) is obtained

ν(isotropic)=4593 (±50) + 56000 + 15980000

= 16040593 ± 50 Hz

Ξ ^{199}Hg (in methylethynylmercury) = 16040593 x 100/89.6

= 17902447 Hz

To calculate ^{199}Hg chemical shift relative to dimethyl mercury using the established convention and

$\Xi(^{199}Hg)$ in Me_2Hg =17910780 Hz

$\delta^{199}Hg$ (CH_3HgCCH) =(17902447-17910780)/17.910780 ppm

= -465.3 ppm

ν(nematic) - ν(isotropic) = 41586 - 60593 Hz

= -19007 ± 50 Hz

$\therefore$ δ(nem) - δ(iso) = -19007/15.98 ppm

Using the convention whereby chemical shifts and shieldings have opposite signs, then

σ (nem)- σ (iso) = +1189 ±3 ppm

for this particular experiment.

From the proton spectra we obtain the value of $^2D(HH)$= +2778.8(±1) Hz which corrected for vibration gives 2876.6 (±1) Hz

Using the internuclear distance between two methyl protons as 1.7845A and the equation for S_{zz};

$S_{zz} = 2 \times r(HH)^3 \times {}^2D(HH)/K(HH)$

$S_{zz} = 1.7845^3 \times 2876.6 / 120067 = 0.2723 \pm .002$

Substituting into equation 3.10 we obtain

$$\triangle o\ (^{199}Hg) = \sigma_{\parallel} - \sigma_{\perp} = 3 \times 1189/\ 2 \times 0.2723$$

$$= + 6550 \pm 20 \text{ ppm}$$

3.3.4 Quadrupole Coupling constant in Methylethynylmercury-d_1

The deuterium quadrupole coupling constant in methylethynylmercury-d_1 ($CH_3HgC{\equiv}CD$) in Phase IV was measured, and is reported in Table 3.7. The quadrupolar coupling (eQV_{zz}/h) is given by the following expression;

$$(eQV_{zz}/h) = 2DS/3S_{zz} \qquad 3.12$$

where DS is the doublet splitting in the deuterium spectrum and S_{zz} is the orientation parameter. The splitting of the doublet is in the order of 100 KHz hence the splitting could only be obtained through two separate spectra showing the positions of the high and low frequency peaks. The magnitude of S_{zz} was determined from $^2D(HH)$ measured from the proton spectrum at the same temperature. The proton spectrum of methylethynylmercury-d_1 in nematic phase is a triplet with splitting of 3.$^2D(HH)$. S_{zz} was determined from Equation 3.6, using the geometry from Table 3.1 and the vibrationally corrected value of $^2D(HH)$. In Table 3.7 the parameters used to calculate the deuterium quadrupole coupling constant from two experiments are reported.

TABLE 3.7

Parameters used to calculate the Quadrupole Coupling in Methylethynylmercury(II)-d_1

	EXPERIMENT 1	EXPERIMENT 2
^1H SPECTRA		
$^2D(HH)$	3020.7 ±1 Hz	3015.0 ±1 Hz
$^2D(HH)$ corrected for vibration	3118.5 ±1 Hz	3112.8 ±1 Hz
S_{zz} [a]	0.2952 ±.002	0.2947 ±.002
^2D SPECTRA		
Position of high frequency peak of doublet	13797830 ±50 Hz	13797780 ±50 Hz
Position of low frequency peak of doublet.	13711416 ±50 Hz	13711465 ±50 Hz
Doublet splitting	86414 ±50 Hz	86315 ±50 Hz
Quadrupolar coupling	195.16 ±.4 KHz	195.3 ±.4 KHz

a) Calculation using Equation 3.9 and r(HH) fixed at 1.7845A

3.4 Discussion

The internuclear distances for HH, HHg, and H'Hg and the inter-bond angles HCHg and HCH, calculated from the nmr of oriented methylethynylmercury and oriented methyl-1-propynyl mercury in the anisotropic phase are summarized in Tables 3.8 and 3.9. Besides the normal errors in the dipolar coupling constants resulting from uncertainties in the line positions, which are caused by temperature gradients in the sample, other errors may arise when calculating geometry by nmr of oriented molecules.

One possible source of error experienced when determining geometrical parameters from the spectra of the oriented molecules is the contribution from anisotropy in the indirect spin-spin couplings. It appears from the geometries deduced here that all J(HH) and J(HgH) couplings are purely isotropic. This is consistent with previous findings [1-10].

Another source of error is the assumption that there exists one unique orientation throughout the anisotropic phase. It is commonly found that in certain small molecules that different orientations may exist at different sites in the anisotropic phase [5,22-24], but again the satisfactory geometries deduced show this source of error is not important here.

3.4.1 Equilibrium Geometry of Methylethynylmercury

The equilibrium geometry of methylethynylmercury is summarized in Table 3.8 and it is based on the internuclear distance r(HH)= 1.7845A. Table 3.8 shows that the largest magnitude of vibrational correction is applied to ^{2}D(HH) and the second largest to ^{2}D(HgH). The vibrational corrections of 6.9% for ^{2}D(HH) and 5% for ^{2}D(HgH) are of the same order of magnitude as found in the calculation for the equilibrium geometry of methyl-trifluoromethylmercury[7]. We can now investigate whether the geometry of methylethynylmercury calculated with vibrational correction is consistent with that determined by other methods. As the structure of methylethynylmercury has not been reported, the geometry determined here is compared with the geometry obtained by transferring geometrical parameters from methyl(trifluoromethyl)mercury[7] and acetylene[25].

Table 3.8

Geometrical Parameters and Dipolar Couplings (with and without vibrational corrections) in Methylethynylmercury

	no vibrational correction	vibrational correction	percentage correction
^2D(HH)/Hz	2604 ±1	2784 ±1	6.75
^5D(HH')/Hz[a]	-97 ±2	-97 ±2	0.14
^2D(HgH)/Hz	-232 ±2	-244 ±2	4.7
^3D(HgH)/Hz	-69 ±2	-70 ±2	2.2
S_{zz}[b]	+0.2464 ±.002	+0.2635 ±.002	
r(HHg)/A	2.588 ±.005	2.606 ±.005	
r(HH')/A	6.64 ±.08	6.78 ±.08	
r(H'Hg)/A	4.19 ±.05	4.31 ±.05	
$r(C_1 Hg)$/A[c]	1.997 ±.005	2.017 ±.005	
∠CHgH	23.4° ±.1°	23.3° ±.1°	
$\angle HHgC_1$	8.9° ±.5°	8.7° ±.5°	

a) H' denotes acetylenic proton

b) Calculation using equation 3.9 with r(HH) fixed at 1.7845A,

c) Calculation from ^2D(HHg), r(CH)= 1.097A and methyl inter-bond angle as 108.85°

The calculated values for r(H-Hg) and the angle $\angle HHgC_1$ with vibrational corrections are 2.6061 ±.005A and 23.2° ±.01° respectively, as obtained from the corresponding dipolar couplings. This corresponds to $r(C_1-Hg)$= 2.0171A ±0.005A assuming that r(CH)=1.097A and the methyl inter-bond angle is

108.85°. The same calculation but without vibrational correction gave $r(C_1-Hg)$ = 1.997A ±.005A. The difference in the two values is of the order of 0.02A and is larger than the experimental error. The internuclear distances for the same parameter in methyl-trifluoromethylmercury obtained by microwave and nmr are 2.05A[26] and 2.03A ±.004A [7] respectively. Hence the vibrationally corrected value for $r(C_1-Hg)$ is a better estimate than that calculated without vibrational correction. The difference between these results and that obtained from methyl-trifluoromethylmercury is in the order of 1 percent, which is within experimental error. The calculated value of r(HH') as determined from $^5D(HH')$ after vibrational corrections was 6.78A ±.08A. This corresponds to $r(C_1-H')$= 6.33A ±.05 with vibrational correction and 6.64A ±.05A without vibrational correction, again assuming r(CH) and methyl inter-bond angle as before. In order to determine the internuclear distance for a particular bond along the linear skeleton, the internuclear distances of three of the bonds are required to be known with reasonable accuracy. As the molecular geometry for this molecule has not been measured, bond lengths have to be assumed from similar molecules. The internuclear distance $r(C_3-H')$ is reported as 1.06A ±.005A [17] and $r(C_1-Hg)$ has already been calculated. Hence using $r(C_1-H')$, $r(C_1-Hg)$ and $r(C_3-H')$ a total of 3.25A is required to be distributed between $r(Hg-C_2)$ and r(C≡C). The nmr study of oriented cyanopropyne with ^{13}C enrichment reported r(C≡C)=1.166A [27] and the microwave value for same internuclear distance is given as 1.20A [28]. Using both values of r(C≡C) the calculated magnitude of $r(Hg-C_2)$ is 2.05A ±.04 with vibrational correction and 1.99A ±.05A without vibrational correction. The latter value is far too small for an

r(C-Hg) bond length[1-10,26] and again the importance of including vibrational corrections when calculating geometries by nmr is shown here. The same results were obtained using $^{3}D(HgH')$. To quote a more precise value for this internuclear distance the dipolar coupling from which this parameter was calculated has to be measured to within 1 percent. In our case $^{5}D(HH')$ and $^{3}D(HgH')$ could only be determined with an error of 4 percent. Hence the use of oriented nmr in obtaining geometry must be restricted to small distances. However the results here do show the importance of including vibrational corrections when determining geometries by nmr.

3.4.2 The Equilibrium Geometry of Methyl-1-propynylmercury

The equilibrium geometry of methyl-1-propynylmercury is reported in Table 3.9. The relative geometry is again based r(H-H)= 1.7845A. In Table 3.9 significant vibrational corrections were found to be necessary for $^{2}D(HH)$, $^{2}D(H"H")$ and $^{2}D(HgH)$. The vibrational corrections to the dipolar couplings $^{2}D(HH)$ and $^{2}D(HgH)$ are twice those observed for the same couplings in methylethynylmercury [this work] and methyl-trifluoromethyl-mercury [7]. This implies that the amplitude of rocking and angle deformation for the methyl that is directly attached to the mercury is larger in the case of methyl-1-propynylmercury. By comparing the geometry as calculated for methyl-1-propynylmercury with and without vibrational corrections it should be possible to tell whether these amplitudes of vibrational corrections are correct.

Table 3.9

Geometrical Parameters and Dipolar Couplings (with and without vibrational corrections) in Methyl-1-propynylmercury

	no vibrational correction	vibrational correction	percentage correction
^2D(HH)/Hz	2943 ±1	3275 ±1	11.3
^2D(H"H")/Hz [a]	2924 ±1	3072 ±1	5.0
^6D(HH")/Hz	-78 ±2	-78 ±2	0.16
^2D(HgH)/Hz	-259 ±2	-285 ±2	9.99
^4D(HgH")/Hz	-44 ±2	-44 ±2	.38
S_{zz} [a]	+0.2785 ±.002	+0.3093 ±.002	
r(H"H")/A	1.784 ±.003	1.823 ±.003	
r(HHg)/A	2.602 ±.005	2.615 ±.005	
r(H"Hg)/A	5.1 ±.05	5.23 ±.05	
<r(HH")>/A	7.62 ±.05	7.67 ±.05	
r(C_1 Hg)/A [c]	2.012 ±.005	2.027 ±.005	
r(C_1C_4)/A [d]	6.63 ±.05	6.81 ±.05	
∠C_1HgH [c]	23.3° ±.1°	23.2° ±.1°	
∠C_4HgH"	11.6° ±.5°	11.6° ±.5°	

a) H" denotes proton belonging to methyl attached to the triple bonded carbon.

b) Calculation using equation 3.9 with r(HH) fixed at 1.7845A.

c) Calculation from ^2D(HHg), r(CH)= 1.097A and methyl inter bond angle of 108.85°.

d) Calculated from ^6D(HH") using methyl geometry as described in c.

The calculated value after vibrational correction for r(H-Hg) is 2.615 A ±.005A which corresponds to 2.027A ±.005A for $r(C_1-Hg)$ on the assumption that $r(C_1-H)$=1.097A and the methyl inter-bond angle is 108.85°. r(C-Hg) calculated without vibrational correction is 2.012A and the difference between the results obtained with and without vibrational corrections exceeds that attributable to experimental error. The value for r(C-Hg) calculated with vibrational correction is consistent within experimental error with that obtained for the same bond length in methylethynylmercury [this work] and methyl-trifluoromethyl-mercury [7]. The value of r(H"H") calculated from $^2D(H"H")$ after vibrational correction is 1.823A ±.003A, and the most reasonable methyl geometry corresponding to this r(H"H") is, r(CH")= 1.1A and ∠H"CH"= 111°. The calculated value for r(H"H") calculated without vibrational correction was 1.785A and the most reasonable methyl geometry corresponding to this value of r(H"H") is r(CH")=1.097A and ∠H"CH"=108.85°. The methyl geometry for cyanopropyne was reported to be 108.8° for the same bond angle and 1.1A for r(CH) [28]. Hence we find a difference of 2.2 percent between the inter-bond angle reported in cyanopropyne and that calculated in methyl-1-propynylmercury after vibrational correction. Such a large difference between the two results might suggest that the applied vibrational correction for $^2D(H'H')$ is incorrect. This cannot be the case because it would lead to inconsistencies in the remaining geometry. However, the difference in the methyl geometry can also be explained in terms of distortion of the methyl inter-bond angle by the movement of the methyl with respect to the anchor atom which in the case of methyl-1-propynylmercury is mercury and cyanopropyne it is carbon. It would be expected that the methyl that is farthest away from

the anchor atom will rock the most. This in turn might cause a slight widening of the methyl inter-bond angle. The methyl that is not directly bonded to the mercury in methyl-1-propynylmercury is then expected to have a larger HCH angle than the corresponding methyl in cyanopropyne.

The value of $r(C_1-C_4)$ was determined from $^6D(HH")$. Before this could be done the knowledge of the conformation of methyl-1-propynylmercury was required. The possible conformations of methyl-1-propynylmercury would be staggered, eclipsed, or free rotation of the methyls. In the calculation using the computer program COM1PM it was found that within experimental error one could not say which conformer is preferred. This is not surprising as similar observation was made in the study of dimethylmercury [6]. However the spectra of oriented ethane were consistent only with the staggered conformation [29]. Hence such tests must be carried out when molecules may have more than one likely conformation. $^6D(HH")$ was then calculated assuming free rotation of the methyl groups. The calculated value of $\langle r(H"H")\rangle$, where $\langle\rangle$ implies the mean value, corresponds to $r(C_1-C_4)$= 6.81A ±.05A with vibrational correction and 6.63A without vibrational correction. Using $r(C_1Hg)$= 2.027A and $r(C\equiv C)$= 1.2A, a total of 3.58A has to be distributed between $r(Hg-C_2)$ and $r(C_3-C_4)$. In cyanopropyne the microwave value for $r(C_3-C_4)$ is 1.46A[28] and the nmr value is 1.43A [30]. The nmr value has not been corrected for molecular vibration. However using both values an average value of 2.11A ±.05A for the vibrationally corrected r(Hg-C) and 1.93A ±.05A without vibrational correction was calculated. The vibrational corrected value is again seen to be the best estimate. A more accurate

value could not be determined from either $^{6}D(HH")$ or $^{4}D(HgH")$ as both couplings could only be measured with an experimental error of 5 percent. Also, as the molecular geometry of methyl-1-propynylmercury to our knowledge has not been measured, we have been transferring geometrical parameters from similar compounds and assuming that this is feasible.

3.4.3 ^{199}Hg Shielding Anisotropy

In the calculation of the mercury shielding anisotropy, the mercury resonance in dimethylmercury was chosen as the external reference signal. It is appropriate at this point to give the reason for the choice before discussing the shielding anisotropies in both compounds. Sens et al have carried out a general study of Mercury-199 Fourier transform nmr and reported why they thought that dimethylmercury was a suitable choice[31]. They state their reasons to be as follows.

i) The ^{199}Hg signal in dimethylmercury lies at one extreme end of the mercury chemical shift scale.

ii) Dimethylmercury is liquid and thus can be used neat, so the problems of concentration and solvent effects are eliminated.

iii) The mercury nmr spectrum of dimethylmercury can be readily obtained with a single pulse, even in a capillary.

iv) Proton decoupling does not cause problems as all the hydrogens are equivalent, although on most spectrometers this is not particularly important.

Another reason that can be added but not included by Sens's group is that dimethylmercury has been extensively studied by double resonance techniques[21,32-33]. The only disadvantages in using

dimethylmercury is its toxicity and the fact that ^{199}Hg signal lies at the high frequency end of the mercury chemical shift range, so that virtually all other mercury chemical shifts are negative. As dimethylmercury is a health hazard there is no need to have a sample of this reagent available when measuring mercury chemical shifts. This is because chemical shifts can be quoted relative to an external reference compound using the value of Ξ (reference).

The errors in the calculation of the mercury shielding anisotropy from the nmr of oriented molecules are those already summarized in Section 3.4. However there is also a further error that might exist because mercury chemical shifts are known to be medium-dependant. This implies that the chemical environment of the mercury in the nematic and isotropic phases may be different. In pyridine and dimethyl sulphoxide the mercury chemical shift can be affected by as much as 100 ppm according to conditions[31,34]. As the isotropic mercury chemical shift of methylethynylmercury and methyl-1-propynylmercury are similar in deuterated benzene and in Phase IV, this source of error can be considered to be unimportant in our case.

The nmr of oriented molecules can give information on the chemical environment at a nucleus from the measurement of the its shielding anisotropy and the isotropic shielding. From the anisotropic and the isotropic shieldings the individual contributions to the shielding for each direction can be calculated. These experimental results can then be discussed with deductions made from the theory of nuclear shielding. A general theory of nuclear shielding has been presented by Ramsey[35] and Gutowsky[36]. Ramsey's theory discussed the observed shielding of

a nucleus (σ(A)) as the sum of the contributions from the paramagnetic and diagmagnetic shieldings.

$$\sigma\ (A) = \sigma_p(A) + \sigma_d(A) \qquad 3.13$$

The diagmagnetic shielding involves the free rotation of the electrons about the nucleus in question and the paramagnetic contribution describes the hindrance or in the terms of Gutowsky the imbalance caused by other electrons and nuclei in the molecule. Many problems arise in the treatment of chemical shifts, but by simplifying the theoretical consideration of shielding, the factors that dominate chemical shifts can be discussed. These factors are as follows

i) the relative importance of local and long range effects is not absolutely known but it can be assumed that the former will dominate the shielding.

ii) There is also uncertainty in the relative importance between the paramagnetic and diagmagnetic contributions and here the paramagnetic shielding will dominate as variations in the diagmagnetic shielding are small.

Hence for our purpose we can assume that the paramagnetic contribution to the shielding will dominate and it will be the local electrons which will have the greatest effect upon the chemical shift. In mercury compounds the local field involves the valence shell; this is mainly composed of <u>s</u> and <u>p</u> orbitals and from the definition of Jameson and Gutowsky, σ_p will be large when the imbalance is greatest in the valance <u>p</u> shell. This is when one <u>p</u> orbital is full and the other two are empty or <u>vice versa</u>.

In linear mercury compounds the mercury shieldings parallel and perpendicular to the linear skeleton will involve circulation and interaction between electrons of nuclei close to the mercury. Hence we can say that the paramagnetic contribution to the shielding can be measured directly from $\sigma_{\parallel}$ and $\sigma_{\perp}$. The observed isotropic shielding is given by;

$$\sigma(\text{iso}) = \tfrac{1}{3}(\sigma_{xx} + \sigma_{yy} + \sigma_{zz}) \qquad 3.14$$

and the shielding anisotropy for a molecule with C_3 symmetry is given by;

$$\Delta\sigma = \sigma_{\parallel} - \sigma_{\perp} = \sigma_{zz} - \sigma_{xx,yy} \qquad 3.15$$

where the z axis is parallel to the C_3 symmetry axis. From the above equations the individual contribution to the shielding can be calculated. For methylethynylmercury $\sigma_{xx} = \sigma_{yy}$ = -2028 ppm and σ_{zz} = +4522 ppm, was obtained, and for methyl-1-propynylmercury it was deduced that $\sigma_{xx} = \sigma_{yy}$ = -1890 ppm and σ_{zz} = +4210 ppm. The shielding contribution parallel to the symmetry axis for dimethylmercury measured by Diehl and for HgMeX (X= Cl,Br,I) measured by Kennedy and McFarlane was +5000 ppm, +4500 ppm, +4550 ppm, and +4740 ppm respectively [1,10]. The contribution to shielding perpendicular to the same axis for the above series was -2500 ppm, -1035 ppm, -1040 ppm, and -740 ppm respectively. The vast difference between shielding perpendicular and parallel to the magnetic field in all the above molecules indicates that the electronic circulation is unhindered about the symmetry axis but highly restricted perpendicular to this direction (i.e. large negative contribution to the shielding). The magnitude of individual contributions to the mercury shielding

in methylethynylmercury and methyl-1-propynylmercury are not as large as observed for dimethylmercury. In dimethylmercury σ_{xx} and σ_{zz} are expected to be close to their extreme values and thus the observed shielding anisotropy can be ascribed to unrestricted electronic circulation when the symmetry axis and the magnetic field direction are parallel with each other and highly restricted when they are perpendicular. In terms of bonding the mercury in dimethylmercury then uses only $6p_z$ orbital and $6p_x$ and $6p_y$ orbitals are left vacant. The decrease in σ_{zz} and increase in $\sigma_{xx,yy}$ going through the series dimethylmercury, methylethynylmercury and methyl-1-propynylmercury suggest electrons are being withdrawn from the mercury's $6p_z$ orbitals. There may also be an increase in the occupation of the $6p_x$ and $6p_y$ orbitals. The adjacent carbon-carbon triple bond present in both methylethynylmercury and methyl-1-propynylmercury must be responsible for withdrawing electrons from the mercury $6p_z$ orbital. The difference in covalent bonding in both methylethynylmercury and methyl-1-propynylmercury from that found in dimethylmercury is also shown in the difference in r(Hg-C) bond lengths. The internuclear distance for r(Hg-C) in dimethylmercury was found to be 2.09A [1] whereas the same internuclear distance in methylethynylmercury and methyl-1-propynylmercury was about 0.07A shorter [this work].

One observation from Table 3.6 is the difference between the magnitude of the shielding anisotropy calculated with and without vibrational correction. The difference of 230 ppm in the case of methylethynylmercury and 600 ppm for methyl-1-propynylmercury and 475 ppm for the shielding anisotropy for mercury in dimethylmercury[1] indicates the importance of including

vibrational corrections throughout the calculation in the nmr of oriented system.

Sometimes a shielding anisotropy experiment can be used to derive the signs of coupling constants when the sign of the shielding anisotropy is known. The sign of the dipolar coupling constant is dependant upon the orientation of the molecule (see equations 3.6 and 3.7), but the sign of the indirect spin-spin coupling is not. In this work the sign of J(HgH) is of interest as it has already been determined by double resonance experiments[21]. The sign of $^2J(HgH)$ can be derived given that sign of the mercury shielding anisotropy is positive. The mercury shielding anisotropy is given by equation 3.10. From Table 3.6 ν(nem)-ν(iso) is negative, so that σ(nem)-σ(iso) is positive. Thus given that $\Delta\sigma(^{199}Hg)$ is positive, then S_{zz} must also be positive. $^2D(HgH)$ is given by the following equation;

$$^2D(HgH) = -K(HHg)\, S_{zz}\, [1 - 2\sin^2(\xi/2)]/r^3_{HgH} \qquad 3.16$$

where ξ is the angle subtended at the mercury by a pair of protons attached to the same carbon. Using the assumed geometry (r(HH)=1.7845A and ξ =46.5°), $1-2\sin^2(\xi/2)$ is found to be positive. As S_{zz} is positive then $^2D(HgH)$ must be negative. The mercury spectrum of the oriented methylethynylmercury is a quartet with splitting of |2.D(HgH)+J(HgH)|. The value of D(HHg) can be calculated from Equation 3.16 using S_{zz} calculated from corresponding proton spectrum. We find that |2.D(HgH)+J(HgH)| is greater than 2.D(HgH) so that $^2D(HgH)$ and $^2J(HgH)$ must have the same sign. Given the sign of $^2D(HgH)$ as being negative then $^2J(HgH)$ must be negative also. This is consistent with double resonance experiments carried out to find the sign of the same

coupling in dimethylmercury [21].

3.4.4 Quadrupolar Coupling in Methylethynylmercury-d_1

Another parameter that can be measured from the nmr of oriented molecules is the quadrupolar coupling constant. The quadrupolar coupling constant corrected for harmonic vibrations for the deuteron in methylethynylmercury-d_1 was determined here to be 195.2 KHz. The value for the same constant without vibrational corrections was found to be 201 KHz. The experimental error was only about ±0.4 KHz. The deuterium quadrupolar coupling constants reported by Millet and Dailey in DCN, C_2D_2, C_6D_6 and CH_3CD_3 were 199 KHz, 198 KHz, 183 KHz and 167 KHz respectively [13]. These measurements did not include vibrational corrections. As the magnitude of the quadrupolar coupling constant can give a qualitative picture of the bond to deuterium, by comparing the uncorrected value of the constant in methylethynylmercury-d_1 with those obtained by Millet and Dailey we can say that the carbon-deuteron bond in this molecule has an sp character, and the carbon-deuteron internuclear distance is about 1.06A. This result is not surprising but it does show that nmr of oriented molecules is a convenient and accurate method for the determination of the deuterium quadrupole coupling constants. Also this exercise shows the importance of including vibrational corrections in the calculation.

3.5 Conclusion

The equilibrium geometries of methylethynylmercury and methyl-1-propynylmercury in the liquid crystal Phase IV have been determined. The bond lengths and inter-bond angles that were

calculated for both molecules are consistent with those which might be reasonably expected[1-10,25,28], and the results here are of value since no other studies on the geometries of these molecules have been reported.

The study of methylethynylmercury and methyl-1-propynylmercury in the liquid crystal has also enabled us to determine the absolute signs of $^{2}J(HgH)$, $^{3}J(HgH)$, and $^{4}J(HgH)$ from the sign of the mercury shielding anisotropy. The sign of the indirect spin-spin coupling $^{2}J(HgH)$ determined by us is in agreement with the sign observed from double resonance experiments carried out on dimethylmercury [21]. The signs of the other two couplings are consistent with geometry and spectral analysis when the sign of $^{2}J(HgH)$ is known.

Shielding anisotropies of +6550 ppm and +6000 ppm for mercury in methylethynylmercury and methyl-1-propynylmercury were obtained by using a nematic liquid crystal and recording the corresponding spectra. These anisotropies when compared with that measured in dimethylmercury [1] indicate that the carbon triple bond in both methylethynylmercury and methyl-1-propynylmercury causes withdrawal of electrons occupying the mercury's $6\underline{p}_z$ orbitals and an increase in occupancy of the mercury's $6\underline{p}_x$ and $6\underline{p}_y$ orbitals. The differences in covalent bonding between dimethylmercury, methylethynylmercury and methyl-1-propynylmercury were also shown in the differences in the Hg-C bond lengths.

The analysis of the nmr spectrum of partially oriented methylethynylmercury-d_1 in Phase IV was found to be an accurate and convenient method to determine the deuterium quadrupolar coupling constant.

APPENDIX 3.1

Listing of the Computer Program COM1PM

```
C       ****** PROGRAM COM1PM ******
        DIMENSION XCOORD(10),YCOORD(10),ZCOORD(10)
        RCHG=2.08
        RHGC=2.05
        RCTC=1.21
        RCC=1.46
        RCH=1.11
        ANGMTH=108.5
        D6HH=76.7
        KHH =120067.
        THETA=ANGMTH
        THETB=0.5*(180.0-THETA)
         RHH  = SIND(THETA)*RCH/SIND(THETB)
         XO   = RHH * SIND(30.)/SIND (120.0)
         ZO   = SQRT((RCH*RCH)-(XO*XO))
        XCOORD(1)= XO
        YCOORD(1)= 0.0
        ZCOORD(1)= 0.0
        DO 10 I=2,6
        XCOORD(I)=0.0
        YCOORD(I)=0.0
10      CONTINUE
        ZCOORD(2)=ZO
        ZCOORD(3)=ZO+RCHG
        ZCOORD(4)=ZCOORD(3)+RHGC
        ZCOORD(5)=ZCOORD(4)+RCTC
        ZCOORD(6)=ZCOORD(5)+RCC
        ZCOORD(7)=ZCOORD(6)+ZO
        ROTAT=0.0
        ATOT=0
20      ROTAT=ROTAT+1.
        IF(ROTAT.GT.360.0)GOTO 40
        ATOT=ATOT+1
        XCOORD(7)=XCOORD(1)*COSD(ROTAT)
        YCOORD(7)=XCOORD(1)*SIND(ROTAT)
        RI=SQRT((ZCOORD(1)-ZCOORD(7))**2+
     1+(YCOORD(1)-YCOORD(7))**2+
     1+(ZCOORD(1)-ZCOORD(7))**2)
        RI3=RI**3
        ALPHAZ=((ABS(ZCOORD(1)-ZCOORD(7)))/RI)**2
        SDR=(3*ALPHAZ-1)/RI3
        TOTSDR=SDR+TOTSDR
        SDR=0.0
        GO TO 20
40      SZZ=D6HH/(KHH*(TOTSDR/ATOT))
        TYPE 30,SZZ,ATOT
30      FORMAT(2F)
        RETURN
        END
```

3.6 References

1 J. Jokisaari and P. Diehl, Org. Mag. Res., 13(5), 359,(1980).

2 J. Jokisaari and K.Räisänen, Mol. Phys., 36, 113(1978).

3 J. Jokisaari and P. Diehl, Mol. Phys., 37, 981(1979).

4 C. Schumann, H. Dreeskamp and K. Hildenbrand, J. Mag. Res., 18, 97,(1975).

5 C.L. Khetrapal and A. Saupe, Mol. Cryst. Liq. Cryst., 19, 195(1973).

6 G. Englert, Z. Naturforsch, 24A, 1075,(1969).

7 J. Jokisaari and J. Kuonanoja, J. Mol. Struct., 68, 173,(1980).

8 J. Jokisaari, K. Räisänen, J. Kuonanoja, P. Pyykkö and L. Lajunen, Mol. Phys., 39, 715(1980).

9 K. Räisänen, J. Kuonanoja and J. Jokisaari, Mol. Phys., 38, 1307(1979).

10 J.D. Kennedy and W. McFarlane, J. Chem. Soc. Farad. Trans. 2, 1653(1976).

11 Y. Imai, F. Watari and K. Aida, Spectrochim Acta, 36A, 233(1980).

12 Y. Imai, F. Watari and K. Aida, Bull. of Chem. Soc. of Japan, 52(10), 2875(1979).

13 F.S. Millet and B.P. Dailey, J. Chem. Phys., 56, 3249(1972).

14 W.J. Caspary, F. Millet, M. Reichbach and B.P. Dailey, J. Chem. Phys., 51, 623(1967).

15 W.J. Caspary, Doctoral Thesis, Columbia University, N.Y. 1968.

16 P. Diehl and C.L. Khetrapal, Can. J. Chem., 47, 1411,(1969).

17 G.P. Ceasar, C.S. Yannoni and B.P. Dailey, J. Chem. Phys., 50, 373(1969).

18 D. Gill, M.P. Klein and G. Kotowyoz, J. Amer. Chem. Soc., 90, 6870(1968).

19 C.M. Woodman, Mol. Phys., 13, 365(1967).

20 S. Sýkora, J. Vogt, H. Bösiger and P. Diehl, J. Mag. Res., 36, 53(1979).

21 K.A. Mclauchlan, D.H. Wiffen and L.W. Reeve, Mol. Phys., 10, 131(1966).

22 E.E. Burnell, J.R. Council and S.E. Ulrich, Chem. Phys. Letts., 31, 395(1975).

23 P. Diehl, M. Reinhold, A.S. Tracey and E. Wullschleger, Mol. Phys., 30, 1781(1975).

24 M. Ayres, K.A. Mclauchlan and J. Wilkinson, Chem Commum, 858(1969).

25 E. Haloui and D. Canet Org. Mag. Res., 6, 537(1974).

26 H. Güntherm, H. Oberhammer and R. Eugen, J. Mol. Struct., 64, 249(1980).

27 E. Haloui and D. Canet, Chem. Phys. Letts., 26, 261(1974).

28 J. Sheridan and L.F. Thomas, Nature, 174, 798(1954).

29 H.S. Spiesecke, private communication.

30 S. Mohanty, Chem. Phys. Letts., 18, 581(1973).

31 M.A. Sens, N.K. Wilson, P.D. Ellis and J.D. Odom, J. Mag. Res., 19, 323, (19)

32 R.R. Dean and W. McFarlane, Mol. Phys., 13, 343(1967).

33 K. Hildenbrand and H. Dreeskamp, Z. Phys. Chem., 69, 671(1970

34 A.P. Tupčiauskas, N.M. Sergeyev, Y.A. Ustynyuk and A.N. Kashin J. Mag. Res., 7, 124(1972).

35 N.F. Ramsey, Phys. Rev., 91, 303(1953).

36 C.J. Jameson and H.S. Gutowsky, J. Chem. Phys., 40, 1714(1964).

Chapter 4

NMR STUDY OF BIS(TRIFLUOROMETHYL)MERCURY ORIENTED IN MERCK PHASE IV AND IN EBBA

4.1 Introduction

As was mentioned in Chapters 2 and 3, the nmr spectra of molecules oriented in nematic liquid crystals permit the determination of nmr parameters which in isotropic solvents average out to zero. Examples of such parameters are chemical shift anisotropies, and dipolar and anisotropic indirect couplings The direct dipolar couplings can be used to determine geometries, and the chemical shift anisotropy can provide insight into the architecture of chemical bonds. Anisotropy in the indirect spin-spin couplings is often difficult to establish as it is closely involved with the direct dipolar couplings, but theoretically it should help in the understanding of the mechanism involved in spin-spin coupling. These anisotropies can also be a nuisance to analytical nmr chemists when trying to accurately determine geometries.

The anisotropy in the indirect spin-spin coupling is not found between all nuclei. There is no evidence at all of anisotropy in the indirect coupling between a pair of protons, but for indirect couplings involving fluorine, this contribution can be significant in certain molecules. It is for this reason that a number of fluorinated compounds partially oriented in the nematic phase have been studied in the present work. These studies show that complications arise in determining molecular geometries when the experimental anisotropic coupling (D^{total}) obtained from the analysis of the anisotropic spectrum is not purely dipolar but

also contains contributions arising from anisotropies in the indirect couplings (D^{indir}). In fluorinated benzenes it was found that D_{FF}^{indir} is very sensitive to small changes in the geometry so that either D_{FF}^{indir} or the correct geometry can be accurately determined, but not both [1]. In trifluoromethyl benzene, D_{FF}^{indir} was found to lie in the range of -41 Hz to +5Hz, according to the geometry assumed [2]. A study of cis and trans 1,2 difluoroethenes [3] showed that only J_{FF}^{trans} and J(CF) have large anisotropic contributions. D_{FF}^{indir} trans was about 5% of the corresponding dipolar coupling whereas D_{CF}^{indir} was less than 1% of its dipolar coupling. The experimentally determined D_{FF}^{indir} was also in agreement with theoretical calculation. The disagreement between the structures obtained from nmr and micro wave results on fluoromethane suggested that there are large anisotropies in the C-F and C-H indirect couplings in this molecule [4]. In difluoromethane and trifluoromethane, J(FH) and/or J(FF) appear to show small anisotropies [5]. A study of phosphoryl fluoride (F_3PO) in the nematic phase also showed disagreement between the geometry determined by nmr and that obtained from electron diffraction data[6]. Again the disagreement was interpreted by suggesting that large anisotropies were present in either or both of J(PF) and J(FF). When the anisotropic contribution from J(PF) was assumed to be zero then D_{FF}^{indir} was about 30% of the corresponding value of its experimental anisotropic coupling. If J(FF) was assumed to have zero anisotropy then D_{FF}^{indir} was about 50% of the corresponding experimental anisotropic coupling. It was found from the equilibrium geometry of methyl-trifluoromethylmercury[7] as derived by nmr that the position of the fluorines could not be determined accurately as a consequence of the error in the

experimental dipolar coupling and/or anisotropic contributions to the geminal indirect FF couplings. Hence, from all these studies it is apparent that anisotropies in indirect spin-spin couplings can be a nuisance, as they can impede our ability to calculate accurate structural data from the nmr spectra of oriented molecules. Where it is known that the indirect couplings are anisotropic, the nmr of oriented species can either determine accurately the geometry, or the contribution from D^{indir}. The nmr of bis(trifluoromethyl)mercury partially oriented in the nematic phase is discussed in this chapter. This study gives information on anisotropies of certain indirect couplings and the part they play in obtaining precise molecular geometries.

Bis(trifluoromethyl)mercury is a particularly suitable compound to study in this way as it has threefold symmetry, and its orientation in the liquid crystal can be described by a single parameter. The compound is also a suitable choice in that the vibrational force field analysis has been reported [8]. From the force field, the anharmonic vibrational corrections to the experimental dipolar couplings can be calculated, and this should improve the relative precision of the direct dipolar coupling constants. This in turn should help to determine quite accurately the anisotropy in the indirect couplings and/or the geometrical parameters. For a molecule to be suited for the determination of such parameters by oriented nmr, the requirements are that the number of anisotropic couplings that can be measured from the anisotropic spectrum should exceed the number of parameters that describe the orientation. In the case of bis(trifluoromethyl)-mercury the number of orientation parameters required is one. To calculate any anisotropies present in the indirect couplings or

the geometry, then at least one of the experimental anisotropic couplings has to be assumed to be purely dipolar so that the orientation parameter can be calculated from it. From studies of trifluoromethane [5] and methyl-trifluoromethylmercury [7] it was found that the geminal spin-spin couplings between pairs of fluorines have negligible anisotropy. Hence for bis(trifluoromethyl)mercury the orientation can be deduced from the anisotropic $^2D(FF)$ coupling. Once the orientation has been determined, the molecular geometry or the anisotropic contribution to an indirect coupling can then be calculated.

Various methods are available for the determination of the absolute signs of the indirect spin-spin couplings, and double resonance experiments are the most commonly used[9]. In double resonance experiments, the assumption is made that the sign of the indirect coupling for a directly bonded C-H is positive[10]. Liquid crystal nmr studies can also be used to determine the absolute signs of indirect couplings[11,Chapter 3]. The method for the determination of the signs of indirect couplings by nmr of molecules oriented in liquid crystals relies on knowing the sign of the orientation parameter, or the absolute sign of the shielding anisotropy. Previous studies on mercury shielding anisotropies in the linear molecules dimethylmercury[12], methylmercury halides[13], methylethynylmercury[Chapter 3] and methyl-1-propynylmercury[Chapter 3] have shown that they are large (greater than 4000ppm) and positive. This is consistent with the theory of mercury shielding as presented by Ramsey [14] and by Gutowsky[15]. It is then expected that the sign of the mercury shielding anisotropy in bis(trifluoromethyl)mercury should also be large and positive, and from it the signs of the indirect

spin-spin couplings $^{2}J(HgF)$ and $^{4}J(FF)$ can be determined. The determination of the shielding anisotropies for the fluorine and mercury in bis(trifluoromethyl)mercury can also be discussed in relation to the existing theories of ^{19}F and ^{199}Hg chemical shifts [14-16].

4.2 Experimental

Bis(trifluoromethyl)mercury was synthesized in our laboratory as described in Chapter 8. Liquid crystalline solvents 4-ethoxy benzylidene-4'-butylaniline (EBBA) and Merck Phase IV were obtained commercially and were used without further purification. Three nematic samples were prepared as described in Chapter 3. Bis(trifluoromethyl)mercury was also studied in a mixture of 20% deuterated benzene and benzene.

^{199}Hg nmr spectra were obtained as described in Chapter 3. All ^{19}F spectra were recorded on an FX90Q spectrometer operating at 84.26 MHz. The anisotropic spectrum was obtained with 16K data points and a spectral width of 12 KHz. The pulse width used was 17μs. The summation of 2000 FIDs was transformed with an artificial line broadening function to give a line width of 1 Hz in the central region of the spectrum and 3 Hz in the outer parts. This number of scans was sufficient to observe the ^{199}Hg satellites. The isotropic ^{19}F spectrum was acquired with the same pulse width and a spectral width of 6 KHz. Fewer scans were needed to observe the ^{199}Hg satellites in this case.

Nmr spectra of oriented molecules were analysed using equations for the line positions derived by Englert[17] and the computer program LAOCOON LC[18]. The calculated spectrum was

plotted as described in Section 3.2.

The harmonic vibrational corrections to the dipolar coupling constants were calculated with the aid of the computer program VIBRA[19], and the force field obtained from Mills[8].

4.3 Results

4.3.1 Anisotropic and Isotropic Couplings

The ^{19}F nmr spectrum with natural abundance ^{199}Hg satellites of bis(trifluoromethyl)mercury oriented in Phase IV at room temperature is shown in Fig 4.1(a). The magnitude and relative sign of $^{4}J(FF)$ in bis(trifluoromethyl)mercury were obtained directly from the analysis of the anisotropic ^{19}F spectrum. In the analysis of nmr spectra a reversal of the signs of all the couplings leaves the nmr spectrum unchanged. In our analysis of the anisotropic ^{19}F spectrum it was found that $^{4}J(FF)$ had the same sign as the corresponding total anisotropic coupling $^{4}D_{FF}^{total}$, but opposite sign to the $^{2}D_{FF}^{total}$ coupling. The absolute signs of all the couplings can then be derived by the knowledge of the sign any one of these three couplings.

The magnitude of $^{2}J(HgF)$ was measured from the satellite region of the isotropic ^{19}F nmr spectrum of bis(trifluoromethyl) mercury in the liquid crystal solvent. The sign of $^{2}J(HgF)$ in bis(trifluoromethyl)mercury has to our knowledge not been determined. Fedorov and coworkers determined the signs of

Fig 4.1 Anisotropic 84.26 MHz ^{19}F nmr spectra including ^{199}Hg satellites of $(CF_3)_2Hg$ in Phase IV; a) Experimental (below) b) Calculated (overleaf)

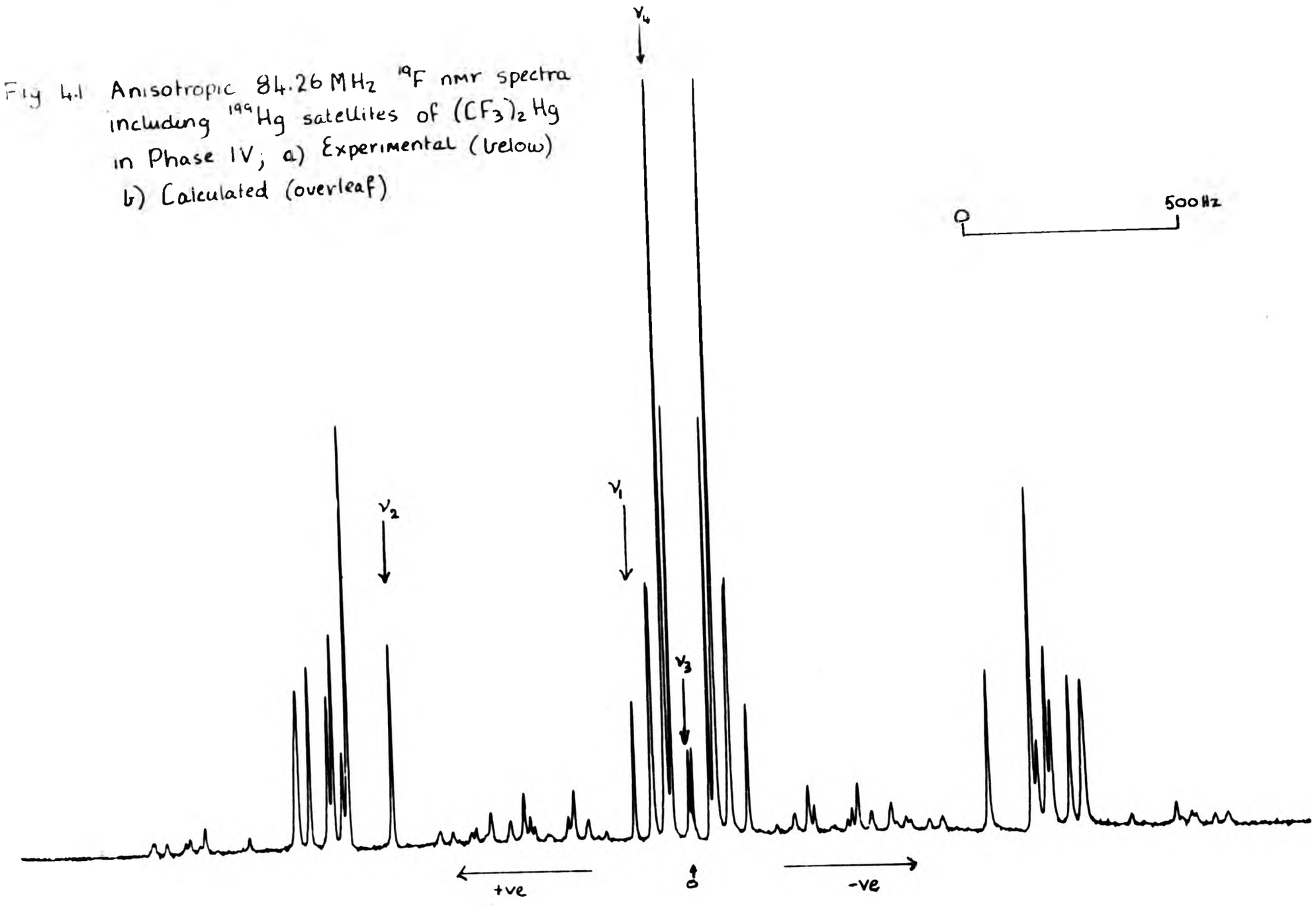

Fig 4.1 (b)

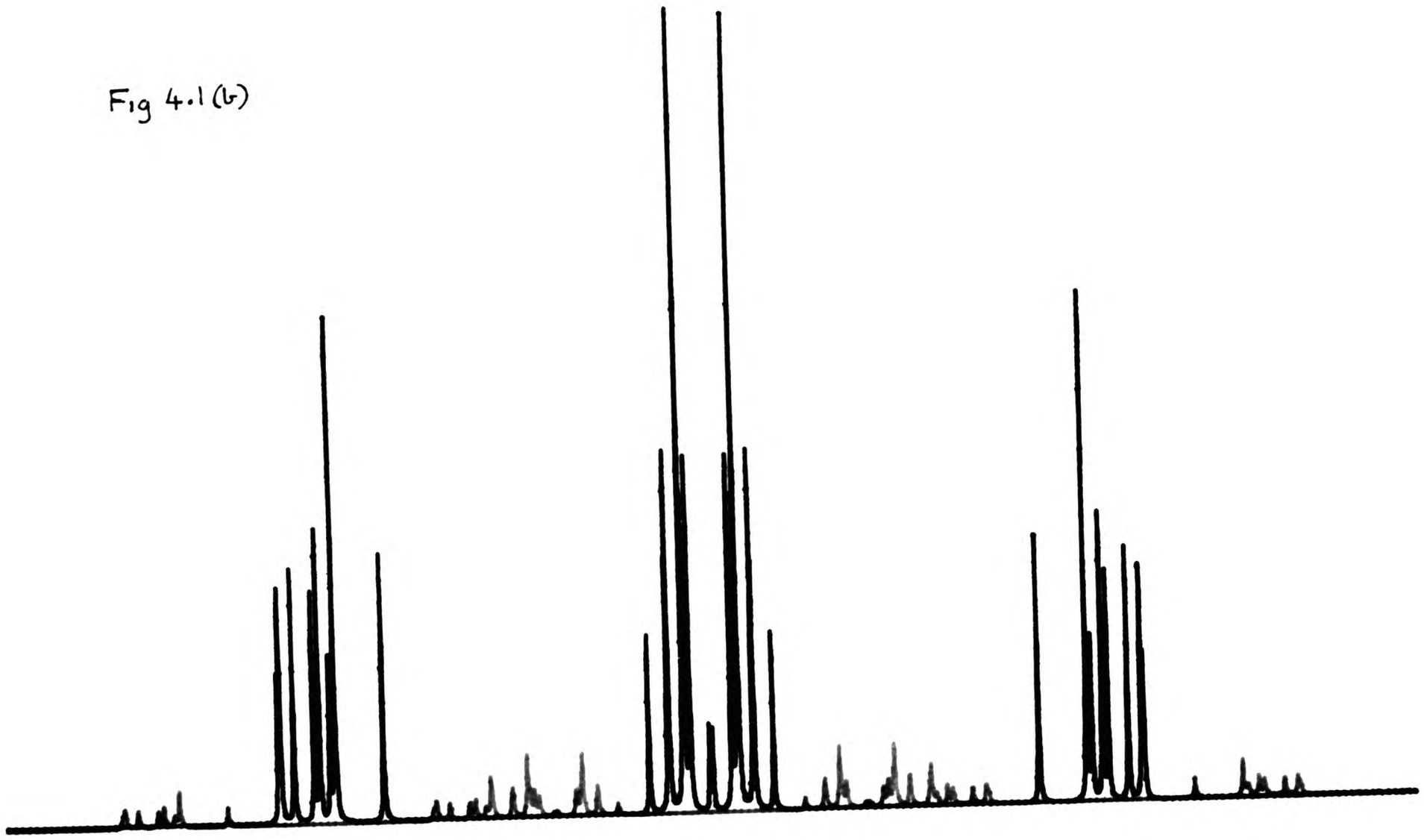

Fig 4.1 (b)

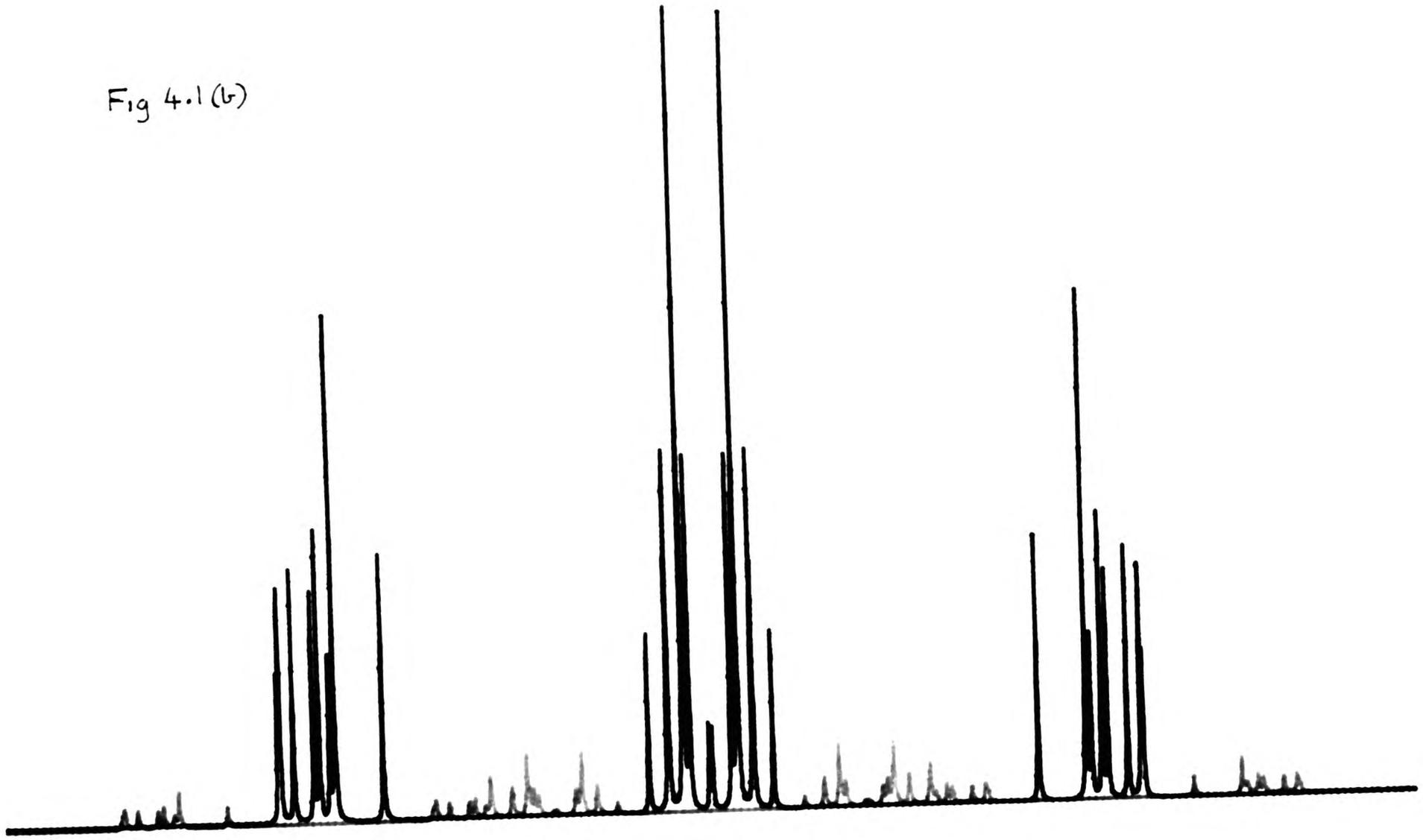

$^2J(HgF)$ couplings in perfluorovinyl compounds[20] and found them to be positive. Goggin reported that $^2J(HgF)$ varies between 1200 and 2000 Hz and was positive in trifluoromethyl mercuric compounds[21]. For the present the sign of $^2J(HgF)$ can be assumed to be positive, but as we shall see later the sign of this coupling can also be determined from the sign of the orientation parameter.

The total anisotropic couplings $^{2,4}D_{FF}^{tot}$ were measured from the ^{19}F spectrum of partially oriented bis(trifluoromethyl)-mercury. The spectrum consists of 34 lines characteristic of an oriented A_3A_3' spin system, of which 28 lines were visible. It was analysed using the equations of Englert[17]. From these equations it was possible to determine the magnitudes and relative signs of both the isotropic and the anisotropic couplings, providing that certain lines were well resolved. The A_3A_3' spectrum is symmetrical about the centre and the positions of these lines (see fig 4.1(a)) measured from the centre are as follows:

$$\nu_1 = + \tfrac{9}{2}\ {}^4D(FF) \qquad 4.1$$

$$\nu_2 + \nu_1 = -3\ {}^2D(FF) \qquad 4.2$$

$$\nu_3 + \nu_4 = +2\ {}^4J(FF) - 2\ {}^4D(FF) \qquad 4.3$$

The magnitudes and relative signs of the couplings were determined by solving equations 4.1 to 4.3. The absolute signs of these couplings can be obtained by either assuming the sign of $^4J(FF)$ or by determining the sign of any one of the anisotropic couplings. The sign of $^4J(FF)$ in bis(trifluoromethyl)mercury- has not been determined, nor is there any information on the sign of $^4J(FCHgCF)$ in a similar molecule. However it is much simpler to derive the sign of one of the anisotropic couplings. This can

be obtained by solving the equation for the direct dipolar coupling. The equation for the geminal fluorine coupling $^2D(FF)$ is;

$$^2D(FF) = K(FF)\ S_{zz}/2r_{FF}^3 \qquad 4.4$$

where S_{zz} is the orientation parameter and the z axis is taken to be parallel to the C_{3v} symmetry axis. From equation 4.4 the sign of S_{zz} is required to determine the sign of $^2D_{FF}^{dir}$. The sign of S_{zz} can be derived directly from the mercury shielding anisotropy. The shielding anisotropy ($\Delta\sigma$) for the mercury in bis(trifluoromethyl)mercury is given by the following expression;

$$\Delta\sigma\ (^{199}Hg) = -3/2\ [\nu(nem) - \nu(iso)]/S_{zz} \qquad 4.5$$

where ν(nem) and ν(iso) are the chemical shifts in the nematic and isotropic phases respectively. From the mercury shielding anisotropy results in dimethylmercury [12] and methylmercuric halides [13], the sign of the mercury shielding anisotropy in bis(trifluoromethyl)mercury can be assumed to be also positive, as pointed out above. The sign of (ν(nem) - ν(iso)) from the mercury shielding anisotropy experiment was positive and given that the mercury shielding anisotropy is also positive, then S_{zz} must be negative. As S_{zz} is negative, then from equation 4.4 $^2D(FF)$ must also be negative. Given that the sign of $^2D(FF)$ is negative, and knowing from spectral analysis that the sign of $^2D(FF)$ is opposite to the sign of $^4D(FF)$, then $^4D(FF)$ and $^4J(FF)$ must be positive.

The total anisotropic coupling between mercury and fluorine was measured from the splitting in the ^{199}Hg spectrum of oriented bis(trifluoromethyl)mercury and also as a check from the

splitting of the satellites in the ^{19}F spectrum of the oriented molecule. The splitting is equal in both spectra to $|2.D(HgF)+J(HgF)|$, where D is the total anisotropic coupling. Using the equation for $^{2}D^{dir}_{HgF}$;

$$^{2}D^{dir}_{HgF} = - K(HgF)(1-2\sin^{2}\xi/2)S_{zz}/r^{3}_{HgF} \qquad 4.6$$

where ξ is the angle subtended at the mercury by two fluorines attached to the same carbon atom. The constant K(HgF) is positive and from the geometry listed in Table 4.2 $(1-2\sin^{2}\xi/2)$ is also positive. Then for a negative S_{zz} derived from the mercury shielding anisotropy, $^{2}D(HgF)$ must be positive. Given that D(HgF) is positive and that splitting $|2\,D(HgF)+J(HgF)|$ is greater than $|J(HgF)|$ then D(HgF) and J(HgF) must have the same sign. Hence $^{2}J(HgF)$ is positive and this is consistent with work on the same coupling in similar compounds [20,21]. This completes the analysis of the ^{19}F spectrum with natural abundance ^{199}Hg satellites of bis(trifluoromethyl)mercury partially oriented in the nematic phase. The nmr parameters obtained in this way from the analysis of the ^{19}F anisotropic spectrum for three different solutions are summarized in Table 4.1. The computed spectrum of bis(trifluoromethyl)mercury partially oriented in Phase IV using the results from Table 4.1 is shown in Fig 4.1(b).

Table 4.1 Selected Nmr Data of Bis(trifluoromethyl)mercury in a Liquid Crystal

Coupling constant/Hz	Sample [a]		
	A	B	C
$^{2}D(^{19}F-^{19}F)$	-550.8 ±1	-554.1 ±1	-1207.8 ±1
$^{4}D(^{19}F-^{19}F)$	+59.0 ±.5	+59.1 ±.5	+130.9 ±.5
$^{2}D(^{199}Hg^{19}F)$	+23.5 ±.4	+24.0 ±.4	+47.4 ±.4
$^{4}J(^{19}F-^{19}F)$	+4.5 ±.5	+4.3 ±.5	+4.4 ±.5
$^{2}J(^{199}Hg-^{19}F)$	+1282.1 ±1	+1282.1 ±1	+1269.0 ±1
$^{4}D(FF)/^{2}D(FF)$	-0.10712 ±.0007	-0.10666 ±.0007	-0.10838 ±.0003
$^{2}D(HgF)/^{2}D(FF)$	-0.04267 ±.0012	-0.04331 ±.0012	-0.0393 ±.0003

a) Phase IV used for A and B, and EBBA used for C.

In Table 4.1 the experimental results for three different solutions of bis(trifluoromethyl)mercury partially oriented in the liquid crystal are reported. Phase IV was used as a liquid crystal in solutions A and B and in solution C, EBBA was used. The three solutions gave different ratios for $^{4}D(FF)/^{2}D(FF)$ and for $^{2}D(HgF)/^{2}D(FF)$. This suggests that both $^{2}J(HgF)$ and $J(FF)$ may have anisotropic contributions. Also the differences in the magnitude of $^{2}J(HgF)$ measured in benzene, Phase IV and EBBA clearly show that the coupling is solvent dependant. As the better quality spectrum was obtained when Phase IV was used, it was decided that the calculations of the equilibrium geometry and anisotropies in the shielding and indirect couplings should be determined using the results from solution A.

Fig 4.2 Geometrical Parameters and Internal Coordinates of Bis(trifluoromethyl)mercury)

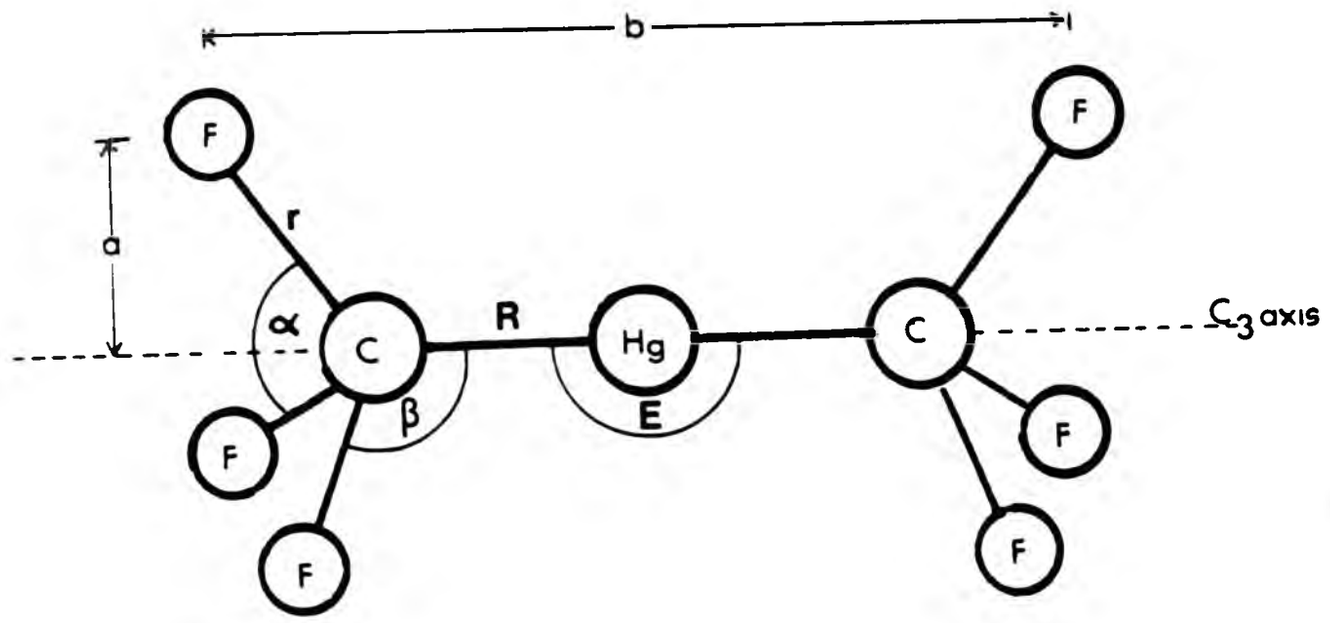

Table 4.2 Preliminary Geometrical Parameters for Bis(trifluoromethyl)mercury(II)

r(CF)	1.33A	r(HgC)	2.2A
r(FF)	2.163A	r(HgF)	2.91A
∠FCF	108.85°	∠FHgC	25.5°

4.3.2 Calculation of the Orientation tensor

The signs and magnitudes of the total anisotropic couplings having been determined, the next stage in the process of determining anisotropic parameters or the geometry is to calculate the orientation tensor. The equations for calculating the orientation parameter S_{zz} from experimental dipolar couplings $^2D(FF)$, $^2D(HgF)$ and $^4D(FF)$ are 4.4, 4.6 and 4.7.

$$^4D(FF) = -K(FF)\langle S/R^3_{FF} \rangle \qquad 4.7$$

In equation 4.7 $S=(3Cos^2\phi-1)$, where ϕ is the variable angle between the z axis and the internuclear distance vector R, so as to incorporate rotation of the trifluoromethyls, and <> implies the mean value. A decision has to be made as to which of the equations 4.4, 4.6 and 4.7 should be used to calculate S_{zz}. The choice depends upon the same factors as discussed in detail in Section 2.5. In summary, the choice depends upon the relative precision of the experimental anisotropic couplings, the accuracy of geometrical parameters needed to calculate S_{zz} and knowledge of any anisotropy in the indirect couplings. The way these factors affect the choice in this study is now discussed.

The error in the measured dipolar couplings is dependant upon the "quality" of the anisotropic spectrum. All the relevant line positions could be measured within ±1Hz. The geometrical parameters required to calculate S_{zz} were taken from Table 4.2. As for the contribution of anisotropy in the indirect spin-spin coupling there is no information about the anisotropy in $^2J(HgF)$ but anisotropy in J coupling between a pair of fluorines is known to exist in some molecules. One way of finding evidence of

anisotropy in the indirect coupling is by calculating the same orientation parameter from different experimental anisotropic couplings. Hence S_{zz} was calculated from equations 4.4, 4.6 and 4.7, and the geometry as given in Table 4.2. If anisotropy in the indirect coupling is evident, then it will show up in the difference in the calculated S_{zz} from the three expressions.

Equations 4.4 and 4.6 are simple to solve as the only "unknowns" are the internuclear distances and bond angles. These "unknowns" can be readily obtained from the assumed geometry of bis(trifluoromethyl)mercury. Before S_{zz} can be calculated from equation 4.5, the knowledge of the preferred configuration of the trifluoromethyl group for the molecule is required. S_{zz} was determined for the staggered and eclipsed conformations and also for free rotation of the trifluoromethyls. The computer program COB3FM was written for this purpose, and its listing is shown in Appendix 4.1, and in Table 4.3 are reported the five values of S_{zz} obtained.

Table 4.3 Calculation of S_{zz} using different dipolar couplings

Method	S_{zz} [a]
$^2D(^{19}F-^{19}F)$	-.1056
$^2D(^{19}F-^{199}Hg)$	-.0412
$^4D(^{19}F-^{19}F)$ (eclipsed geometry)	-.1134
$^4D(^{19}F-^{19}F)$ (staggered geometry)	-.1139
$^4D(^{19}F-^{19}F)$ (methyl rotation)	-.1136

a) S_{zz} calculated using the Equations 4.4, 4.6 and 4.7 and the geometry listed in Table 4.2.

In Table 4.3 it is found that there are small differences in S_{zz} calculated from the observed $^2D(FF)$ and $^4D(FF)$. Also the calculations using equation 4.7 show that it is not possible to discriminate between the three conformations of bis(trifluoro methyl)mercury. The small variations in the calculated S_{zz} from $^2D_{FF}^{total}$ and $^4D_{FF}^{total}$ can be attributed to

i) Neglect of vibrational effects,

ii) Small contributions from anisotropy in the indirect spin-spin coupling.

However, S_{zz} calculated from $^2D(HgF)$ differs considerably from the values calculated from the FF dipolar couplings. The difference again would be attributed to vibrational effects, but the difference is too large to be solely caused by this effect, and it has to be said that there are significant contributions from the anisotropy in one or more of the indirect spin-spin couplings $^{2,4}J(FF)$ and $^2J(HgF)$.

Hence, as there are variations in the value of S_{zz} calculated from the three observed dipolar couplings, to continue any further it is necessary to decide which dipolar coupling should be used to determine S_{zz}. In the studies of oriented trifluoromethane [5] and methyl-trifluoromethylmercury [7] it was reported that there is only a small contribution from the anisotropy in $^2J(FF)$, and it was therefore decided to calculate S_{zz} from $^2D(FF)$. To improve the precision of S_{zz} from experimental dipolar couplings, harmonic vibrational corrections to the direct dipolar couplings were determined.

4.3.3 Force Field for bis(trifluoromethyl)mercury

The Urey Bradley force field and the geometry of bis(trifluoromethyl)mercury were obtained from Miles et al[8]. The force constants were given as diagonal elements of an F matrix. From the original force field only 5 force constants could be expressed as internal coordinates and they are reported in Table 4.4. The geometry used is reported in Table 4.2 and the description of the internal coordinates is shown in Fig 4.2. The harmonic corrections to the direct dipolar coupling were calculated with the aid of computer program VIBRA[19].

Table 4.4

Force constants for bis(trifluoromethyl)mercury[a] in Internal coordinate representation

Internal Coordinate[b]	Force constant (mdyne/A)	Internal Coordinate[b]	Force constant (mdyne/A)
f(r)	7.24	f(E)	0.1006
f(R)	2.56	f(β)	0.287
f(∝)	0.786		

a) ref[8]

b) As in Fig 4.2

4.3.4 Calculation of ^{19}F and ^{199}Hg Shielding Anisotropies

The ^{199}Hg and ^{19}F shielding anisotropies in bis(trifluoromethyl)mercury were determined as described in Chapter 3. The parameters used to calculate both shielding anisotropies are reported in Table 4.5.

Table 4.5

Selected Nmr data for determining ^{19}F and ^{199}Hg Shielding Anisotropies

Parameter	^{19}F [a]	^{19}F [b]	^{199}Hg
ν(nem)-ν(iso) /Hz [c]	-485 ±17	-233 ± 11	+5129 ±50
δ(nem)-δ(iso) /ppm	-5.8 ±.2	-2.8 ±.2	+324 ±3
$^2D_{(FF)}$	-1208.2 ±1	-609.6 ±1	-609.6 ±1
$^2D_{(FF)}$ (vib. corr.)	-1231.2 ±1	-621.0 ±1	-621.0 ±1
S_{zz} [d]	-.2323 ±.003	-.1172 ±.003	-.1172 ±.003
S_{zz} (vib. corr.) [d]	-.2367 ±.003	-.1194 ±.003	-.1194 ±.003
$\Delta\sigma$ /ppm	-37 ±1	-35 ±1	+4148 ±50
$\Delta\sigma$ /ppm (vib. corr.)	-36 ± 1	-34 ±1	+4071 ± 50

a) Using EBBA.

b) Using Phase IV

c) Positive value indicates negative shielding

d) S_{zz} calculated from geometry in Table 4.2

Plot of ^{199}Hg chemical shift against Temperature for $(CF_3)_2Hg$ in Phase IV

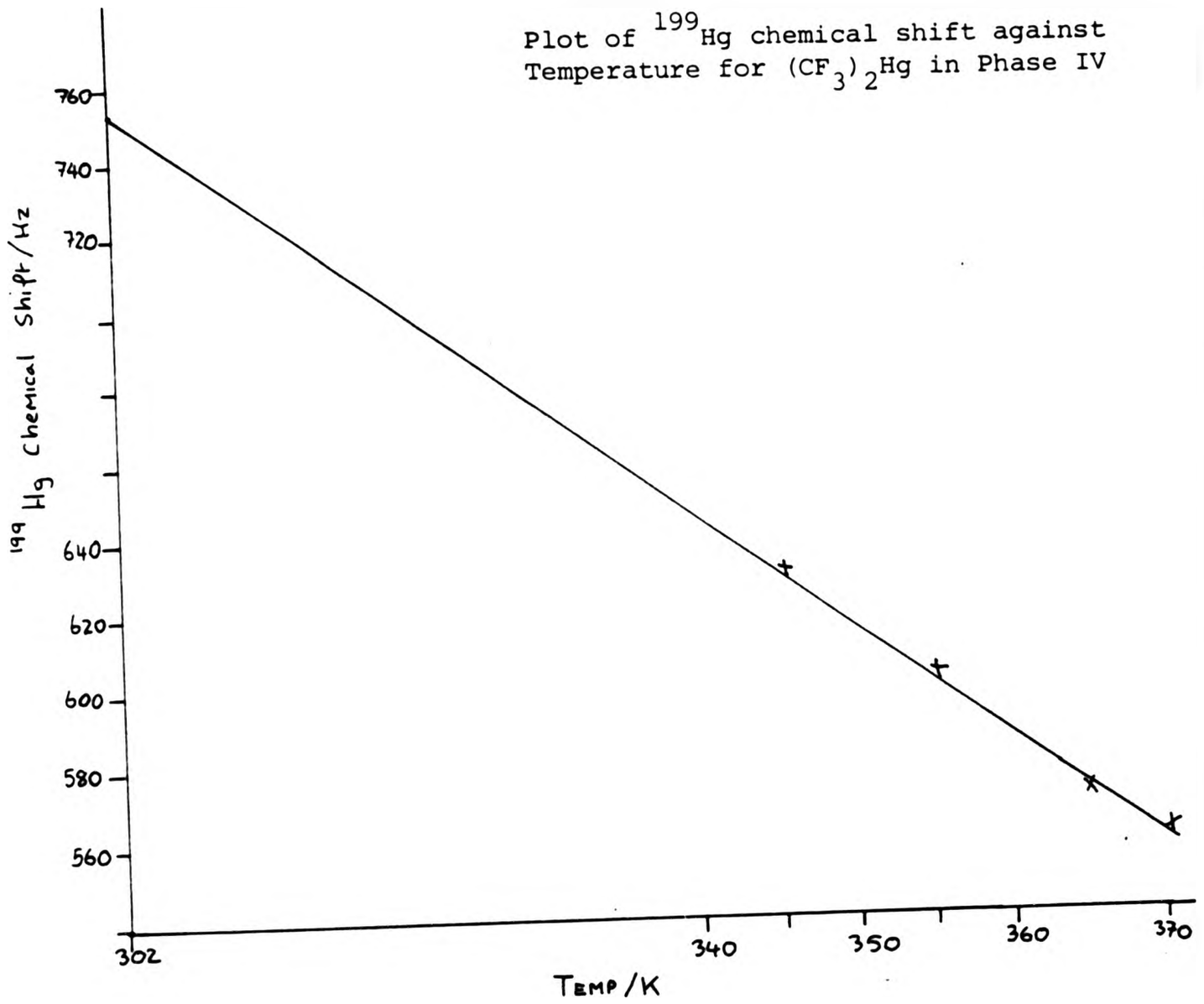

Plot of ^{19}F chemical shift against Temperature for $(CF_3)_2Hg$ in Phase IV

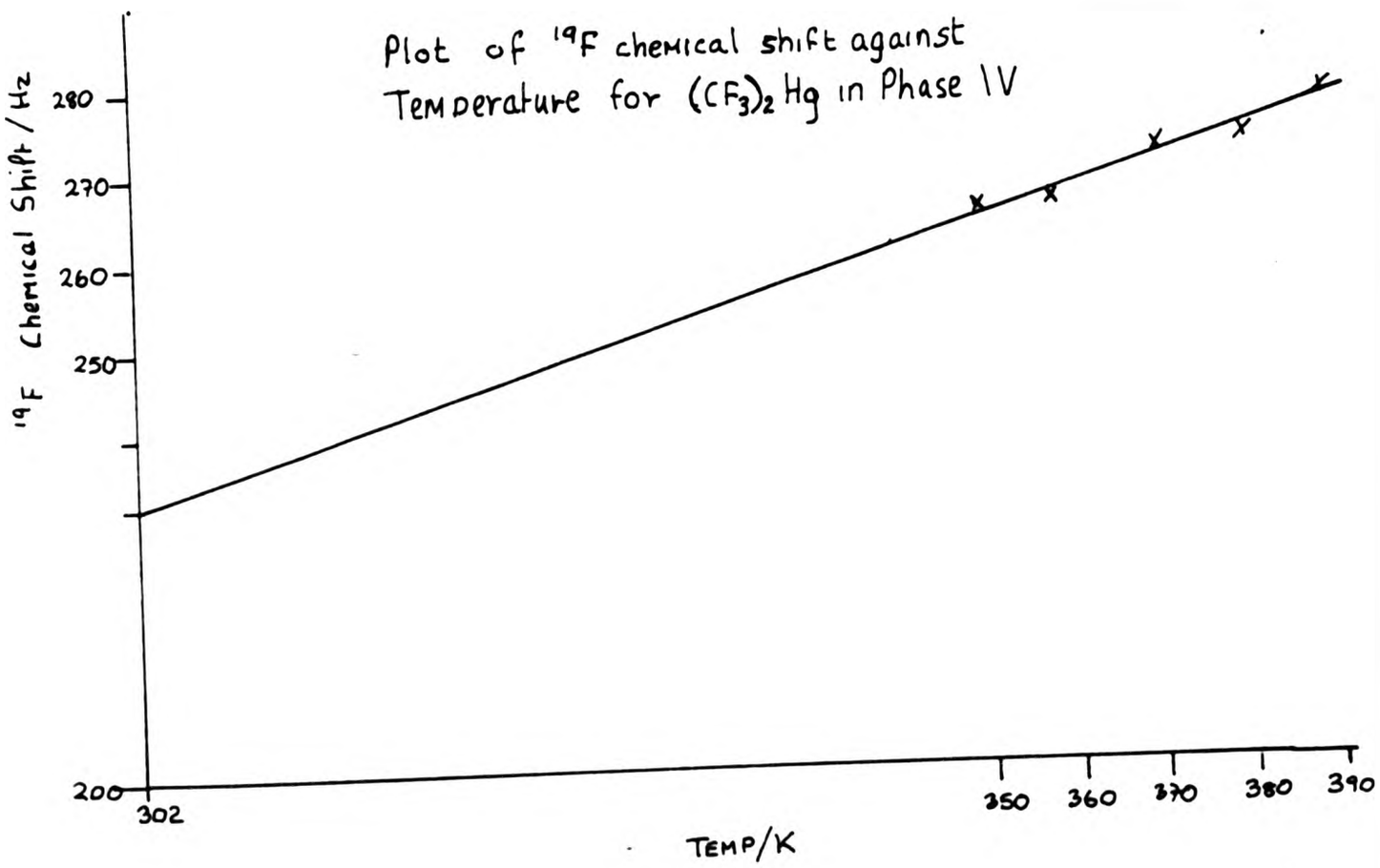

4.3.5 Calculation of the Anisotropy of the Indirect Spin-spin Coupling

The anisotropic contribution from the indirect spin-spin coupling D^{indir} was determined using the following equation.

$$D^{total} = D^{e} + D^{indir} \qquad 4.8$$

where D^{total} is the total (observed) anisotropic coupling and D^{e} is the direct dipolar coupling calculated from the equilibrium geometry with the assumption that the anisotropy from the corresponding J coupling is zero.

4.4 DISCUSSION

4.4.1 Equilibrium Geometry and J Anisotropies

The equilibrium structure of bis(trifluoromethyl)mercury is reported in Table 4.6. The determination of geometrical data from nmr spectra of oriented species relies on the same factors as listed in Sections 2.5 and 3.4. It was decided to calculate the orientation parameter S_{zz} from $^{2}D(FF)$ using the trifluoromethyl geometry as listed in Table 4.2. From the calculated value of S_{zz} the aim was to derive the geometry and/or the anisotropy in the indirect coupling from the other two measured anisotropic couplings.

One of the problems of calculation of anisotropic parameters from the nmr of oriented molecules is that they depend upon the orientation. It would be very useful if calculations were independent of orientation. Englert and coworkers [17] calculated the ratio a/b for two freely rotating groups using the ratio of $^{2}D(FF)$ and $^{4}D(FF)$.

In our case it is shown that;

$$\frac{^4D(FF)}{^2D(FF)} = -\frac{3\sqrt{3}}{\pi}\int_0^{2\pi}\frac{(\frac{a^2}{b^2}-1+\cos\phi)\,d\phi}{(\frac{a^2}{b^2}+2-2\cos\phi)^{5/2}} \qquad 4.9$$

where a is the perpendicular distance from the fluorine atom to the symmetry axis, b is the separation between 2 parallel planes containing the fluorine atoms (see fig 4.2) and ϕ is the relative rotational angle between the CF_3 groups. The value of a/b is now no longer dependant upon the orientation of the molecule and can be obtained by solving the integral numerically as described in Appendix 4.2. A value for a can be derived from the assumed geometry of the trifluoromethyl segment and from it b can be determined. This in turn will give the internuclear distance r(C-Hg). Using the value for $^4D(FF)/^2D(FF)$ with vibrational corrections, r(C-F) = 1.33A and the interbond angle for the trifluoromethyl group as 108.8°, r(C-Hg) is calculated as 2.158A ±.006A. The same calculation but without vibrational correction gave r(C-Hg) =2.134A ±.006A. The value given by Miles is 2.2A [8] but this is uncorrected for vibration and the value of 2.158 ±0.07A for the same parameter was obtained by Jokisaari and Kuonanoja in their study of methyl-trifluoromethylmercury [7]. The latter value was corrected for vibrational effects but had also a large range for the error. It is therefore not possible to say conclusively that the present results are consistent with those observed in methyl-trifluoromethylmercury, because of the large error range reported by Jokisaari and Kuonanoja. Equation 4.9 can also be used to calculate $^4D_{FF}^{ind}$ using $^2D(FF)$ and a/b for a range of methyl geometries. A graph of $^4D_{FF}^{ind}$ against a likely range of FCF inter-bond angles is shown in Fig 4.3.

Table 4.6 Calculated Geometrical Parameters and Anisotropy in $^2J(HgF)$ coupling in Bis(trifluoromethyl)mercury using Vibrationally Corrected Dipolar Couplings

	no vibrational correction	vibrational correction	percentage correction
$^2D(FF)$/Hz	-550.3 ±1	-561.1 ±1	1.94
$^4D(FF)$/Hz	+59.1 ±.5	+58.9 ±.5	0.30
$^2D(HgF)$/Hz (expt)	+23.5 ±1	+24.3 ±1	1.2
$^2D(HgF)$/Hz (calc)	+63.7	+63.8	
$^4D(FF)/^2D(FF)$	-0.1074 ±.004	-0.1050 ±.001	
S_{zz} [a]	-0.1048 ±.003	-0.1069 ±.003	
a/b [b]	4.152 ±.005	4.191 ±.005	
r(CHg)/A [c]	2.134 ±.006	2.160 ±.006	
r(HgF)/A	2.887 ±.006	2.900 ±.006	
∠ CHgF	25.7° ±.1°	25.5° ±.1°	
$^2D^{ind}(HgF)$/Hz [d]	-40.2 ±1	-39.4 ±1	
$^2J^{aniso}(HgF)$/Hz [e]	+400 ±10	+ 553 ±16	

a) Assuming r(FF)= 2.1629A and anisotropy in $^2J(FF)$ FF coupling is zero.

b) Calculated from Equation 4.9

c) Calculated from a/b where a=1.2487A and anisotropy in $^4J(FF)$ is zero

d) From Equation 4.8

e) From Equation 4.10

Fig 4.3 Plot of $^4D_{FF}^{ind}$ against Trifluoromethyl Interbond Angle

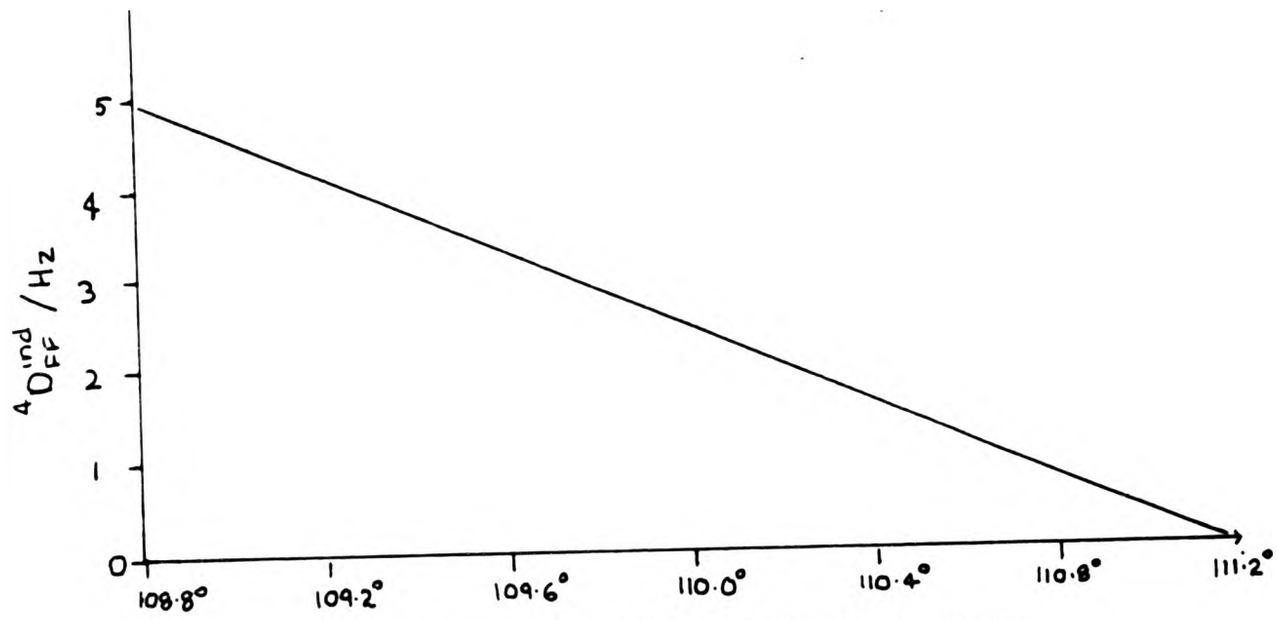

The graph shows that $^4D_{FF}^{ind}$ can vary between 0 and 5.0 Hz which is up to 9% of the experimental coupling. The results show that the importance of having the correct geometry when calculating anisotropies in the indirect couplings.

The internuclear distances r(C-Hg) and r(F-Hg) could also be determined from equation 4.6 and S_{zz} calculated from equation 4.4. $^2D(HgF)$ was determined from the splitting of the mercury satellites in the ^{19}F spectrum of the oriented molecule. The splitting is equal to $|2 . D_{HgF}^{total} + {}^2J(HgF)|$ where $^2J(HgF)$ is the isotropic spin-spin coupling measured at the same temperature as the nematic spectrum. To obtain this, $^2J(HgF)$ was measured at various temperatures above the nematic/isotropic transition temperature of the solution, and it was found that $^2J(HgF)$ was temperature independent. This procedure assumes that J(HgF) in the isotropic and nematic phases is the same. From J(HgF) and the Hg-F splitting, D_{HgF}^{total} was calculated as +24.3 Hz. The expected

direct dipolar coupling for F-Hg using the geometry calculated from the long range FF dipolar coupling was +63.0 Hz. It was possible in the case of $^4D^{total}_{FF}$ to make reasonable changes in the apparent geometry such that the difference between the observed dipolar coupling and the dipolar coupling calculated from the geometry was zero. However as there is large differences between observed and calculated F-Hg dipolar couplings the same process could not be performed here. It is possible to account for this discrepancy by:

i) A change in $^2J(HgF)$ in going from the isotropic to the nematic phase might be responsible. This explanation is unlikely as J(HgF) was found to be temperature independent at various temperatures above the nematic/isotropic transition temperature. To make D^{indir}_{HgF} vanish in equation 4.8, $^2J(HgF)$ would have to be around 1243Hz (experimental $^2J(HgF)$ = +1283 ±1 Hz), and such a change is unlikely[7].

ii) The value of r(C-Hg) in bis(trifluoromethyl)mercury is not necessarily the same as in methyl-trifluoromethylmercury. Again this is unlikely as the geometry to make D^{indir}_{HgF} vanish would correspond to a value of r(C-Hg) equal to 3.612 A and this is well outside the expected bond length (2.16 ±.05A) [7,12,13, Chapter 3].

iii) There is contribution from the anisotropy in the indirect J(HgF) coupling.

This last suggestion is probably the best explanation for the discrepancy and is not unreasonable as anisotropies in indirect couplings involving fluorines have been reported from experimental and theoretical studies[1-7]. For molecules with 3-fold symmetry

the anisotropic contribution in the indirect coupling (J^{aniso}_{HgF}) can be determined from

$$D^{indir}_{HgF} = 2.J^{aniso}_{HgF} .S_{zz} (3Cos^2\gamma-1)/3 \qquad 4.10$$

and

$$J^{aniso}_{HgF} = J^{\parallel}_{HgF} - J^{\perp}_{HgF} \qquad 4.11$$

In equation 4.11, γ is the angle the internuclear vector Hg-F makes with the z axis (or C_{3v} symmetry axis), and $J^{\parallel}$ and $J^{\perp}$ are the indirect couplings measured parallel and perpendicular to the symmetry axis. S_{zz} was calculated from the experimental $^2D(FF)$ and D^{indir}_{HgF} from equation 4.8. J^{aniso}_{HgF} was calculated as +390 Hz, which is 30% of the corresponding isotropic coupling, assuming that the discrepancy to be completely due to the anisotropy in $^2J(HgF)$. There are no theoretical or experimental estimates previously reported on anisotropy in any Hg-F couplings, but it is not unreasonable to expect large anisotropies in indirect couplings involving fluorines[1-7].

$^2D^{indir}_{FF}$ and $^2D^{indir}_{HgF}$ were calculated by assuming that the measured anisotropic coupling $^4D(FF)$ was purely dipolar for a range of geometries. From equations 4.8 and 4.9 it can be seen that by varying the FCF inter-bond angle between 108.8^o and 109.3^o, $^2D^{indir}_{FF}$ can vary by up to 4% of the value of the corresponding experimental dipolar coupling. For the same calculation D^{indir}_{HgF} varies between 370-390Hz depending on the geometry. Thus the results show that $^{2,4}D^{indir}$ couplings are very sensitive to geometry whereas J^{aniso}_{HgF} is not.

4.4.2 ^{199}Hg Shielding Anisotropy

The theory of mercury chemical shifts and its application to linear mercuric molecules have been discussed in Section 3.4.3 . It is predicted from the theory that in the linear molecule dimethylmercury the mercury shielding anisotropy should be close to its maximum value; in terms of covalent bonding this implies that the atom mercury in dimethylmercury uses only $6p_z$ orbitals, the $6p_x$ and $6p_y$ orbitals being left vacant. The observed shielding anisotropy for the mercury in dimethylmercury was +7500ppm which corresponds to $\sigma_\perp$ = -2500ppm and $\sigma_{\parallel}$ = +5000ppm where $\sigma_{\parallel}$ and $\sigma_\perp$ are shieldings when the applied magnetic field direction and the symmetry axis are parallel and perpendicular to each other [14]. These magnitudes of shieldings about the two axes corresponds to the electrons in the close vicinity of the mercury having unrestricted electronic circulation when the symmetry axis and the magnetic field direction are parallel, and highly restricted when they are perpendicular. In bis(trifluoromethyl)mercury, $\Delta\sigma(^{199}Hg)$ and the isotropic mercury shielding were observed to be +4071 ppm and +1430 ppm (relative to mercury in dimethylmercury) respectively. This corresponds to $\sigma_{zz} = \sigma_{\parallel}$ = +3998 ppm and $\sigma_\perp = \sigma_{xx} = \sigma_{yy}$ =-73 ppm. Comparison with the dimethylmercury results show an increase in $\sigma_\perp (=\sigma_{xx,yy})$ and decrease in $\sigma_{\parallel}(\sigma_{zz})$ in bis(trifluoromethyl)mercury. This implies that the electronic circulation about the mercury in bis(trifluoromethyl)-mercury is reduced parallel to the symmetry axis and increased perpendicular to the same axis. In terms of covalent bonding for the Hg-C bond it can be said that there is an increase in occupancy in the mercury $6p_x$ and $6p_y$ orbitals and reduced occupancy in the $6p_z$ orbitals in bis(trifluoromethyl)mercury

when compared with the mercury in dimethylmercury. The change observed between dimethylmercury and bis(trifluoromethyl)mercury can be said to be due to the electron attracting power of the fluorines.

4.4.3 ^{19}F Shielding Anisotropy

The theory of fluorine chemical shifts has been discussed along the same lines as mercury chemical shifts[16]. As a first approximation, the paramagnetic contribution to the shielding will be dominant and one would expect the local electrons around the fluorine to have the greatest effect upon the fluorine chemical shifts. However problems can arise in theoretical studies of ^{19}F chemical shifts from the presence of rotational and conformational isomerism, especially in the calculation of fluorine shielding constants in saturated fluorinated organic molecules. The fluorine shielding anisotropy in bis(trifluoromethyl)mercury was measured as -35ppm ±1ppm. The shielding anisotropy measurements of molecules partially oriented in liquid crystal can only yield the anisotropy relative to the symmetry axis[22]. In the case of the mercury shielding anisotropy measurements we were able to calculate the shielding anisotropy about the C-Hg-C linear skeleton because the symmetry axis and the C-Hg-C direction coincided. Also axial symmetry, i.e $\sigma_{xx}=\sigma_{yy}$ can be assumed. The fluorine shielding anisotropy measurement as determined from one orientation is relative to the symmetry axis and not along a particular bond. The fluorine shielding anisotropy calculated using equation 4.5 also assumes axial symmetry and this can be argued to be not completely correct. In order to calculate the fluorine shielding anisotropy along the CF

bond the following transformation is made:

$$\Delta\sigma\,(\text{bond})\ [3\text{Cos}^2\psi-1] = \Delta\sigma\,(\text{sym axis}) \qquad 4.12$$

and $$\Delta\sigma\,(\text{bond}) = \sigma_{zz} - \tfrac{1}{2}(\sigma_{xx} + \sigma_{yy}) \qquad 4.13$$

where ψ is the angle the bond direction makes with the symmetry axis. Equation 4.14 assumes unaxial symmetry. From the observed $\Delta\sigma$ (sym), $\Delta\sigma$ (bond) is calculated as +107 ppm. The positive anisotropy when calculated along the CF bond is what one would expect from the theory of covalent bonding[12,13,23]. A study of trifluoromethane trapped in p-quinol clathrates gave the fluorine shielding anisotropy $\sigma_{\parallel} - \sigma_{\perp} = +105 \pm 20$ppm, where $\sigma_{\perp}$ is the average of the two components of the shielding tensor perpendicular to the CF bond direction[23]. The result with respect to the symmetry axis was -35ppm ±10ppm. However a study of the same molecule in a liquid crystal and assuming axial symmetry gave a value for $\Delta\sigma\,(^{19}F)$ along the CF bond direction of +260ppm[24]. Other results on fluorine shielding anisotropies along the CF bond in CF_3 derivatives determined from nmr studies of oriented molecules in liquid crystals show they can vary between -157 and +230ppm[25]. As our results are in agreement with theoretical results obtained for the fluorine shielding anisotropy about the CF bond, it appears that the calculation of fluorine shielding in bis(trifluoromethyl)mercury need only include shielding from the immediate electron cloud surrounding the fluorine. However it can be argued from the range of fluorine shielding anisotropies about the CF bond reported on a series of saturated fluorinated organic compounds, that agreement in our case may be coincidental. There are no experimental results reported on molecules similar to bis(trifluoromethyl)mercury to compare with the present one. However the former argument is preferred on the grounds that the

mercury in bis(trifluoromethyl)mercury is some distance away from the CF_3 group, and the approximation of only including the shielding from the immediate electron cloud around the fluorine nucleus is valid. The discrepancy in the experimental results of fluorine chemical shifts on small saturated organic molecules containing fluorines can be due to the problem of obtaining a unique orientation over the whole anisotropic phase. This is a problem sometimes experienced in the nmr of molecules oriented in liquid crystal where it has been found that molecules may take up more than one orientation in the anisotropic phase[26]. In the case of bis(trifluoromethyl)mercury the long linear skeleton ought to eliminate problems of different orientations at different sites over the anisotropic phase. The geometry deduced in the present work confirms this.

4.5 Conclusion

The use of nematic liquid crystal has permitted the determination of the equilibrium geometry and sign of indirect couplings in bis(trifluoromethyl)mercury. The assignments of the signs of the indirect couplings were made from the sign of the mercury shielding anisotropy. Both the equilibrium geometry and the sign of $^2J(HgF)$ are consistent with those obtained from other methods, and in similar molecules. The sign of $^4J(FCHgCF)$ was shown to be positive in this molecule.

The results show definite evidence of anisotropy in $^2J(HgF)$ and this is 30% of the value of the isotropic coupling. There is no theoretical or previous experimental evidence of anisotropic contributions to this coupling, but it is not unreasonable to

mercury in bis(trifluoromethyl)mercury is some distance away from the CF_3 group, and the approximation of only including the shielding from the immediate electron cloud around the fluorine nucleus is valid. The discrepancy in the experimental results of fluorine chemical shifts on small saturated organic molecules containing fluorines can be due to the problem of obtaining a unique orientation over the whole anisotropic phase. This is a problem sometimes experienced in the nmr of molecules oriented in liquid crystal where it has been found that molecules may take up more than one orientation in the anisotropic phase[26]. In the case of bis(trifluoromethyl)mercury the long linear skeleton ought to eliminate problems of different orientations at different sites over the anisotropic phase. The geometry deduced in the present work confirms this.

4.5 Conclusion

The use of nematic liquid crystal has permitted the determination of the equilibrium geometry and sign of indirect couplings in bis(trifluoromethyl)mercury. The assignments of the signs of the indirect couplings were made from the sign of the mercury shielding anisotropy. Both the equilibrium geometry and the sign of $^2J(HgF)$ are consistent with those obtained from other methods, and in similar molecules. The sign of $^4J(FCHgCF)$ was shown to be positive in this molecule.

The results show definite evidence of anisotropy in $^2J(HgF)$ and this is 30% of the value of the isotropic coupling. There is no theoretical or previous experimental evidence of anisotropic contributions to this coupling, but it is not unreasonable to

expect large anisotropic contributions to J(HgF), as there are numerous examples of anisotropies involving fluorines, and in some cases they also have large magnitudes[1-7].

The anisotropic contributions to $^{4}J(FF)$ and/or $^{2}J(FF)$ appear to be small in bis(trifluoromethyl)mercury, and by small (and reasonable) changes in the geometry these apparent contributions can be made to vanish. This is a problem experienced in determining geometries by nmr of oriented molecules in that either the geometry or the anisotropic contribution in the indirect coupling can be calculated. However the latter parameter can be accurately determined if the geometry is known and the geometry is independent of orientation.

The mercury shielding anisotropy in bis(trifluoromethyl)-mercury was observed to be +4071 ppm, which is about half the value obtained for the mercury shielding anisotropy in dimethylmercury. This suggests that the replacement of protons by fluorines must cause an overall orbital electron imbalance and hence change the shielding environment at the mercury nucleus in bis(trifluoromethyl)mercury. In terms of bonding, the mercury in $(CH_3)_2Hg$ uses only $6p_z$ orbitals and the $6p_x$ and $6p_y$ orbitals are left vacant, whereas the mercury in $(CF_3)_2Hg$ there now exist occupancy of $6p_x$ and $6p_y$ orbitals but a reduced occupancy in $6p_z$ orbitals (compared to dimethylmercury).

The fluorine shielding anisotropy along the CF bond in bis(trifluoromethyl)mercury was calculated to be +107 ppm and is consistent with that determined experimentally and theoretically by Harris on trifluoromethane[23]. The results here suggest that the paramagnetic contribution to the fluorine shielding dominates

and it is the local electrons which contribute to the fluorine chemical shift.

APPENDIX 4.1

Listing of the Computer Program COB3FM

```
C       ***** PROGRAM COB3FM.FOR *****
        DIMENSION XCOORD(2),YCOORD(2),ZCOORD(2)
        RCHG=2.23
        RCF=1.33
        ANGMTH=109.3
        D6FF=59.0
        KFF =106265.
        THETA=ANGMTH
        THETB=0.5*(180.0-THETA)
         RFF  = SIND(THETA)*RCF/SIND(THETB)
         XO   = RFF * SIND(30.)/SIND (120.0)
         ZO   = SQRT((RCF*RCF)-(XO*XO))
        XCOORD(1)= XO
        YCOORD(1)= 0.0
        ZCOORD(1)= 0.0
        XCOORD(2)=0.0
        YCOORD(2)=0.0
        ZCOORD(2)=2*(RCHG++ZO)
        ROTAT=0.0
        ATOT=0
20      ROTAT=ROTAT+1.
        IF(ROTAT.GT.360.0)GOTO 40
        ATOT=ATOT+1
        XCOORD(2)=XCOORD(1)*COSD(ROTAT)
        A(2)=XCOORD(1)*SIND(ROTAT)
        RI=SQRT((XCOORD(1)-XCOORD(2))**2+
     1+(YCOORD(1)-YCOORD(2))**2+
     1+(ZCOORD(1)-ZCOORD(2))**2)
        RI3=RI**3
        ALPHAZ=((ABS(ZCOORD(1)-ZCOORD(2)))/RI)**2
        SDR=(3*ALPHAZ-1)/RI3
        TOTSDR=SDR+TOTSDR
        SDR=0.0
        GO TO 20
40      SZZ=2.*D6FF/(KFF*(TOTSDR/ATOT))
        TYPE 30,SZZ,ATOT
30      FORMAT(2F)
        RETURN
        END
```

APPENDIX 4.2

Computation of Integral in Equation 4.9

Using Simpson's rule :

$$f(x)dx = -[f(o) + f(2n) + 4(f(1)+f(3)+f(5)+....+f(2n+1) + 2(f(2)+f(4)+f(6)+....+f(2n-2)] \quad 4.14$$

where $$f(x)dx = -\frac{3\sqrt{3}}{\pi}\int_{0}^{2\pi}\frac{(\frac{a^2}{b^2}-1+\cos\phi)\,d\phi}{(\frac{a^2}{b^2}+2-2\cos\phi)^{5/2}}$$

and $$f(n)dx = \frac{\frac{a^2}{b^2}-1+\cos(n)}{\left(\frac{a^2}{b^2}+2-2\cos(n)\right)^{5/2}}$$

and h= interval, and f(n)= n^{th} point.

The following computer program was used to calculate the integral in Equation 4.12.

```
C          ****DRATIO.FOR****
13       type 10
10       format(' A/B')
         ACCEPT 20,ADB
20       FORMAT (4F)
         DRATIO=0.0
         ADB2=ADB**2
         CONST=3*SQRT(3.0)/3.14159
         S=0.0
63       CONTINUE
         IF(S.EQ.0.0)GOTO 60
         IF(S.EQ.360.0)GOTO 60
         ANUMER=ADB2-1.0+COSD(S)
         DENOM=(ADB2+2-(2*(COSD(S))))**2.5
         DRATIO=DRATIO+(4*ANUMER/(DENOM))
         S=S+1.0
         ANUMER=ADB2-1.0+COSD(S)
         DENOM=(ADB2+2-(2*(COSD(S))))**2.5
         DRATIO=DRATIO+(2*ANUMER/(DENOM))
         GOTO 61
60       DENOM=(ADB2+2-(*COSD(S))))**2.5
         ANUMER=ADB2-1.0+COSD(S)
         DRATIO=DRATIO+(ANUMER/(DENOM))
61       S=S+1.0
         IF(S.GE.360.0) GOTO 62
         GOTO 63
62       DRATIO=DRATIO*CONST*2*3.14159/(360.0*3)
         TYPE 20,ADB,DRATIO
         TYPE 21
```

```
21      FORMAT(' ?')
        ACCEPT 20,ANGLE
        HALF=0.5*(180.-ANGLE)
        RFF=1.33*SIND(ANGLE)/SIND(HALF)
        A=RFF*SIND(30.)/SIND(120.0)
        B=A*ADB
        CO=SQRT(1.33**2-A**2)
        CHG=0.5*(B-(2*CO))
        WRITE (5,20),ADB,DRATIO,CHG
        GOTO 13
        RETURN
        END
```

4.6 References

1 J. Gerritsen and C. MacLean, Spectrchimica Acta, 27A, 1495(1971); J. Gerritsen and C. MacLean, Rec. Trav. Chim. Pays-Bas 91, 1393(1972); J. Gerritsen, G. Koopmans, H.S. Rollema and C. MacLean, J. Mag. Res., 8, 20(1972); G J. den Otter, J. Gerritsen and C. MacLean, J. Mol. Struct, 16, 379(1973); G.J den Otter, W. Heijser, and C. MacLean, J. Mag. Res., 13, 11(1974); G.J. den Otter, W. Heijser, and C. MacLean, J. Mol. Struct., 31, 47(1976).

2 J. Degelaen, P. Diehl and W. Niederberger, Org. Mag. Res., 4, 721(1972).

3 G.J. den Otter and C. MacLean, J. Mag. Res., 20, 11(1975).

4 T.R. Krugh and R.A. Bernheim, J. Amer. Chem. Soc., 91, 2385 (1969).

5 G.J. den Otter, J. Bulthuis and C.A. deLange, J. Mag. Res., 20, 67(1975).

6 J. Bulthuis and C.A. deLange, J. Mag. Res., 14, 13(1974).

7 J. Jokisaari and J. Kuonanoja, J. Mol. Struct., 68, 173(1980).

8 M.G. Miles, J.H. Patterson, C.W. Hobbs, M.J. Hooper, J. Overend, R S. Tobais, Inorganic Chemistry, 7, 1725(1968).

9 K.A. Mclauchlan, D.H. Wiffen and L.W. Reeve, Mol. Phys., 10, 131(1966); A.D. Buckingham and K.A. McLauchlan, Prog. in

Nmr., 2, 63(1967); E.L. Mackor and C. MacLean, J. Chem. Phys., 42, 64(1966); E.L. Mackor and C. MacLean, Proc. Phys. Soc. (London), 88, 342(1966).

10 M. Karplus and D.M. Grant, Proc. Nat. Acad. Sci. U.S., 45, 1269(1959); N. Muller and D.E. Pritchard, J. Chem. Phys., 31, 768(1959); ibid 1471(1959); J.N. Shoolery, J. Chem. Phys., 31, 1427(1959).

11 G. Englert and A. Saupe, Mol. Cryst., 1, 503(1966); R.A. Bernheim and B.J. Lavery, J. Amer. Chem. Soc, 89, 1279(1967); T.R. Krugh and R.A. Bernheim, J. Chem. Phys, 52, 4942(1970).

12 J. Jokisaari and P. Diehl, Org. Mag. Res., 13(5), 359,(1980).

13 J.D. Kennedy and W. McFarlane, J. Chem. Soc. Farad. Trans. 2, 1653(1976).

14 C.J. Jameson and H.S. Gutowsky, J. Chem. Phys., 40, 1714(1964).

15 N.F. Ramsey, Phys. Rev., 91, 303(1953).

16 M. Karplus and D.J. Day, J. Chem. Phys., 34, 1683(1961).

17 G. Englert, Z. Naturforsch, 24A, 1075,(1969).

18 C.M. Woodman, Mol. Phys., 13, 365(1967)

19 S. Sýkora, J. Vogt, H. Bösiger and P. Diehl, J. Mag. Res., 36, 53(1979).

20 L.A. Fedorov, Z.A. Stumbrevichyute and E.I. Fedin, J. Strukt. Chem., 16, 899(1975).

21 P.L. Goggin, (unpublished work).

22 A Saupe, Z Naturforsch, A19, 161(1964).

23 A.B. Harris, E. Hunt, and H. Meyer, J. Chem. Phys., 42, 2851 (1965).

24 R.A. Bernheim, D.J. Hoy, T.R. Krugh, and B.J. Lavery, J. Chem. Phys., 50, 1350(1969).

25 P.K. Bhattacharya and B.P. Dailey, J. Mag. Res., 13. 317(1974); T.R. Krugh and R.A. Bernheim, J. Amer. Chem. Soc, 89, 6784(1967); D.N Silverman and B.P. Dailey, J. Chem. Phys., 51, 623(1969); G.P. Ceasar, C.S. Yannoni and B.P Dailey, J. Chem. Phys., 54 4021(1971).

26 L.C. Snyder and S. Meiboom, J. Chem. Phys., 44, 4057(1966); P. Diehl, M. Reinhold, A.S. Tracey and E. Wullschleger, Mol. Phys., 30, 1781(1975); E.E. Burnell, J.R. Council and S.E. Ulrich, Chem. Phys. Letts., 31, 395(1975).

Chapter 5

STUDY OF THE PENTAFLUOROPHENYL PHOSPHORUS SYSTEM ORIENTED IN MERCK PHASE IV AND V

5.1 Introduction

Aromatic substituted phosphines of the form $(C_6X_5)_3P$ are of interest as some of their structures have been determined by X-ray diffraction[1-3], and the geometrical parameters obtained by nmr can then be compared with previously reported values. Where their structures have not been previously determined, their geometries can be assumed from those of similar molecules. For example the structural data for tris(pentafluorophenyl)phosphine can be obtained by transferring the relevant geometrical parameters from triphenylphosphine and pentafluorobenzene. In order to determine geometry by liquid crystal nmr it is necessary to analyse the appropriate anisotropic spectrum, and this may not always be possible for molecules with a large number of spins. For instance, the proton spectrum of oriented triphenylphosphine involves the analysis of a 16 spin (15 protons and one phosphorus) system, and even if all the lines were well resolved this would not be feasible. However, by isotopic substitution and proton decoupling the effective number of spins can be reduced, and hence the anisotropic nmr spectrum can be simplified. In the case of triphenylphosphine substitution of deuterons for protons in two of the phenyl groups would simplify the anisotropic spectrum into a six spin system, which can be analysed using existing computer programs[4,5]. Even so, the analysis is not entirely straightforward because of the small chemical shift differences between different types of protons. Another interesting molecule

similar to triphenylphosphine is tris(pentafluorophenyl)phosphine. In order to obtain the relevant information to determine its geometry, it would again be necessary to analyse a 16 spin (15 fluorines and one phosphorus) system. By replacement of the fluorines in two of the pentafluorophenyl groups by protons (to give pentafluorophenyldiphenylphosphine) the symmetry of the molecule can be reduced, and the analysis of its ^{19}F anisotropic spectrum would now involve a six spin system, if proton decoupling is used. The analysis of this anisotropic spectrum can now yield the relevant anisotropic parameters and the geometry of the pentafluorophenyl phosphorus system ($P(C_6F_5)$).

Various fluorinated benzenes partially oriented in liquid crystals have been studied to obtain information on geometries, orientations and anisotropy in the indirect couplings[6-10]. Earlier work involved estimating the geometry and anisotropic parameters from proton and ^{19}F nmr spectra. Later on, the determination of natural abundance carbon-13 satellites was included in the calculations[9]. These results showed that geometries deduced by nmr were in good agreement with those obtained from micro-wave and electron diffraction data. Analysis of the nmr spectra of ortho-difluorobenzene[9] and several tetrafluorobenzenes [6,10] partially oriented in a nematic solvent also provided evidence of anisotropic contributions from the $^{19}F-^{19}F$ indirect spin-spin couplings. The F-F indirect couplings had up to 3 percent anisotropy relative to the corresponding direct dipolar couplings. In the case of $D^{indir}_{FF(meta)}$ in tetrafluorobenzenes there was also good agreement with theoretical calculations[10]. A study of pentafluorobenzene[10] in a liquid crystal was also used to estimate the

anisotropic contributions from the indirect FF couplings, and the geometry determined after taking into account these contributions was consistent with that obtained for similar molecules. The present study of the pentafluorophenyl phosphorus system in pentafluorophenyldiphenylphosphine ($P(C_6F_5)(C_6H_5)_2$) by oriented nmr similarly permits the determination of its geometry and the anisotropy of the indirect F-F couplings.

Very little work has been carried out on the nmr of fluorinated phosphines oriented in liquid crystals, and so little is known about the anisotropy of J(PF) couplings. The geometries of phosphorus trifluoride[11] and thiophosphoryl fluoride (F_3PS) [12] determined by oriented nmr were in good agreement with micro-wave and electron diffraction results. In phosphoryl fluoride (F_3PO) the value for the FPF inter-bond angle estimated by oriented nmr was smaller by 3^o than that obtained by electron diffraction [13]. The disagreement between the two results was explained in terms of anisotropic contributions to the indirect F-F and/or P-F couplings, or by a variation of the molecule's geometry with orientation in the anisotropic phase. The present study permits determination of anisotropies of J(PF) couplings in the pentafluorophenyl phosphorus system.

The absolute signs of indirect spin-spin couplings have often been obtained from the nmr study of molecules oriented in a liquid crystal[14, Chapter 4]. The sign of $^3J(PF)$ cannot be determined directly from the analysis of the ^{19}F or the ^{31}P isotropic spectra of the $P(C_6F_5)$ system. However it can be determined from the analysis of the anisotropic ^{19}F spectrum provided a sufficiently accurate geometry of the $P(C_6F_5)$ unit is available.

5.2 Experimental

Pentafluorophenyldiphenylphosphine was synthesized using the method described elsewhere[15]. The nematic samples were prepared in Merck Phase IV and V as described in Chapter 3. The solute concentrations employed were approximately 3.5 to 4.0% by weight.

All ^{19}F spectra were recorded as described in Chapter 4. ^{31}P nmr spectra were obtained on a Jeol FX90Q spectrometer operated in the FT mode, and equipped for variable temperature operation, at a measuring frequency of 36.2 MHz. The anisotropic spectrum was recorded with a spectral width of 1000 Hz and a pulse width of 22μs. The transformation of the FIDs from 500 scans gave an average line width of 10 Hz for this spectrum. For the recording of the isotropic spectrum fewer scans were needed and the line width was about 1 Hz over the whole spectrum. All ^{19}F and ^{31}P spectra were acquired with external ^{2}D lock and complete proton decoupling.

The nmr spectra from the oriented samples were analysed using the computer program LAOCOON LC[5] and the isotropic spectrum was analysed using the computer program LAOCOON 1968[16]. The calculated spectrum was plotted as described in Section 3.2.

5.3 Results

5.3.1 Anisotropic and Isotropic Couplings

The $^{31}P\ \{^{1}H\}$ and $^{19}F\ \{^{1}H\}$ isotropic nmr spectra of pentafluorophenyldiphenylphosphine dissolved in Phase V above its nematic/isotropic transition temperature are shown in Figs 5.1 and 5.2 respectively. The ^{31}P spectrum is a triplet with splitting

corresponding to $^{3}J(PF)$. The indirect spin-spin couplings $^{4}J(PF)$ and $^{5}J(PF)$ could not be determined from the isotropic ^{31}P spectrum as their magnitudes were smaller than the line width in this spectrum (less than 1Hz). However they were obtained from the study of the same molecule in benzene by Graham and Hogben [17].

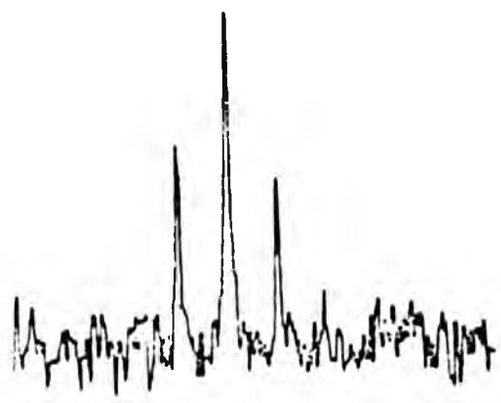

Fig 5.1 ^{31}P $\{^{1}H\}$ Isotropic nmr spectrum of Pentafluorophenyldiphenylphosphine in Phase V.

The isotropic ^{19}F nmr spectrum of the phosphorus pentafluorophenyl system was analysed along the same lines as described by Hogben and Graham[17], and by Grant, Hirst and Gutowsky[18]. The absolute signs of all the indirect ^{19}F-^{19}F couplings were transferred from spin-tickling experiments carried out by Lustig et al[19]. The correctness of our analysis was verified by comparing the experimental isotropic spectrum with that calculated using the computer program LAOCOON 1968[16]. The isotropic coupling constants and the chemical shifts obtained in

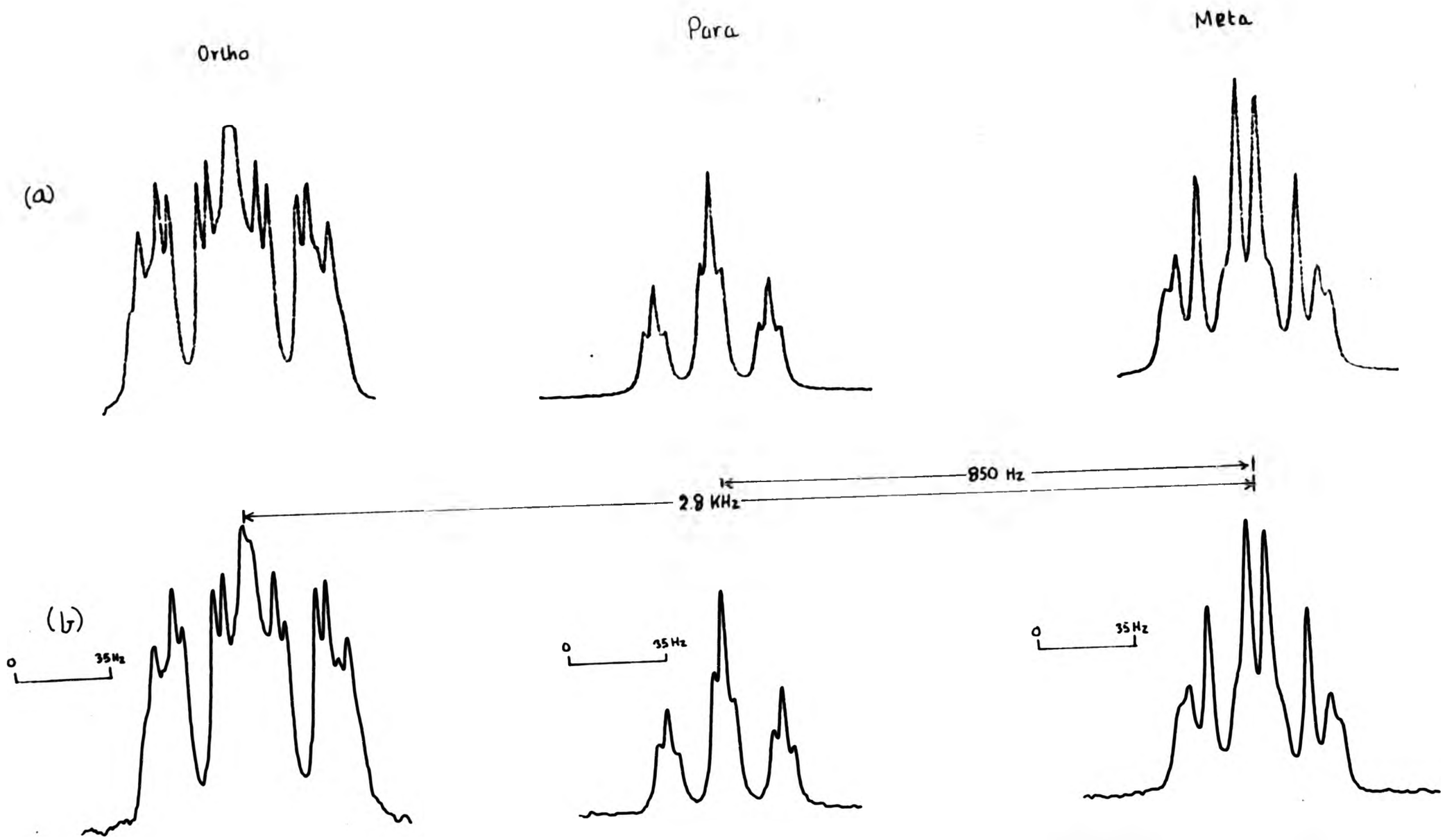

Fig 5.2 84.26 MHz $^{19}F\{^1H\}$ isotropic nmr spectra of $(C_6F_5)(C_6H_5)_2P$ in Phase V (a) Computed, (b) Experimental

this way for the pentafluorophenyl phosphorus system are reported in Table 5.1. The ^{19}F spectrum calculated using these parameters is shown in Fig 5.2(b).

Table 5.1 (^{19}F ^{19}F) and (^{31}P ^{19}F) Isotropic Couplings in the Phosphorus Pentafluorophenyl System.

	J^a		J^a
$^3J(PF_2)=^3J(PF_6)$	36.6	$^4J(F_2F_4)=^4J(F_4F_6)$	+4.0
$^4J(PF_3)=^4J(PF_5)$	0.6	$^4J(F_2F_6)$	-4.5
$^5J(PF_4)$	0.6	$^4J(F_3F_5)$	-1.5
$^3J(F_2F_3)=^3J(F_5F_6)$	-24.1	$^5J(F_2F_5)=^5J(F_3F_6)$	+9.5
$^3J(F_3F_4)=^3J(F_4F_5)$	-20.9		

a) Indirect coupling constants in Hz Numbering as in Figure 5.5.

The ^{31}P nmr spectrum of the oriented pentafluorophenyl phosphorus system is shown in Fig 5.3. It is a triplet of triplets of doublets. The spacing within each multiplet is equal to $|2\,D(PF)+J(PF)|$, where D is total anisotropic coupling and J is the appropriate indirect spin-spin coupling. The spacings a and b (see fig 5.3) correspond to $|2\,^3D(PF)+^3J(PF)|$ and $|2\,^4D(PF)+^4J(PF)|$ respectively, and c yields $|2\,^5D(PF)+^5J(PF)|$. As the signs of the splittings and the indirect couplings are unknown there is more than one value of each D(PF) coupling determined from the splitting, and the corresponding indirect coupling. Hence, from the splittings $|2D+J|$ and the J couplings measured from the isotropic spectrum, several possible values of D(PF) for each PF interaction were determined. However, the correct set of values of D(PF) for each P-F interaction was

obtained from the analysis of the oriented ^{19}F spectrum and an assumed geometry.

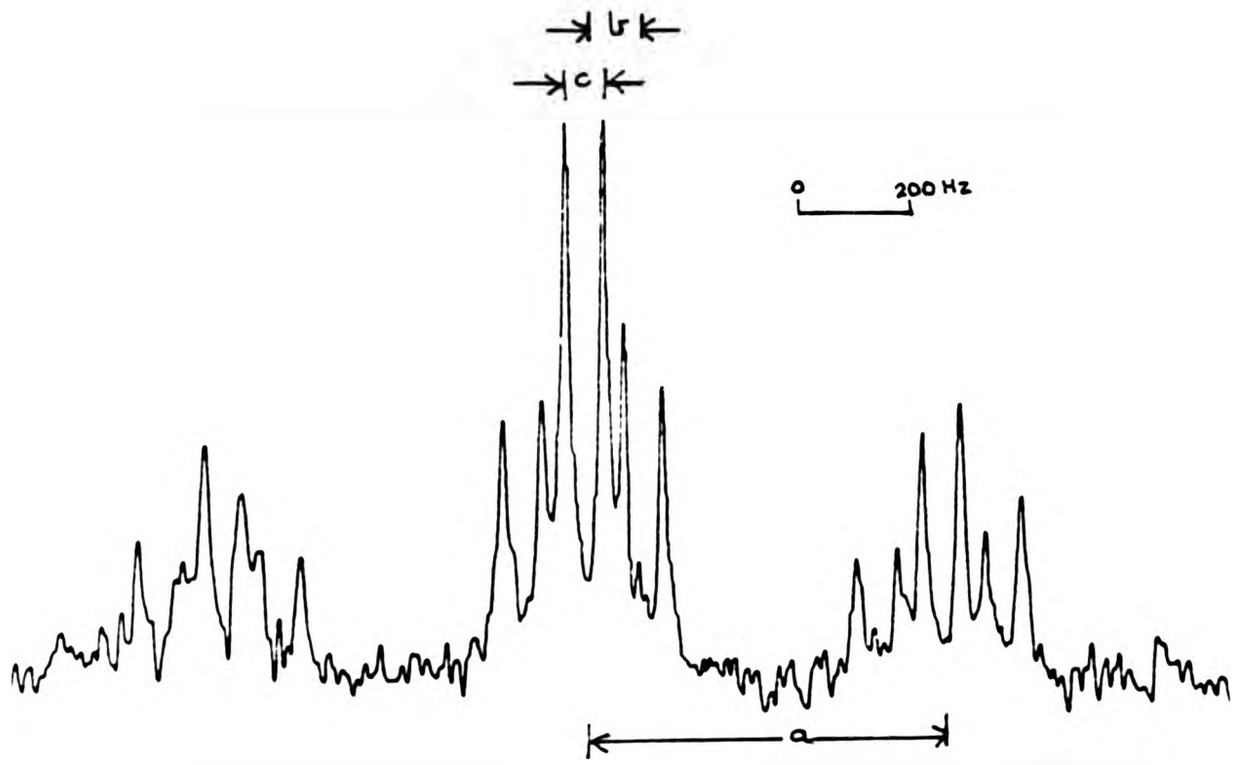

Fig 5.3 $^{31}P\{^{1}H\}$ nmr spectrum (36.2MHz) of $P(C_6F_5)(C_6H_5)_2$
Partially oriented in Phase V

The ^{19}F spectrum of the oriented pentafluorophenyl phosphorus system is depicted in Fig 5.4. It was analysed as that of an AA'BB'CX spin system (A=B=C=^{19}F and X=^{31}P) using the computer program LAOCOON LC[5]. The analysis involved calculating trial spectra from a set of chemical shifts, and indirect spin-spin and anisotropic couplings, using the computer program until the computed spectrum and the experimental spectrum were "visually alike". Visually alike means that the calculated and the experimental spectra look similar in all the major structural features of the spectrum. For a more accurate analysis, the iteration option available in the program was then used to obtain the parameters that gave the best fit to the experimental spectrum.

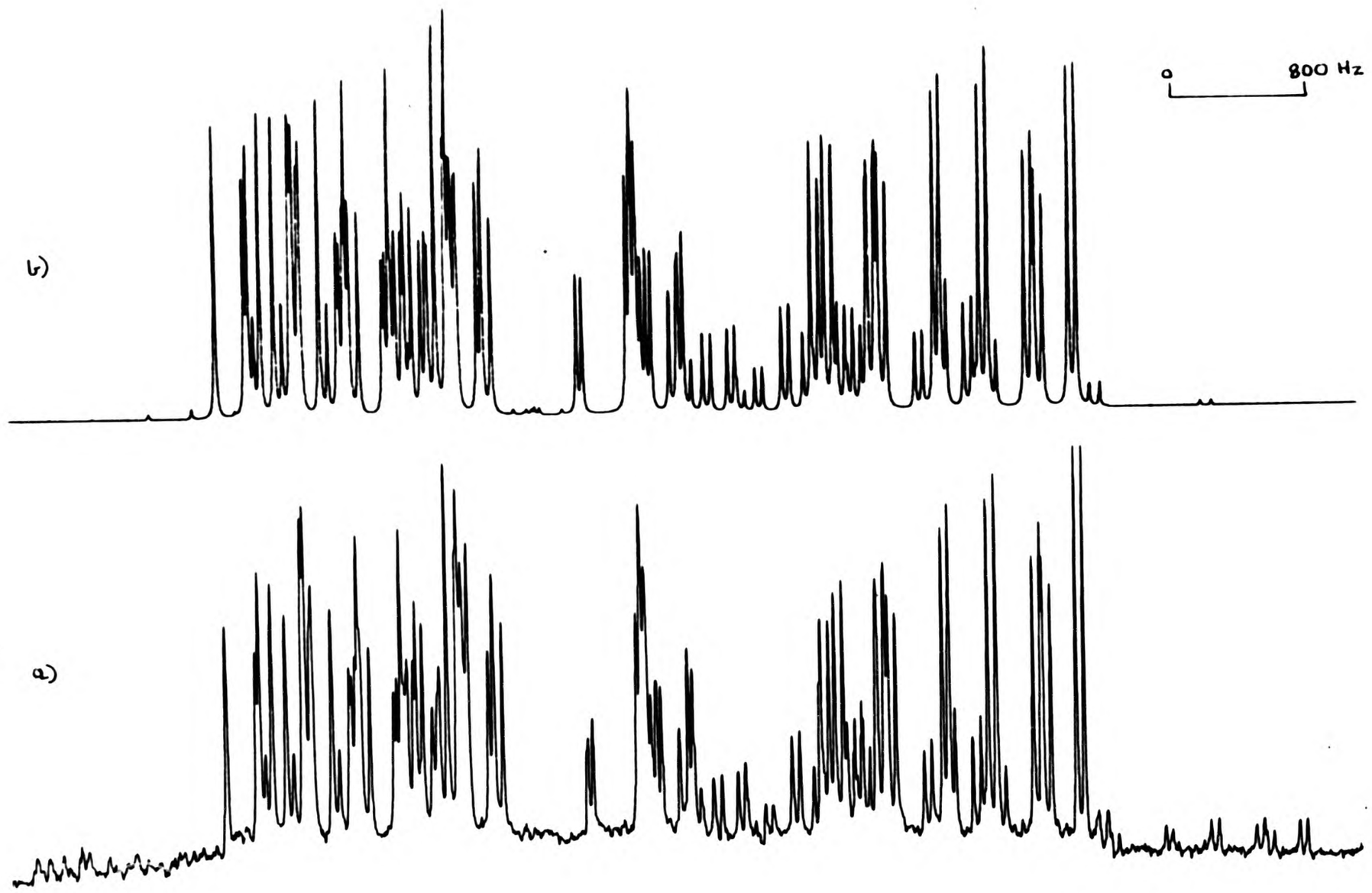

Fig 5.4 84.26 MHz Experimental (lower) and Computed (upper) $^{19}F\{^1H\}$ nmr spectra of $(C_6F_5)(C_6H_5)_2P$ partially oriented in Phase V

As a first approximation the indirect spin-spin couplings and the chemical shifts were taken from the results in the isotropic phase, and the PF anisotropic couplings were obtained from the nematic ^{31}P spectrum. All that was then needed to use LAOCOON LC were estimates of the FF anisotropic couplings. Anisotropic couplings can be estimated from an assumed geometry and the orientation of the molecule. The geometry of the pentafluorophenyl phosphorus system was assumed by transferring the relevant geometrical data from triphenylphosphine[1] and pentafluorobenzene[10]. For the pentafluorophenyl phosphorus system as shown in Fig 5.5 two independent orientation parameters are required to describe its orientation in the liquid crystal.

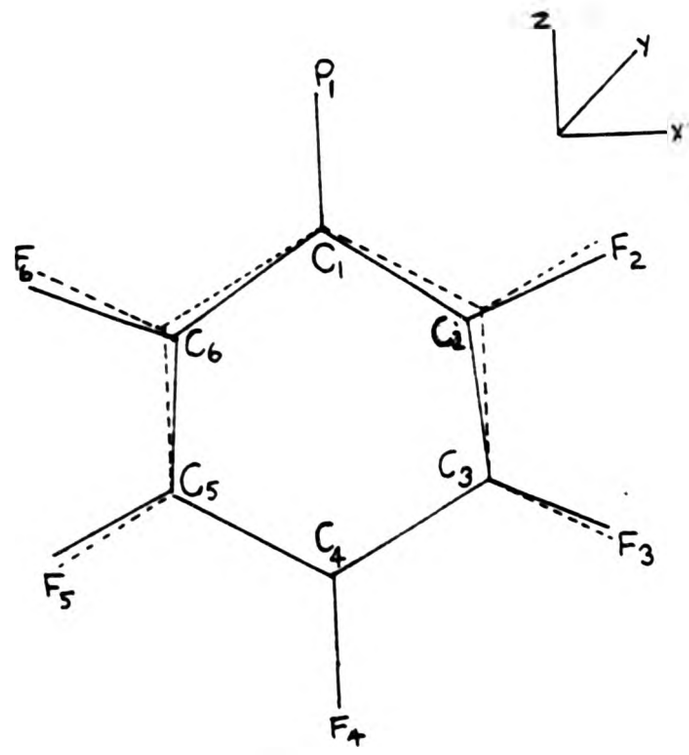

Fig 5.5

The Pentafluorophenyl unit showing deformation (exaggerated) from Hexagonal Symmetry (dashed lines).

The two parameters S_{xx} and S_{zz} are related to $D_{2,3}$ and $D_{3,4}$, where the numbering refers to fluorines as labelled in Fig 5.5, and the z axis is parallel with the two-fold axis (see Fig 5.5), by;

$$S_{zz} = -D^{dir}_{2,3} \times r^3_{2,3} / K(FF) \qquad 5.1$$

$$S_{xx} = -\frac{4}{3}\left[\frac{r^3_{3,4}}{K(FF)}\right](D^{dir}_{3,4} - \frac{1}{4}D^{dir}_{2,3}) \qquad 5.2$$

Also

$$S_{xx} + S_{yy} + S_{zz} = 0 \qquad 5.3$$

and $$D^{dir}_{i,j} = K(i,j) \times S_{i,j}/r^3 \qquad 5.4$$

where $$S_{ij} = S_{xx}\cos^2\theta_{ijx} + S_{yy}\cos^2\theta_{ijy} + S_{zz}\cos^2\theta_{ijz}$$

and θ_{ijp} is the angle the vector ij makes with the axis p. Using equations 5.1 to 5.5 reasonable estimates of all the required anisotropic couplings can be calculated, once $D^{dir}_{2,3}$ and $D^{dir}_{3,4}$ have been determined from the experimental anisotropic spectrum. Owing to the complexity of the observed anisotropic ^{19}F spectrum, it was not possible to approximate $D^{dir}_{2,3}$ and $D^{dir}_{3,4}$ directly from the splitting patterns in the spectrum. However the anisotropic couplings determined from the ^{31}P anisotropic spectrum can also be used to determine S_{zz} and S_{xx}. Under conditions of regular hexagonal symmetry the vector joining the phosphorus and fluorine 4 is parallel to the vector joining fluorines 2 and 3, and the vector joining the phosphorus and fluorine 6 is very nearly parallel to the vector joining fluorines 3 and 4, so that equations similar to 5.1 and 5.2 can be used. They are:

$$S_{zz} = -D^{dir}_{1,4} \times r^3_{1,4} / K(PF) \qquad 5.6$$

and $$S_{xx} = -\frac{4}{3}\left[\frac{r^3_{1,2}}{K(FF)}\right](D^{dir}_{1,2} - \frac{1}{4}D^{dir}_{1,4}) \qquad 5.7$$

Estimates of the orientation parameters were calculated using Equations 5.6 and 5.7, and then equations 5.3 to 5.5 were used to determine the remaining anisotropic couplings. In order to perform these calculations the computer program CALPF5.FOR was written; its listing is shown in the appendix 5.1. As $D_{1,4}$ and $D_{1,6}$ were obtained from the moduli of the splittings in the ^{31}P anisotropic spectrum and the sign of $^{3}J(PF)$ is unknown, the orientation parameters calculated from equations 5.5 and 5.6 can have more than one possible value. However, if the initial geometry is sufficiently precise and the experimental spectrum has a reasonable number of well resolved lines, then only one set of nmr parameters calculated from a particular set of orientation parameters will correspond to a calculated spectrum that accurately resembles the experimental one. It was observed that for each set of anisotropic parameters the chemical shifts of the fluorines were required to be varied. Starting with the isotropic chemical shifts then each chemical shift was varied over a range of ±200Hz. The number of trial spectra computed before a satisfactory fit was achieved was about six. Once the computed spectrum resembled the anisotropic spectrum, iteration was used to obtain accurate values for the chemical shifts and the anisotropic couplings. The indirect couplings were not iterated upon. The parameters that gave the best fit to the anisotropic spectra for two different orientations are reported in Table 5.2 and the computed ^{19}F spectrum of the pentafluorophenyl phosphorus system oriented in Phase V is shown in Fig 5.4(b).

Table 5.2

Selected Anisotropic Couplings in the Pentafluorophenyl Phosphorus system in Phase IV and V

	Anisotropic Coupling/Hz[a]	
	Liquid Crystal	
	Phase IV	Phase V
$^3D(PF_2)=^3D(PF_6)$	-133.1 ±1	-152.1 ±1
$^4D(PF_3)=^4D(PF_5)$	-21.1 ±1	-23.2 ±1
$^5D(PF_4)$	-10.4 ±2	-13.6 ±1
$^3D(F_2F_3)=^3D(F_5F_6)$	-321.6 ±1	-347.2 ±1
$^3D(F_3F_4)=^3D(F_4F_5)$	-473.4 ±1	-544.2 ±1
$^4D(F_2F_4)=^4D(F_4F_6)$	-69.1 ±1	-76.5 ±1
$^4D(F_2F_6)$	-95.2 ±1	-111.0 ±1
$^4D(F_3F_5)$	-99.5 ±1	-117.1 ±1
$^5D(F_2F_5)=^5D(F_3F_6)$	-57.4 ±1	-72.8 ±1
$^3D(PF)/^3D(F_3F_4)$	0.2812	0.2795
$^5D(PF)/^3D(F_2F_3)$	0.0323	0.0392

a) Numbering as in Figure 5.5. The anisotropic couplings were determined using the computer program LAOCOON LC.

5.3.2 Calculation of Anisotropy in the Indirect Couplings

The anisotropic contributions to the indirect spin-spin couplings D^{indir} were determined from the differences between the calculated and experimental anisotropic couplings (cf. Section 4.3.4).

5.4 Discussion

The equilibrium geometry of the pentafluorophenyl phosphorus system was determined using the anisotropic couplings PF and FF obtained from the analysis of the anisotropic ^{19}F spectrum. The calculations were based on the following assumptions:

i) The bond length for the directly bonded PC is the same as the bond length found in triphenylphosphine[1].

ii) The orientation of the pentafluorophenyl system in the anisotropic phase can be described by two independent orientation parameters.

iii) All the indirect spin-spin couplings required for the analysis of the anisotropic spectrum can be obtained from the isotropic spectrum using the same solvent.

iv) The vibrational corrections to the experimental dipolar couplings can be ignored.

v) Anisotropies in the indirect spin-spin couplings have to be based on previously reported values.

Justifications of these assumptions are now discussed. Any change in P-C bond length should not affect the geometry of the pentafluorophenyl system but will cause discrepancies in the calculated anisotropies of the indirect P-F couplings and also in the calculated P-F internuclear distances.

The analysis of the ^{19}F and the ^{31}P spectra of the oriented pentafluorophenyl system was simplified by using the coordinate system shown in Fig 5.5 and by using the indirect spin-spin couplings measured from the isotropic spectrum. This approach has been used when determining geometries of other molecules with two-fold symmetry and as the results obtained were consistent with those obtained by other methods [10,20-23], it seems reasonable to follow the same approach here.

The PF and FF experimental dipolar couplings were not corrected for harmonic vibrations as the vibrational force field for the molecule has not been previously reported. However it is possible to transfer a force field from a similar molecule so as to estimate the magnitudes of the corrections required. In the study of ortho-difluorobenzene, the vibrational corrections applied to the ortho FF direct couplings were of the order of 1 Hz in 400 Hz[9]. Such a small correction should not influence the calculated geometry and hence it can be ignored here. As all the other dipolar couplings correspond to longer range couplings, then it seems that the vibrational corrections to all the dipolar couplings can be ignored in this problem.

Studies of a number of fluorinated benzenes partially oriented in liquid crystals have been reported and they show that complications arise in the determination of molecular geometries

when the experimental anisotropic couplings $^{19}F-^{19}F$ are not purely dipolar, but have significant contributions from the anisotropy in the indirect spin-spin couplings[6-10]. In the study of oriented pentafluorobenzene [10], ortho D_{FF}^{indir} was negligible, meta D_{FF}^{indir} was 3.3 percent relative to the experimental experimental $^4D(FF)$, and para D_{FF}^{indir} was 3.8 percent with respect to $^5D_{FF}^{exp}$. Only the meta D_{FF}^{indir} was in agreement with theoretical calculation, whereas the ortho D_{FF}^{indir} was sensitive to the assumed geometry. However, using these values for D_{FF}^{indir}, the geometry of pentafluorobenzene determined by nmr compared well with those obtained in similar molecules. It was decided to calculate the geometry of the pentafluorophenyl phosphorus system assuming the ortho D_{FF}^{indir} to be zero and meta D_{FF}^{indir} to be of the same order of magnitude as observed in pentafluorobenzene oriented in Phase IV. Hence S_{zz} and S_{xx} were calculated from the experimental $^3D(FF)$ couplings using equations 5.1 and 5.2, and the positions of the fluorine atoms were varied until the calculated values of the meta D(FF) couplings were consistent with the experimental meta D(FF) couplings after their anisotropic contributions to the indirect couplings were taken into account. The calculation also assumed that the phenyl ring is a regular hexagon and that r(C-C)=1.397A. The geometry calculated using these assumptions is summarized in column A of Table 5.3, and the deformation of the CCF inter-bond angles from 120^o is shown in Fig 5.5. Comparison of these sets of results with that obtained for pentafluorobenzene[10] shows that the value for r(C-F) bond length is the same in both molecules, but the deformation of angle $C_1C_2F_2$ is larger by approximately 3.5^o in the pentafluorophenyl phosphorus system.

Table 5.3 Calculated Dipolar Couplings and, Orientation and Geometrical Parameters in the Pentafluorophenyl Phosphorus System.

	DIPOLAR COUPLINGS IN HZ		
	Expt [a]	CALCULATED[b]	
		A	B
$^3D(PF_2)=^3D(PF_6)$	-152.1	147.0	-145.6
$^4D(PF_3)=^4D(PF_5)$	-23.2	-24.1	-23.9
$^5D(PF_4)$	-13.6	-12.6	-12.4
$^3D(F_2F_3)=^3D(F_5F_6)$	-347.2	-347.2	-347.2
$^3D(F_3F_4)=^3D(F_4F_5)$	-544.2	-544.2	-544.2
$^4D(F_2F_4)=^4D(F_4F_6)$	-111.0	-114.7	-114.7
$^4D(F_2F_6)$	-76.5	-78.8	-78.8
$^4D(F_3F_5)$	-117.1	-121.4	122.1
$^5D(F_2F_3)=^5D(F_3F_6)$	-72.8	-70.3	-70.8
S_{xx} [b]		-0.1230	-0.1243
S_{zz} [b]		-0.05867	-0.05762
$r(CF_2)/A$		1.34 ±.01	1.34 ±.01
$r(CF_3)/A$		1.34 ±.01	1.34 ±.01
Bond Angle $C_1C_2F_2$		125.0° ±.5°	124.0° ±.5°
Bond Angle $C_4C_3F_3$		120.8° ±.5°	121.0° ±.5°
Bond Angle $C_2C_1F_6$		120.0°	118.3° ±.5°

a) Experimental Results from $^{19}F\{H\}$ spectrum of $P(C_6F_5)(C_6H_5)_2$ in Phase V at room temperature.

b) See text

When compared with tetramesityldiphosphine[2] and trimesityl-phosphine[3] for the same bond angle (but with F_2 now corresponding to the ortho methyl carbon) the difference is only larger by $1^{o} \pm .5^{o}$. The enlargement of the angle $C_1C_2F_2$ in $P(C_6F_5)$ is understandable in that it allows the phenyl rings to rotate more freely. The deformation of the $C_4C_3F_3$ inter-bond angle is of the same magnitude as found in both of the phosphines[2,3] and in pentafluorobenzene[10].

The geometries of the phenyl rings in trimesitylphosphine [3], tetramesityldiphosphine [2], and chlorinated [24-26] and fluorinated [6,9,10,27,28] benzenes that have been previously reported show a deviation from regular hexagonal symmetry. The structures of trimesitylphosphine and tetramesityldiphosphine were studied by X-ray diffraction, and the chlorinated and fluorinated benzene geometries were obtained from micro-wave, electron diffraction and oriented nmr. The geometry of the pentafluorophenyl phosphorus system was calculated as before, but this time the inter-bond angle $C_2C_1C_6$ was allowed to vary and the positions of carbons C_3, C_4 and C_5 were held fixed. The geometry determined using this scheme is reported in column B of Table 5.3, and the deformation of the phenyl ring from regular hexagonal symmetry is shown in Fig 5.5. The value of the inter-bond angle $C_2C_1C_6$ calculated in this way was $118.3^{o} \pm .25^{o}$ which is smaller by 0.5^{o} in comparison with that from a similar calculation carried out on pentafluorobenzene [10]. The same bond angle determined in trimesitylphosphine [3], tetramesityldiphosphine [2] and triphenylphosphine [1] has values of 119.2^{o}, 118.4^{o} and 119.4^{o} respectively. These results on the phosphines also showed that the determined value of r(C-C) can

vary between 1.363A and 1.410A whereas in the calculations of geometry by nmr, this bond length was kept constant at 1.397A. The calculated value of the inter-bond angles $C_1C_2F_2$ and $C_4C_3F_3$ corresponding to the value of $\angle C_2C_1C_6$ in the phosphorus pentafluorophenyl system were $122.0^{\circ} \pm .5^{\circ}$ and $120.0^{\circ} \pm .5^{\circ}$ respectively. Hence both geometries in Table 5.3 show that the inter-bond angle $C_1C_2F_2$ is larger in the pentafluorophenyl phosphorus system than in pentafluorobenzene. The geometries determined by nmr, X-ray and electron diffraction on various fluorinated and chlorinated benzenes, and for triphenyl and mesityl phosphines suggest that for the pentafluorophenyl phosphorus system the hexagon is distorted.

These measurements also yield the anisotropic contributions to the indirect PF couplings which are based on assumed anisotropic contributions to J(FF) couplings and an assumed geometry. The value for r(P-C) of 1.825A used in this study was obtained by taking the average of the three P-C bond lengths determined in solid triphenylphosphine. The same bond lengths in trimesitylphosphine and tetramesityldiphosphine are larger by 0.01 and 0.02A respectively. This change in the value of r(P-C) does not change the value of the calculated D(PF) by a great deal. $^3D_{PF}^{indir}$ was calculated as 3.4% ±0.7% relative to the corresponding experimental anisotropic coupling. The other two contributions were about 1.5% ±1%. The results show definite evidence of anisotropy in $^3J(PF)$ if the calculated geometry is correct. There is very little reported on the anisotropy in indirect couplings between phosphorus and fluorines[11-13], but as anisotropic contributions from J(CF) [29] and J(HgF) [Chapter 4] have been reported, then it seems not unreasonable to expect

anisotropy in J(PF) also.

Nmr spectra of oriented molecules can be used to determine the absolute signs of couplings [14, Chapters 3 and 4], if the experimental spectrum is sufficiently well resolved and the calculated geometry is sufficiently accurate. The analysis of the nmr spectrum of the oriented $P(C_6F_5)$ unit was based on knowing the signs of all the indirect FF couplings. The anisotropic couplings obtained from the analysis of the experimental spectrum are consistent with the geometry of similar molecules. The combination of the chemical shifts, and the indirect and the anisotropic couplings yields from the analysis of the experimental spectrum a negative $^3D(PF)$ and a positive $^3J(PF)$. From the analysis of anisotropic spectrum the values of $^3D(PF)$ and $^3J(PF)$ cannot be determined separately, but the spectrum does yield $|2.^3D(PF)+^3J(PF)|$. This implies that if $^3J(PF)$ is positive (as reported in Table 5.2) then the value of the corresponding total experimental anisotropic coupling leads to an anisotropic contribution in $^3J(PF)$, which is about 3% relative to the experimental dipolar coupling. However, if $^3J(PF)$ is assumed negative, then the required increase in the total anisotropic coupling would have to be as large as $^3J(PF)$ itself for the anisotropic spectrum to remain unchanged. This increase in the total anisotropic coupling would yield an anisotropic contribution from $^3J(PF)$ of about 30%, when the same geometry is used. Very few phosphorus compounds containing fluorines have been studied by liquid crystal nmr[11-13] and only the study of phosphoryl fluoride[13] suggested that J(PF) had anisotropic contributions. In this molecule when J(FF) was considered to have no anisotropic contributions then J(PF) was calculated to have 50%

anisotropic contribution with respect to its total anisotropic coupling so as to make the geometry calculated by oriented nmr consistent with the geometry determined by electron diffraction. However, the discrepancy between the nmr and electron diffraction structures was also explained by the same authors in terms of an orientation-dependant geometry. This problem of molecules having slightly different geometries at different orientations in the anisotropic phase in a liquid crystal is sometimes found in the nmr study of oriented molecules[30]. In our study of tris(orthofluorophenyl)phosphine[Chapter 6] the sign of $^{3}J(PF)$ was determined as positive, so it seems likely that anisotropic contribution in $^{3}J(PF)$ in the pentafluorophenyl phosphorus system is about 3%. The signs of $^{4}J(PF)$ and $^{3}J(PF)$ couplings could not be determined in the same way as described for $^{3}J(PF)$ because of the small magnitudes of both couplings, when compared with the line width in the anisotropic ^{19}F nmr spectrum and the $^{3}D_{PF}^{total}$ couplings.

5.5 Conclusions

The geometry of the pentafluorophenyl phosphorus system has been determined by liquid crystal nmr, and is consistent with that found in similar molecules[1-3,10]. The results show that the phenyl ring in the molecule deviates from regular hexagonal symmetry and the greatest deformation in the inter-bond angle is in $C_1C_2F_2$. It was not possible to determine a complete and accurate geometry, although in principle this would be possible if ^{13}C satellites were taken into consideration. However, our results confirm that if the geometry determined in the present study is reasonably accurate then the contributions from

anisotropy in the indirect F-F couplings are similar to those found in pentafluorobenzene[10].

This nmr study of the pentafluorophenyl phosphorus system showed evidence of anisotropy in $^{3}J(PF)$, and its magnitude was 3% when J was taken as positive and about 30% if J was negative. Both percentage contributions are calculated relative to the experimental anisotropic coupling. The contribution of 3% is more likely because this agrees with the sign of the $^{3}J(PF)$ coupling determined from the nmr study of tris(orthofluorophenyl)-phosphine[Chapter 6]. In addition, the nmr studies of phosphorus trifluoride[11], thiophosphoryl fluoride[12] and phosphoryl fluoride[13] confirm that anisotropy in J(PF) is expected to be small.

APPENDIX 5.1

Listing of the Computer Program CALPF5.FOR

```
C       ****** PROGRAM CALPF5.FOR ******
        DIMENSION X1(12),Z1(12),X2(12),Z2(12),X3(12)
        DIMENSION Y3(12),Z3(12),Y1(12),Y2(12)
        DIMENSION R(12,12),R3(12,12)
        DIMENSION ALPHAY(12,12),ALPHAX(12,12),ALPHAZ(12,12)
        DIMENSION CONST(12,12),D(12,12)
82      TYPE 798
798     FORMAT(' ANGLE C2C1C6')
        ACCEPT 55,C2C1C6
        X1(8)= -1.397*SIND(C2C1C6)
        X1(9)=-1.21
        X1(11)=1.21
        X1(12)= 1.397*SIND(C2C1C6)
        Z1(1)=-3.237
        Z1(4)=2.6985
        Z1(7)=-1.397
        Z1(10)= 1.397
        Z1(8)=1.397*COSD(C2C1C6)
        Z1(9)= 0.6985
        Z1(11)= 0.6985
        Z1(12)=1.397*COSD(C2C1C6)
        TYPE 30
30      FORMAT(' CF BOND LENGTH')
        ACCEPT 55,RCF2,RCF3
```

```
      IF (RCF2.EQ.0.0)GO TO 83
55    FORMAT(3F)
      TYPE 201
201   FORMAT(' ANGLE C3 C2 F2 and angle c2 c3 f3?')
      ACCEPT 55,c3c2f2,c2c3f3
      C3C2F2=240-C3C2F2-90
      C2C3F3=240-C2C3F3-90
      X2(2)=X1(8)-(COSD(C3C2F2)*RCF2)
      Z2(2)=Z1(8)-(SIND(C3C2F2)*RCF2)
      X2(6)=-X2(2)
      X2(8)=-1.21
      X2(9)=-1.21
      X2(11)=1.21
      X2(12)=1.21
      X2(3)=X1(9)-(COSD(C2C3F3)*RCF3)
      Z2(3)=Z1(9)+(SIND(C2C3F3)*RCF3)
      X2(5)=-X2(3)
      Z2(1)=-3.227
      Z2(6)= Z2(2)
      Z2(5)= Z2(3)
      Z2(4)=Z1(10)+RCF3
      Z2(7)=-1.397
      Z2(10)= 1.397
      Z2(8)=-0.6985
      Z2(9)= 0.6985
      Z2(11)= 0.6985
      Z2(12)=-0.6985
      ANGLE2=0.0
      ANGLE1=0.0
C ANGLE2=ANGLE IN XZ PLANE
      DO 29 I=1,12
      IF (I.EQ.2) GO TO 27
      IF (I.EQ.6) GO TO 34
      X3(I)=X2(I)
      Y3(I)=Y3(I)
      GO TO 29
27    X3(I)= (X2(I)*COSD(ANGLE1))+(SIND(ANGLE1)*Y2(I))
      Y3(I)= (Y2(I)*COSD(ANGLE1))-(SIND(ANGLE1)*X2(I))
      GO TO 29
34    X3(I)=-X3(2)
      Y3(I)=Y3(2)
29    CONTINUE
      RCP=-(Z2(1)-Z2(7))
      C2C3F3=240.-(90.+C2C3F3)
      C3C2F2=240.-(90.+C3C2F2)
      WRITE(22,63)RCF2,RCF3,RCP,C2C3F3,C3C2F2,C2C1C6
63    FORMAT(/3X,' RCF2 = ',F5.3,3X,' RCF3 = ',F5.3,3X,
     1' RCP = ',F5.3,/,3X,
     2' ANGLE C4 C3 F3 =',F7.3,3X,' ANGLE C1 C2 F2 =',F7.3,/
     3' ANGLE C2 C1 C6 =',F7.3,/)
      DO 91 I=1,3
      DO 92 J=2,6
      IF (I.EQ.J)GO TO 92
      R(I,J)=SQRT((Z2(I)-Z2(J))**2+(X3(I)-X3(J))**2
     1+(Y3(I)-Y3(J))**2)
      R3(I,J)=R(I,J)**3
92    CONTINUE
91    CONTINUE
62    FORMAT(3X,9(2X,F7.1))
      DO 101 I=1,3
```

```
      DO 102 J=2,6
      IF (I.EQ.J)GO TO 102
      ALPHAX(I,J)=((ABS(X2(I)-X2(J)))/R(I,J))**2
      ALPHAY(I,J)=((ABS(Y2(I)-Y2(J)))/R(I,J))**2
      ALPHAZ(I,J)=((ABS(Z2(I)-Z2(J)))/R(I,J))**2
102   CONTINUE
101   CONTINUE
      DO 103 I=1,3
      DO 104 J=2,6
      IF(I.EQ.J)GO TO 104
      CONST(I,J)=106268.8
      IF(I.EQ.1)CONST(I,J)=45728.4
104   CONTINUE
103   CONTINUE
      TYPE 344
344   FORMAT(' D23,D34')
      ACCEPT 55,D23,D34
      SZZ=(R3(2,3)*D23)/(CONST(2,3)*ALPHAZ(2,3))
      SXX=((D34*R3(3,4)/CONST(3,4))-(SZZ*ALPHAZ(3,4)))/
     1 ALPHAX(3,4)
      SYY=-(SXX+SZZ)
      WRITE (22,105)SXX,SZZ,SYY
105   FORMAT(/3X,' S(XX) = ',F10.6,3X,' S(ZZ) = ',F10.6,
     13X,' S(ZZ) = ',F10.6/)
      DO 111 I=1,3
      DO 112 J=2,6
      IF(I.EQ.J)GO TO 112
      D(I,J)=(CONST(I,J)/R3(I,J))*((SXX*ALPHAX(I,J))+
     1(SZZ*ALPHAZ(I,J))+(SYY*ALPHAY(I,J)))
112   CONTINUE
111   CONTINUE
      WRITE(22,69)
70    FORMAT(/3X,' DIPOLAR COUPLING'/3X,18('-')/)
69    FORMAT(3X,'    12       13       14       23
     134      24       26       35       25'/,3X,70('-')/)
      WRITE(22,62)D(1,2),D(1,3),D(1,4),D(2,3),D(3,4),
     1D(2,4),D(2,6),D(3,5),D(2,5)
      GO TO 82
83    RETURN
      END
```

5.6 References

1 J.J.Daley, J. Chem. Soc., 3799(1964).

2 S.G. Baxter, A.H. Cowley, R.E. Davies and P.E. Riley, J. Amer. Chem. Soc., 103, 1699(1981).

3 J.F. Blount, C.A. Maryanoff and K.Mislow, Tetrahedron Lett., 913 (1975).

4 P. Diehl C.L. Khetrapal and H.P. Kellarhals, Mol. Phys., 15, 333(1968); P. Diehl H.P. Kellarhals and W. Niederberger,

J. Mag. Res., 4, 352(1971).

5 C.M. Woodman, Mol. Phys., 13, 365(1967).

6 S.A. Spearman and J.H. Goldstein, J. Mag. Res., 4, 93(1971) and the references cited therein.

7 P. Diehl, H.P. Kellarhals and U. Lienhard, Org. Mag. Res., 1, 93(1969).

8 A.S. Tracey, Mol. Phys., 33, 339(1977).

9 T. Väänänen, J. Jokisaari and J. Lounila, J. Mag. Res., 49, 73(1982).

10 G.J. den Otter and C. MacLean, J. Mol. Struct., 31, 47(1976).

11 N. Zumbulyadis and B.P. Dailey, Mol. Phys., 26, 777(1973).

12 A.J. Montana, N. Zumbulyadis and B.P. Dailey, J. Chem. Phys., 66, 1850(1977).

13 P.K. Bhattacharya and B.P. Dailey, Mol. Phys., 28, 209(1974); J. Bulthuis and C.A. deLange, J. Mag. Res., 14, 13(1974).

14 References 27 and 28 in Chapter 4.

15 R.D.W. Kemmitt, D.I. Nichols and R.D. Peacock, J. Chem. Soc. (A), 2149(1968).

16 S. Castellano and A.A. Bother-By, J. Chem. Phys., 41, 3863(1964).

17 M.G. Hogben and W.A.G. Graham, J. Amer. Chem. Soc., 91, 3863(1964).

18 D.M. Grant, R.C. Hirst and H.S. Gutowsky, J. Chem. Phys., 38, 470(1963).

19 E. Lustig, W. Moniz, P. Diehl and R. Bodmer, J. Chem. Phys., 49, 4550(1968).

20 L.C. Snyder, J. Chem. Phys., 43, 4041(1965).

21 J. Gerritsen and C. MacLean, Rec. Trav. Chim. Pays-Bas, 91, 1393(1972).

22 G.J. den Otter, J. Gerritsen and C. MacLean, J. Mol. Struct,

16, 379(1973).

23 J.W. Emsley J.C. Lindon and J. Tabony, J. Chem. Soc. Farad. Trans 2, 71, 579(1975); K.J. Orrell and V. Sik, J. Chem. Soc. Farad. Trans 2, 71, 1360(1975).

24 J. Jokisaari and P. Diehl, J. Mol. Struct., 53, 55(1979).

25 H. Bösiger and P. Diehl, J. Mag. Res., 35, 367(1979).

26 G. Dombi, J. Amrein and P. Diehl, Org. Mag. Res., 13, 224(1980).

27 E.E. Babcock, R.C. Long Jr. and J.M. Goldstein, J. Mol. Struct., 74, 111(1981).

28 A. Hatta, C. Hirose, K. Kozima, Bull. of Chem. Soc. of Japan, 41, 1088(1968).

29 G.J. den Otter and C. MacLean, J. Mag. Res., 20, 11(1975).

30 References 12-14 in Chapter 2.

CHAPTER 6

STUDY OF TRIS(FLUOROPHENYL)PHOSPHINES ORIENTED IN MERCK PHASE V

6.1 Introduction

As discussed in Chapters 2 to 5, the nmr of molecules partially oriented in nematic liquid crystals has been successfully used to obtain structural information, absolute signs of indirect spin-spin couplings, quadrupolar coupling constants, and anisotropies in the indirect couplings and chemical shifts. The technique has been also applied to molecules where the intramolecular motions are important[1,2]. Studies of intramolecular motion by nmr depend upon three different time scales.

i) The time scale for the nmr experiment T_{nmr}, which is between 1 and 10^{-3} sec.

ii) The time scale for the reorientation of the molecule, T_{or}. There have been no accurate measurements for this time scale in liquid crystals but it is believed to be of the same order of magnitude or greater than those in isotropic liquids[3], which implies it is between 10^{-6} and 10^{-9} sec.

iii) The time scale for any intramolecular motion, T_{imm}.

If the time scale for the reorientation of the molecule is greater than the time scale for the intra-molecular motion then the nmr spectrum yields one set of orientation parameters. If $T_{nmr} > T_{imm} > T_{or}$, then the spectrum again yields one set of orientation parameters but the anisotropic couplings are averaged over the various species present at that orientation. However, if

the time scale for the intramolecular motion is long compared to the time scale of the nmr experiment and the reorientation of the molecule, then the observed spectrum is a superposition of as many spectra as there are different species.

In most systems so far studied by oriented nmr, the intramolecular motion is fast on the nmr time scale, and it is not possible to study each conformer independently or to determine energy barriers to rotation. However the method has been applied with success to determine the mode of rotation and conformational preferences in some selected molecules. From a study of oriented substituted bithienyl derivatives (Fig 6.1) [4] it was possible to demonstrate the absence of free rotation about the carbon-carbon bond linking the two rings, and show that the anisotropic spectrum was consistent with the presence of two isomers, of which the cis was less stable than the trans. This deduction agreed with X-ray and esr results. The nmr spectra of oriented biphenyls [5,6] showed that such molecules exist in the liquid crystal phase in a "twisted" conformation. It was also possible to determine fairly accurately the angle between the planes of the phenyl rings, and the data obtained by nmr was in agreement with electron diffraction results. A nmr study of bipyrimidine (Fig 6.2) in the nematic phase made it possible to determine the barrier to internal rotation about the carbon-carbon bond[7].

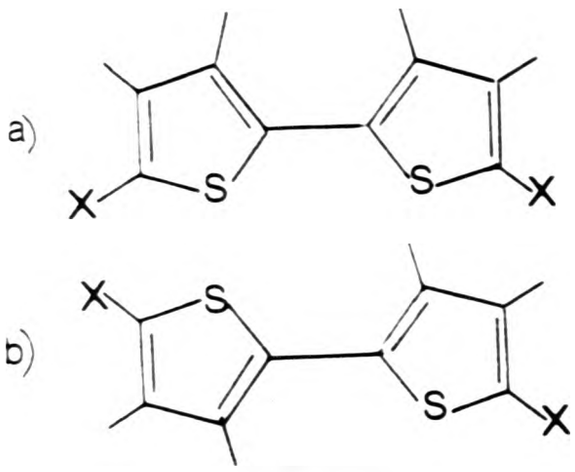

Fig. 6.1 (a) Cis and (b) trans disubstituted bithienyl X = Cl, Br, NO_2

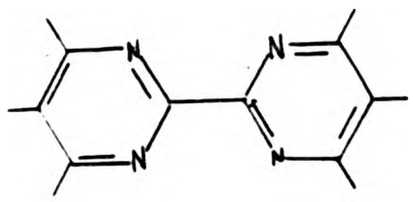

Fig 6.2

Bipyrimidine

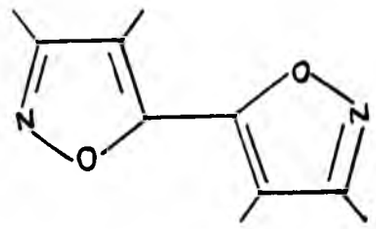

Fig 6.3

Bis-iso-oxazole

The nmr spectrum of oriented substituted toluenes [8-13] permitted the determination of the barrier for the methyl rotations about the carbon-carbon bonds as well as giving complete structures of these molecules. It was possible to interpret the data from the nmr spectra of oriented bis-iso-oxazoles (Fig 6.3) in terms of a model involving conformational equilibria in solution[14,15].

However, not all studies have been successful in reporting accurate parameters to describe the intramolecular motions that may be taking place. A study of tropolone (Fig 6.4) by oriented nmr showed that various models gave good agreement with the experimental data, but an exact solution was not possible from the available information [16]. The nmr method in all such cases relies on information from other sources, and the problem can only then be solved after

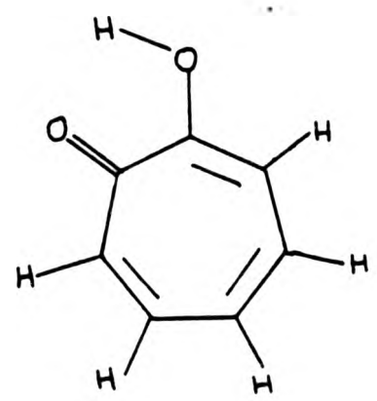

Fig. 6.4 Tropolone

assumptions are made regarding conformations and certain geometrical parameters. To solve such problems where it is expected that the intramolecular motion is important involves setting up reasonable models, and then selecting ones which reproduce the experimental data. This method may not always give accurate results when applied to conformational analysis, but it does provide some information on conformational preferences and the interconversion processes.

The present study involves analysis of nmr spectra of oriented ortho, meta and para tris(fluorophenyl)phosphines ($(C_6FH_4)_3P$) to obtain information about their geometries and conformational preferences. The study also permitted the determination of the signs of PF couplings, and anisotropies of PF and FF indirect couplings. In order to derive the signs of the indirect couplings, the ^{31}P shielding anisotropies were determined.

6.2 Experimental

Para, meta, and ortho tris(fluorophenyl)phosphines were synthesized as described in Chapter 8. The nematic samples were prepared in Merck Phase V as described in Chapter 3. The solute concentrations employed were approximately 2.0 to 6.0% by weight.

^{19}F and ^{31}P spectra were recorded on a Jeol FX90Q spectrometer as described in Chapter 5. ^{31}P nmr spectra were also obtained on a Jeol FX60 spectrometer in the FT mode, equipped for variable temperature operation, and operating at 24.2 MHz. The anisotropic spectra were recorded from overnight runs so as to detect ^{13}C satellites (natural abundance 1.1%). A spectral

width of 1000 Hz and a pulse width of 9μs were used. All ^{19}F and ^{31}P spectra were acquired with external ^{2}D lock and complete proton decoupling.

Nmr spectra of oriented molecules were analysed as described by Englert[17].

6.3 Results

6.3.1 Anisotropic and Isotropic Couplings

The ^{31}P $\{^{1}H\}$ spectrum with carbon-13 satellites and the ^{19}F $\{^{1}H\}$ spectrum of tris(o-fluorophenyl)phosphine partially oriented in Phase V are shown in Figs 6.5 and 6.6.

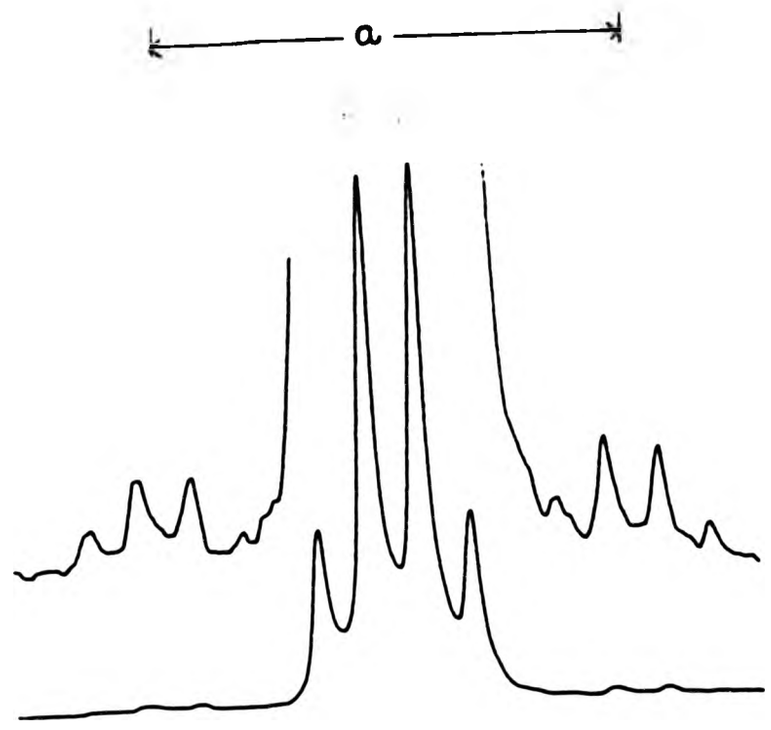

Fig 6.5 24.2 MHz $^{31}P\{^{1}H\}$ Nmr Spectrum including ^{13}C satellites of $(o\text{-}C_6FH_4)_3P$ partially oriented in Phase V

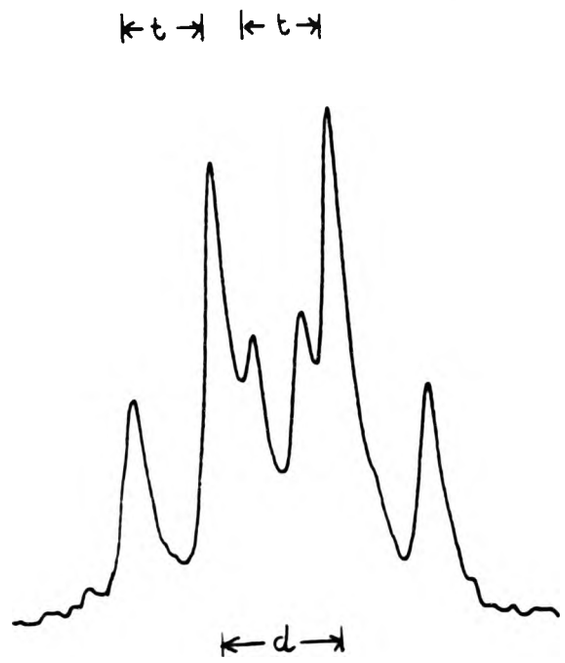

t = triplet splitting

d = doublet splitting

Fig 6.6 84.2 MHz $^{19}F\{^1H\}$ Nmr Spectrum of $(o\text{-}C_6FH_4)_3P$ partially oriented in Phase IV

The nematic spectra of the other tris(fluorophenyl)phosphines have the same structure and thus they can all be analysed similarly. The oriented spectra were analysed as AX_3 spin systems with effective C_3 symmetry, where $A=^{31}P$ and $X=^{19}F$. The ^{31}P anisotropic spectrum is a 1:3:3:1 quartet, with each component of the quartet being flanked by ^{13}C satellites. The spacings in the ^{31}P spectrum and the separation of the satellites (defined by a in Fig 6.5) are equal to $|2.D(i,j)+J(i,j)|$, where $D(i,j)$ is the total anisotropic coupling and $J(i,j)$ is the isotropic coupling. The anisotropic ^{19}F spectrum of each molecule is a triplet of doublets. The splitting in the doublet corresponds to $|2.^iD(PF)+^iJ(PF)|$ (i=3,4,5) and the spacing in the triplet is $|3D(FF)|$. The magnitudes of the isotropic couplings were determined from the appropriate isotropic spectrum measured at 70°C, and their signs where possible were obtained from

previously reported values. Only the signs of $^{1}J(PC)$ [18] and $^{5}J(PF)$ [19] have been reported and they are both negative. However the determination of the signs of the dipolar and the indirect couplings is sometimes possible from the analysis of the anisotropic spectrum [20].

The determination of the signs of the dipolar couplings in tris(p-fluorophenyl)phosphine was conducted as follows. From the anisotropic spectra the following splittings are obtained:

$$\text{splitting(PC)} = |2.{}^{1}D(PC) + {}^{1}J(PC)|$$

$$\text{splitting(PF)} = |2.{}^{5}D(PF) + {}^{5}J(PF)|$$

$$\text{splitting(FF)} = |3.D(FF)|$$

In order to determine the absolute values of the dipolar couplings the signs of the corresponding splittings are required, and these can be found by solving the equations for the dipolar couplings. The equations for dipolar couplings $^{1}D(PC)$, $^{5}D(PF)$ and $D(FF)$ are;

$$^{1}D^{dir}_{PC} = -K(PC)(1-2\sin^{2}\xi/2)S_{zz}/r^{3}_{PC} \qquad 6.1$$

$$^{5}D^{dir}_{PF} = -K(PF)(1-2\sin^{2}\xi/2)S_{zz}/r^{3}_{PF} \qquad 6.2$$

$$D(FF) = K(FF)\,S_{zz}/2r^{3}_{FF} \qquad 6.3$$

where S_{zz} is the orientation parameter, ξ is the CPC inter-bond angle and the z axis is parallel to the C_3 symmetry axis. From Equations 6.1 to 6.3 and using an assumed geometry, $^{1}D(PC)$ and $^{5}D(PF)$ were found to have the same signs, but to be opposite in sign to D(FF). By combining equations 6.2 and 6.3 the value of ξ can be related to the ratio of the dipolar couplings D(PF)/D(FF). The geometries of the tris(fluorophenyl)phosphines have not been reported, so they have been assumed to be similar to that obtained by transferring geometrical parameters from the X-ray study of triphenylphosphine[21] and the nmr study of the pentafluorophenyl

phosphine system[22]. This assumed geometry has been used throughout this study. Using the assumed value of ξ (109°) [21], this ratio of D(PF)/D(FF) is found to be less than one. This leads to a negative splitting (PF) and a negative $^5D(PF)$, assuming that $^5J(PF)$ is -4.6Hz. As $^1D(PC)$ and $^5D(PF)$ have the same signs, this follows that D(PC) is also negative. The signs determined in this way are also consistent with the negative sign of S_{zz} determined from the sign of the ^{31}P shielding anisotropy (positive) in tris(p-fluorophenyl)phosphine, which is expected to have the same sign as in triphenylphosphine[23]. The absolute values of all the couplings from three different orientations of tris(p-fluorophenyl)phosphine obtained in this way are summarized in Table 6.1.

Table 6.1 Selected Nmr Data of Tris(p-fluorophenyl)phosphine

Nmr Parameter	Sample		
	A	B	C
$^1J(PC)$ /Hz	-12.4	-12.4	-12.4
$[^1J(PC)+2.\ ^1D(PC)]$ /Hz	-160.5 ±1	-127.0 ±1	-146.0 ±1
$^1D(PC)$ /Hz	-74.1 ±.5	-57.3 ±.5	-66.8 ±.5
$^5J(PF)$ /Hz	-4.6	-4.6	-4.6
$[^5J(PF)+2.\ ^5D(PF)]$ /Hz	-18.4 ±.2	-12.4 ±.2	-16.0 ±.5
$^5D(PF)$ /Hz	-6.9 ±.25	-3.9 ±.25	-5.7 ±.25
D(FF) /Hz	+10.0 ±.25		+9.0 ±.15
D(PF) /D(PC)	0.09312	0.06807	0.08533
D(FF) /D(PC)	-0.1350		-0.13473

The proton-decoupled ^{31}P anisotropic spectrum with ^{13}C satellites of oriented tris(o-fluorophenyl)phosphine was analysed as described for tris(p-fluorophenyl)phosphine. It was possible in the case tris(p-fluorophenyl)phosphine to determine the absolute sign of $^{1}D(PC)$ from the assumed geometry and its dipolar coupling D(PF), as both the dipolar couplings D(PC) and D(PF) are independent of conformation. In the ortho substituted compound D(PF) is dependant upon conformation. This implies that the sign of $^{1}D(PC)$ can only be derived from the sign of the orientation parameter S_{zz} using equation 6.1. The sign of the orientation parameter can be determined from the sign of the ^{31}P shielding anisotropy, which is given by

$$\Delta\sigma\,(^{31}P) = -3/2\,(\nu(nem) - \nu(iso))/S_{zz} \qquad 6.4$$

where ν(nem) and ν(iso) are the chemical shifts in the nematic and isotropic phases respectively. ^{31}P shielding anisotropies have been determined for a number of phosphines by liquid crystal nmr [23-27] and solid state nmr[28], and they were found to be positive. Even when the magnitude of this shielding anisotropy was small as in the case of trimethylphosphine (7.6ppm) [25,27], the positive anisotropy was consistent with the correct sign of the J(PCH) coupling. In the case of tris(o-fluorophenyl)phosphine the ^{31}P shielding anisotropy was small and the sign of $^{3}J(PF)$ is unknown. If the ^{31}P shielding anisotropy is assumed to be positive as observed in other phosphines, then by solving equation 6.4, S_{zz} was found to be negative. However the sign of S_{zz} can also be inferred by consideration of the shape of the molecule and assuming that molecules with similar shapes can be expected to orient similarly in the same liquid crystal and thus their orientation parameters will have the same sign. Since the

structures of triphenylphosphine and tris(p-fluorophenyl)phosphine bear similarity to tris(o-fluorophenyl)phosphine then the sign of S_{zz} can be assumed to be the same in all three cases, which implies that they are all negative. It is not possible to continue with the analysis of the nmr spectrum of oriented tris(o-fluorophenyl)phosphine without these assumptions. It then follows that the sign of $^1D(PC)$ must be the same for all the solutions. The magnitude of $^1D(PC)$ from the nematic spectrum of tris(o-fluorophenyl)phosphine was obtained in the same way as described for the para compound. As for the corresponding $^1D(PC)$ from the nematic spectrum of oriented tris(m-fluorophenyl)phosphine this was not obtained because the ^{13}C satellites were hidden by the signals from the main spectrum. The absolute values for D(FF) and D(PF) from the spectrum of oriented ortho and meta tris(fluorophenyl)phosphine could not be determined in the same way as described from the analysis of the spectrum of oriented tris(p-fluorophenyl)phosphine. This is because the equations for D(FF) and D(PF) are not the same as the ones derived for para-substituted compound. In the case of the para-substituted molecule the angle between the vector PF and the magnetic field direction is constant throughout the rotation of the fluorophenyl rings about the PC bond. For the ortho and meta substituted compound this is not the case. However the sign of J(i,j) relative to D(i,j) can be determined as long as the magnitudes of the splittings (i,j) and J(i,j) are relatively large. From a plot of the splitting (i,j) against various temperatures below the isotropic/nematic transition temperature, the relative sign of J(I,J) can be deduced (Table 6.2).

Table 6.2 PF Splitting in $(o\text{-}C_6FH_4)_3P$ at various temperatures

Temp/°C	|PF splitting| /Hz
20	62.3
30	51.9
40	39.7
50	25.
70 (isotropic)	50.7

As Table 6.2 shows J(PF) and D(PF) have opposite signs in tris(o-fluorophenyl)phosphine. At the present, nothing can be said about the sign of D(FF) in both the meta and ortho tris(fluorophenyl)phosphines, and because of the small value of J(PF) in the meta compound, its sign relative to $^4D(PF)$ could not be determined either. The parameters obtained in this way from the nmr spectra of oriented meta and ortho tris(fluorophenyl)phosphines are reported in Table 6.3.

Table 6.3 Selected Nmr Data of ortho and meta tris(fluorophenyl)phosphines

Nmr Parameters	ortho	meta
$^1J(PC)$ /Hz	-12.4	-12.4
$^1J(PC)+2.\,^1D(PC)$ /Hz	-90.8 ±1	
$^1D(PC)$ /Hz	-39.2 ±.5	
$^5J(PF)$ /Hz	+56.2 ±.5	-0.8
$^5J(PF)+2.\,^5D(PF)$ /Hz	-70.2 ±.2	-30.5 ±.5
D(PF) /Hz	-63.2 ±.25	-16.5 ±.5
D(FF) /Hz	-16.7 ±.25	-6.0 ±.25

6.3.2 ^{31}P Shielding Anisotropies

The ^{31}P shielding anisotropies of tris(fluorophenyl)-phosphines were determined using equation 6.4 and they are reported in Table 6.4 Two method were employed to obtain the isotropic chemical shifts.

i) ν(iso) was determined at various temperatures above the isotropic/nematic transition temperature of the so ution, and the results were extrapolated to the nematic temperature. An explanation of this method is given in detail in Chapter 3.

ii) The chemical shift for different values of S_{zz} (obtained by varying the concentration of solute in solvent) was measured and extrapolated to $S_{zz} = 0$ to give the isotropic chemical shift.

Table 6.4 Parameters used to calculate ^{31}P Shielding Anisotropies in Ortho and Para $(C_6FH_4)_3P$

	Para[a]		ortho
	Method 1	Method 2	Method 1
$^1D(PC)$/Hz	-66.8 ±1	-66.8 ±1	-39.2 ±1
S_{zz}[b]	-.1489	-.1489	-.08739
ν(nem) - ν(iso)/Hz	-135 ±3[c]	-105 ±3[c]	-13 ±2[d]
$\sigma_\parallel - \sigma_\perp$/ppm	+37 ±2	+44 ±2	+6 ±2

a) See text

b) Calculated using equation 6.1

6.4 Discussion

6.4.1 Geometry and J Anisotropies

The molecular geometry, anisotropies in the indirect couplings, and conformational preferences of tris(fluorophenyl) phosphines were deduced using the experimental dipolar couplings D(PC), D(PF) and D(FF), and an assumed geometry [21,22]. The main sources of error are similar to those listed in Section 6.4. In summary, the errors in this study originate from the normal error in the experimental couplings resulting from uncertainties in the line positions and neglect of vibrational averaging[29]. All the relevant line positions in the main spectrum could be measured within ±0.3Hz and the lines in the satellite regions were obtained within ±1.0Hz. Studies have shown[29] that vibrational corrections can be neglected when the expected internuclear distance is relatively large and the atoms involved are other than protons. Hence vibrational averaging of the experimental anisotropic couplings PF, PC, and FF can be neglected here. The way the errors from the uncertainties in the line positions contribute to the final solution are discussed separately for each molecule studied.

Tris(p-fluorophenyl)phosphine

The estimated geometry and contributions from anisotropy in the indirect $^{5}J(PF)$ and J(FF) couplings are reported in Table 6.5. The calculations were based on an S_{zz} derived from $^{1}D(PC)$ and the assumption that the CPC inter-bond angle and r(PC) bond length are the same as that in triphenylphosphine[21]. In Table 6.1 the results in column B obtained from $^{5}D(PF)$ were eliminated because of the relative inaccuracy in the measured

coupling compared to the experimental error.

Table 6.5 Anisotropies in J(PF) and J(FF) couplings in para $(C_6FH_4)_3P$

	Sample	
	A	C
$^1D(PC)$/Hz	-74.1 ±.5	-66.8 ±.5
S_{zz} [a]	-0.16519 ±.0011	-0.14891 ±.0011
$^5D(PF)$/Hz (expt)	-6.9 ±.25	-5.7 ±.5
$^5D(PF)$/Hz (calc)	-7.97 ±.25	-7.19 ±.5
D(FF)/Hz (expt)	+10.00 ±.25	+9.03 ±.1
D(FF)/Hz (calc)	+10.73 ±.25	+9.67 ±.1
$^5D_{FF}^{indir}$/Hz	1.07 ±.25	0.63 ±.1

a) Calculated using equation 6.1

The value of the internuclear distance r(PF) calculated using equation 6.2 and results from columns A and C was 6.4 ±.1A. This value corresponds to r(CF)=1.7 ±.1A assuming that r(CC)=1.397A and r(PC)=1.83A, and that the experimental anisotropic coupling is purely dipolar. This is well outside the expected value for this internuclear distance (r(CF)=1.33 ±.02A)[30], and the difference is larger than the experimental error. This implies that $^5J(PF)$ has an anisotropic contribution, and this is not surprising as similar observations were made in the study of the pentafluorophenyl phosphorus system oriented in Phase V[22]. The calculated value for r(FF) from D(FF) was found to be 9.57A, whereas the expected value is 9.36A, when using the same geometry. Again the discrepancy between the calculated value and the

expected value for r(FF) can be removed by assuming that there is contribution from anisotropy in J(FF) [31]. Evidence for anisotropy in J(PF) and J(FF) was also deduced from the ratios of D(PF)/D(PC) and D(FF)/D(PC) at three different orientations. However, equation 6.1 can be solved for the CPC inter-bond angle using S_{zz} derived from the expected value of r(FF) and the experimental D(FF). The value of the angle obtained in this way was $109.9^{o} \pm .5^{o}$ which is reasonable when compared with same bond angle in triphenylphosphine.

The present study of tris(p-fluorophenyl)phosphine has enabled the determination of the sign of $^{1}J(PC)$ and $^{5}J(PF)$ couplings and anisotropies in the PF and FF indirect couplings. The study has also permitted the determination of the CPC inter-bond angle on the assumption that the experimental D(FF) was purely dipolar. Very little could be said about conformational preferences of this molecule in the "liquid" state. What could be deduced from the anisotropic ^{19}F and ^{31}P nmr spectra is that this molecule retains effective C_3 symmetry which implies that the three fluorophenyl rings are equivalent.

Tris(o-fluorophenyl)phosphine

Unlike the $^{19}F\{^{1}H\}$ and $^{31}P\{^{1}H\}$ anisotropic spectra of the para substituted compound, the corresponding spectra of tris(o-fluorophenyl)phosphine should in principle give information about conformational preferences. The experimentally determined anisotropic couplings obtained from tris(o-fluorophenyl)phosphine oriented in Phase V have to be examined using various likely models in order to determine whether any of these can be chosen unambiguously. Both the proton decoupled ^{19}F and the ^{31}P nmr

spectra of the oriented species show a typical oriented AX_3 spin system[17]. The results from the analysis of these spectra then may arise from any one of the following models.

i) The phenyl rings undergo completely free rotation about the PC bond at a rate that is faster than the time scale for the nmr experiment and reorientation of the molecule. In such a situation the orientation of the molecule can be described by a single parameter S_{zz}. Using this model $^3D(PF)$ can be related to r(PF) by using an equation derived by McFarlane and Kennedy[25] in the study of ^{31}P shielding anisotropies for organo phosphines.

$$^3D(PF) = K(PF)\ S_{zz} \langle 3\cos^2\Phi - 1\rangle / 2r_{PF}^3 \qquad 6.5$$

and

$$\langle \cos^2\Phi \rangle = \cos^2\gamma \cos^2\beta + \tfrac{1}{2} \sin^2\gamma \sin^2\beta \qquad 6.6$$

where γ is the angle between the symmetry axis and PC bond and β is the angle the vector PF makes with the PC bond (cf. Fig 6.7). Solving equations 6.5 and 6.6, and using S_{zz} determined from D(PC) and assuming its sign to be negative, r(PF) was calculated as 1.02 A. The expected value is 3.01A. Such a large disagreement cannot be accounted for by the experimental error. This can imply that the discrepancy in the calculated value of r(PF) is caused by:

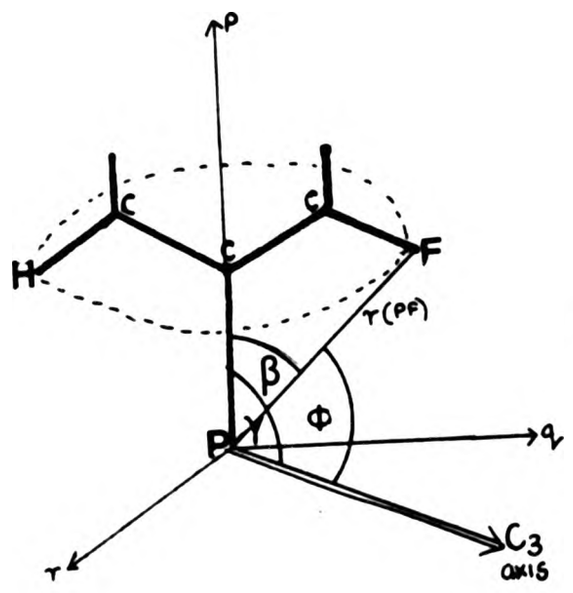

Fig. 6.7

a) An incorrect assumed geometry.

b) A significant contribution from anisotropy in $^3J(PF)$.

The dependence of the results on the geometry was tested by modifying the geometry by reasonable quantities and it was observed that this was not a major contributing factor. (b) was similarly rejected because by using an assumed geometry, $^{3}D(PF)$ was calculated as 2.3Hz which corresponds to a value D_{PF}^{indir} which is most unlikely. This model was also eliminated because the value of S_{zz} calculated from Equation 6.4, assuming that the experimental D(PF) as being purely dipolar and an assumed geometry, was -2.2163, which is impossible[32]. This latter observation also eliminates discrepancies caused by a) and b).

ii) A single conformation of tris(o-fluorophenyl)phosphine may exist in the nematic phase. Furthermore, from the anisotropic ^{19}F and ^{31}P nmr spectra this conformation must have effective C_3 symmetry. To calculate a conformation that satisfies the experimental dipolar couplings D(PC), D(PF), and D(FF) simultaneously involves determining these dipolar couplings for each likely "rigid" structure of tris(o-fluorophenyl)phosphine. To do this the computer program COPF3.FOR was written and its listing is shown in the appendix. The program sets up the molecule initially with the planes of the fluorophenyl rings all parallel to the C_3 symmetry axis. Then it generates other possible configurations by rotating the rings independently in 5^{o} intervals from the previous position, and calculates the averages of the $^{3}D(PF)$ and the D(FF) couplings using S_{zz} derived from $^{1}D(PC)$. To save computing time the program does not generate conformers which are permutations of one another. For example, if a conformer has phenyl ring A in Θ position, phenyl ring B in Ω position and phenyl ring C in Ψ position; then it does not generate a conformer where the phenyl ring A is now in

the Ω position, phenyl ring B is in the ψ position and phenyl ring C in the Θ position. However the model does assume rapid interconversion, relative to the nmr time scale, between conformers that are permutations of one another so as to retain C_3 symmetry. The program also rejected certain conformers that were unacceptable. The acceptable conformers were:

a) Conformers that gave an average value of D(PF) and D(FF) which were within ±7Hz of the experimental dipolar couplings. This allowed for any anisotropy in PF and FF indirect couplings, and errors in the measurement of the anisotropic couplings.

b) Conformers were excluded when the internuclear distance between two fluorine atoms was less than the value of 2 covalent radii for fluorine (2.8A) [33,34].

A list of 15 conformers calculated in this way is given in Table 6.6, but of course if the interval of rotation of the fluorophenyl rings was reduced from 5^{o}, then additional intermediate acceptable conformers would appear. The results from this calculation show that any one of the conformers in Table 6.6 may exist in the nematic phase. Furthermore on inspection of Table 6.6, the 15 conformers can be realisticly reduced to only two substantially different conformations, I and II.

iii) There is more that one conformer present in the anisotropic phase and examples of the likely conformers are summarized in Table 6.6. However, besides these conformers, any of which alone may not give average values of D(PF) and D(FF) couplings that reproduce the experimental ones, but when combined with other conformers, will do so. To calculate a list of the latter set of conformers would be unrealistic because of the large number of possible solutions generated. Furthermore it can be

Table 6.6 Conformers of ortho $(C_6FH_4)_3P$ calculated using the computer program COPF3.FOR.

	Conformer[a]			Dipolar Coupling[b]/Hz	
	A	B	C	D(PF)[c]	D(FF)[d]
I	20	65	275	-55.3	-19.4
	20	70	275	-55.3	-18.8
	25	55	275	-55.4	-15.4
	25	60	275	-56.1	-15.5
	25	65	275	-56.5	-15.4
	25	70	275	-56.5	-15.1
	25	75	275	-56.0	-14.4
	25	80	275	-55.1	-13.4
II	85	280	335	-55.1	-13.4
	85	285	335	-56.0	-14.4
	85	290	335	-56.5	-15.1
	85	290	340	-55.3	-18.8
	85	295	335	-56.5	-15.4
	85	295	340	-55.3	-19.4
	85	305	335	-55.4	-15.4

a) Conformers with phenyl rings in positions A, B, and C degrees (see text)

b) Dipolar couplings couplings calculated using S_{zz} determined from D(PC).

c) Experimental=-63.2 ±.3 Hz

d) Experimental=-16.7 ±.3 Hz

said that there is rapid interconversion between preferred conformers because the line width in both the anisotropic ^{19}F and the ^{31}P spectra is what is normally expected in nematic solution. From our calculation using this model it was found that the sign of D(PF) from all possible conformation was negative. This implies that $^{3}J(PF)$ is positive.

Tris(m-fluorophenyl)phosphine

The method of selection of models that are consistent with the ^{19}F and ^{31}P anisotropic spectra of oriented tris(m-fluorophenyl)phosphine should in principle be the same as applied in the ortho case. However in practice this was not possible because the orientation parameter from $^{1}D(PC)$ could not be calculated from the $^{31}P\ \{^{1}H\}$ spectrum with carbon-13 satellites of oriented tris(m-fluorophenyl)phosphine because the satellite region was hidden by the main spectrum. The sign of the orientation parameter may be assumed from that found for other molecules which have similar structure, but its magnitude cannot be assumed to be the same as observed from the para and the ortho tris(fluorophenyl)phosphine nematic samples when the same concentrations are employed. This is because the orientation of the molecule is dependant upon the chemical and physical properties of both the molecule and the liquid crystal solvent. These reasons make it impossible to determine conformational preference for this molecule at present.

6.4.2 ^{31}P Shielding Anisotropies

The ^{31}P shielding anisotropies for para and ortho tris(fluorophenyl)phosphines are reported in Table 6.4. The results from tris(p-fluorophenyl)phosphine using two different methods for determining the isotropic chemical shift show that there is a difference of about 5ppm which exceeds that allowed for experimental error. This implies that the technique of determining shielding anisotropies from oriented nmr suffers from

its inability to determine accurately the chemical shift at zero orientation. The method is also influenced by the inaccuracy in the orientation parameter. However, in addition to the above suggestions the discrepancy could also be due to conformational problems. Where intramolecular motion is important in the studies of molecules oriented in liquid crystals, it is expected that different orientations may cause the molecule to have different preferred conformations in the "liquid" state. This observation was also reported by Robert and Wiesenfield when they determined ^{31}P shielding anisotropies of several phosphine oxides, sulphides and selenides by solid state nmr[28] and liquid crystal nmr[23]. With these possible errors in mind comparison between the ^{31}P shielding anisotropies for the three phosphines are now discussed.

The values of ^{31}P shielding anisotropies reported in Table 6.3 show that they are positive, which indicates that shielding is more effective when the magnetic field is directed along the C_3 axis than when it is perpendicular to this axis. Only the sign of ^{31}P shielding anisotropy in tris(o-fluorophenyl)phosphine was assumed. The results from tris(p-fluorophenyl)phosphine show that the ^{31}P shielding anisotropy in this molecule is larger by 17ppm ±2ppm when compared with triphenylphosphine (+23ppm)[23]. One would expect that both these molecules would have similar shielding anisotropies as the fluorine in tris(p-fluorophenyl)phosphine is some distance away from the phosphorus. This suggests that the two molecules may have different conformations in the liquid crystal. The comparison of tris(o-fluorophenyl)phosphine and triphenylphosphine shows that ^{31}P shielding anisotropy in this fluoro molecule is smaller by about 20ppm.

Again the difference can be accounted for by conformational differences in the two molecules, but as the fluorine atom in tris(o-fluorophenyl)phosphine is close to the phosphorus, then a reduced anisotropy in comparison to triphenylphosphine is expected, because of the electronegativity of the fluorine.

6.5 Conclusion

The nmr study of tris(p-fluorophenyl)phosphine has shown evidence of anisotropy in the indirect PF and FF couplings. The inter-bond CPC angle was determined as $109.9^{\circ} \pm .5^{\circ}$ in this molecule when the anisotropies in $^{1}J(PC)$ and $J(FF)$ were assumed to be zero. Assuming that the signs of the ^{31}P shielding anisotropies in triphenylphosphine and tris(p-fluorophenyl)-phosphine are the same, then the signs of $^{1}J(PC)$ and $^{5}J(PF)$ were determined to be negative. This is consistent with other work[18,19].

In the study of tris(o-fluorophenyl)phosphine oriented in a liquid crystal, the nmr analysis showed conclusively the absence of free rotation about the PC bonds. However, it was consistent with the presence of a single conformation or rapid interconversion between preferred conformers. From the present study, the sign of $^{3}J(PF)$ was determined as positive on the assumption of the sign of the ^{31}P shielding anisotropy in triphenylphosphine.

^{31}P shielding anisotropies for the ortho and the para tris(fluorophenyl)phosphines were determined. In the case of the tris(p-fluorophenyl)phosphine the shielding anisotropy was observed to be positive and for tris(o-fluorophenyl)phosphine it

was determined as positive assuming S_{zz} to be negative. In the previous chapters limitations from studying nmr in liquid crystal solvents have been discussed. In summary they are: the need to know the orientation parameters which characterize the orientation of the molecule, anisotropies in the indirect couplings and corrections to the dipolar couplings from molecular vibrations. This study has shown that the method also suffers from conformational problems, when intramolecular motion is important, and the determination of the isotropic chemical shift at zero orientation when determining chemical shift tensors.

APPENDIX 6.1

Listing of the Computer Program COPF3.FOR

```
C           ***PROGRAM COPF3.FOR***
            DIMENSION X2(36),Y2(36),Z2(36)
            DIMENSION X11(12),Y11(12),Z11(12)
            DIMENSION R(36,36),R3(36,36)
            DIMENSION ALPHAX(36,36),ALPHAY(36,36),ALPHAZ(36,36)
            DIMENSION CONST(36,36),D(36,36),TOTD(35,35),AVE(35,35)
            DO 150  I=2,4
            CONST(1,I)=45728.4
 150        CONTINUE
            DO 151  I=2,3
            DO 152  J=3,4
            IF (I.EQ.J)GO TO 152
            CONST(I,J)=106269.
 152        CONTINUE
 151        CONTINUE
            X11C=1.21
            z11C=-.6985-1.83
C           C1C2F2=123.
            CCFANG=240.-123.-90.
            X112=X11C+(COSD(CCFANG)*1.33)
            Z112=Z11C+(SIND(CCFANG)*1.33)
            SZZ=-.0873851
            SXX=-0.5*SZZ
            SYY=SXX
            ANG2Z=64.46892
 509        format(f)
            DO 801 IANG=5,360,5
            DO 802 JANG=IANG,360,5
            DO 803 KANG=JANG,360,5
            ROT(2)=IANG
```

```
      ROT(3)=JANG
      ROT(4)=KANG
      DO 29 I=2,4
      ROTAT=ROT(I)
      BETA = 120.*(I-2)
      X2I=0.0
      X2I=X112*COSD(ANG2Z)*COSD(ROTAT)-(Z112*SIND(ANG2Z))
      X2(I)=X2I*COSD(BETA)+(X112*SIND(BETA)*SIND(ROTAT))
      Y2I=0.0
      Y2I=-Z112*SIND(ANG2Z)+(COSD(ROTAT)*COSD(ANG2Z)*X112)
      Y2(I)=X112*SIND(ROTAT)*COSD(BETA)-(Y2I*SIND(BETA))
      Z2(I)=Z112*COSD(ANG2Z)+(X112*SIND(ANG2Z)*COSD(ROTAT))
29    CONTINUE
      DO 91 I=1,3
      DO 92 J=2,4
      IF (I.EQ.J)GO TO 92
      R(I,J)=SQRT((Z2(I)-Z2(J))**2+(X2(I)-X2(J))**2
     1+(Y2(I)-Y2(J))**2)
      IF(R(I,J).LT.2.80) GOTO 803
      R3(I,J)=R(I,J)**3
92    CONTINUE
91    CONTINUE
      DO 153 I=1,3
      DO 154 J=2,4
      IF (I.EQ.J)GO TO 154
      ALPHAX(I,J)=((ABS(X2(I)-X2(J)))/R(I,J))**2
      ALPHAY(I,J)=((ABS(Y2(I)-Y2(J)))/R(I,J))**2
      ALPHAZ(I,J)=((ABS(Z2(I)-Z2(J)))/R(I,J))**2
154   CONTINUE
153   CONTINUE
      DO 155 I=1,3
      DO 156 J=2,4
      IF (I.EQ.J)GO TO 156
      D(I,J)=-(CONST(I,J)/R3(I,J))*((SXX*ALPHAX(I,J))
     1+(SZZ*ALPHAZ(I,J))+(SYY*ALPHAY(I,J)))
156   CONTINUE
155   CONTINUE
      AVEPF=(D(1,2)+D(1,3)+D(1,4))/3.0
      IF(ABS(AVEPF).LT.55.0) GOTO 803
      IF(ABS(AVEPF).GT.70.0) GOTO 803
      AVEFF=(D(2,3)+D(2,4)+D(3,4))/3.0
      IF(ABS(AVEFF).LT.10.0) GOTO 803
      IF(ABS(AVEFF).GT.22.0) GOTO 803
      OPEN(UNIT=23,ACCESS='APPEND')
      WRITE(23,445)IANG,JANG,KANG,AVEPF,AVEFF
      CLOSE(UNIT=23)
      AVEFF=0.0
      AVEPF=0.0
803   CONTINUE
802   CONTINUE
801   CONTINUE
751   CONTINUE
445   FORMAT(3(2X,I5),4(2X,F7.1))
      RETURN
      END
```

6.6 References

1 C.L. Khetrapal and A.C. Kunwar, Advances in Magnetic Resonance Vol 9, 301(1977).

2 Nmr Spectroscopy using Liquid Crystal Solvents, J.W. Emsley and J.C. Lindon, Pergamon, N.Y. 1975;

3 L. Lunazzi, G.F. Pedulli, M. Tiecco and C.A. Veracini, J. Chem. Soc. Perkin Trans. 2, 755(1973);
R.Y. Dong, J. Mag. Res. , 7, 60(1972).

4 P.L. Barili and C.A. Veracini, Mol. Phys., 24, 673(1972); C.A. Veracini, D.Macciantelli and L. Lunazzi, J. Chem. Soc. Perkin Trans. 2, 1396(1973); P. Bucci, M. Longeri, C.A. Veracini, and L. Lunazzi, J. Amer. Chem. Soc., 96, 1305 (1974).

5 A. d'Annibale, L. Lunazzi, A.C. Boicelli and D. Macciantelli, J. Chem. Soc. Perkin Trans. 2, 1396(1973);

6 W. Niederberger, L. Lunazzi and P. Diehl, Mol. Phys., 26, 571(1793).

7 J. Courtieu, Y. Gounelle, C. Duret, P. Gonord and S.K. Kan, Org. Mag. Res., 6, 622(1974).

8 P. Diehl, C.L. Khetrapal and W.Niederberger, J. Mag. Res. 4,352(1971).

9 P. Diehl, P.H. Henrichs and W. Niederberger, Mol. Phys., 20, 139(1971).

10 P. Diehl, C.L. Khetrapal, W. Niederberger and P. Partington, J. Mag. Res., 2 181(1970).

11 P. Diehl, H.P. Kellarhals and W. Niederberger, J. Mag. Res., 2 230(1970)

12 P. Diehl, P.H. Henrichs, W. Niederberger and J. Vogt Mol. Phys., 21 377(1971).

13 E.E. Burnell and P. Diehl, Mol. Phys., 24 489(197).

14 P. Bucci, P.F. Franchini, A.M. Serra, and C.A. Veracini, Chem. Phys. Letts. ,8 421(1971).

15 P. Bucci, and C.A. Veracini, J. Chem. Phys., 56 1290(1973).

16 J.W. Emsley, J.C. Lindon and D.S. Stephenson, Mol. Phys. 27 641(1974).

17 G. Englert, Z. Naturforsch, 24A, 3799(1964).

18 T. Bundgaard and H.J Jakobsen, Act. Che,. Scand., 26, 2548(1972); Tetrahedron Lett., 3353(1972).

19 W. McFarlane, Org. Mag. Res., 1, 3(1969).

20 References 27,28 in Chapter 4.

21 J.J. Daly, J. Chem. Soc., 3799(1964).

22 Chapter 5.

23 J.B. Robert and L.Wiesenfield, J. Mag. Res., 38 357(1980).

24 N. Zumbulyadis and B.P. Dailey, Mol. Phys., 26, 777(1973); ibid. 27, 633(1974); P.K. Bhattacharya and B.P. Dailey, Mol. Phys., 28, 209(1974); J. Montana, N. Zumbulyadis and B.P. Dailey, J. Chem. Phys., 65, 4571(1965).

25 J.D. Kennedy and W. McFarlane, J. Chem. Soc. Chem. Commun., 666(1976).

26 J. Pierre, A.L. Brand, A.Cogne and J.B. Robert, Chem. Phys. Letts., 48, 524(1977); J. Amer. Chem. Soc., 100, 2600(1978).

27 J. Montana, N. Zumbulyadis and B.P. Dailey J. Amer. Chem. Soc., 99, 319(1977).

28 J.B. Robert and L.Wiesenfield, Mol. Phys., 44 319(1981).

29 Section 2.6.

30 References 6,9,10,27,28 in Chapter 5.

31 Section 2.8.

32 Section 2.5.

33 A. Bondi, J. Chem. Phys., 68, 441(1964);

34 J.E. Huheey, Inorganic Chemistry, Harper and Row Publishers N.Y.

Chapter 7

THE CONFORMATIONAL ANALYSIS OF TRIMESITYLPHOSPHINE AND TETRAMESITYLDIPHOSPHINE

7.1 Introduction

The structure and stereochemistry of tri-coordinate phosphorus compounds have been extensively studied, and in this work nmr has played an enormous part [1-7]. Tri-coordinated phosphorus compounds such as phosphine itself and tri-substituted organophosphines adopt a pyramidal structure with the electron lone pair pointing away from the apex of the pyramid (Fig 7.1). The degree of flattening of the pyramid or, as in Fig 7.1, the RPR inter-bond angle is of course dependent on the substituent R. For instance, for R = methyl the inter-bond angle is 98.6° [8], whereas when R is phenyl the inter-bond angle becomes 108.8° [9].

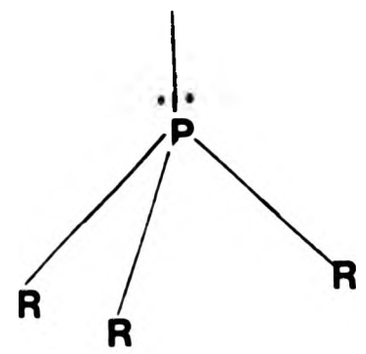

Fig 7.1

These variations arise as a consequence of the different sizes of the group R. In addition when the group R is very bulky, there may be steric interference between the substituents on the phosphorus, and this can restrict the rotation about the phosphorus-carbon bonds. Thus when R is a phenyl group the ortho protons on the same ring might become nonequivalent, and the dynamics of the internal rotation could then be studied by nmr. Similar considerations apply to diphosphines R_2PPR_2 where in addition it is also necessary to take into account the rotation

about the PP bond. The present chapter reports on the study of this kind behaviour in 2,4,6-trimethylphenyl phosphorus compounds which will be referred to in future as mesityl compounds.

In principle, variations in coupling constants or in chemical shifts could be used to provide detailed information about the particular configuration adopted; in practice considerably more is known about the relationship between geometry and the magnitudes of coupling constants, than about the corresponding relationship for chemical shifts. For example with regard to two-bond coupling, work has been carried out on $J(^{1}H\ ^{15}N)$, $J(^{13}C\ ^{15}N)$, $J(^{13}C\ ^{31}P)$, and $J(^{1}H\ ^{31}P)$ [10-17], and for three-bond coupling on $J(^{1}H\ ^{31}P)$, $J(^{13}C\ ^{31}P)$, $J(^{1}H\ ^{19}F)$ and $J(^{1}H\ ^{15}N)$ [7,18,19,20]. It is also known that long range couplings are sensitive to the orientation of the lone pair [7]. These studies all show the existence of a Karplus type of relationship, i.e a correlation between magnitude of the coupling constant and the dihedral angle α (fig 7.2) [21].

Fig 7.2

For example from the study of cis and trans isomers of 1,2-dimethyl-3-phospholene (Fig 7.3a,b) it is known that $^{2}J(PC)$

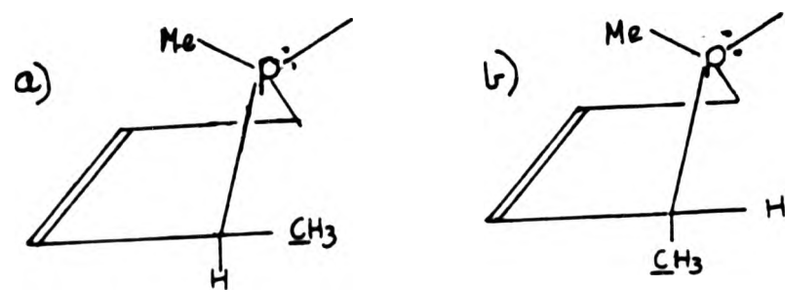

Fig 7.3

1,2-dimethyl-3-phospholene a) cis isomer b) trans isomer.

is very small for the cis isomer and large for the trans (ca 32 Hz)[22]. Similarly, Gray and Cremer [23] reported that in phosphetan, the same coupling to Me_A was very small (0-5 Hz) and that to Me_B was large (27-34 Hz) (Fig 7.3c). Thus the general rule can be given that large coupling occurs in systems where the dihedral angle is small, and small coupling occurs when the same dihedral angle is large.

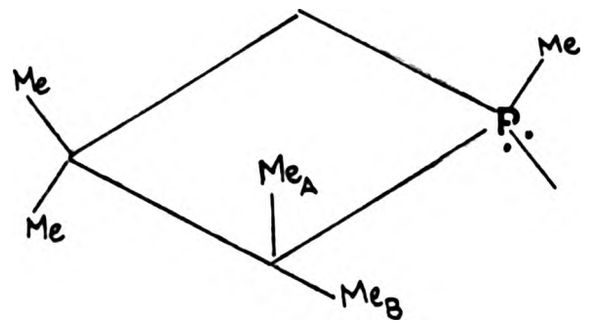

Fig 7.3 c
Pentaphenyl Phospheten

We can now turn to triphenylphosphine. Inspection of a model of triphenylphosphine indicates if all three phenyl rings were to adopt a configuration with their planes parallel to the C_3 symmetry axis (Fig 7.4a) then the ortho protons marked X would be so close to each other that this configuration can be disregarded.

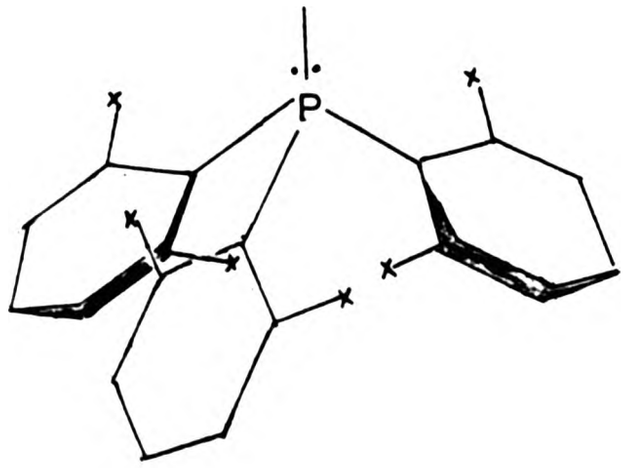

fig 7.4a

Triphenylphosphine

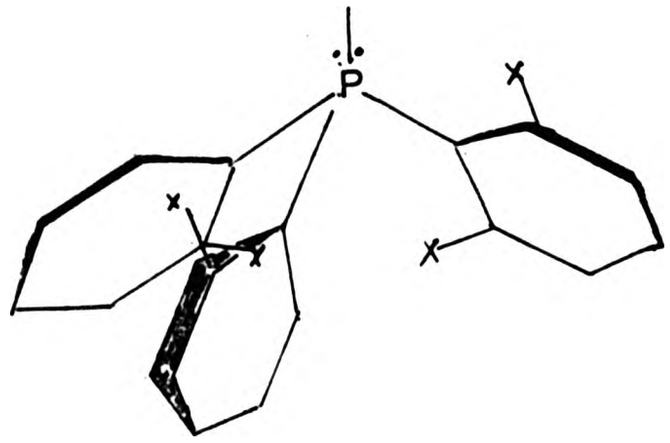

fig 7.4b

Triphenylphosphine

An alternative structure is one in which each phenyl ring is rotated through 90° from the previous position, but this is also unlikely as it again would create steric overcrowding (Fig 7.4b). Therefore it seem likely that triphenylphosphine adopts a configuration that is intermediate between the extremes described. This structure has a propeller-like twist which can either be of a left handed or right handed sense, so that the molecule would be chiral (compare the triphenylcarbonium ion[24]), although interconversion of the enantiomers might not involve a very large energy barrier, especially if geared rotation was possible. It is clear in this kind of structure that in any particular ring the ortho protons are inequivalent, as are the ortho carbons, but our measurements of the ^{13}C spectrum of triphenylphosphine at temperatures as low as -83°C gave a single doublet with $^{2}J(PC)$ = +19.7 Hz for the ortho ^{13}C resonance, implying that rotation about the PC bond is still fast. By contrast it was found that in tris-2-methylphenylphosphine at 32°C the ortho carbons were nonequivalent, and more importantly had remarkably different values of $^{2}J(PC)$ (+26.4, +0.4 Hz) [25], implying a pronounced dominance of a conformer in which one of these carbons has a large dihedral angle with respect to phosphorus lone pair, while the other has not. In this compound the three-bond coupling between methyl carbon and phosphorus was also relatively large (21.8 Hz). Similar results were obtained from substituted thienylphosphines (Fig 7.5a,b) [17].

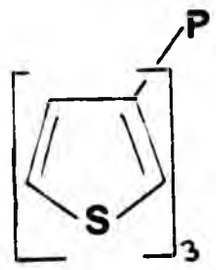

fig 7.5a

Trithienylphosphine

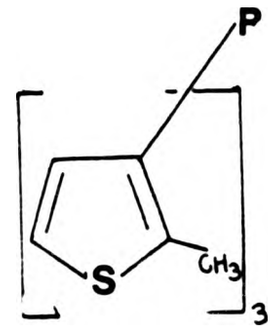

fig 7.5b

Tri(orthomethyl) thienylphosphine

In the foregoing examples the various nuclei exhibiting coupling constants of different sizes are also chemically nonequivalent and thus even when internal rotation is fast no coalescence phenomena are observed, and whilst it is possible to draw conclusions about the various conformers present, nothing can be said about the dynamics of the interconversion process. By contrast, the higher symmetry of the mesityl group leads to relatively simple ^{13}C and proton nmr spectra for mesityl phosphorus derivatives at and above room temperature when internal rotations are rapid on the nmr time scale, whereas at lower (but readily accessible) temperatures much more complicated spectra are obtained, indicating that various conformers are "frozen out". Band-shape analysis at intermediate temperatures can therefore in principle produce thermodynamic parameters for these processes of internal rotation [26,27]. In the case of trimesitylphosphine these processes refer to the internal rotation about the PC bond, whereas in tetramesityldiphosphine rotation about PP bond must also be taken into account. As expected, individual rotation of the methyl groups is too rapid to affect the spectrum at

temperatures available to us.

This chapter describes the determination of the energy barriers and conformational preferences at various temperatures in trimesitylphosphine and tetramesityldiphosphine. The first detailed reports of nmr experiments on mesityl compounds were from Stephonov's group [28,29]. They observed that the ^{13}C chemical shifts, and two and three-bond J(PC) coupling constants were dependant on relative orientation of the lone pair in trimesitylphosphine and tri(2,3,5,6-tetramethylphenyl)phosphine. Proton nmr and X-ray crystallography studies on tetramesityldiphosphine were reported by Baxter et al [30] who concluded that tetramesityldiphosphine adopted the anti conformation in both the solid and low temperature liquid states.

7.2 Experimental

Samples were examined in 10mm nmr tubes using dichloromethane as the solvent together with about 20% deuterated benzene to provide the internal frequency lock. In the case of tetramesityldiphosphine at temperatures above $-40^{o}C$ low solubility and long relaxation times for the carbons lead to poor signal to noise ratios, which were improved by adding $Cr(acac)_3$ (0.04g/4.5mls of solution)

^{13}C and ^{31}P nmr spectra were obtained on Jeol FX90Q and Jeol FX60 Fourier transform spectrometers. The operating frequencies for ^{13}C and ^{31}P on the FX90Q were 22.6 and 36.2 MHz respectively and on the FX60 the ^{13}C and ^{31}P frequencies were 15.0 and 24.2 MHz respectively. Both spectrometers had proton decoupling, but the FX60 was modified with an additional frequency synthesizer to

permit phosphorus decoupling together with proton decoupling. The required ^{31}P irradiation frequency was determined by direct measurement. Low temperature spectra were obtained with 2.5 KHz spectral width and 4K data points, and with an artificial line broadening window of about 0.5 Hz. Typically for the dynamic nmr experiments it was necessary to acquire 2000 transients and use an artificial line broadening weighting of the FID prior to transformation of 1-1.5 Hz to optimize the signal to noise ratio.

Both the Jeol FX60 and FX90Q were equipped for variable low temperature operation, using a flow of cold nitrogen to the probe. The rate of flow of nitrogen to the probe and hence the sample temperature was controlled and monitored on a Jeol temperature control unit. The temperature control unit was calibrated using a capillary containing a compound of known melting point placed in a dummy solution, and the melting process was observed by quickly taking out the tube from the probe. After each change in temperature or removal of sample from the probe the sample was allowed to equilibrate for about 10 minutes. The accuracy of temperature measurements in dynamic nmr has a direct consequence on the determination of activation parameters; hence the importance of this exercise.

Theoretical spectra were calculated using the program POLY obtained from the Daresbury NMR Library and partly written by Chan and Reeves[31]. The program as obtained from the library was slightly modified so that it could be used on our computer. Initially the format statements had to be modified. Secondly POLY was modified so that its output was a list of line positions and intensities. The table of line intensities and line positions was plotted with a Lorentzian line shape on a Tetronix graphical

display unit using our own program. POLY calculates nmr band shapes for exchange between a specified number of uncoupled sites which have spin 1/2 nuclei. The exchange which produces a modified band shape is computed from first order rate constants, arranged as a matrix, provided the line-width in the absence of exchange is known. The line-width in absence of exchange which is entered as T2 is obtained by varying T2 until the line-width in the experimental spectrum for the slow exchange limit is similar to that obtained in the calculated spectrum when rate constant is 0 sec^{-1}. A typical input and output for POLY is illustrated in Appendix 7.1. Then, the best fit rate constants were determined by direct comparison of simulated with experimental spectra.

7.3 Results And Discussion

Trimesitylphosphine

The ^{13}C nmr spectra of trimesitylphosphine at $-68^{o}C$ and room temperature with complete proton decoupling ($^{13}C\ \{^{1}H\}$) are depicted in Fig 7.6a,b. The results are reported in Table 7.1. As can be seen that there are approximately twice as many lines in the low temperature spectrum as in the one at room temperature. This implies that at low temperature certain conformers of trimesitylphosphine have been "frozen out". Comparison of the low temperature ^{13}C nmr with both proton and phosphorus decoupling ($^{13}C\ \{^{1}H, ^{31}P\}$) and the same spectrum but this time with proton decoupling only ($^{13}C\ \{^{1}H\}$) indicates that some of the lines that were doublets in the proton-decoupled spectrum collapse into singlets when both proton and phosphorus decoupling is carried out (fig 7.7a,b).

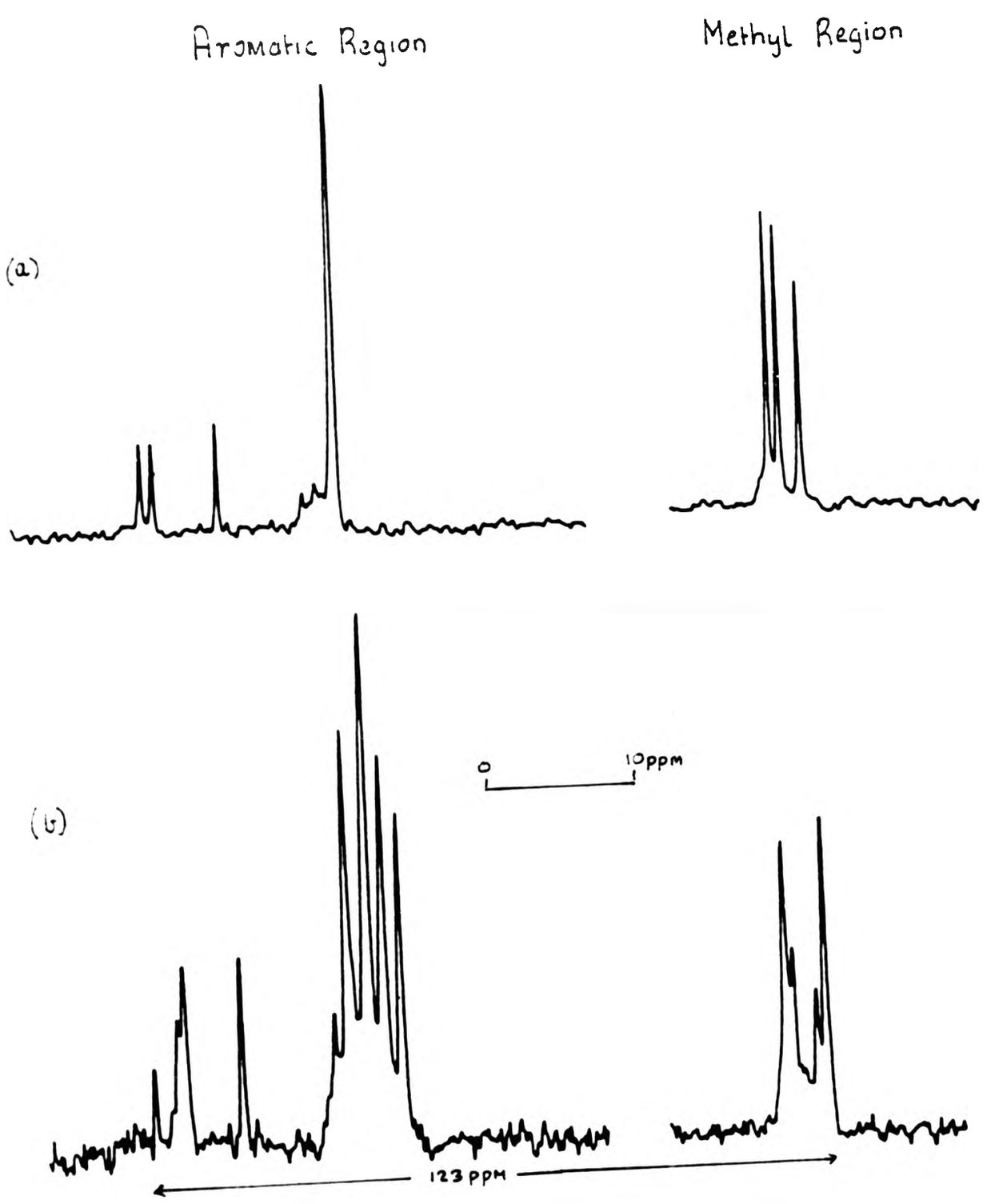

Fig 7.6 15 MHz $^{13}C\{^1H\}$ nmr spectra of Trimesitylphosphine at a) room temperature and b) -63°C

Fig 7.7 15 MHz ^{13}C nmr spectrum of Trimesitylphosphine at -68°C. (a) Phosphorus and proton decoupled, (b) proton decoupled.

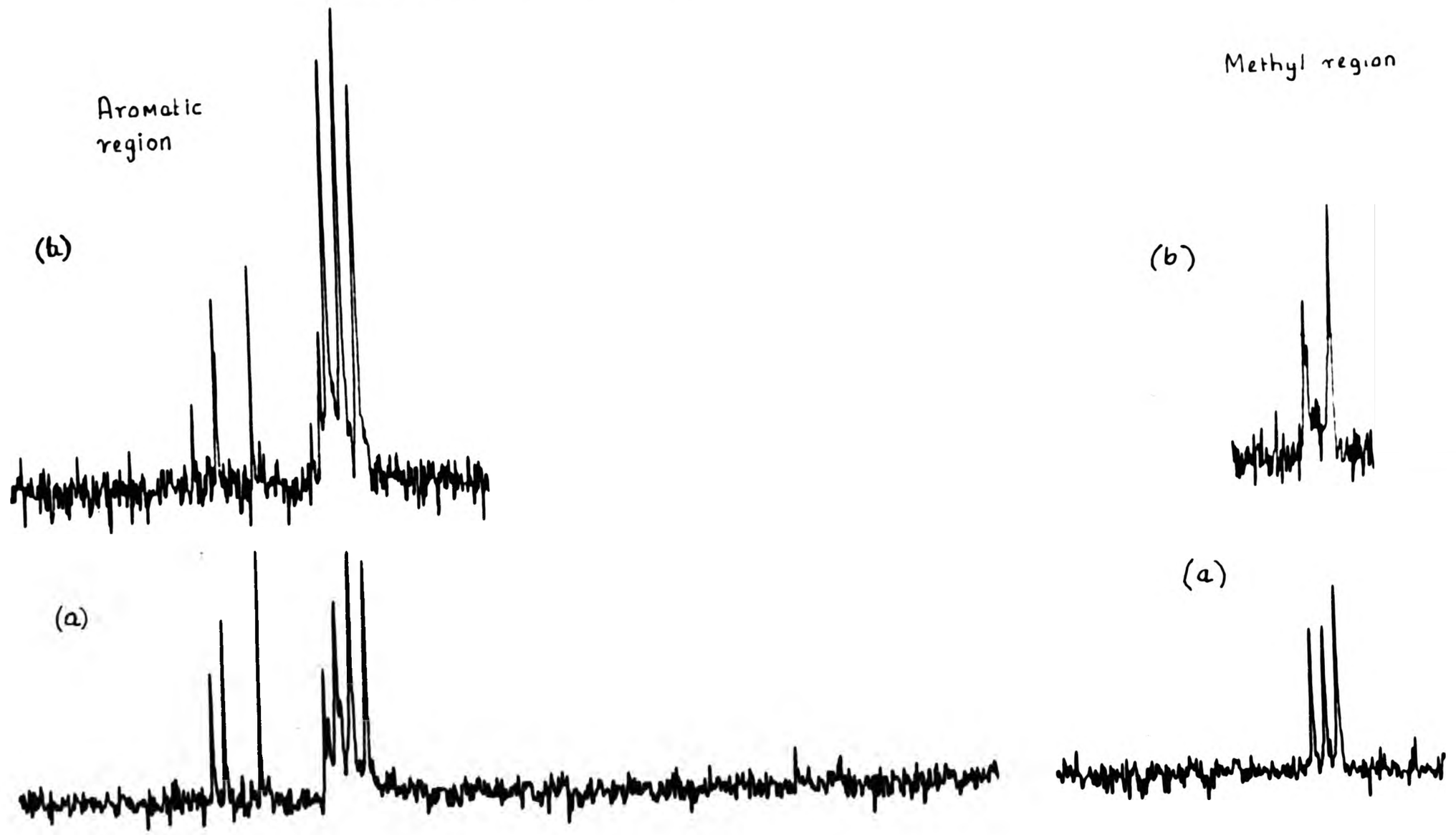

Table 7.1 NMR data of Trimesitylphosphine

Carbon[b]	^{13}C CHEMICAL SHIFT[a]			
	AROMATIC CARBONS		METHYL CARBONS	
	210K	303K	210K	303K
2	142.5	141.8	22.1	22.7
4	137.4	137.4	20.7	20.7
6	141.4	141.8	23.3	22.7

i^b	$^{13}C-^{31}P$ COUPLING CONSTANT			
	$^2J(P\ C_i)$		$^3J(P\ C_i)^c$	
	210K	303K	210K	303K
2	37.1	17.6	33.2	16.6
6	0.0	17.6	0.0	16.6

a) chemical shift in ppm to high frequency of $SiMe_4$

b) labelling refers to Fig 7.8

c) carbon refers to methyl carbon

Considering the methyl region ($\delta^{13}C$=21.0 to 24.0 ppm) of trimesitylphosphine with both proton and phosphorus decoupling there are three signals corresponding to the two ortho methyls C-2 and C-6 (see Fig 7.7) and the para methyl C-4 (labelling refers to Fig 7.8). The ^{13}C spectrum with proton decoupling only (Fig 7.7b)

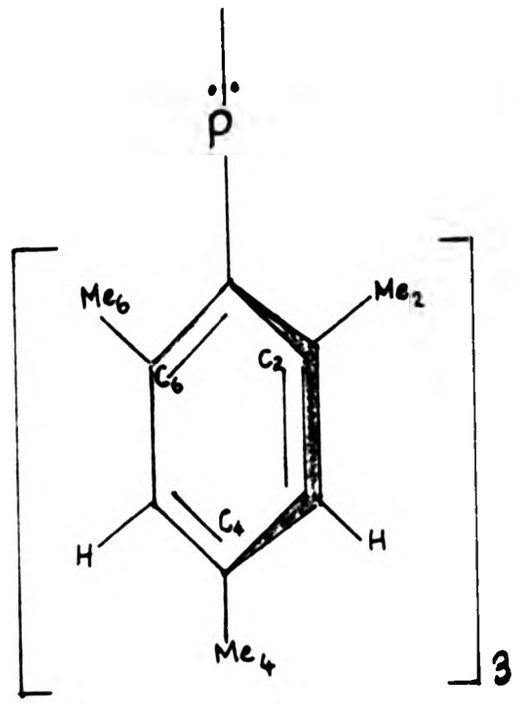

Fig 7.8
Trimesitylphosphine

has peaks at $\delta^{13}C$=23.3 ppm and $\delta^{13}C$=20.7 ppm which have small splittings that could not be resolved, whereas the peak at $\delta^{13}C$=22.1 ppm has a splitting of 33.2 Hz. This coupling can be taken to be positive from the results obtained upon similar compounds[23]. As the magnitude of $^{3}J(^{13}C-^{31}P)$ is related to the position of the methyl with respect to the lone pair at the phosphorus atom then the methyl with chemical shift of 22.1 ppm must be an ortho methyl trans to the lone pair. To determine which of the two other peaks can be assigned to the other ortho methyl a ^{13}C variable temperature nmr experiment was required. In the slow exchange limit (-68°C) trimesityl phosphine is locked in one particular configuration. As the temperature is raised the rotation about the PC bond will commence and eventually this rotation will become rapid with respect to the nmr time scale, causing the ortho aromatic carbons become equivalent and give a signal at their mean frequency. Over this temperature range we would observe coalescence between the two ortho methyl carbon signals in the ^{13}C nmr spectrum. In parallel the position of the para methyl carbon signal will remain unchanged. From Fig 7.9a it is found that the peak at $\delta^{13}C$=20.7 ppm corresponds with the other ortho methyl and the splitting is very small or equal to zero. From the magnitude of the coupling it can be concluded that this ortho methyl must be cis to the lone pair.

Comparison of the low temperature $^{13}C\ \{^{1}H\}$ and $^{13}C\ \{^{1}H, ^{31}P\}$ nmr spectra of the aromatic region (δ^{13}=135 ppm to $\delta^{13}C$=143 ppm) in trimesitylphosphine shows that there are three signals corresponding two ortho aromatic carbons and one para aromatic carbon. These resonances can be assigned to quaternary carbons because of the chemical shifts

observed and their low intensities (due to the absence of nuclear Overhauser effect and long relaxation times) compared with those from the rest of the aromatic carbons. In the $^{13}C\ \{^1H\}$ spectrum, one of the ortho aromatic carbons has a splitting of 37.0 Hz and the others have little or zero splitting. The corresponding spectrum at room temperature indicated that the signal at $\delta^{13}C$ =137.4 ppm was from the para aromatic carbon, as the position of this signal remained unchanged at low and room temperatures. The ^{13}C nmr signals at $\delta^{13}C$ =142.5 ppm and $\delta^{13}C$ = 141.4 ppm must belong to ortho carbons trans to the lone pair and cis to the lone pair respectively (from the magnitudes of their couplings). These observations from both $^{13}C\ \{^1H\}$ nmr spectra (at room and at low temperature) of trimesitylphosphine do show that the molecule at the low temperature prefers the chiral structure.

The next object of this study was to determine the energy barrier for the rotation about the PC bond. The energy of activation (E_a) was calculated for PC rotation in trimesityl-phosphine using Equation 7.1, where k is the rate constant in sec^{-1} and T is the absolute temperature.

$$k = - A \ln (E_a/RT) \qquad 7.1$$

Fig 7.9a shows spectra at 7 different temperatures covering the range in which the signals from the two ortho methyl carbons coalesce and Fig 7.9b shows matching computed spectra for a set of different rate constants k. From the plot of ln(k) against 1/T (Fig 7.9c) the energy of activation for the PC bond rotation was calculated. In Table 7.2 energy barrier for the PC bond rotation in trimesitylphosphine is reported.

Fig 7.9 Temperature dependant 15 MHz $^{13}C\{^1H, ^{31}P\}$ nmr spectra of trimesitylphosphine (upper) and the corresponding calculated spectra (lower)

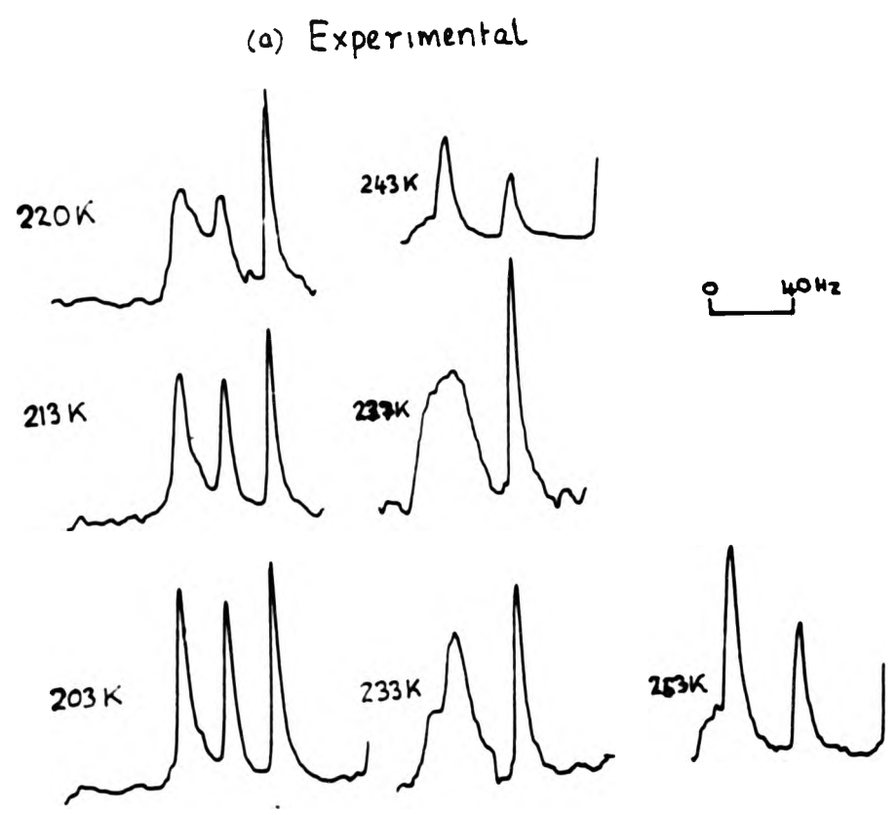

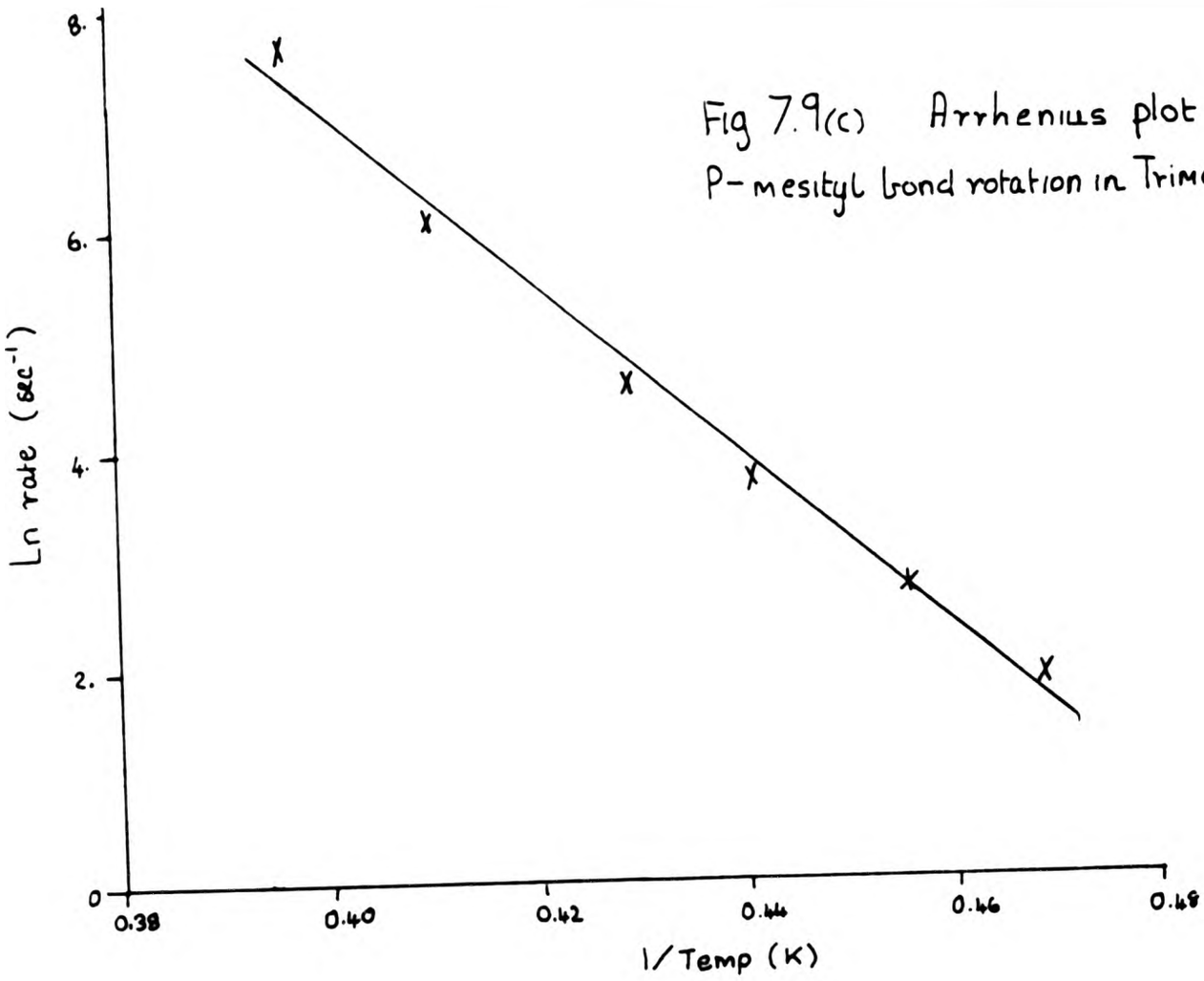

Fig 7.9(c) Arrhenius plot for the P-mesityl bond rotation in Trimesitylphosphine

Table 7.2 Energy Barrier Results For the Rotation about the P-Mesityl bond in Trimesitylphosphine from ^{13}C nmr data

$\Delta\nu$/Hz[a]	21.3 ±1
T(coalescence)/K[b]	223 ±2
E_a / KJ mol^{-1}	70.0 ±3

a) Separation between ortho methyl carbon signals for trimesitylphosphine before exchange.

b) Temperature at which the ortho methyl carbon signals in trimesitylphosphine coalesce.

Tetramesityldiphosphine

Low temperature (-48°C) and room temperature (+22°C) ^{13}C nmr spectra of tetramesityldiphosphine are depicted in Fig 7.10 and the results of their analysis are reported in Table 7.3.

Table 7.3 NMR data of Tetramesityldiphosphine

Carbon[b]	^{13}C CHEMICAL SHIFT[a]			
	AROMATIC CARBONS		METHYL CARBONS	
	230K	303K	230K	303K
2,7	146.4,144.9	144.9	23.3,22.0	22.0
4,9	138.4,136.6	137.5	20.5,20.3	20.4
6,11	142.3,141.7	144.9	22.0,21.8	22.0
	$^{13}C-^{31}P$ COUPLING CONSTANT/Hz			
	N[c]		N[d]	
i[b]	230K	303K	230K	303K
2,7	38.1,31.2		23.0,24.4	22.0
6,11	4.4,4.0		11.6,5.5	22.

a) chemical shift in ppm to high frequency of $SiMe_4$

b) labelling refers to Fig 7.12

c) $N=^2J(PC_i)+^3J(PC_i)$; C_i denotes aromatic carbon

d) $N=^3J(PC_i)+^4J(PC_i)$; C_i denotes methyl carbon

Once again we observe in the spectra that the number of lines at low temperature exceeds the number of lines at room temperature. Again one can say that at low temperature certain conformers of tetramesityldiphosphine are present and at higher temperature when rotation about the PC and PP bonds becomes fast with respect to

Fig 7.10 22.6 MHz $^{13}C\{^1H\}$ nm spectra of Tetramesityldiphosphine at
a) room temperature b) at -48°C

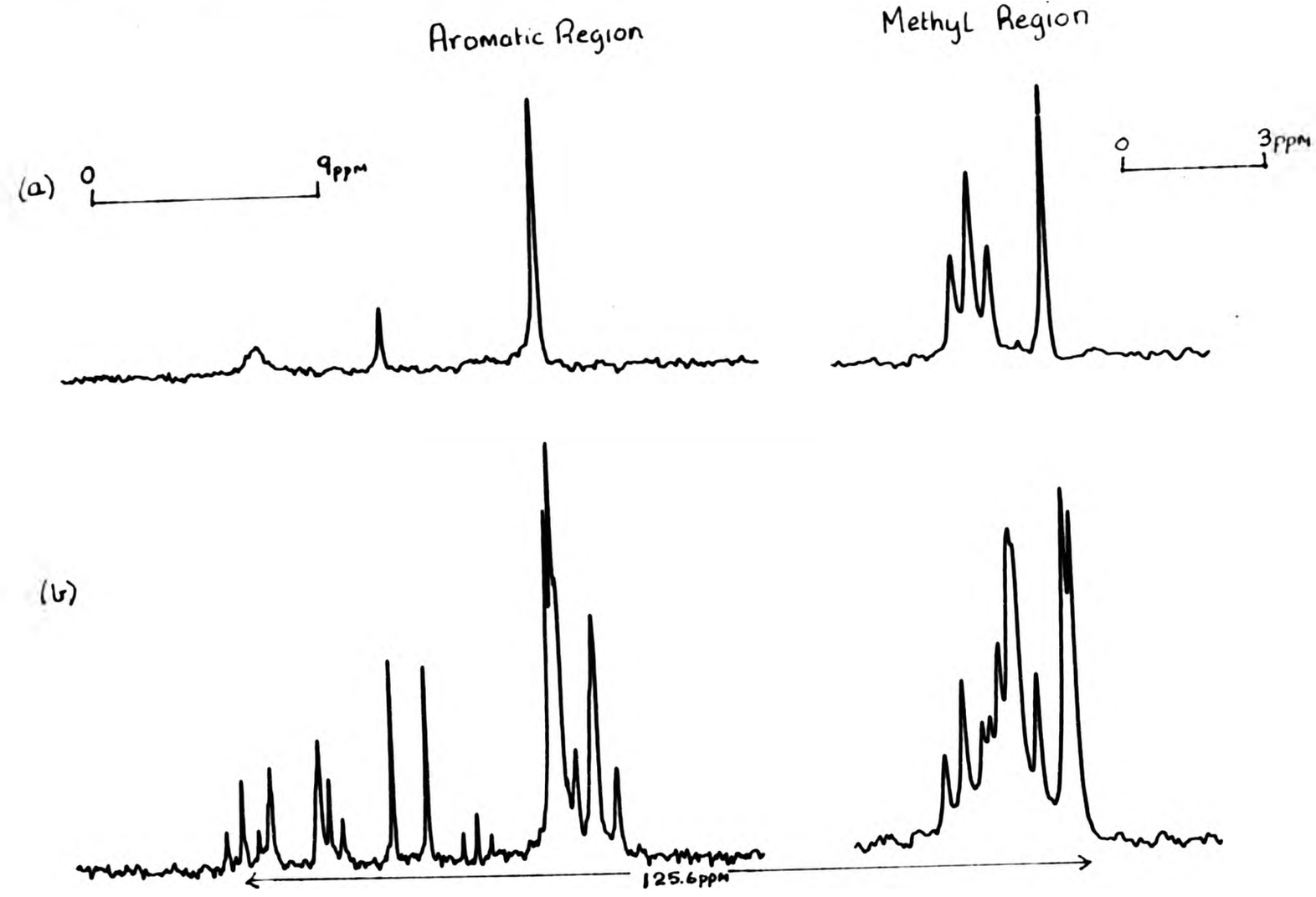

Fig 2.11 15 MHz ^{13}C nmr spectra of the Aromatic region of Tetramesityldiphosphine at -48°C
(a) proton decoupled (b) proton and phosphorus decoupled

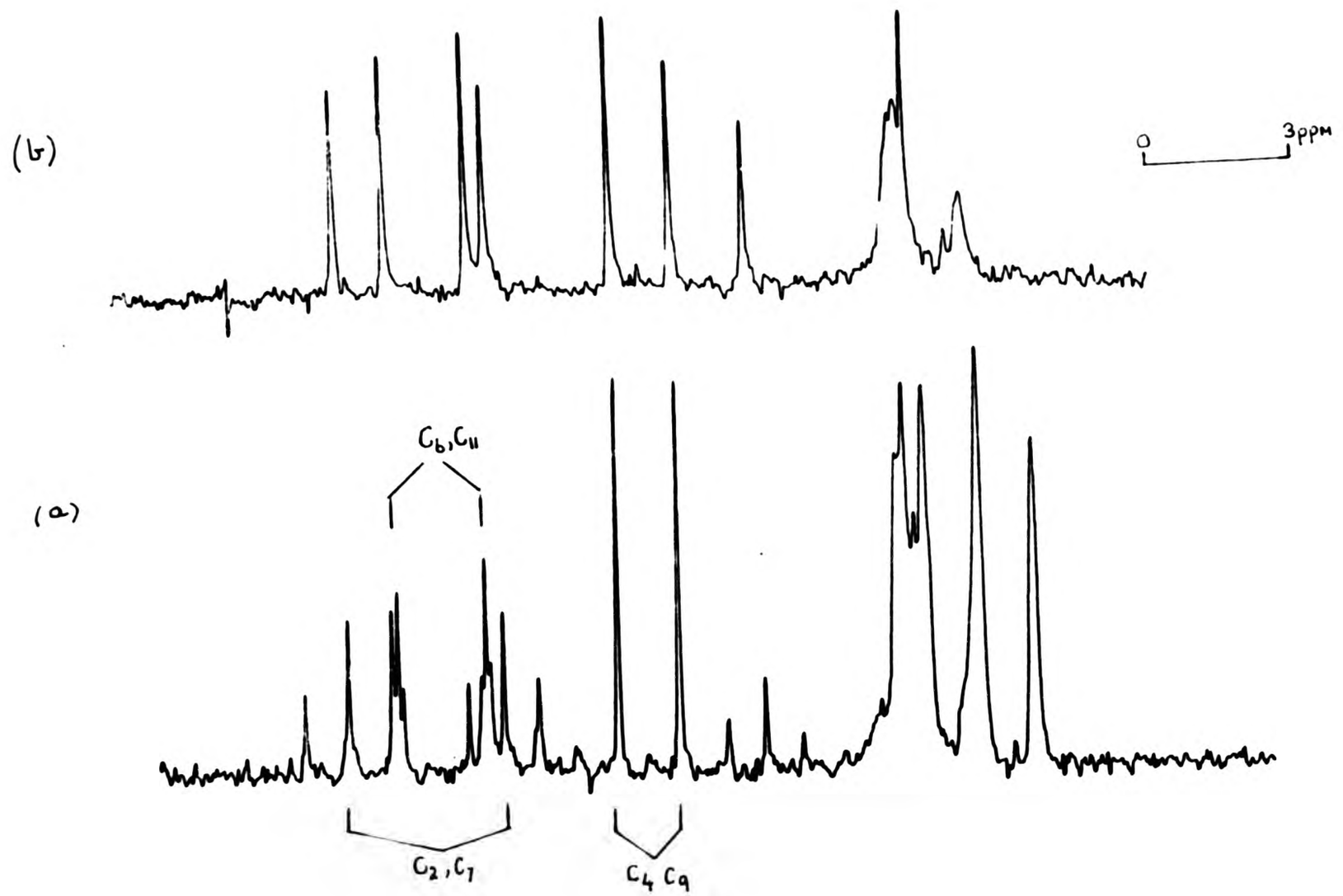

the nmr time scale, then the average signal between all the possible conformers will be present. As was found in the analysis of the $^{13}C\{^{1}H\}$ spectrum of trimesitylphosphine at low temperature, both $^{13}C\{^{1}H\}$ and $^{13}C\{^{1}H,^{31}P\}$ experiments were required to analyse the low temperature spectrum of tetramesityldiphosphine. From the low temperature $^{13}C\{^{1}H\}$ spectrum of the aromatic region (Fig 7.11a) (between $\delta^{13}C$=120.0 ppm and $\delta^{13}C$=150.0 ppm) it was found that there are four triplets and two singlets which collapse into 6 single peaks upon ^{31}P decoupling (Fig 7.11b). This region is that of quaternary carbon resonances and thus we can label the triplets as originating from ortho aromatic carbons and the singlets from the two para aromatic carbons. The low temperature ^{31}P nmr spectrum indicated a single phosphorus environment. If tetramesityl-diphosphine in the slow exchange limit adopted the trans configuration then only two ortho aromatic carbon signals and one para aromatic carbon signal would be expected. The cis conformer can be also excluded as this would cause steric overcrowding. The conclusion from both the ^{13}C and ^{31}P spectra is that tetramesityldiphosphine at low temperature prefers the gauche configuration (Fig 7.12).

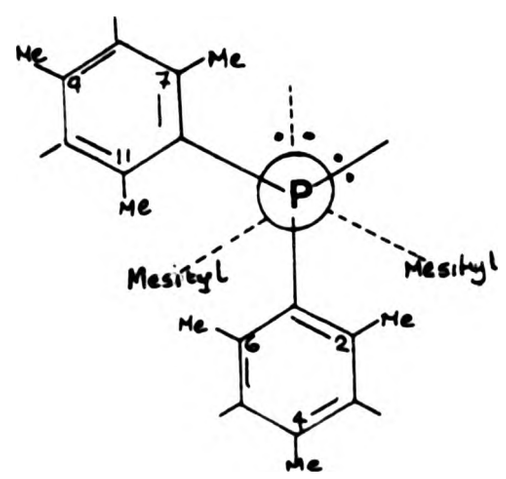

Fig 7.12 Gauche Configuration of Tetramesityldiphosphine

Similar findings were reported by Harris for tetra-t-butyl-diphosphine [1]. On raising the temperature the signals from the para aromatic carbons should coalesce as a consequence of the rotation about the phosphorus-phosphorus bond. As Fig 7.10a shows, signals at $\delta^{13}C$= 138.4 ppm and 136.6 ppm do indeed coalesce and thus they correspond to the para aromatic carbons C-4 and C-9 in Fig 7.17. The coupling constants ^{5}J(PPCCCC) and ^{4}J(PCCCC) are 0 Hz as expected from results of trimesityl-phosphine [this work] and triphenylphosphine[23]. As we cannot use differences in magnitudes of coupling constants to determine the positions of the para aromatic carbons with respect to the direction of the phosphorus lone pair, correlations between chemical shift positions and dihedral angle can be applied. Rankin [20] and Jorden [32] demonstrated that nuclei cis to the lone pair resonate at higher frequency than those trans to the lone pair. Hence from Fig 7.12 C-9 will be at higher frequency than C-4.

The ortho aromatic region of tetramesityldiphosphine (^{13}C =141.5 ppm to 147 ppm) consisted of pseudo triplets (Fig 7.11). These triplets are described as pseudo triplets and not "normal" triplets (as found in the X spectrum for an A_2X spin system). The differences between the two types of triplet are their splittings. In A_2X spin system the splitting is J(AX) which is not the case for pseudo triplets. The reason for obtaining pseudo triplets is that when there are two different magnetic environments of A, we no longer have an A_2X system but rather an AA'X spin system. In our case A=A'=^{31}P and X=^{13}C. It is the presence of ^{13}C nuclei which has only 1% natural abundance (one ^{13}C nucleus per molecule) that reduces the symmetry and causing

Similar findings were reported by Harris for tetra-t-butyl-diphosphine [1]. On raising the temperature the signals from the para aromatic carbons should coalesce as a consequence of the rotation about the phosphorus-phosphorus bond. As Fig 7.10a shows, signals at $\delta^{13}C$= 138.4 ppm and 136.6 ppm do indeed coalesce and thus they correspond to the para aromatic carbons C-4 and C-9 in Fig 7.17. The coupling constants ^{5}J(PPCCCC) and ^{4}J(PCCCC) are 0 Hz as expected from results of trimesityl-phosphine [this work] and triphenylphosphine[23]. As we cannot use differences in magnitudes of coupling constants to determine the positions of the para aromatic carbons with respect to the direction of the phosphorus lone pair, correlations between chemical shift positions and dihedral angle can be applied. Rankin [20] and Jorden [32] demonstrated that nuclei cis to the lone pair resonate at higher frequency than those trans to the lone pair. Hence from Fig 7.12 C-9 will be at higher frequency than C-4.

The ortho aromatic region of tetramesityldiphosphine (^{13}C =141.5 ppm to 147 ppm) consisted of pseudo triplets (Fig 7.11). These triplets are described as pseudo triplets and not "normal" triplets (as found in the X spectrum for an A_2X spin system). The differences between the two types of triplet are their splittings. In A_2X spin system the splitting is J(AX) which is not the case for pseudo triplets. The reason for obtaining pseudo triplets is that when there are two different magnetic environments of A, we no longer have an A_2X system but rather an AA'X spin system. In our case A=A'=^{31}P and X=^{13}C. It is the presence of ^{13}C nuclei which has only 1% natural abundance (one ^{13}C nucleus per molecule) that reduces the symmetry and causing

the magnetic environment of the two ^{31}P nuclei be different. For an AA'X spin system, the X part of the spectrum contains 6 lines (Fig 7.14).

Fig 7.14 X Region of an AA'X spin system

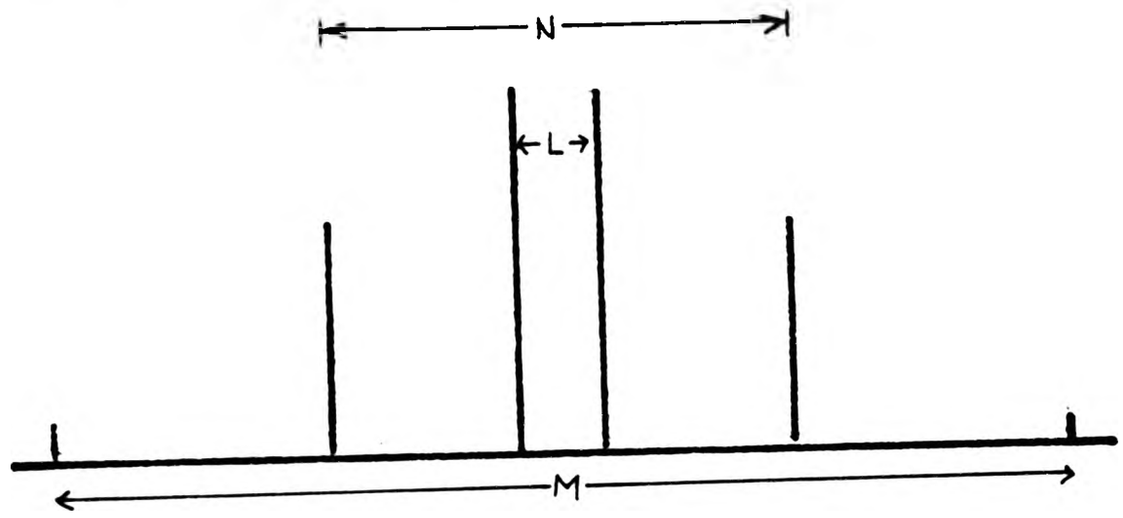

$$N = J(A'X) + J(AX)$$

$$L = 2|D_+ - D_-|$$

$$M = 2|D_+ + D_-|$$

$$D = -\ [\nu_A - \nu_{A'} + \tfrac{1}{2}(J(AX) - J(A'X))]^2 + J_{AA'}^2\ ^{1/2}$$

For such a system D_+ and D_- are identical as the chemical shift difference $\nu_A - \nu_{A'}$ is expected to be zero. Hence L becomes zero and the inner two lines come together. The magnitude of J(PP) of 220 Hz was observed by McFarlane and McFarlane [6] in 1,2-dimethyl-1,2- diphenylbiphosphine. Thus we can safely say that the magnitude of J(PP) for tetramesityldiphosphine is many times greater than N and thus the two outer most lines (separation M) move further apart from the centre of the spectrum, and their intensities are transferred to the centre band. Thus for this AA'X system, we have the following relationships

$$\nu(A) = \nu(A')$$

$$J(AA') >> J(AX + A'X)$$

and the X region should consist of a triplet, the central band being an unresolvable doublet and N ($=^{n}J(C-P)+^{n+1}J(C-P)$) is taken as the separation of the outer lines of the triplets. No attempt was made to investigate the sign of N, but from work on similar compounds the sign of N is positive, when N is large; but when N is small a reversal of its sign may occur as was revealed by Albrand's group [33]. However what is interesting is the magnitude of N. The sizes of N found in this work could be separated into two groups. One group had N in the order of 31 to 38 Hz and the other in the order of 4 Hz. This suggests that rings are twisted as observed in trimesitylphosphine, and by the same argument used in the analysis of trimesitylphosphine and assuming that $^{n+1}J(^{13}C-^{31}P)$ is very close to zero then the larger splitting belongs to the aromatic carbon which is <u>trans</u> to the lone pair and smaller N originating from the <u>ortho</u> aromatic <u>cis</u> to the lone pair. Hence using the notation in Fig 7.12 and the spectrum in Fig 7.11, it can be concluded that carbons C-6 and C-11 are <u>cis</u> to the lone pair and that carbons C-2 and C-7 are <u>trans</u> to the lone pair.

The low temperature $^{13}C\ \{^{1}H, ^{31}P\}$ spectrum of tetramesityldiphosphine in the methyl region ($\delta^{13}C$ =20 ppm to $\delta^{13}C$ =24 ppm) consists of 4 signals of equal intensity and one signal with double intensity (Fig 7.15a). From the low temperature spectrum but with proton decoupling only, two of the signals remained unsplit and 4 of signals showed they had splitting (Fig 7.15b). The signals that show no splitting in the low temperature proton decoupled spectrum were assigned to the <u>para</u> methyls and this assignment was confirmed by observation of the same spectrum at higher temperature. The couplings involving

the methyl carbons were determined by comparison between spectra with and without phosphorus decoupling.

Fig 7.15 ^{13}C nmr spectrum of the methyl region of Tetramesityldiphosphine at $-48^{o}C$ a) with proton decoupling, b) with proton and phosphorus decoupling

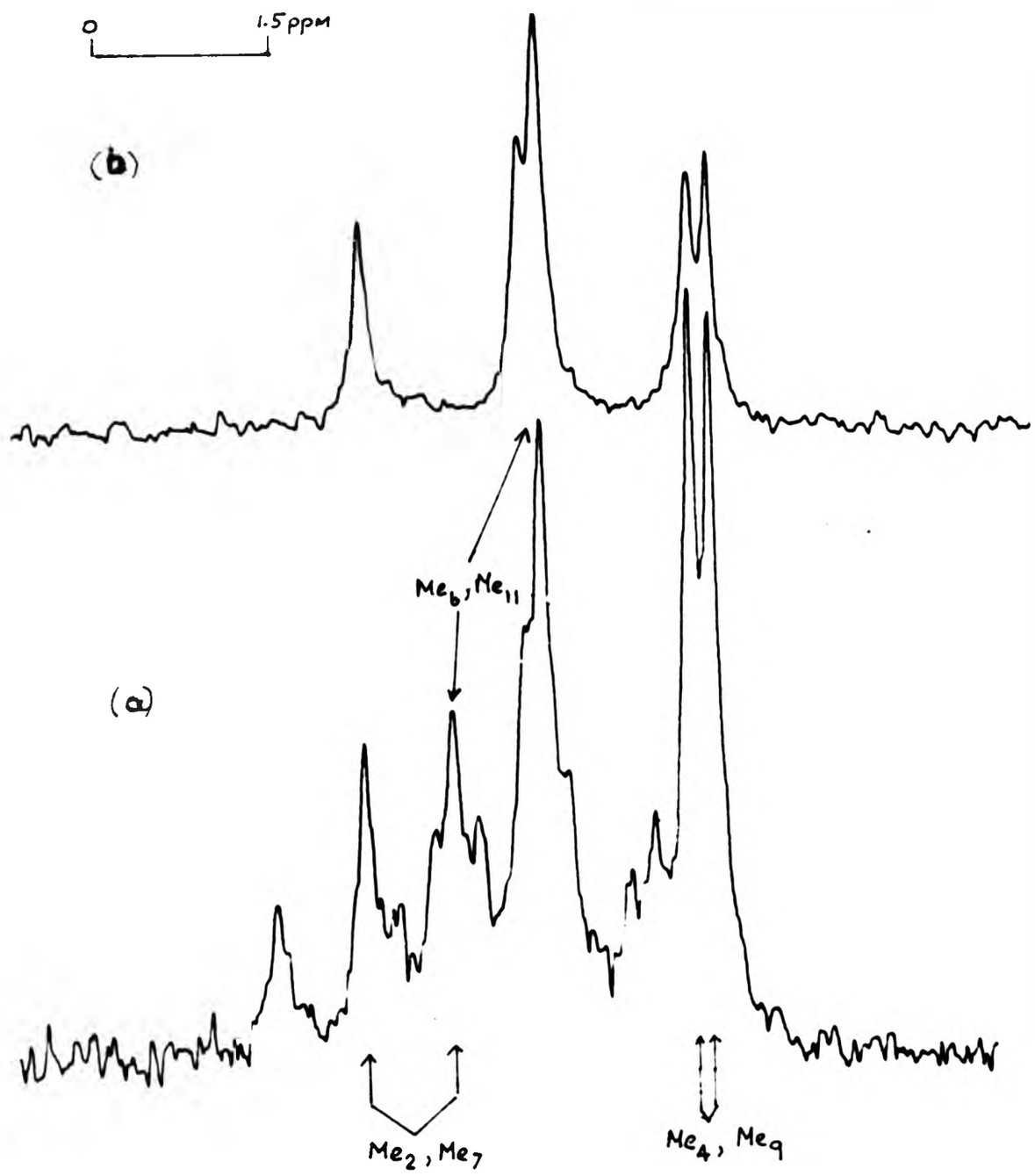

The next object of this exercise was to determine the energy barriers for rotation about both the PC and PP bonds in tetramesityldiphosphine. The energy associated with the PP bond rotation was calculated by observing the coalescence between the 2 para aromatic signals at different temperatures, since these are unaffected by the rotation about the PC bonds. Fig 7.16a shows spectra at 7 different temperatures covering the range in which the signals from the two para aromatic signals coalesce and Fig 7.16b shows matching computed spectra. From the plot of rate versus 1/T (Fig 7.16c) the energy of activation for the PP bond rotation was calculated using equation 7.1. Once the barrier for the PP rotation is known there should be no problem in calculating the energy barriers for PC rotation as this would be obtained through observation of coalescence of appropriate pairs of carbon peaks. In practice it was found that up to $-30^{o}C$ the rotation about the PP bond had already started but there was no sign of the P-mesityl bond rotation. Above this temperature the quality of the spectra began to deteriorate and it became impossible to obtain satisfactory spectra from which to calculate the energy barrier for the rotation about the P-P bond. The poor quality spectra at high temperatures may have been due to slight dissociation of Mes_4P_2 into free radicals of Mes_2P . The reason for this may be due to the bulkiness of the mesityl group which would weaken the PP bond, in some cases causing the PP bond to break thus leading to the presence of free radicals in solution. In Table 7.4 energy barrier to rotation about the PP bond in tetramesityldiphosphine are reported.

(a) Calculated

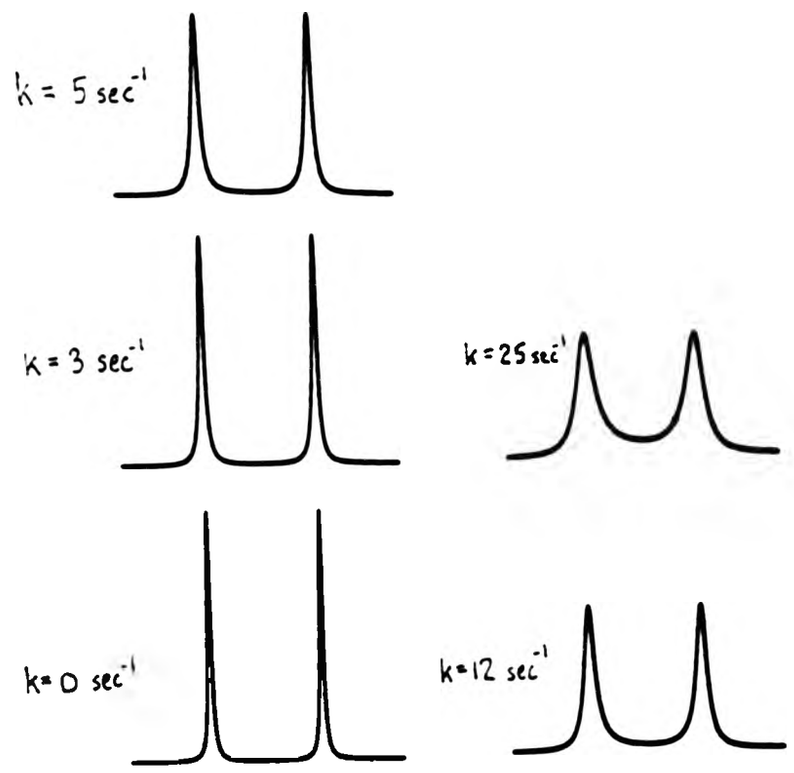

(b) Experimental

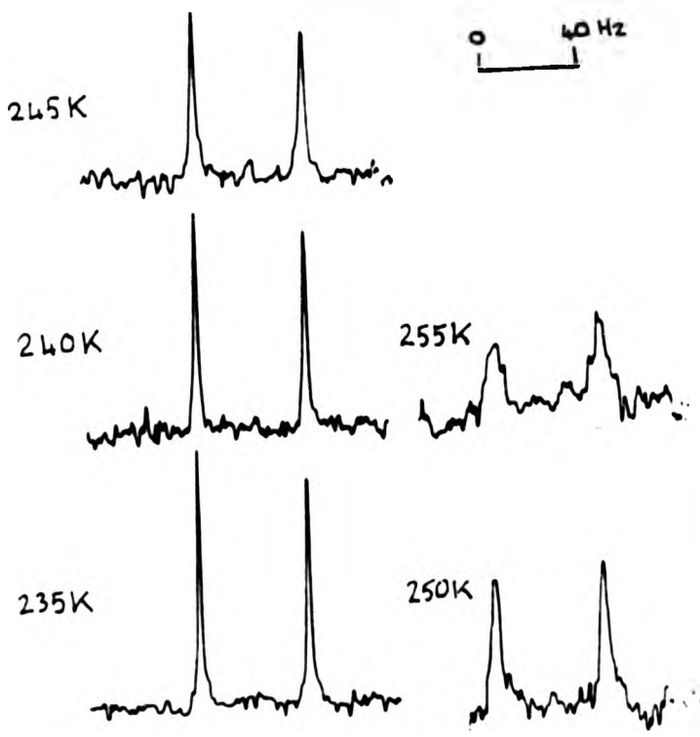

Fig 7.1b Experimental (lower) and Calculated (upper) Temperature Dependant 15MHz $^{13}C\{^1H\}$ nmr spectra of the para aromatic region in Tetramesityldiphosphine.

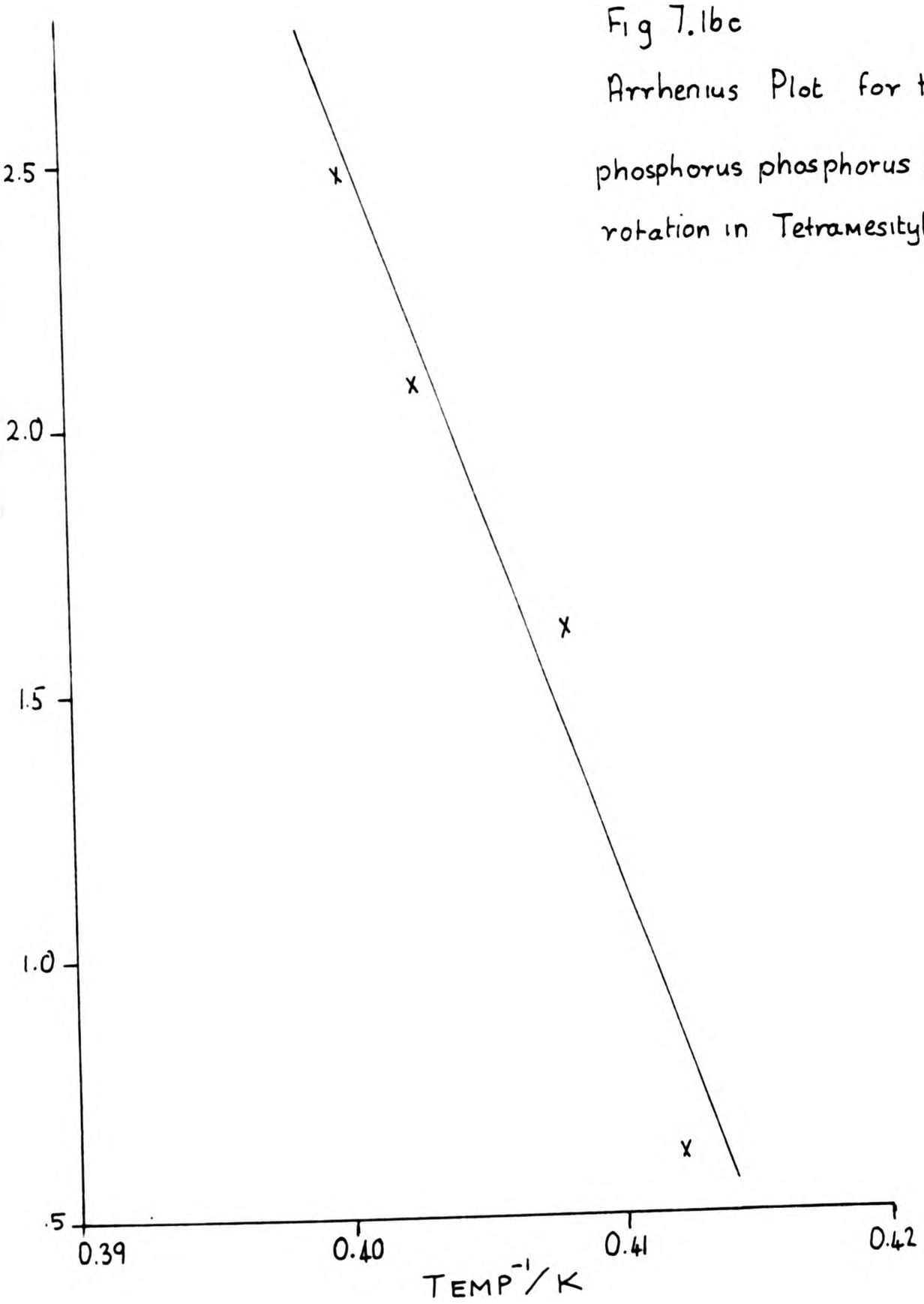

Fig 7.16c

Arrhenius Plot for the

phosphorus phosphorus bond

rotation in Tetramesityl diphosphine

Table 7.4 Energy Barrier Results For the P-P Rotation in Tetramesityldiphosphine from ^{13}C nmr data

$\Delta\nu$/Hz[a]	7.8 ±.5
T(coalescence)/K[b]	249 ±2
E_a / KJ mol^{-1}	90.5 ±5

a) Separation between para aromatic carbon signals for tetramesityldiphosphine before exchange.

b) Temperature at which the para aromatic carbon signals in tetramesityldiphosphine coalesce.

7.4 Conclusions

Tetramesityldiphosphine and trimesitylphosphine have been studied by nmr. The results of this study reveal that trimesitylphosphine adopts the chiral structure at low temperatures and tetramesityldiphosphine adopts a gauche conformation with respect to rotation about the PP bond, and has similar propeller twist of the mesityl rings. The structures of the conformers have been determined from the magnitudes of the two and three-bond phosphorus-carbon couplings; the method similarly used to obtain structural information on triphenyl and tris(ortho-tolyl)phosphine. In Table 7.5 comparisons of two and three-bond phosphorus carbon couplings for four phosphines are reported. In triphenylphosphine at temperatures as low as -83°C only one coupling is observed between the ortho carbons and phosphorus.

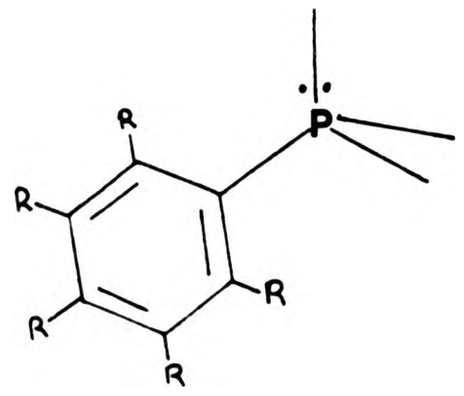

fig 7.17

Phenyl phosphine segment of a tri-substituted phosphine where R = proton or methyl.

Table 7.5 Ortho carbon phosphorus coupling constant in Aryl Phosphines

Ortho $J(^{13}C-^{31}P)$/Hz	$(Ph)_3P$	R_3P[a]	Mes_3P	Mes_4P_2[b]
Reference	9	8	tw	tw
Aromatic carbon				
trans to lone pair	19.65	26.44	37.1	31.2,38.1
cis to lone pair		0.41	0.0	4.0,4.4
Methyl carbon				
trans to lone pair		21.82	33.2	23.0,24.4
cis to lone pair			0.0	3.0,11.6

tw= This work

a) R= $(o\text{-}CH_3C_6H_5)_3P$

b) coupling constant corresponds to N where N is equal to $^{n}J(^{13}C-^{31}P)+^{n+1}J(^{13}C-^{31}P)$

This suggests that at this temperature rotation about the phosphorus-carbon bond is fast compared to nmr time scale. In trimesitylphosphine at the same temperature we obtain two different values for this coupling, and this can be interpreted by suggesting that trimesitylphosphine takes up the chiral structure at low temperature. However at room temperature when rotation about the PC bond is fast relative to the nmr time scale an averaging of the two couplings is expected. This was observed to have a value of 16.6 Hz (the calculated average is 16.6 Hz) for the PC coupling where the C belongs to the ortho methyl carbon. For PC coupling where C is the ortho aromatic carbon the observed value was 17.6 Hz (the calculated average is 18.5 Hz). It was not possible due to poor quality of the spectrum to obtain values of the ^{2}J(PC) coupling constant in tetramesityldiphosphine at room temperature (see Fig 7.10a). In tetramesityldiphosphine the splitting between phosphorus and the ortho methyl ^{13}C at room temperature was now 23 Hz (the calculated average is 18 Hz). The results indicate an increase in three-bond phosphorus carbon (methyl) coupling from trimesitylphosphine to tetramesityl-diphosphine at room temperature implying that the dihedral angle between the phosphorus lone pair direction and the ortho carbon atom has decreased. The implication of this is that the ortho aromatic carbons move closer to the phosphorus lone pair. This is understandable in that a more bulky substituent could rotate more freely if the wings of the pyramid are more spread out.

The structure of "frozen out" tetramesityldiphosphine reported from our observation favouring the lone pairs to be gauche is not consistent with Baxter's findings [30]. Baxter found from X-ray crystallography that tetramesityldiphosphine

prefers the anti state (Fig 7.18). From this and liquid state ^{1}H nmr he concludes that tetramesityldiphosphine favours the anti configuration also in the low temperature liquid state. Assuming the X-ray observation is correct the nmr analysis can be examined thoroughly. The low temperature proton nmr spectrum shows 4 equal intensity aromatic peaks and 6 equal intensity methyl peaks. This is consistent with our ^{13}C nmr experiments. The six methyl signals at high temperature collapse to three signals which can be attributed to two ortho and one para methyl sites. Baxter concludes from proton nmr that these observations are consistent with the X-ray picture. Although in principle the anti forms of tetramesityldiphosphine would give this number of proton signals, the energy barriers for the interconversion between the two mirror image anti forms (see fig 7.19) would surely be too low permit separate signals. Isomers I and III will give signals in both ^{13}C and proton nmr spectra as already described, but their exchange will lead at all accessible temperatures to half this number of signals, since the symmetrical transition intermediate II is of relatively low energy. Hence it appears that tetramesityldiphosphine in the solid state may favour an anti configuration but in frozen out liquid state the compound prefers the gauche configuration.

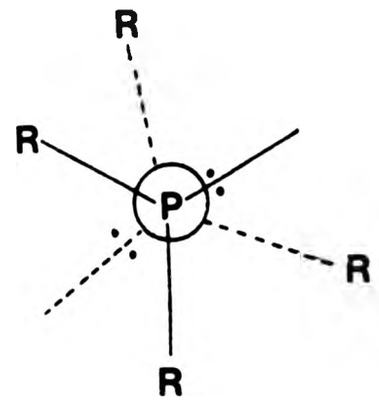

Fig 7.18 Anti Configuration of Tetramesityldiphosphine (R=Mesityl)

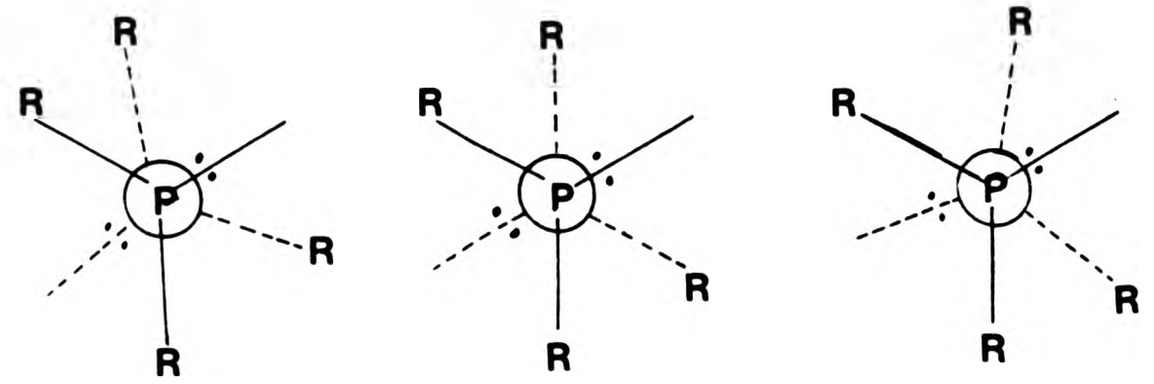

I Transition Intermediate II III

Fig 7.19 Possible Isomers of the Anti states of Tetramesityldiphosphine (R=Mesityl)

This is consistent with work carried out on diphosphines by Harris's group[1] and Mislow [34]. Their conclusions were that the likelihood of the molecule preferring the gauche configuration at the slow exchange limit was increased as the steric bulk of the substituent on the phosphorus is increased.

The disappointing aspect of this study was that we were unable to obtain the energy barrier for the hindered rotation about the P-mesityl bond in tetramesityldiphosphine. This seems not surprising as in similar work upon 1,1,2,2-tetramesityl-disilane there is no report on Si-mesityl energy barriers, but only on the energy barriers for the Si-Si rotation [35].

What this study illustrates is that the dihedral angle dependence of two and three-bond phosphorus-carbon coupling constants and variable temperature nmr makes simple the determination of the stereochemistry of trimesitylphosphine and tetramesityldiphosphine. Also dynamic ^{13}C nmr has permitted us

to determine energy barriers for the rotation about the PC bond in trimesitylphosphine and the rotation about the PP bond in tetramesityldiphosphine. Summarizing we find that nmr is a valuable technique for structure determination and providing kinetic parameters (as long as the kinetics for any particular process is within the nmr time scale) for a vast range of organic molecules.

APPENDIX 7.1

INPUT FOR POLY

```
1,2,1,1
50.,120.,.025,3.2
100
66.4,107.8
.5,.5
12.
```

OUTPUT OF POLY

```
          ***** MULTIPLE SITE EXCHANGE PROGRAM *****
  CASE NUMBER      1

  CHEMICAL EXCHANGE BETWEEN    2 SITES
FREQUENCY RANGE FROM 50.0 TO 120.00 IN  0.025 HZ INCREMENTS
NORMALISATION FACTOR =  .1000E+03
LINEWIDTH IN THE ABSENCE OF EXCHANGE =      3.20 HZ

          ***** SITE PARAMETERS *****
        SITE     1      SHIFT =    66.40      POPULATION=      0.50
        SITE     2      SHIFT =   107.80      POPULATION=      0.50

          ***** RATE CONSTANTS *****
            R( 1, 2)  = -.1200E+02
            R( 2, 1)  = -.1200E+02

TRACE  =  0.4410618E+02 + -0.1094530E+04I
SUMEIG =  0.4410618E+02 + -0.1094530E+04I

          ***** CALCULATED SPECTRUM *****

FREQUENCY    INTENSITY    FREQUENCY    INTENSITY
  50.0000       0.0766      50.0250       0.0768
  50.0500       0.0771      50.0750       0.0773
  50.1000       0.0775      50.1250       0.0778
     .             .           .             .
     .             .           .             .
 119.9000       0.1412     119.9250       0.1407
 119.9500       0.1401     119.9750       0.1395
 120.0000       0.1390
```

7.5 References

1 S. Aime, R.K. Harris, E.M. McVicker and M. Fild, J. Chem. Soc. Chem. Comm., 426(1974).

2 E.G. Finer and R.K. Harris. Prog. Nmr Specty., 6, 61(1970).

3 W. McFarlane, Quart. Review, 23, 187(1969).

4 E.G. Finer and R.K. Harris, Chem. Comm., 110(1968).

5 R.W. Rudolph and R.A. Newmark, J. Amer. Chem. Soc., 92, 1195(1970).

6 H.C.E. McFarlane and W. McFarlane, Chem. Comm., 1589(1971).

7 G.W. Buchanan and C. Benezra, Can. J. Chem., 54, 231(1976).

8 L.S. Bartell, J. Chem. Phys., 32, 832(1960).

9 J.J. Daly, J. Chem. Phys., 3799(1964).

10 J.P. Kintzinger and J.M. Lehn, Chem. Commun., 660(1967).

11 D. Crepaux and J.M. Lehn, Mol. Phys., 14, 547(1968).

12 T. Yonezawa, I. Morishmima, K. Fukuta and Y. Ohmori, J. Mol. Spectrosc., 31, 341(1969).

13 M.S. Gopinathan and P.T. Narisimhan, Mol.Phys., 22, 473(1971).

14 R.L. Lichter and J.D. Roberts, J. Amer. Chem. Soc., 93, 5218(1971).

15 P.S. Pregosin, E.W. Randall and A.I. White, J. Chem. Soc., Perkin Trans. 2, 1(1972).

16 J.P. Albrand, D. Gagniare, J. Martin and J.B. Robert, Bull.Soc. Chim Fr, 40(1969)

17 S. Sorensen, R.S. Hanson and H.J. Jakobsen, J. Amer. Chem. Soc., 94, 5900(1972)

18 T. Axenrod, Tetra Letts, 5293(1968).

19 W. Witanowski, Ann. Reports nmr specty., 5A, 44(1972).

20 D.W.H. Rankin and J.G. Wright, J. Chem. Soc. Dalton Trans., 1070(1977).

21 M. Karplus, J. Chem. Phys., 30, 11(1959).

22 S.I. Fetherman, S.O. Lee and L.D. Quin, J.Org.Chem., 39(19), 2899(1974).

23 G.A. Gray and S.E. Gemer, Chem. Comm., 367(1972).

24 R.T. Morrison and R.N. Boyd, Organic Chemistry, 4th Edition, Allyn and Bacon.

25 T. Bundgaard and H.G. Jakobsen, Acta Chem. Scand., 26, 2548(1972).

26 B.E. Mann, Prog in nmr specty.,11, 95(1977).

27 Practical Nmr Spectroscopy, M.L. Martin, G.J. Martin, and J.J. Delpuech. Heydon Press 1980.

28 V.V. Negrebetskii, A.I. Bokanov, N.A. Rozanel'skaya, L.Ya. Bogel'fer and B.I. Stepanov, Zh. Strukt Khim., 19(4), 545(1978).

29 V.V. Negrebetskii, A.I. Bokanov, N.A. Rozanel'skaya and B.I. Stepanov, Zh. Obshch Khim., 49(7), 1304 (1979).

30 S.G. Baxter, A.H. Cowley, R.E. Davies and P.E. Riley, J. Amer. Chem. Soc., 103, 1699(1981).

31 S.O. Chan and L.W. Reeves, J. Amer. Chem. Soc., 95, 670(1973).

32 G.J. Jorden and D.L.R. Grist, Org. Mag. Res., 9, 322(1977).

33 J.P. Albrand, Chem. Comm., 89, 6612(1968).

34 S.G. Baxter, D.A. Dougherty, J.P. Hummel and K. Mislow, J. Amer. Chem. Soc., 100, 7795(1978).

35 J.F. Blount, C.A. Maryanoff and K. Mislow, Tetrahedron Lett., 913(1975).

Chapter 8

PREPARATIONS

8.1 Trimesitylphosphine $[(CH_3)_3C_6H_3]_3P$

$$2RBr + 2Mg \longrightarrow 2RMgBr \xrightarrow{PCl_3} [R_2PCl] \xrightarrow{2RMgBr} R_3P$$

$$R=2,4,6-(CH_3)_3C_6H_3$$

The Grignard reagent was prepared by adding slowly under nitrogen, 15.92g of bromomesitylene in 40mls of tetrahydrofuran to 1.94g of magnesium. The solution was then cooled and kept cooled during the addition of 1.8mls of phosphorus trichloride in 10mls of tetrahydrofuran. After the addition was complete the mixture was refluxed under nitrogen for about 2 hours. The mixture was cooled and then 100mls of benzene followed by 50mls of aqueous ammonium chloride were added. Upon settling, the organic layer was removed from the mixture, and washed thoroughly with water and soda solution. The solvent from the organic layer was evaporated under vacuum. The residue was washed with alcohol and crystallised from a mixture of alcohol and benzene. m.pt 192°C (lit. 192-193° [1]). $\delta^{31}P$ -36.5 ppm. (with respect to 85% phosphoric acid)

8.2 Tetramesityldiphosphine $[(CH_3)_3C_6H_3]_4\ P_2$

$$4RBr + 4Mg \longrightarrow 4RMgBr \xrightarrow{2PCl_3} 2[R_2PCl] \xrightarrow{Mg} R_4P_2$$

$$R=2,4,6-(CH_3)_3C_6H_3$$

The preparation of tetramesityldiphosphine was similar to that of trimesitylphosphine but with the following changes. 19.95g of bromomesitylene and 2.92g of magnesium were used, and

then followed by 3.6mls of phosphorus trichloride. $\delta^{31}P$ was -30.8ppm (with respect to 85% phosphoric acid).

8.3 Bistrifluoromethylmercury $(CF_3)_2Hg$

$$2CF_3COOH + HgO \xrightarrow{-[H_2O]} (CF_3COO)_2Hg \xrightarrow{K_2CO_3} (CF_3)_2Hg$$

23g of mercuric oxide was added slowly to 22.5mls of trifluoroacetic acid. Small quantities of mercuric oxide were further added until a small amount of undissolved mercuric oxide remained. After warming for 10 minutes the excess mercuric oxide was filtered off, and the solvent was removed by evaporation at 40°C under vacuum. The residue was dried overnight under vacuum over dried phosphorus pentoxide giving anhydrous trifluoromethylmercuric acetate. 8.0g of dried product was placed with about 8g of anhydrous potassium carbonate in a vacuum sublimer. The mixture was heated at an oil bath temperature between 180 and 200°C under vacuum, and the crystals of $(CF_3)_2Hg$ collected on the side of the condenser. $\delta^{19}F$ of $(CF_3)_2Hg$ in benzene was 41.99ppm (with respect to trifluoroacetic acid); lit. value -41.59 ppm[2].

8.4 Tris(o-fluorophenyl)phosphine $(o\text{-}C_6FH_4)_3P$[3]

$$2RBr + 2Mg \longrightarrow 2RMgBr \xrightarrow{PCl_3} [R_2PCl] \xrightarrow{2RMgBr} R_3P$$

$$R = (o\text{-}C_6H_4F)$$

The Grignard reagent was prepared by adding under nitrogen, 12.0g (68.5m mol) of o-bromofluorobenzene in 100mls of tetrahydrofuran (THF) to 1.68g of completely dry magnesium. After

the addition was complete the mixture was stirred at room temperature for 2hrs. The mixture was then cooled to -80°C and then to it a solution of 2.35g of phosphorus trichloride in 50mls of THF was added slowly. The mixture was stirred for 3hrs after which it was treated with 20% aqueous ammonium chloride followed by 50mls of water. The THF was then removed by evaporation and the aqueous solution extracted with ether. The ether extract was dried and the solvent was removed using a rotary evaporator. The crude tris(o-fluorophenyl)phosphine was crystallised from methanol. The purity of the compound was checked by ^{19}F and ^{31}P nmr.

Meta and para tris(fluorophenyl)phosphine were prepared in our laboratory in identical manner using the appropriate bromofluorobenzene.

8.5 References

1 B.I. Stepanov, E.N. Karpova and A.I. Bokanov, Zh. Obshch Khim., 48(7), 1899(1978).

2 M.D. Marvin and J.R.V. Wazer, Inorganic Chemistry, 3, 763(1964).

3 J. Chatt and F.A. Hart, J. Chem. Soc., 2807(1960).